DESY 99–070
August 1999
hep-ph/9908433
v.2 (02/2000)

ZFITTER v.6.21

A Semi-Analytical Program for Fermion Pair Production in e^+e^- Annihilation

D. Bardin[1,†], M. Bilenky[2], P. Christova[1,3,*], M. Jack[4],
L. Kalinovskaya[1,†], A. Olchevski[1,5], S. Riemann[4], T. Riemann[4,‡]

[1] Laboratory of Nuclear Problems, Joint Institute for Nuclear Research, Dubna, Russia

[2] Institute of Physics, Academy of Sciences, Prague, Czech Republik

[3] Faculty of Physics, Bishop Preslavsky University, Shoumen, Bulgaria

[4] DESY Zeuthen, Germany

[5] EP Division, CERN, Geneva, Switzerland

Abstract

We describe ZFITTER, a Fortran program based on a semi-analytical approach to fermion pair production in e^+e^- annihilation at a wide range of centre-of-mass energies, including the PETRA, TRISTAN, LEP1/SLC, and LEP2 energies. A flexible treatment of complete $\mathcal{O}(\alpha)$ QED corrections and of some higher order contributions is made possible with three calculational chains containing different realistic sets of restrictions in the photon phase space. Numerical integrations are at most one-dimensional. Complete $\mathcal{O}(\alpha)$ weak loop corrections supplemented by selected higher-order terms may be included. The program calculates Δr, the Z width, differential cross-sections, total cross-sections, integrated forward-backward asymmetries, left-right asymmetries, and for τ pair production also final-state polarization effects. Various interfaces allow fits to be performed with different sets of free parameters.

Submitted to Computer Physics Communications

† Supported by European Union with grant INTAS-93-744 and by German-JINR Heisenberg-Landau program

‡ Supported by European Union with grant CHRX-CT920004

* Supported by European Union with grant CIPD-CT940016 and by Bulgarian Foundation for Scientific Researches with grant Φ–620/1996

ZFITTER v.6.21

A Semi-Analytical Program for Fermion Pair Production in e^+e^- Annihilation

D. Bardin [a] *, M. Bilenky [b], P. Christova [a c] †, M. Jack [d], A. Olchevski [a e], L. Kalinovskaya [a] ‡, S. Riemann [d] and T. Riemann [d] §

[a]Laboratory of Nuclear Problems, Joint Institute for Nuclear Research, Dubna, Russia

[b]Institute of Physics, Academy of Sciences, Prague, Czech Republik

[c]Faculty of Physics, Bishop Preslavsky University, Shoumen, Bulgaria

[d]DESY Zeuthen, Germany

[e]EP Division, CERN, Geneva, Switzerland

We describe ZFITTER, a Fortran program based on a semi-analytical approach to fermion pair production in e^+e^- annihilation at a wide range of centre-of-mass energies, including the PETRA, TRISTAN, LEP1/SLC, and LEP2 energies. A flexible treatment of complete $\mathcal{O}(\alpha)$ QED corrections and of some higher order contributions is made possible with three calculational chains containing different realistic sets of restrictions in the photon phase space. Numerical integrations are at most one-dimensional. Complete $\mathcal{O}(\alpha)$ weak loop corrections supplemented by selected higher-order terms may be included. The program calculates Δr, the Z width, differential cross-sections, total cross-sections, integrated forward-backward asymmetries, left-right asymmetries, and for τ pair production also final-state polarization effects. Various interfaces allow fits to be performed with different sets of free parameters.

*Supported by European Union with grant INTAS-93-744 and by German-JINR Heisenberg-Landau program

†Supported by European Union with grant CIPD-CT940016 and by Bulgarian Foundation for Scientific Researches with grant Φ–620/1996

‡Supported by European Union with grant INTAS-93-744 and by German-JINR Heisenberg-Landau program

§Supported by European Union with grant CHRX-CT920004

PROGRAM SUMMARY

Title of the program: ZFITTER version 6.21 (26 July 1999)
Computer: any computer with FORTRAN 77 compiler
Operating system: UNIX, program tested e.g. under HP-UX and Linux, but also under IBM, IBM PC, VMS, APOLLO, and SUN
Programming language used: FORTRAN 77
High-speed storage required: < 2 MB
No. of cards in combined program and test deck: about 24,000
Keywords: Quantum electrodynamics (QED), Standard Model, electroweak interactions, heavy boson Z, e^+e^--annihilation, radiative corrections, initial-state radiation (ISR), final-state radiation (FSR), QED interference, LEP1, LEP2, Linear Collider, TESLA
Nature of the physical problem: Fermion pair production is important for the study of the properties of the Z-boson and for precision tests of the Standard Model at LEP and future linear colliders at higher energies. QED corrections and combined electroweak and QCD corrections have to be calculated for this purpose with high precision, including higher order effects. For multi-parameter fits a program is needed with sufficient flexibility and also high calculational speed. ZFITTER combines the two aspects by at most one-dimensional numerical integrations and a variety of flags, defining the physics contents used. The Standard Model predictions are typically at the per mille precision level, sometimes better.
Method of solution: Numerical integration of analytical formulae.
Restrictions on the complexity of the problem: Fermion pair production is described below the top quark production threshold. Photonic corrections are taken into account with relatively simple cuts on photon energy, or the energies and acollinearity of the two fermions, and *one* fermion production angle. Bhabha scattering is treated poorly.
Typical running time: On a Pentium II PC installation (400 MHz), Linux 2.0.34, approximately 140 sec are needed to run the standard test with subroutine ZFTEST. This result is for a *default/recommended* setting of the input parameters, with *all* corrections in the Standard Model switched *on*. ZFTEST computes 12 cross-sections and cross-section asymmetries for 8 energies with 5 interfaces, i.e. about 360 cross-sections in 140 seconds.

Contents

List of Figures

List of Tables

Introduction

The ZFITTER project was started in 1983 by D. Bardin, O. Fedorenko and T. Riemann. A first program package, ZBIZON, was shortly used in 1989 at LEP by the DELPHI and L3 Collaborations but got immediately replaced by the ZFITTER package.

The Fortran program ZFITTER [1], with the packages DIZET [2] and BHANG, was originally intended for the description of fermion pair production around the Z resonance at the e^+e^- colliders LEP1 and SLC in the Standard Model using the on mass shell renormalization scheme [3,4]. The 1989 version of DIZET was described in [5], and the corresponding 1992 versions ZFITTER v.4.5, DIZET v.4.04, and BHANG in [6]. The actual version 6.21 of ZFITTER [7–11] was improved in many respects and is now also intended for considerably smaller and higher energies thus covering two fermion production physics ranging from PETRA to LEP2:

$$e^+e^- \longrightarrow f\bar{f}(\mathrm{n}\gamma), \quad f = \mu, \nu_\mu, \tau, \nu_\tau, u, d, c, s, b. \tag{I.1}$$

Applications at higher energies have not been carefully tested so far.

ZFITTER, when it is used with the DIZET package allows for the description of data in the Standard Model. ZFITTER calculates radiative corrections to the muon decay constant [3,4,12–14], the decay width of the Z boson [12–14], and improved Born cross-sections [8,13,14] for reaction Eq. (I.1) with virtual electromagnetic, electroweak, and QCD corrections. Photonic corrections with different cuts and for different observables are described as convolutions of improved Born cross-sections with radiator functions (flux functions) [15,9–11].

The Fortran program package ZFITTER consists of three parts:

- The main package ZFITTER itself.
  The authors of ZFITTER are:
  D. Bardin, M. Bilenky (1987-1994), A. Chizhov (1987-1991), P. Christova (since 1997), O. Fedorenko (1990), M. Jack (since 1997), L. Kalinovskaya (since 1997), A. Olshevsky, S. Riemann, T. Riemann, M. Sachwitz (1987-1991), A. Sazonov (1987-1991), Yu. Sedykh (1989-1991), I. Sheer (1991-1992), L. Vertogradov (1990).

- The package ZFITTER calculates the virtual corrections in the Standard Model with the Fortran program DIZET.
  The authors of DIZET are:
  A. Akhundov (1985-1989), D. Bardin, M. Bilenky (1987-1994), P. Christova, L. Kalinovskaya (since 1997), S. Riemann, T. Riemann, M. Sachwitz (1987-1991), H. Vogt (1989).

- The package ZFITTER has a branch for Bhabha scattering, the Fortran program BHANG. BHANG calculates QED corrections and determines the improved Born cross-section with the aid of DIZET.
  The author of BHANG is M. Bilenky.

This article describes ZFITTER, version 6.21 and DIZET, version 6.21, and the parts of BHANG, version 4.67, which determine the improved Born cross-section [16,14] for the reaction

$$e^+e^- \longrightarrow e^+e^-. \tag{I.2}$$

Alternatively to the Standard Model, several so-called "semi–model-independent" approaches may be used in ZFITTER, see Section 3.7. In addition, it can be used to fit the experimental data with the S-matrix approach, package SMATASY [17–20] and to theories that go beyond the Standard Model, package ZEFIT [21,22]. These packages are to be run together with ZFITTER.

ZFITTER is based on a semi-analytical approach to radiative corrections. It relies on formulae which are either differential in the scattering angle ϑ as defined in Fig. I.1 or, alternatively, are analytically integrated over a finite angular region.

ZFITTER calculates:

- Δr – Standard Model corrections to G_μ, the muon decay constant
- M_W – the W boson mass from M_Z, M_H, other masses, and Δr
- $\Gamma_Z = \sum_f \Gamma_f$ – total and partial Z boson decay widths
- $d\sigma/d\cos\vartheta$ – differential cross-sections
- σ_T – total cross-sections
- A_{FB} – forward-backward asymmetries
- A_{LR} – left-right asymmetries
- A_{pol}, A_{FB}^{pol} – final state polarization effects for τ leptons

Total cross-sections and asymmetries may be calculated in a non-symmetric angular interval:

$$\sigma_T(c_1,c_2) = \int_{c_1}^{c_2} d\cos\vartheta \frac{d\sigma}{d\cos\vartheta}, \tag{I.3}$$

$$A_{FB}(c_1,c_2) = \frac{\sigma_{FB}(c_1,c_2)}{\sigma_T(c_1,c_2)}, \tag{I.4}$$

where

$$\sigma_{FB}(c_1,c_2) = \left[\int_0^{c_2} d\cos\vartheta - \int_{c_1}^{0} d\cos\vartheta\right] \frac{d\sigma}{d\cos\vartheta}. \tag{I.5}$$

Analogous definitions of other asymmetries are given in Section 3.8. Two cases of special physical interest are:

$$\sigma_T(c) = \int_{-c}^{c} d\cos\vartheta \frac{d\sigma}{d\cos\vartheta}, \tag{I.6}$$

$$\sigma_{FB}(c) = \left[\int_0^{c} d\cos\vartheta - \int_{-c}^{0} d\cos\vartheta\right] \frac{d\sigma}{d\cos\vartheta}. \tag{I.7}$$

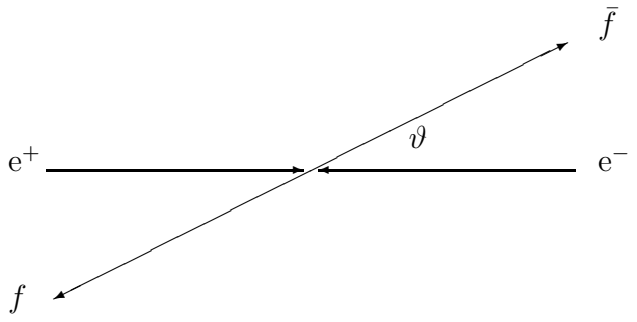

Figure I.1. *Scattering angle ϑ*

In ZFITTER, the expressions Eq. (I.3) and Eq. (I.4) are constructed from the following integral:

$$\sigma(0,c) \equiv \int_0^c d\cos\vartheta \frac{d\sigma}{d\cos\vartheta} = \frac{1}{2}\left[\sigma_T(c) + \sigma_{FB}(c)\right]. \tag{I.8}$$

Corresponding to $c_1 = \cos\vartheta_1 < \cos\vartheta < c_2 = \cos\vartheta_2$, the maximal and minimal polar angles for the integrated cross-sections are:

$$\texttt{ANG1} \;=\; \vartheta_2, \tag{I.9}$$

$$\texttt{ANG0} \;=\; \vartheta_1. \tag{I.10}$$

For a symmetrical angular region, it is

$$\vartheta_2 \;=\; 180^\circ - \vartheta_1. \tag{I.11}$$

If the angles related by Eq. (I.11), an internal flag ISYM is set equal to 1 in subroutine ZCUT and the integrated quantities $\sigma_{T,FB}(c) = [\sigma(0,c) \pm \sigma(0,-c)]$ are simply twice the contributions calculated by calls to subroutines SFAST or SCUT. We mention this here since in SFAST and SCUT the cross-section contributions are by a factor two smaller than the (integrated) corresponding quantities in subroutine COSCUT from the branch for the calculation of angular distributions.

With ZFITTER cross-sections may be calculated in two ways: without and with photonic corrections. The Born approximation and, if electroweak corrections are applied, the improved Born approximation, are based on analytic formulae. Photonic corrections are realized as *one-dimensional numeric integrations* over the invariant mass of the fermion pair:

$$s' \equiv (p_f + p_{\bar{f}})^2 = \left(1 - \frac{2E_\gamma}{\sqrt{s}}\right) s, \tag{I.12}$$

where p_f ($p_{\bar{f}}$) is the fermion (antifermion) momentum and E_γ the energy of the emitted photon. Often we will also use a related variable v:

$$\Delta = v_{\max} \geq v \;=\; \frac{2E_\gamma}{\sqrt{s}} = 1 - \frac{s'}{s}. \tag{I.13}$$

The cut conditions for Δ, $s'_{\min}$, and $E_\gamma^{\max}$ are trivially related by Eq. (I.13).

The photonic corrections are implemented by convoluting the corresponding (improved) Born cross-sections σ_A^0, $A = T, FB$, with photonic radiator functions R_A^a, $a = ini, int, ini+fin$. For initial state radiation, e.g., the correction to the differential cross-section is:

$$\frac{d\sigma^{ini}}{d\cos\vartheta} \sim \int_{4m_f^2 \le s'_{\min}}^{s} \frac{ds'}{s} \left[R_T^{ini}(s, s', \cos\vartheta)\, \sigma_T^0(s') + R_{FB}^{ini}(s, s', \cos\vartheta)\, \sigma_{FB}^0(s') \right]. \tag{I.14}$$

The QED radiators are defined in Chapter 1. The pseudo-observables are defined for the Standard Model in Chapter 2 and the improved Born cross-sections in Chapter 3. The latter two Chapters make intensive use of one-loop amplitudes collected in Appendix A. Initialization and use of the program are described in Section 4.1 and Section 4.2. Section 4.3 documents the various *interfaces*. Section 4.4 contains a description of the contents of some of the common blocks of `ZFITTER` and Appendix B an example of the use of the program.

`ZFITTER` is a self-contained package, but contains some routines of other authors:

- Subroutines `SIMPS` [23], written by I. Silin, and `FDSIMP` [24], written by Yu. Sedykh, perform self adapting one-dimensional numerical integrations without and with mapping.

- Subroutines `TRILOG` and `S12` [25], written by T. Matsuura, calculate polylogarithms Li_3 and $S_{2,1}$.

- Package with main subroutine `hadr5`, version 24/02/1995, written by F. Jegerlehner [26], calculates the contribution of light hadrons to the hadronic vacuum polarization [27] (default, flag `VPOL`=1).

- Another calculation of this contribution is subroutine `HADRQQ`, written by H. Burkhardt [28,29] (flag `VPOL`=3).

- Package `m2tcor`, version 2.0 (Oct 1996), written by G. Degrassi [30], calculates the electroweak corrections of the order $\mathcal{O}(G_\mu^2 m_t^2 M_Z^2)$ and $\mathcal{O}(G_\mu^2 m_t^4)$ to Δr, $\sin^2\theta_{\rm eff}^{\rm lept}$ and to the partial Z boson widths [31–36] (default, flag `AMT4`=4).

- Package `pairho.f`, version 16/07/99, written by A. Arbuzov [37], contains a rather complete treatment of higher order initial state pair production corrections to e^+e^- annihilation (default, flag `ISPP`=2).

- A package for the computation of functions $V(r)$, $A(r)$, and $F(x)$, needed for the calculation of $\mathcal{O}(\alpha\alpha_s)$ corrections to bosonic self-energies, written by B. Kniehl [38] (default, flag `IQCD`=3).

Finally we would like to draw the attention of the reader to the comprehensive presentation of many subtleties of the underlying formulae given in [39], and to some quite recent numerical comparisons with the results of other programmes given in [40,41].

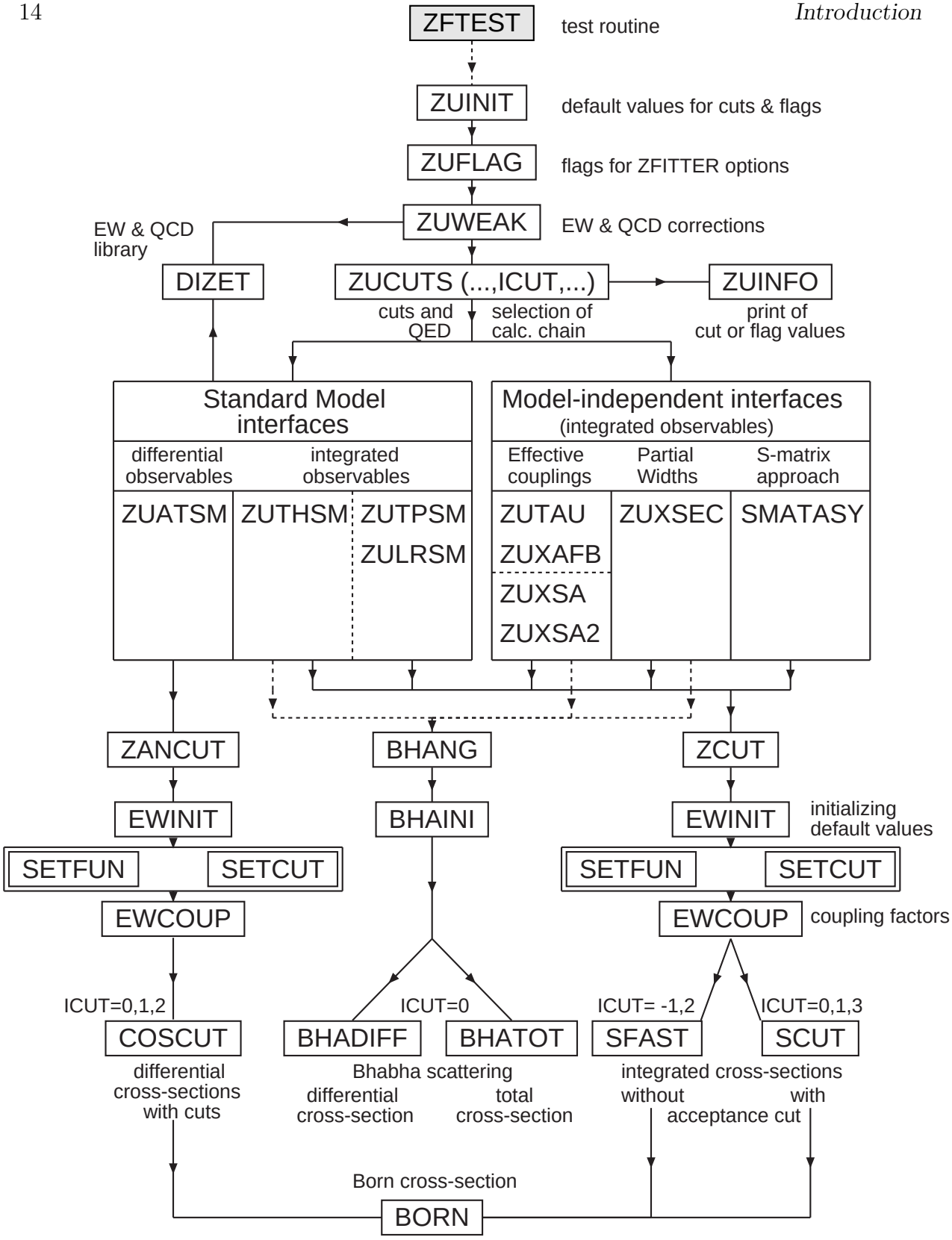

Figure I.2. *Logical structure of the package* ZFITTER

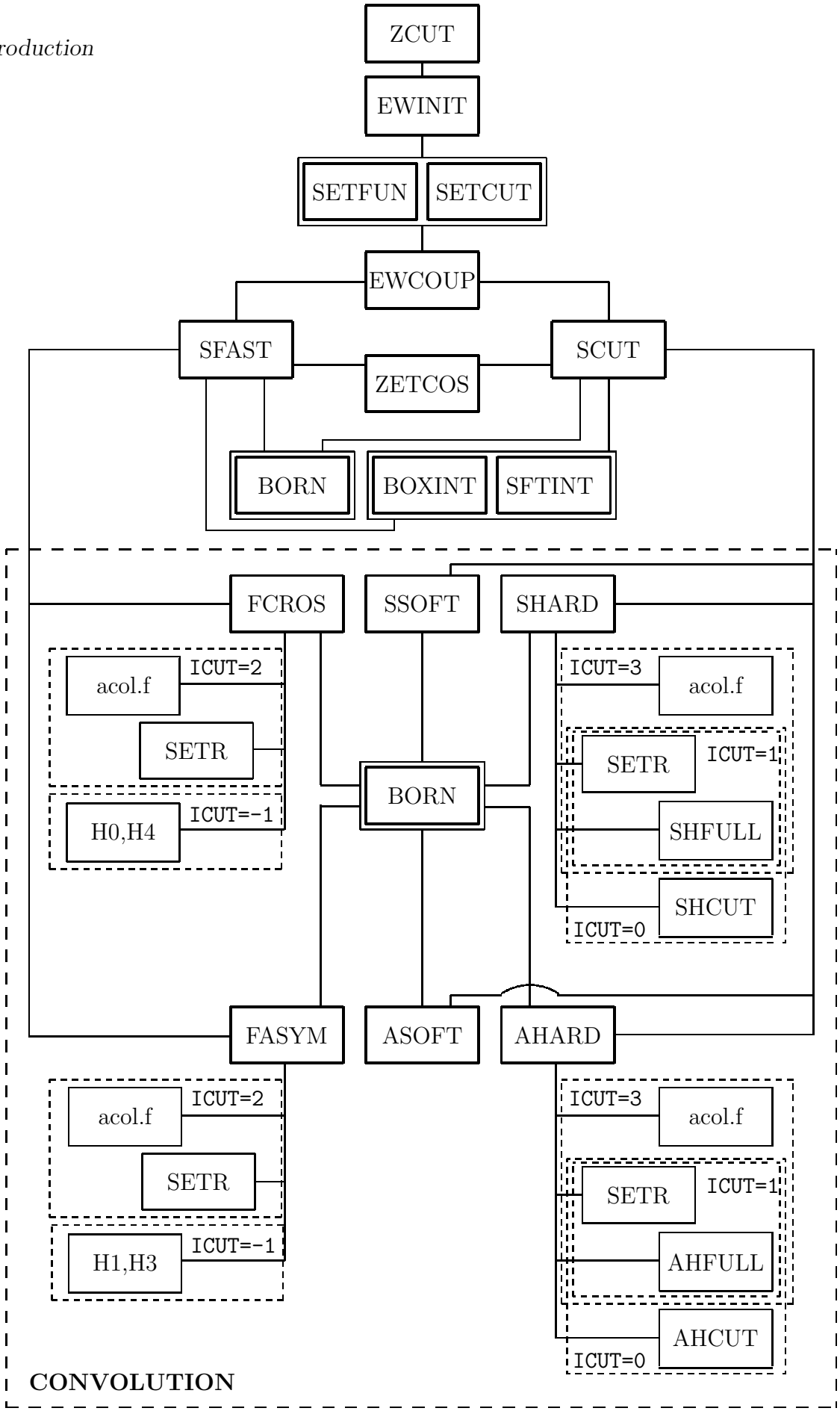

Figure I.3. Logical structure of subroutine `ZCUT`

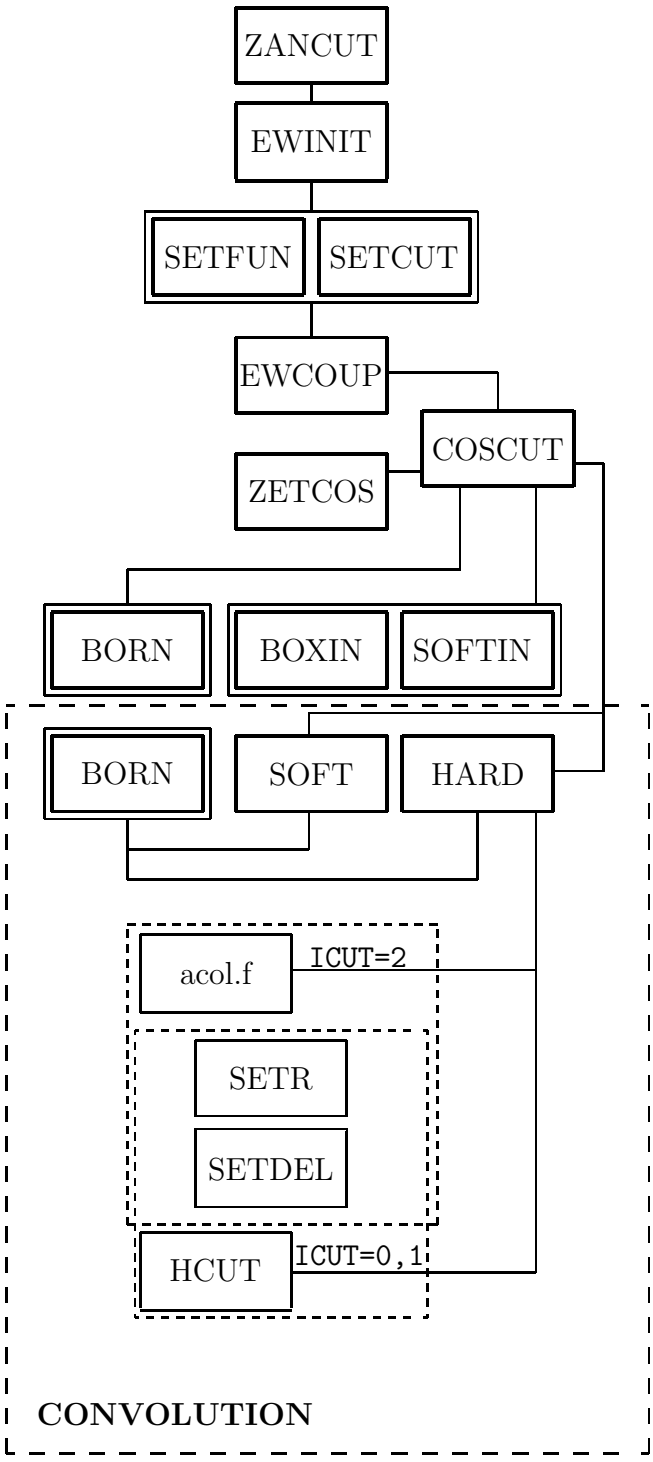

Figure I.4. Logical structure of subroutine `ZANCUT`

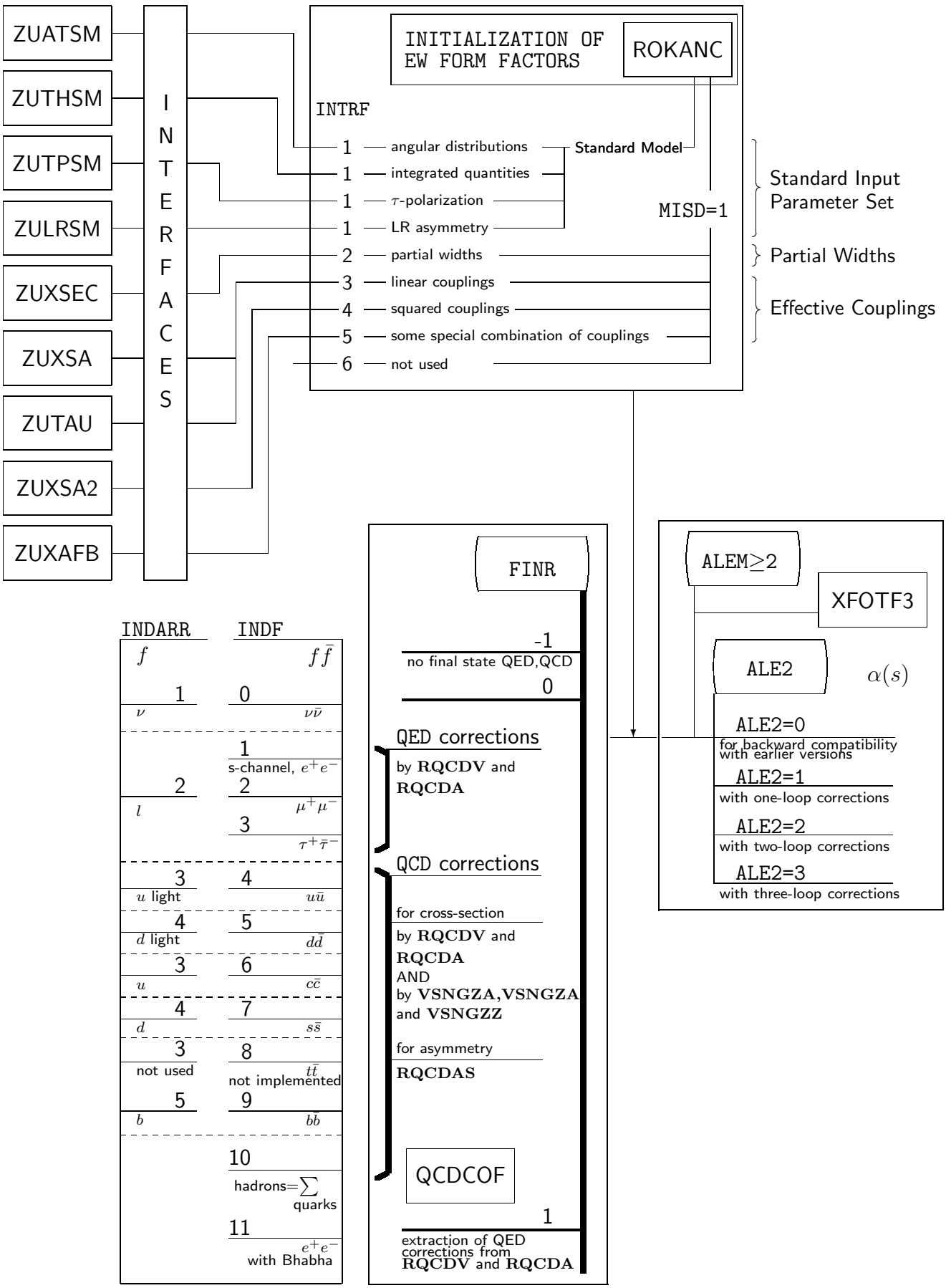

Figure I.5. *Preparations for the* ZFITTER *interfaces in subroutine* EWCOUP

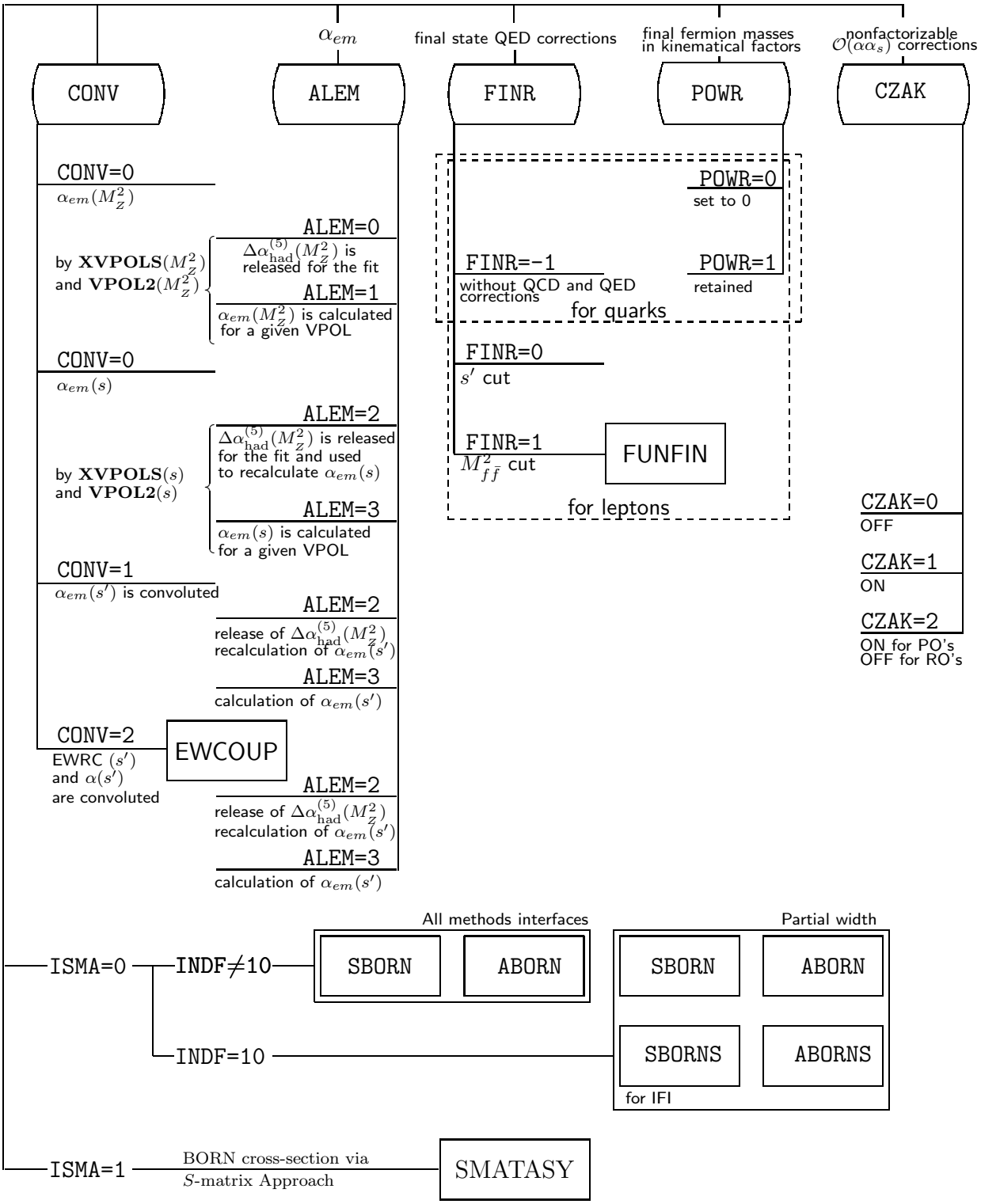

Figure I.6. *Logical structure of subroutine* BORN

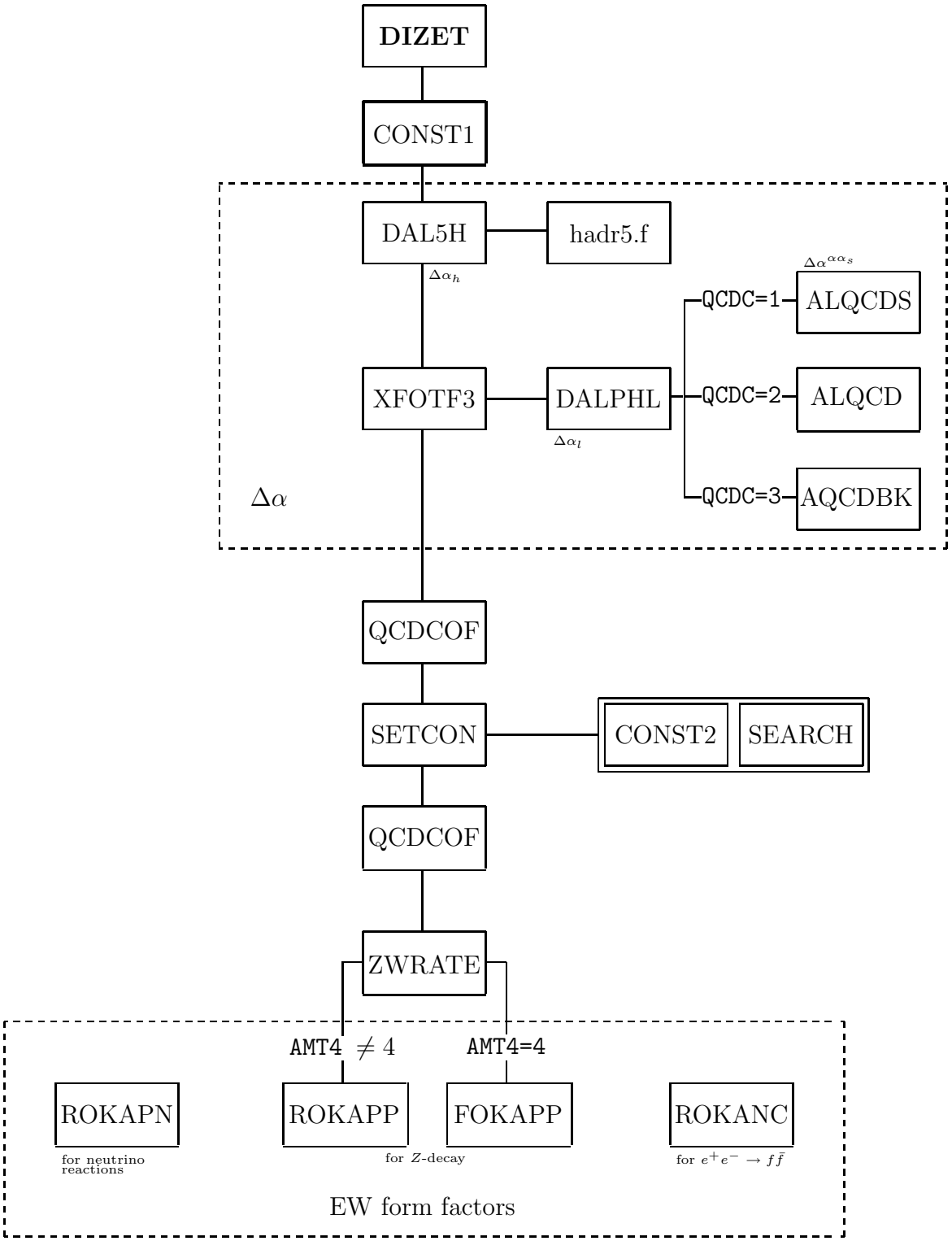

Figure I.7. *Logical structure of the package* DIZET

CHFLAG	IVALUE	CHFLAG	IVALUE	CHFLAG	IVALUE
AFBC	1	AFMT	1	ALEM	3
ALE2	3	AMT4	4	BARB	2
BORN	0	BOXD	1	CONV	1
CZAK	1	DIAG	1	EXPF	0
EXPR	0	FINR	1	FOT2	3
FSRS	1	FTJR	1	GAMS	1
GFER	2	HIGS	0	HIG2	0
INTF	1	ISPP	2	IPFC	5
IPSC	0	IPTO	3	MISC	0
MISD	1	PART	0	POWR	1
PREC	10	PRNT	0	QCDC	3
SCAL	0	SCRE	0	VPOL	1
WEAK	1				

Table I.1
Flag settings for ZFITTER*; the flags are listed in alphabetical order. The numerical values are the default settings*

Final-state fermions	$\nu\bar{\nu}$	e^+e^-	$\mu^+\mu^-$	$\tau^+\tau^-$	$u\bar{u}$	$d\bar{d}$	$c\bar{c}$	$s\bar{s}$	$t\bar{t}$	$b\bar{b}$	hadrons	Bhabha
INDF	0	1	2	3	4	5	6	7	8	9	10	11

Table I.2
Indices for the selection of final states. Note that INDF *= 0,1 returns only s-channel observables,* INDF *= 8 always returns zero, and* INDF *= 10 indicates a sum over all open quark channels.*

I	'FLAG'	name in programs	Position in NPAR(1:21) (DIZET)	Position in NPAR(1:30) (ZFITTER)	default
1	AFBC	IAFB		13	1
2	SCAL	ISCAL	9	15	0
3	SCRE	ISCRE	6		0
4	AMT4	IAMT4	2	16	4
5	BORN	IBORN		14	0
6	BOXD	IBOX		4	1
7	CONV				1
8	FINR	IFINAL		9	1
9	FOT2	IPHOT2		10	3
10	GAMS			5	1
11	DIAG			7	1
12	INTF	INTERF		8	1
13	BARB	IBARB	10		2
14	PART	IPART		17	0
15	POWR				1
16	PRNT				0
17	ALEM	IALEM	7	20	3
18	QCDC	IQCD	3	3	3
19	VPOL	IHVP	1	2	1
20	WEAK	IWEAK		1	1
21	FTJR	IFTJR	11		1
22	EXPR	IFACR	12		0
23	EXPF	IFACT	13	19	0
24	HIGS	IHIGS	14		0
25	AFMT	IAFMT	15		1
26	CZAK	ICZAK	17		1
27	PREC				10
28	HIG2	IHIG2	18		0
29	ALE2	IALE2	19	21	3
30	GFER	IGFER	20		2
31	ISPP	ISRPPR			1
32	FSRS				1
33	MISC	IMISC			0
34	MISD	IMISD			1
35	IPFC	IPFC			5
36	IPSC	IPSC			0
37	IPTO	IPTO			3
		IMOMS	4		1
		IMASS	5		0
		IMASK	8		0
		IEWLC	16		1
		IDDZZ	21		1

Table I.3

Flag settings for ZFITTER *and* DIZET*; the flags are listed in the order of vector* IFLAGS*. The corresponding names used internally in the programs, the position of the flags in vector* NPAR(1:21) *of* DIZET *and* NPAR(1:30) *of* ZFITTER *and the default values are given.*

Chapter 1

Photonic Corrections

1.1. Born Cross-Sections

Born cross-sections are calculated in ZFITTER for two purposes:

- If the user wants to calculate a Born cross-section;
- In order to be convoluted during the calculation of a QED corrected cross-section.

Born approximations are calculated with ZFITTER by choosing flag BORN=1 in subroutine ZUFLAG[1]. The fermion production channel is chosen with flag INDF. For a list of the fermion indices see Tab. I.2[2]. There are two different cases:

- Calculation of a differential cross-section $d\sigma^{\rm Born}/d\cos\vartheta$. This is foreseen within the Standard Model only and initiated by the user with the interface ZUATSM[3]. Subroutine ZANCUT is called, which calls subroutines EWCOUP and COSCUT. The latter calls subroutine BORN. The Born cross-section $d\sigma^{\rm Born}/d\cos\vartheta$ is calculated in subroutine COSCUT.
- Calculation of an integrated cross-section $\sigma_T^{\rm Born}$ (or angular asymmetry $A_{FB}^{\rm Born}$): This may be initialized by any of the other interfaces. For the Standard Model, e.g., subroutine ZUTHSM calls subroutine ZCUT, which calls subroutines EWCOUP and SFAST (without angular acceptance cut) or subroutines EWCOUP and SCUT (with angular acceptance cut). Then subroutine SFAST or subroutine SCUT calls subroutine BORN and calculates the integrated Born cross-section $\sigma_T^{\rm Born}$ and angular asymmetry $A_{FB}^{\rm Born}$.

In all cases it is subroutine EWCOUP (see Section 3.7) where the coupling constants of the cross-section are determined. Polarization effects are also taken into account there. Then, in subroutine BORN (see Section 3.8) the angular independent pieces of the Born cross-section are composed.

In this Section we will describe the Born formulae for the simplest case of photon and Z exchange with constant, real-valued vector and axial vector couplings. This corresponds

[1] The logical structure of ZFITTER is shown in Fig. I.2.
[2] A systematic presentation of the initialization of ZFITTER is given in Appendix 4.2.
[3] A systematic presentation of the interfaces of ZFITTER is given in Appendix 4.3.

e.g. to the tree level Standard Model (interfaces `ZUATSM` or `ZUTHSM`) or to a semi-model-independent ansatz (e.g. interface `ZUXSA`).

The differential Born cross-section `SIGBRN` is:

$$\frac{d\sigma^{\rm Born}}{d\cos\vartheta} = D_{\scriptscriptstyle T}(\cos\vartheta)\,\sigma^0_{\scriptscriptstyle T}(s) + \frac{4m_f^2}{s}\,D^m_{\scriptscriptstyle T}(\cos\vartheta)\,\sigma^{0,m}_{\scriptscriptstyle T}(s) + D_{\scriptscriptstyle FB}(\cos\vartheta)\,\sigma^0_{\scriptscriptstyle FB}(s), \tag{1.1.1}$$

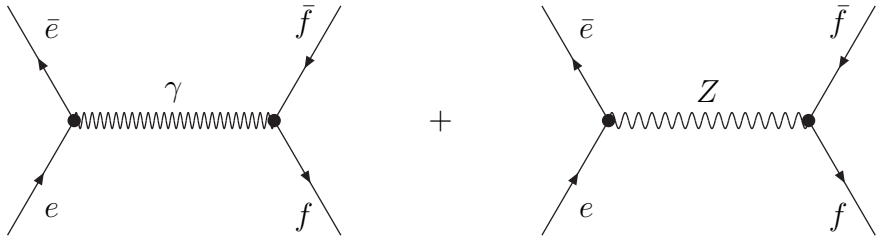

Figure 1.1. *Born approximation for* $e\bar{e} \to (Z,\gamma) \to f\bar{f}$

with

$$\sigma^0_{\scriptscriptstyle T}(s) = \frac{\pi\alpha^2}{s}\beta_f(s)\left[K_{\scriptscriptstyle T}(\gamma) + K_{\scriptscriptstyle T}(I)\,\Re e\chi_{\scriptscriptstyle Z}(s) + K_{\scriptscriptstyle T}(Z)\,|\chi_{\scriptscriptstyle Z}(s)|^2\right], \tag{1.1.2}$$

$$\sigma^{0,m}_{\scriptscriptstyle T}(s) = \frac{\pi\alpha^2}{s}\beta_f(s)\left[K^m_{\scriptscriptstyle T}(\gamma) + K^m_{\scriptscriptstyle T}(I)\,\Re e\chi_{\scriptscriptstyle Z}(s) + K^m_{\scriptscriptstyle T}(Z)\,|\chi_{\scriptscriptstyle Z}(s)|^2\right], \tag{1.1.3}$$

$$\sigma^0_{\scriptscriptstyle FB}(s) = \frac{\pi\alpha^2}{s}\beta_f(s)\left[K_{\scriptscriptstyle FB}(I)\Re e\chi_{\scriptscriptstyle Z}(s) + K_{\scriptscriptstyle FB}(Z)\,|\chi_{\scriptscriptstyle Z}(s)|^2\right], \tag{1.1.4}$$

and

$$D_{\scriptscriptstyle T}(\cos\vartheta) = \frac{1}{2}\left(1+\cos^2\vartheta\right), \tag{1.1.5}$$

$$D^m_{\scriptscriptstyle T}(\cos\vartheta) = \frac{1}{2}\sin^2\vartheta, \tag{1.1.6}$$

$$D_{\scriptscriptstyle FB}(\cos\vartheta) = \cos\vartheta, \tag{1.1.7}$$

$$\beta_f(s) = \sqrt{1-\frac{4m_f^2}{s}}\,. \tag{1.1.8}$$

For hadrons, we sum over u, d, c, s, b quarks (above their production thresholds). Masses of quarks are usually treated together with QCD corrections, see Section 3.6. Some deviating choice of inclusion of final state masses is possible for hadronic final states with flags `FINR`=-1 and `POWR`, see Appendix 4.2.2.

The Z propagator is contained in the factor:

$$\chi_Z(s) = \frac{G_\mu}{\sqrt{2}}\frac{M_Z^2}{8\pi\alpha}\frac{s}{s-m_Z^2}, \tag{1.1.9}$$

$$m_Z^2 = M_Z^2 - iM_Z\Gamma_Z(s). \tag{1.1.10}$$

An s independent width may be taken into account with the transformation of constants as introduced in [42]. This is realized in ZFITTER as described in Section 3.2. For the calculation of Γ_Z in the Standard Model we refer to Section 2.4. We also define accordingly for the photon propagator:

$$\chi_\gamma(s) = 1, \tag{1.1.11}$$

and use the following conventions:

$$|Q_e| = 1, \tag{1.1.12}$$
$$a_f = 1, \tag{1.1.13}$$
$$v_f = 1 - 4|Q_f|s_W^2. \tag{1.1.14}$$

Further, the coupling functions are:

$$K_T(\gamma) = K_T^m(\gamma) = Q_e^2Q_f^2c_f, \tag{1.1.15}$$

$$K_{FB}(\gamma) = 0, \tag{1.1.16}$$

$$K_T(I) = K_T^m(I) = 2|Q_eQ_f|v_ev_fc_f, \tag{1.1.17}$$

$$K_{FB}(I) = 2|Q_eQ_f|a_ea_f\beta_fc_f, \tag{1.1.18}$$

$$K_T(Z) = (v_e^2+a_e^2)(v_f^2+a_f^2\beta_f^2)c_f, \tag{1.1.19}$$

$$K_{FB}(Z) = 4v_ea_ev_fa_f\beta_fc_f, \tag{1.1.20}$$

$$K_T^m(Z) = (v_e^2+a_e^2)v_f^2c_f, \tag{1.1.21}$$

$$\bar{K}_T^m(Z) = (v_e^2+a_e^2)a_f^2c_f, \tag{1.1.22}$$

where c_f is the color factor 1(3) for leptons (quarks). We added the definition of $\bar{K}_T^m(Z)$ for later use.

Later on, in Chapter 2 and 3 the corrections from weak loop insertions, from the running QED coupling and, for quark production, from QCD will be absorbed in the couplings K_A and in the prediction for the Z width[4]. In model independent approaches, the K_A will be, together with M_Z and Γ_Z, the parameters to be determined; see Section 3.7.

[4]Note however that corrections from ZZ and WW box diagrams have a complicated angular dependence; see Subsection 3.3.2.

The most general expressions for four different polarizations of the fermions are given explicitely in Section 3.7.1. Weak higher order corrections influence also exclusively the combinations K_{A}.

QED corrections depend only on $M_Z, \Gamma_Z, \cos\vartheta, s$ and, due to mass singularities, on fermion masses. The explicit expressions for the QED corrections will contain *effective* Born cross-section factors with a reduced invariant mass s':

$$\sigma^0_{A}(s') = \sum_{m,n=\gamma,Z} \sigma^0_{A}(s',s';m,n), \tag{1.1.23}$$

$$\sigma^0_{A}(s,s') = \sum_{m,n=\gamma,Z} \sigma^0_{A}(s,s';m,n), \tag{1.1.24}$$

$$\sigma^0_{A}(s,s';m,n) = \frac{\pi\alpha^2}{s'} K_{A}(m,n) \frac{1}{2} \left[\chi_m(s)\chi^*_n(s') + \chi_m(s')\chi^*_n(s)\right], \quad A = T, FB. \tag{1.1.25}$$

The $K_{A}(m,n)$ are those defined in Eqs. (1.1.15)–(1.1.22). Further, we use the correspondences $(\gamma\gamma, \gamma Z + Z\gamma, ZZ) \sim (\gamma, I, Z)$. The functions $\sigma^0_{A}(s,s')$ are needed when we treat the interference of initial state radiation (with scale s') and final state radiation (with scale s).

After angular integration, the total Born cross-section $\texttt{SBORN} = \sigma^{\rm Born}_{T}(s,c)$ and forward-backward asymmetry $\texttt{ABORN} = A^{\rm Born}_{FB}(s,c)$ become:

$$\sigma^{\rm Born}_{T}(s,c) = C_{T}(c)\,\sigma^0_{T}(s) + \frac{4m_f^2}{s}\,C^m_{T}(c)\,\sigma^{0,m}_{T}(s), \tag{1.1.26}$$

$$A^{\rm Born}_{FB}(s,c) = \frac{\sigma^{\rm Born}_{FB}(s,c)}{\sigma^{\rm Born}_{T}(s,c)}, \tag{1.1.27}$$

$$\sigma^{\rm Born}_{FB}(s,c) = C_{FB}(c)\,\sigma^0_{FB}(s). \tag{1.1.28}$$

Here, we allow for an angular acceptance cut,

$$C_{T}(c) = \int_{-c}^{c} d\cos\vartheta\, D_{T}(\cos\vartheta) = c\left(1 + \frac{c^2}{3}\right), \tag{1.1.29}$$

$$C^m_{T}(c) = \int_{-c}^{c} d\cos\vartheta\, D^m_{T}(\cos\vartheta) = c\left(1 - \frac{c^2}{3}\right), \tag{1.1.30}$$

$$C_{FB}(c) = \left\{\int_0^c - \int_{-c}^0\right\} d\cos\vartheta\, D_{FB}(\cos\vartheta) = c^2. \tag{1.1.31}$$

The usual normalization factors $C_{T}(1) = 4/3, C_{FB} = 1$ are obtained if the full scattering region is explored. In the program, we often use the abbreviations $\texttt{COPL3} = c + c^3/3$ and $\texttt{COPL2} = 1 + c^2$.

Finally we should mention that mass effects in the improved Born cross-sections of ZFITTER are contained in only three factors:

$$\texttt{THRESH} = \beta_f(s), \tag{1.1.32}$$

$$\texttt{CORF2} \;=\; c_1(m_f) = 1 + 2\frac{m_f^2}{s}, \tag{1.1.33}$$

$$\texttt{CORF3} \;=\; c_2(m_f) = -6\frac{m_f^2}{s}. \tag{1.1.34}$$

Further, there are mass dependent QCD corrections, see Subsection 3.6.2.

The mass factors Eqs. (1.1.32)–(1.1.34) are valid for integrated cross-sections without cuts. For differental cross-sections and for those with cuts applied, they have to be considered as approximations. This seems to be no numerical problem for final state fermions foreseen in ZFITTER. We just remind that ZFITTER does not yet cover t-quark production.

1.2. Photonic Corrections. Overview

The branches with different treatments of photonic cuts are chosen with flag ICUT in subroutine ZUINIT when calling subroutine ZUCUTS: the values $-1, +1, +2, +3$ correspond to the application of: no cuts but an s' cut, the s' cut plus acceptance cut, the acollinearity cut without/with acceptance cut. In the case of the angular distribution $d\sigma/d\cos\vartheta$, the flag values are reduced to $+1, +2, +3$ where ICUT $= +1$ means an s' cut, and ICUT $= +2$ (and for checking purposes equivalently $+3$) treats an acollinearity cut.

The numerical values of the cut variables are set by the user when calling subroutine ZUCUTS, see Appendix 4.2.4. Real photonic corrections are influenced by the following additional flags: INTF, FINR, FOT2.

In this Section, we will describe real photonic corrections to $d\sigma/d\cos\vartheta$, $\sigma_{_T}(c)$ and $\sigma_{_{FB}}(c)$. A complete treatment of photonic corrections also includes the running of the electromagnetic coupling constant. This will be discussed in Section 3.8. For the calculation of reaction Eq. (I.1) to order $\mathcal{O}(\alpha)$, the cross-sections σ are split into contributions from initial state radiation, σ^{ini}, final state radiation, σ^{fin}, and their interference, σ^{int}. In order to get a finite, gauge invariant result, real photon bremsstrahlung from the diagrams of Fig. 1.2 is combined with photonic vertex corrections of Fig. 1.3 for initial or final state radiation, and with the box diagram corrections of Fig. 1.4 for their interference.

In ZFITTER, initial and final state corrections may be combined in different ways thus reaching different numerical accuracy. The simplest choice, with flag FINR=0, is to take final state corrections into account by a numerical factor ($A = T, FB$):

$$\sigma_{_A} \;=\; \sigma_{_A}^{ini}\left(1 + \delta_{_A}^{fin}\right) + \sigma_{_A}^{int}, \tag{1.2.1}$$

$$\delta_{_T}^{fin} \;=\; \frac{3}{4}\frac{\alpha}{\pi}Q_f^2, \tag{1.2.2}$$

$$\delta_{_{FB}}^{fin} \;=\; 0. \tag{1.2.3}$$

The factor $\delta_{_A}^{fin}$ has been given here for the massless case without cuts. The contribution σ^{int} comes from initial-final state interferences and may be switched on or off with flag INTF. The calculation of complete $\mathcal{O}(\alpha)$ corrections, $\sigma = \sigma^{ini} + \sigma^{fin} + \sigma^{int}$, is not foreseen in ZFITTER since initial state radiation contains necessarily soft photon exponentiation. The default approach to photonic bremsstrahlung for leptons is a *common* soft photon exponentiation for initial and final state radiation (with flag NPAR(9) = FINR=1):

$$\sigma = \sigma^{ini+fin} + \sigma^{int}. \tag{1.2.4}$$

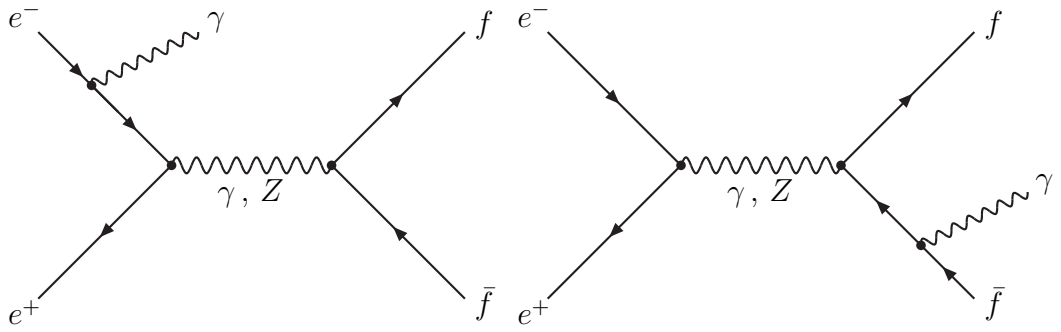

Figure 1.2. *Examples for real photon emission*

In such an approach higher order non-factorizing QCD and QED corrections can be treated only approximately, since they are known only for an inclusive setup.

An alternative, of some practical importance for the production of b quark pairs e.g., is the common treatment of final state QED and QCD corrections with account of running mass effects. For this case, higher order results are available and replace successfully the exponentiation of final state soft photonic corrections. For details see Section 3.6.

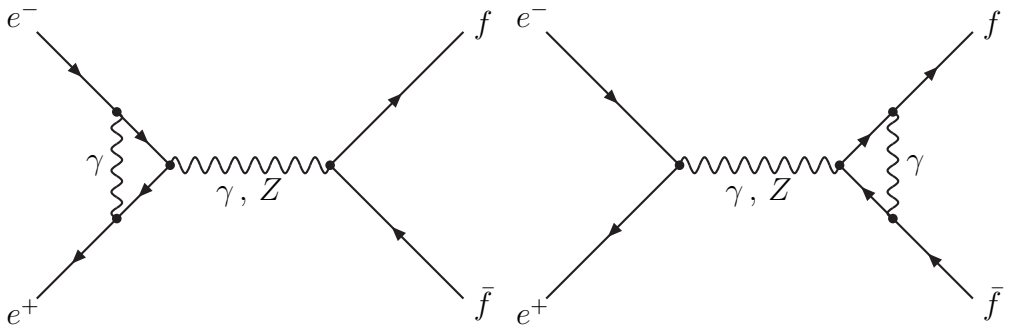

Figure 1.3. *The photonic vertex corrections*

In the other cases, the recommended cross-section is Eq. (1.2.4) and we give here the generic formula as an instructive example:

$$\sigma_{_T}(c) \;=\; \int_0^{1-4m_f^2/s} dv \left[\sigma^0_{_T}(s')\, R^{ini+fin}_{_T}(v,c) + \sum_{m,n=\gamma,Z} \sigma^0_{_{FB}}(s,s',m,n) R^{int}_{_T}(v,c,m,n)\right]. \tag{1.2.5}$$

In Eq. (1.2.5), we assume for definiteness no cuts on the final state. The variable c is to be understood as either $\cos\vartheta$ (then σ_T is the differential cross-section part, symmetric in the scattering angle) or as the integration limit for the cut angular integration (for $c = 1$, σ_T is the total cross-section). When replacing index T by FB, Eq. (1.2.5) expresses a forward-backward anti-symmetric combination.

The photonic corrections consist of Born-like virtual+soft parts S, photonic box parts B, and hard parts H:

$$\begin{aligned}\sigma_T(c) &= \int_0^{1-4m_f^2/s} dv \left\{ \left[\sigma_T^{Born}(s',c)\left(1+\bar{S}^{ini}\right)\beta_e v^{\beta_e-1} + \sigma_T^0(s')\bar{H}_T^{ini}(v,c)\right]\bar{R}_T^{fin}(v) \right. \\ &\quad \left. + \sigma_{FB}^0(s,s')\left[H_T^{int}(v,c) - \frac{\sigma_{FB}^0(s)}{\sigma_{FB}^0(s,s')}H_T^{int,sing}(v,c)\right]\right\} \\ &\quad + \sigma_{FB}^0(s,c)\bar{S}_T^{int} + \sum_{m,n=\gamma,Z}\sigma_{FB}^0(s,s,m,n)B_T(c,m,n). \end{aligned} \tag{1.2.6}$$

Here, the $\sigma_T^{Born}(s,c), \sigma_T^0(s)$ etc. are generic expressions denoting either effective Born angular distributions or integrated effective Born cross-sections. They are defined in Section 1.1, Section 3.7, and Section 3.8. The other expressions will be explained in the next Sections.

Technically, the integration is performed as a numerical integration over variable R:

$$R = \frac{s'}{s} = 1 - v, \tag{1.2.7}$$

and the variable v was defined in Eq. (I.13). The expression to be calculated with `ZFITTER` is (see also Eq. (1.2.15) below):

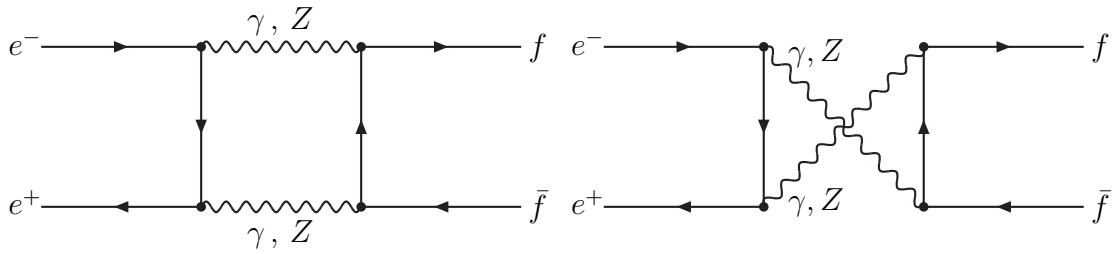

Figure 1.4. *The $\gamma\gamma$ and γZ box diagrams*

$$\sigma_T(c) = \int_{4m_f^2/s}^1 dR \left[\beta_e(1-R)^{\beta_e-1}\right]\mathcal{R}(R,c)$$

$$+ \sigma^0_{FB}(s,c)\bar{S}^{int}_T + \sum_{m,n=\gamma,Z} \sigma^0_{FB}(s,s,m,n)B_T(c,m,n), \tag{1.2.8}$$

with

$$\mathcal{R}(R,c) = \left[\sigma^{Born}_T(s',c)\left(1+\bar{S}^{ini}\right) + \sigma^0_T(s')\,\bar{H}^{ini}_T(v,c)\,\mathcal{Y}\right]\bar{R}^{fin}_T(v)$$
$$+ \sigma^0_{FB}(s,s')\left[H^{int}_T(v,c) - \frac{\sigma^0_{FB}(s)}{\sigma^0_{FB}(s,s')}H^{int,sing}_T(v,c)\right]\mathcal{Y}, \tag{1.2.9}$$

and

$$\mathcal{Y} = \left[\beta_e(1-R)^{\beta_e-1}\right]^{-1}. \tag{1.2.10}$$

The integrand is smoothened with the following variable transformation (mapping), using functions `FACT(R)` $= F$ and `FACINV(F)` $= R$:

$$dF = \beta_e(1-R)^{\beta_e-1}\,dR, \tag{1.2.11}$$

$$F = -(1-R)^{\beta_e}, \tag{1.2.12}$$

$$R = 1-(-F)^{1/\beta_e}. \tag{1.2.13}$$

Further, at $R \to 1$ the function $\mathcal{R}$ is smooth:

$$\mathcal{R}(1,c) = \sigma^{Born}_T(s,c)\left(1+\bar{S}^{ini}\right)\bar{R}^{fin}_T(0). \tag{1.2.14}$$

This allows to perform the integral explicitly in the neighborhood of that limit. In subroutine `SFAST`, the following expression is calculated numerically:

$$\sigma_T(c) = \mathcal{R}(1,c)\,\epsilon_s^{\beta_e} - \int_{F(1-\epsilon_s)}^{F(4m_f^2/s)} dF\,\mathcal{R}\left(1-(-F)^{1/\beta_e},c\right)$$
$$+ \sigma^0_{FB}(s,c)\bar{S}^{int}_T + \sum_{m,n=\gamma,Z} \sigma^0_{FB}(s,s,m,n)B_T(c,m,n), \tag{1.2.15}$$

with typically $\epsilon_s = 10^{-12}$. The integration is done this way with subroutine `FDSIMP` for the integrated QED corrections without cuts.

Subroutine `FDSIMP` has, among others, the arguments `FUNCT, DFUN, DFUNIN`. They denote the integrand function and functions `FACT, FACINV` in `ZFITTER`.

Alternatively, one may split the integrand into two pieces; a soft one with the soft photon factor, and the hard rest. This is done in subroutines `COSCUT` and `SCUT`. It suffices to map the soft part and to directly integrate the rest (hard corrections)[5]:

$$\sigma_T(c) = \mathcal{R}(1,c)\,\epsilon_s^{\beta_e} - \int_{F(1-\epsilon_s)}^{F(R_{min})} dF\,\mathcal{R}^{soft}\left(1-(-F)^{1/\beta_e},c\right)$$

[5]The choice of an s' cut (`ICUT`=1) or cuts on acollinearity and fermion energy (`ICUT`=2,3) is of no influence for the presentation here. The decision between these two sets of cuts leads only to different expressions for the hard corrections H.

$$+\int_{R_{min}}^{1-\epsilon_h} dR \left\{ \sigma_T^0(s')\bar{H}_T^{ini}(v,c)\bar{R}_T^{fin}(v) \right.$$
$$\left. + \sigma_{FB}^0(s,s') \left[H_T^{int}(v,c) - \frac{\sigma_{FB}^0(s)}{\sigma_{FB}^0(s,s')} H_T^{int,sing}(v,c) \right] \right\}$$
$$+ \sigma_{FB}^0(s,c)\bar{S}_T^{int} + \sum_{m,n=\gamma,Z} \sigma_{FB}^0(s,s,m,n) B_T(c,m,n), \tag{1.2.16}$$

with

$$\mathcal{R}^{soft}(R,c) = \sigma_T^{Born}(s',c)\left(1+\bar{S}^{ini}\right)\bar{R}_T^{fin}(v). \tag{1.2.17}$$

Further, it is typically $\epsilon_h = 10^{-5}$ and the second, direct integration over dR in Eq. (1.2.16) is done with subroutine `SIMPS` [23].

From the above it is seen that `ZFITTER` performs *one-fold numerical integrations* for the contributions introduced in Eqs. (1.2.1)–(1.2.6):

$$\frac{d\sigma_A^{ini}}{d\cos\vartheta} = \int_\Omega dv\, \sigma_A^0(s')\, R_A^{ini}(v,\cos\vartheta), \tag{1.2.18}$$

$$\frac{d\sigma_A^{ini+fin}}{d\cos\vartheta} = \int_\Omega dv\, \sigma_A^0(s') R_A^{ini}(v,\cos\vartheta)\, \bar{R}_A^{fin}(v), \tag{1.2.19}$$

$$\frac{d\sigma_A^{int}}{d\cos\vartheta} = \int_\Omega dv \sum_{m,n} \sigma_{\bar{A}}^0(s,s';m,n)\, R_A^{int}(v,\cos\vartheta;m,n), \tag{1.2.20}$$

$$\sigma_A^{ini}(c) = \int_\Omega dv\, \sigma_A^0(s')\, R_A^{ini}(v,c), \tag{1.2.21}$$

$$\sigma_A^{ini+fin}(c) = \int_\Omega dv\, \sigma_A^0(s')\, R_A^{ini}(v,c)\, \bar{R}_A^{fin}(v), \tag{1.2.22}$$

$$\sigma_A^{int}(c) = \int_\Omega dv \sum_{m,n} \sigma_{\bar{A}}^0(s,s';m,n)\, R_A^{int}(v,c;m,n), \tag{1.2.23}$$

where $A = T, FB$, $\bar{A} = FB, T$, and $m,n = \gamma, Z$. The initial-final state interference contributions from γ and Z exchange and from their interference have to be separated. This is unavoidable since the $\gamma\gamma$ and γZ boxes differ. We further would like to stress that for the initial-final state interferences the C even and the C odd properties of the basic cross-section (see the couplings' labels) are opposite to those of Born terms or of initial or final state radiation.

The integral over s', or, equivalently, over R, has to be performed numerically since soft photon exponentiation makes a complicated integrand. The radiator functions $R_A^a(v,\cos\vartheta)$ and $R_A^a(v,c)$, $A = T, FB$, are obtained from two-fold and three-fold analytic phase space integration, respectively:

$$R_A^a(v,\cos\vartheta[,m,n]) = \int dv_2 \int d\phi_\gamma \left|\chi_A^a(s,v,v_2,\cos\vartheta,\phi_\gamma)\right|^2, \tag{1.2.24}$$

$$R_A^a(v,c[,m,n]) = \int_{-c}^{c} d\cos\vartheta \int dv_2 \int d\phi_\gamma \left|\chi_A^a(s,v,v_2,\cos\vartheta,\phi_\gamma)\right|^2, \tag{1.2.25}$$

where the squared matrix elements $|\chi_A^a|^2$ are the result of a Feynman diagram calculation. Further, $s' = M_{ff}^2$, $v_2 = M_{f\gamma}^2/s$, and ϕ_γ is one of the photon angles in the (γ, f) rest system. More details on the definition of the phase space parameterization used are given in Section 1.5.

The s' integration region is indicated by the symbol Ω. Several different cases have been prepared in ZFITTER:

- Born cross-sections (flag BORN=1); option is described in Section 1.1 and Section 3.8;
- no cut but a simple cut on s' (flag ICUT=–1); option is available for $\sigma_{T,FB}$ [15] and is described in Section 1.3;
- cut on s' for $d\sigma/d\cos\vartheta$ [9] and on s' and $\cos\vartheta$ for $\sigma_{T,FB}$ [10] (flag ICUT=1); option is described in Section 1.4;
- cut on s' in the course of numerical integration, combined with cuts on v_2 applied in the analytical integration (flag ICUT=2,3); their combination creates combined cuts on acollinearity and minimal energy of the fermions [11,43]; for the s' integration this means in effect that in different s' regions different analytical expressions are integrand; option is described in Section 1.5.

The angular acceptance cut, $c_1 \leq \cos\vartheta \leq c_2$, limits the scattering angle ϑ of the final-state *anti*fermions (see Fig. I.1). The scattering angle of *fermions* remains unrestricted if the other cut(s) do not imply an implicit restriction (see Section 1.5). In ZFITTER, the QED contributions include the complete $\mathcal{O}(\alpha)$ corrections, plus soft photon exponentiation, plus selected higher order photonic corrections (chosen with flag FOT2). As a matter of fact, we mention that the radiator functions (flux functions), R_A^a, *differ* for different observables (i.e. different index A) and for different bremsstrahlung types ($a = ini, fin, int$). Only close around the Z resonance where hard photon emission is suppressed and for loose cuts some of the radiator functions agree approximately [44,15].

Finally we mention that it is foreseen in ZFITTER to calculate the following contributions:

$$\frac{d\sigma_A^{fin}}{d\cos\vartheta} = \sigma_A^0(s)\int_\Omega dv R_A^{fin}(v,\cos\vartheta), \tag{1.2.26}$$

$$\sigma_A^{fin}(c) = \sigma_A^0(s)\int_\Omega dv\, R_A^{fin}(v), \tag{1.2.27}$$

i.e. *singly deconvoluted* observables — with FSR but without ISR corrections. This is achieved by setting FOT2=-1.

1.3. Photonic Corrections with s' Cut

The calculational chain with s' cut is chosen when calling subroutine ZUCUTS with flag ICUT=–1. (The internal flag IFAST is set equal to 1.) The treatment of photonic $\mathcal{O}(\alpha)$ corrections is based on [15]. Higher order QED corrections depend on the flaggs FOT2 and ISPP For references for this, see Section 4.2.2.

In this calculational chain, the cross-sections σ_T and σ_{FB} are calculated with formulae that assume *no angular cuts* being applied to the final state phase space. It is computationally fast. The integrations are performed with subroutine `FDSIMP` as described in Eq. (1.2.15) and Eqs. (1.2.9)–(1.2.14).

In the notations introduced, the phase space is bounded by the values:

$$c = 1, \tag{1.3.1}$$

$$E_\gamma^{\max} = \frac{\sqrt{s}}{2}\Delta. \tag{1.3.2}$$

Equivalently to Eq. (1.3.2),

$$\Delta \leq 1 - \frac{4m_f^2}{s}, \tag{1.3.3}$$

$$s'^{\min} = 4m_f^2. \tag{1.3.4}$$

Thus, the radiative corrections may depend on fermion masses even for light quarks and leptons. For their choice, see Section 2.2.1. This dependence can be important when total cross-sections are determined from experimental data, and *is* often of special importance when comparing results from other programs.

`ZFITTER` returns the cross-section Eq. (1.2.1) with QED corrections (`SIGQED`, asymmetry `AFBQED`) and without (`SIGBRN, AFBBRN`) from subroutine `ZCUT`. Technicalities of the calculation are described in Section 1.2. Subroutines `FCROS` and `FASYM` are used for the calculation of the symmetric and anti-symmetric cross-sections, respectively.

1.3.1. Initial state corrections with soft photon exponentiation and higher order corrections

Cross-sections with initial state QED corrections as introduced in Eq. (1.2.21) are understood to include soft photon exponentiation plus, optionally, further higher order corrections and are calculated as follows [15]:

$$\sigma_A^{\rm ini}(1) = \int_0^\Delta dv\, \sigma_A^0(s')\, R_A^{\rm ini}(v,1), \tag{1.3.5}$$

$$R_A^{\rm ini}(v,1) = C_A(1)\left[\left(1+\bar{S}^{ini}\right)\beta_e v^{\beta_e-1} + \bar{H}_A^{ini}(v,1)\right], \qquad A = T, FB, \tag{1.3.6}$$

with

$$\beta_e = \frac{2\alpha}{\pi}Q_e^2\left(L_e - 1\right), \tag{1.3.7}$$

$$L_e = \ln\frac{s}{m_e^2}. \tag{1.3.8}$$

The soft plus virtual corrections $\bar{S}^{ini}$ = `SOFTER` are calculated according to Eq. (50) of [9] in subroutine `SETFUN` in the course of initialization of `ZFITTER`:

$$\bar{S}^{ini} = \frac{\alpha}{\pi}Q_e^2\left[\frac{3}{2}\left(L_e - 1\right) + \frac{\pi^2}{3} - \frac{1}{2}\right] + S^{(2)} + S^{pairs}. \tag{1.3.9}$$

The higher order virtual and soft photonic corrections, $S^{(2,3)}$, and pair production corrections, S^{pairs}, are described in Section 1.6.1. They are calculated depending on flag `FOT2` and `ISPP` The hard photon corrections $\bar{H}_T^{ini}$ = `H0` in subroutine `FCROS` and $\bar{H}_{FB}^{ini}$ = `H3` in subroutine `FASYM` are, respectively:

$$\bar{H}_T^{ini}(v,1) = \frac{\alpha}{\pi}Q_e^2(L_e-1)\left[\frac{1+(1-v)^2}{v}\right] - \frac{\beta_e}{v} + H_T^{(2)}(v), \tag{1.3.10}$$

$$\bar{H}_{FB}^{ini}(v,1) = \frac{\alpha}{\pi}Q_e^2\left[(L_e-1) - \ln\frac{1-v}{(1-\frac{1}{2}v)^2}\right]\left[\frac{1+(1-v)^2}{v}\frac{1-v}{(1-\frac{1}{2}v)^2}\right] - \frac{\beta_e}{v} + H_{FB}^{(2)}(v). \tag{1.3.11}$$

The higher order corrections $H_T^{(2,3)}$ and $H_{FB}^{(2,3)}$ also depend on flaggs `FOT2` and `ISPP` and are described in Section 1.6.2.

1.3.2. Final state radiation

The final state photonic corrections are calculated in dependence on flag `IFINAL` = `FINR`. All options of flag `FINR` are possible.

Details may be found in Section 1.4.2.

1.3.3. Initial-final state interference corrections

The QED corrections from the interference of initial and final state radiation are taken into account for flag setting `INTF`=1. Combined with the interference of the $\gamma\gamma$ and γZ box diagrams with the Born matrix element, they give the following cross-section contributions:

$$\sigma_A^{\rm int}(1) = \int_0^\Delta dv \sum_{m,n}\sigma_{\bar{A}}^0(s,s';m,n)R_A^{\rm int}(v,1;m,n), \tag{1.3.12}$$

with

$$R_A^{int}(v,1,m,n) = \delta(v)\left[\bar{S}_A^{int}(1) + B_A(1,m,n)\right] + \bar{H}_A^{int}(v,1). \tag{1.3.13}$$

We use $\sigma_A^0(s,s';m,n)$ from Eq. (1.1.25), $\bar{S}_A^{int}(c)$ from Eq. (1.4.75) and Eq. (1.4.76), $B_A(c,m,n)$ from Eq. (1.4.77). When $A=T$, it is $\bar{A}=FB$ and vice versa.

In `ZFITTER`, the soft photon corrections `SFTIS, SFTIA` from subroutine `SFTINT` as well as the photonic box corrections `BOXIS, BOXIA` from subroutine `BOXINT` for integrated cross-sections are called in subroutine `SFAST` and calculated as functions of c taken by fixing there $c=1$. So, for details we may refer to Section 10. The hard correction to the total cross-section is calculated in the combination $(\sigma_{FB}^0\bar{H}_T^{int}) \sim$ `(H4*ABORN+8/v*ABORN0)` and is added in subroutine `SFAST` after an integration over the function `FCROS`. Analogously, $(\sigma_T^0\bar{H}_{FB}^{int}) \sim$ `[H1*SBORN+4*(8*AL2+1)/(3v)*SBORN0]` results from the integration over the function `FASYM` and contributes to the forward-backward asymmetry.

The $H_T^{int}(v,1) \sim$ `H4` is given in Eq. (29) and $H_{FB}^{int}(v,1) \sim$ `H1` in Eq. (22) of [9]. From these functions, the barred ones are derived:

$$\sigma_{FB}^0(s,s')\bar{H}_T^{int}(v,1) = \frac{\alpha}{\pi}Q_eQ_f\left[\frac{3}{v}(1-v)(v-2)\sigma_{FB}^0(s,s') + \frac{6}{v}\sigma_{FB}^0(s)\right], \tag{1.3.14}$$

$$\begin{aligned}\sigma_T^0(s,s')\bar{H}_{FB}^{int}(v,1) &= \frac{\alpha}{\pi}Q_eQ_f\Bigg\{\frac{2}{3v}\Bigg[2\frac{1-v}{2-v}\left(v^2+2v-2\right)\\ &+ (1-v)\left(5v^2-10v+8\right)\ln(1-v)\\ &- \left(5v^2-2v+8\right)(2-v)\ln(2-v)\Bigg]\sigma_T^0(s,s')\\ &+ \frac{4}{3v}\left(8\ln 2+1\right)\sigma_T^0(s)\Bigg\}. \qquad (1.3.15)\end{aligned}$$

These functions are constructed such that they are finite at $v \to 0$. The subtracted pieces were integrated analytically and combined with the soft photon corrections. This makes the soft corrections (artificially) dependent on integration boundaries (if any) but cancels the dependence on the infrared cut-off.

1.4. Photonic Corrections with Cuts on s' and $\cos\vartheta$

Cross-sections with s' cut and cut on the acceptance angle are chosen by flag `ICUT`=1.

The calculation of differential cross-sections is also possible. Differential cross-sections are calculable with the interface `ZUATSM`. The calculation is organized by subroutine `ZANCUT` and the cross-section is determined in subroutine `COSCUT`. Integrated cross-sections may have an acceptance cut in the production angle. They are accessible by all the other interfaces, e.g. `ZUTHSM` for Standard Model calculations, and go via subroutine `ZCUT` with call of subroutine `SCUT`

Integrations are done with subroutines `SIMPS` and `FDSIMP` following Eq. (1.2.16) with Eq. (1.2.14) and Eq. (1.2.17).

The minimal invariant mass of the final state fermion pair, $R_{\min}$, may be restricted by choosing the cut variable Δ:

$$\Delta = 1 - R_{\min} = v_{\max}, \qquad (1.4.1)$$

$$4m_f^2 \le s'_{\min} = R_{\min}s \le s. \qquad (1.4.2)$$

For single photon emission, this may be re-interpreted as a cut on the maximum allowed photon energy of the bremsstrahlung photon:

$$\Delta = \frac{E_\gamma^{\max}}{E_{beam}}. \qquad (1.4.3)$$

The Dalitz plot in Fig. 1.5 shows this cut in the variable R.

In the ultra-relativistic limit, the allowed region in the v_2, R plane is a triangle. It is independent of the scattering angle.

For the integrated cross-sections, the s' cut may be combined with an angular acceptance cut:

$$c_1 \le \cos\vartheta \le c_2. \qquad (1.4.4)$$

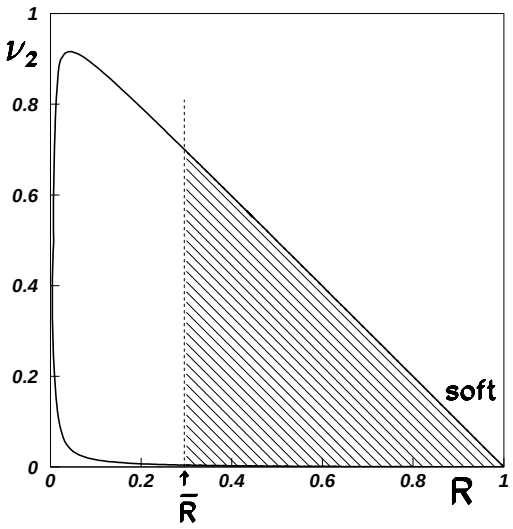

Figure 1.5. *Dalitz plot with a cut on s'*

For a symmetric choice of the angular cuts, $c_1 = -c_2$, we use the abbreviation

$$c = |c_1| = c_2. \tag{1.4.5}$$

As a matter of convention this cut is imposed on the antifermion. Because of CP invariance the cut could equally well be applied on the fermion instead. However, it may not be understood as being applied to both fermions at once.

In the notion of `ZFITTER`, for the s' cut case, it is $R > R_{min} =$ `RECUT2`. This is used for some branchings in the course of calculation. More details on the notion of cut defining variables will be given in Section 1.5.

At the end of these introductory remarks, we should comment on the normalizations. This is easiest studied with the Born cross-sections. From subroutine `SCUT`, we get e.g.:

$$\sigma^0_{\scriptscriptstyle T}(c) = \frac{3}{8}\,\texttt{CSIGNB}\cdot\texttt{SBORN0}\cdot\texttt{COPL3}. \tag{1.4.6}$$

The corresponding definitions are chosen such that `CSIGNB` contains a factor 4/3 (and the conversion factor), `SBORN0` contains no numerical constant (i.e. equals one for muon pair production with photon exchange), and `COPL3` gets 4/3 if no angular acceptance cut is applied. If we write in this article, e.g.:

$$\sigma^0_{\scriptscriptstyle T}(c) = \sigma^0_{\scriptscriptstyle T}(s)\, C_{\scriptscriptstyle T}(c), \tag{1.4.7}$$

then there is a difference by a factor of 2 between Eq. (1.4.6) and Eq. (1.4.7) since $\sigma^0_{\scriptscriptstyle T}(s)$ has no numerical factor, and $C_{\scriptscriptstyle T}(c) =$ `COPL3`. This is exactly the numerical factor mentioned

in Section 1.2. For symmetrical acceptance cut, the normalization is correct in subroutine ZCUT where the cross-section finally is prepared for output. In the following, this kind of numerical overall factor will be assumed to be controlled when we say, e.g., $\sigma_T^0(c) =$ SBRN in subroutines SCUT and SFAST. The program returns correct quantities.

Another remark concerns contributions of the form $\ln c_\pm$ etc, which get singular if $\cos\vartheta = \pm 1$ or $c = \pm 1$. This happens already in subroutine SFAST with simple s' cut. A careful analysis of the corresponding expressions shows that they usually result from expressions like e.g.

$$c_\pm = \frac{1}{2}\left(1 \pm \sqrt{1 - \frac{4m_e^2}{s}}\cos\vartheta\right) \approx \frac{1}{2}(1 \pm \cos\vartheta) \mp \frac{m_e^2}{s}\cos\vartheta. \tag{1.4.8}$$

These expressions never get smaller than m_e^2/s and thus their logarithms are well-defined. In subroutine ZETCOS this is specially arranged to be fulfilled.

1.4.1. Initial state corrections with soft photon exponentiation and higher order corrections

Differential cross-sections

The differential cross-sections are determined with subroutine COSCUT. Common exponentiation of initial and final state radiation is described in Section 1.4.2. Here, we restrict ourselves to the case of only initial state radiation. According to Eq. (1.2.18), it is:

$$\frac{d\sigma^{ini}}{d\cos\vartheta} = \sum_{A=T,FB} \int_0^\Delta dv \sigma_A^0(s') R_A^{ini}(v, \cos\vartheta), \tag{1.4.9}$$

with

$$R_A^{ini}(v,\cos\vartheta) = D_A(\cos\vartheta)\left[1 + \bar{S}^{ini}\right]\beta_e v^{\beta_e - 1} + \bar{H}_A^{ini}(v,\cos\vartheta), \tag{1.4.10}$$

with $\bar{S}^{ini}$ from Eq. (1.3.9) and

$$\bar{H}_A^{ini}(v,\cos\vartheta) = H_A^{ini}(v,\cos\vartheta) + D_A(\cos\vartheta)\left[-\frac{\beta_e}{v} + H_A^{(2)}(v)\right]. \tag{1.4.11}$$

The functions D_A are defined in Eq. (1.1.5) and Eq. (1.1.7), functions $H_A^{(2)}$ in Eq. (1.6.2), and the symmetrized (anti-symmetrized) hard photon parts $\bar{H}_T^{ini} =$ H0 and $\bar{H}_{FB}^{ini} =$ H3 are:

$$H_{T,FB}^{ini}(v,\cos\vartheta) = \frac{\alpha}{2\pi}Q_e^2\left[h_{T,FB}^{ini}(v,\cos\vartheta) \pm h_{T,FB}^{ini}(v,-\cos\vartheta)\right]. \tag{1.4.12}$$

They are calculated in function HARD. The functions $H_{T,FB}^{ini}(v,\cos\vartheta)$ (with same variable names) are calculated in subroutine HCUT, and $h_T^{ini}(v,\cos\vartheta) =$ H0M and $h_{FB}^{ini}(v,\cos\vartheta) =$ H3M in subroutine HINIM, region $(-,+)$:

$$\begin{aligned}\frac{v^3}{R}h_T^{ini}(v,\cos\vartheta) &= \frac{L_c}{\gamma^2}r_2\left(r_2 - \frac{2R}{\gamma}r_1 + \frac{2R^2}{\gamma^2}\right) + \left(-\frac{2}{3R}r_4 + \frac{10}{3}r_2 - 4R + \frac{2}{3\gamma R}r_2 r_3\right)\\ &\quad - \frac{1}{\gamma^2}\left(3r_4 + 8Rr_2 + \frac{26}{3}R^2\right) + \frac{R}{\gamma^3}\left(8r_3 + \frac{44}{3}Rr_1\right)\\ &\quad - \frac{R^2}{\gamma^4}\left(\frac{22}{3}r_2 + 4R\right),\end{aligned} \tag{1.4.13}$$

$$\frac{v^2}{R}h_{FB}^{ini}(v,\cos\vartheta) = r_2\frac{L_c}{\gamma^2}\left(r_1 - \frac{2R}{\gamma}\right) + \frac{2}{\gamma}r_2 - \frac{4}{\gamma^2}r_1(r_2 + R) + \frac{2R}{\gamma^3}(3r_2 + 2R). \tag{1.4.14}$$

Functions $h_A^{ini}(v,\cos\vartheta)$ were given in Eqs. (37) and (38) of [9][6]. The following abbreviations are used:

$$L_c = \ln\frac{\gamma^2}{R} + L_e, \tag{1.4.15}$$

$$R = 1 - v, \tag{1.4.16}$$

$$r_n = 1 + R^n, \tag{1.4.17}$$

$$C_\pm = \frac{1}{2}(1 \pm \cos\vartheta), \tag{1.4.18}$$

$$\gamma = C_+ + RC_-. \tag{1.4.19}$$

Integrated cross-sections delta cut

The Born plus initial state corrections are:

$$\sigma_A^{ini}(c) = \int_0^\Delta dv\ \sigma_A^0(s')R_A^{ini}(v,c), \qquad A = T, FB, \tag{1.4.20}$$

$$R_A^{ini}(v,c) = C_A(c)\left(1+\bar{S}^{ini}\right)\beta_e v^{\beta_e-1} + \bar{H}_A^{ini}(v,c). \tag{1.4.21}$$

The cross-section is calculated in subroutine `SCUT`. The function $\bar{S}^{ini}$ is defined in Eq. (1.3.9). The hard photon corrections $\bar{H}_T^{ini}$=`H0` and $\bar{H}_{FB}^{ini}$=`H3` are calculated by a numerical integration of functions `SHARD` and `AHARD`, respectively:

$$\bar{H}_A^{ini}(v,c) = \frac{\alpha}{\pi}Q_e^2\left[\frac{h_A^{ini}(v,c)}{v} - C_A(c)\frac{\beta_e}{v}\right] + C_A(c)H_A^{(2)}, \qquad A = T, FB. \tag{1.4.22}$$

The second order hard photonic corrections $H_A^{(2)}, A = T, FB$, are described in Section 1.6.2 and the $C_A(c)$ are defined in Eq. (1.1.29) and Eq. (1.1.31). Further, it is:

$$\begin{aligned} h_T^{ini}(v,c) = {} & \frac{4}{3}r_2\left[\frac{\ln\gamma_+}{\gamma_+^3}\left(c_+^3 - R^3c_-^3\right) - \frac{\ln\gamma_-}{\gamma_-^3}\left(c_-^3 - R^3c_+^3\right)\right] \\ & + \frac{2c}{\gamma_-^3\gamma_+^3}\Bigg\{Rr_2\left[(L_e-1) - \ln R\right]\left[\frac{2}{3}R^2(1-c_+c_-) + v^2c_+c_-(R + r_2c_+c_-)\right] \\ & + 2v^2R(c_+c_-)^2\left(r_2R - r_4 + \frac{4}{3}\frac{R^2}{c_+c_-} - \frac{22}{3}R^2\right) \\ & + 2v^4(c_+c_-)^3\left(\frac{5}{3}r_2R - 2R^2 - \frac{1}{3}r_4\right)\Bigg\}, \end{aligned} \tag{1.4.23}$$

$$\begin{aligned} h_{FB}^{ini}(v,c) = {} & 8R\frac{r_2}{r_1^2}\ln\frac{r_1}{2} + \frac{2R}{\gamma_-^2\gamma_+^2}\Bigg\{\left[(L_e-1) - \ln R\right]\Bigg[2r_2\frac{R^2}{r_1^2} \\ & - r_2^2c_+c_- + 4r_2c_+c_-\frac{v^2}{r_1^2}(R + r_2c_+c_-)\Bigg] \\ & + v^2c_+c_-\left[4R - 4c_+c_-r_1^2 + v^2\right]\Bigg\} - 4Rr_2c_+c_-\left(\frac{\ln\gamma_-}{\gamma_-^2} + \frac{\ln\gamma_+}{\gamma_+^2}\right). \end{aligned} \tag{1.4.24}$$

[6]There are printing errors in the corresponding Eqs. (13) and (14) of [45].

For the s' cut, the square brackets in Eq. (1.4.22) are calculated in the functions SHFULL and AHFULL.

The following abbreviations are used:

$$c_\pm = \frac{1}{2}(1 \pm c), \tag{1.4.25}$$

$$\gamma_\pm = c_\pm + Rc_\mp. \tag{1.4.26}$$

1.4.2. Final state radiation

Final state radiation may be treated in quite different ways in ZFITTER. The treatment is chosen by flag IFINAL=FINR and described in detail in Section 3.8. The default value is FINR=1 for *leptons*. A common exponentiation of initial and final state radiation will be performed when FINR=1 is chosen. This situation is described in Section 1.4.2. For FINR=0, final state photonic corrections are treated as a simple factors to $\sigma^0_A(s')$ in Eq. (1.4.9) and in Eq. (1.4.20) according to Eqs. (1.2.3)–(1.2.1). This situation is described in Section 3.6 and Section 3.7. Here we mention only that for the two effective Born cross-sections σ^0_T and σ^0_{FB} the factors are different. For FINR=–1, no final state QED or QCD corrections are applied. For *neutrinos*, FINR=0 is fixed and in effect no final state radiation contributes. For details see subroutine EWCOUP where the generalized weak couplings are set.

Common exponentiation of initial and final state radiation

Common exponentation of initial and final state soft photon radiation is done for flag FINR=1 and follows Section 5.3 of [9].

The cross-section contributions are:

$$\frac{d\sigma^{ini+fin}}{d\cos\vartheta} = \sum_{A=T,FB} \int_0^\Delta dv \sigma^0_A(s') R^{ini}_A(v,\cos\vartheta) \bar{R}^{fin}_A(v), \tag{1.4.27}$$

$$\sigma^{ini+fin}_A(c) = \int_0^\Delta dv \sigma^0_A(s') R^{ini}_A(v,c) \bar{R}^{fin}_A(v), \qquad A = T, FB. \tag{1.4.28}$$

For the definitions of $\sigma^0_A(s'), R^{ini}_A(v,\cos\vartheta), R^{ini}_A(v,c)$ see Section 1.1 and Section 1.4.1.

We mention here that the case of no cuts (but a simple s' cut) is chosen with $c = 1$. In this case the subroutine SCUT returns numbers identical to subroutine to SFAST. [7].

The integrations in Eqs. (1.4.27)–(1.4.28) are performed in subroutines COSCUT and SCUT. The final state factors $\bar{R}^{fin}_T(v)$ = SFIN and $\bar{R}^{fin}_{FB}(v)$ = AFIN are calculated by calls of subroutine FUNFIN from subroutine BORN:

$$\bar{R}^{fin}_A(v) = \Delta'^{\beta'_f}\left[1 + \bar{S}^{fin}(\beta'_f)\right] + \bar{G}_A(v), \tag{1.4.29}$$

The virtual and soft photon part $\bar{S}^{fin}(\beta'_f)$ = (SOFTFR + 3/2*ADD) has a rescaled argument β'_f:

$$\bar{S}^{fin}(\beta'_f) = \frac{3}{4}\beta'_f + \frac{\alpha}{\pi}Q^2_f\left(\frac{\pi^2}{3} - \frac{1}{2}\right), \tag{1.4.30}$$

[7] Subroutine SFAST is called in subroutine ZCUT when flag IFAST=1. For further comments see Section 1.3.2.

$$\beta'_f = \frac{2\alpha}{\pi} Q_f^2 \left(\ln \frac{s'}{m_f^2} - 1 \right). \tag{1.4.31}$$

The effective s' cut $\Delta' =$ `ALIM = A` is also rescaled:

$$\Delta' \equiv 1 - \frac{s'_{\min}}{s'} = \frac{\Delta - v}{1 - v}. \tag{1.4.32}$$

Due to this rescaling, the soft corrections for the final state $\bar{S}^{fin}$ have to be calculated in parallel to the hard corrections and may not be predetermined in the initialization phase as is done for the initial state corrections $\bar{S}^{ini}$.

The hard parts are:

$$\bar{G}_{A}(v) = \frac{1}{4}\beta'_f \Delta' \left(\Delta' - 4\right) + \frac{\alpha}{\pi} Q_f^2 \left[-2\mathrm{Li}_2(\Delta') + g_{A}\left(\Delta'\right) \right], \tag{1.4.33}$$

where

$$g_{T}(\Delta') = \frac{1}{2}\left(1 - \Delta'\right)\left(3 - \Delta'\right) \ln\left(1 - \Delta'\right) - \frac{1}{4}\Delta'\left(\Delta' - 6\right) - \frac{\Delta'^2}{2}\,\mathcal{G}, \tag{1.4.34}$$

$$g_{FB}(\Delta') = \frac{1}{2}\Delta'^2. \tag{1.4.35}$$

In subroutine `FUNFIN`, it is $\bar{G}_{A} + (\alpha/\pi) Q_f^2 g_{A} =$ `FIN - FINS`. The nonuniversal hard final state correction $g_{T}(\Delta')$ contains an approximation since it contains a term, which arises from the angular integration of the product of the (angular dependent) initial state factor with

$$\mathcal{G}(\cos\vartheta) = \left(3 - \frac{4}{1 + \cos^2\vartheta}\right), \tag{1.4.36}$$

and which has been approximated in Eq. (1.4.34) by

$$\mathcal{G} = 0. \tag{1.4.37}$$

1.4.3. Initial-final state interference corrections

The initial-final state interference corrections are added when flag `INTERF`=1 is chosen.

The corresponding cross-sections have the following generic structure:

$$\frac{d\sigma^{int}}{d\cos\vartheta} = \sum_{m,n} \int_0^{\Delta} dv\, \Re e \Big[\sigma^0_{FB}(s, s'; m, n)\, R^{int}_{T}(v, \cos\vartheta; m, n) + \sigma^0_{T}(s, s'; m, n)\, R^{int}_{FB}(v, \cos\vartheta; m, n) \Big], \tag{1.4.38}$$

$$\sigma^{int}_{T} = \sum_{m,n} \int_0^{\Delta} dv\, \Re e \Big[\sigma^0_{FB}(s, s'; m, n)\, R^{int}_{T}(v, c; m, n) \Big], \tag{1.4.39}$$

$$\sigma^{int}_{FB} = \sum_{m,n} \int_0^{\Delta} dv\, \Re e \Big[\sigma^0_{T}(s, s'; m, n)\, R^{int}_{FB}(v, c; m, n) \Big]. \tag{1.4.40}$$

In all these formulae, m, n take the values γ, Z and we use $\sigma^0_{A}(s, s'; m, n)$ from Eq. (1.1.25).

The initial-final state interference corrections have the following property (for a proof see preprint version of [46]):

$$R_A^{int}(v,C;m,n) = \frac{1}{2}\left[R_A^{int}(v,C;m,m) + R_A^{int}(v,C;n,n)^*\right], \quad m,n = \gamma, Z. \tag{1.4.41}$$

Here, the * means complex conjugation and C may be either c or $\cos\vartheta$ and $A = T, FB$. This property allows to determine the γZ interference from the γ and Z exchange corrections. In ZFITTER, the photon functions are the conjugated ones. It is important to use Eq. (1.4.41) in accordance with Eq. (1.1.25).

Differential cross-sections

Differential cross-sections are calculated in subroutine COSCUT. Up to some normalizations to be discussed yet, it is calculated for Eq. (1.4.38):

$$\begin{aligned} R_A^{int}(v,\cos\vartheta;m,n) &= \frac{\alpha}{\pi}Q_eQ_f\Big\{\delta(v)\left[D_{\bar{A}}(\cos\vartheta)\bar{S}^{int}(\Delta,\cos\vartheta) + B_A(\cos\vartheta,m,n)\right] \\ &\quad + \bar{H}_A^{int}(v,\cos\vartheta)\Big\}. \end{aligned} \tag{1.4.42}$$

Here, $D_{\bar{A}}(\cos\vartheta)$ is defined in Eq. (1.1.5) and Eq. (1.1.7). The functions R^{int} consist of soft bremsstrahlung S, hard bremsstrahlung H, and $\gamma\gamma$ and γZ box terms B. The soft correction factor $\bar{S}^{int}(\Delta,\cos\vartheta)$ is independent of m,n and also of $A = T, FB$ and $\bar{A} = FB, T$. It does depend on the cut Δ. This is an artefact of a regularization of the hard photonic corrections $H_A^{int}(v,\cos\vartheta)$ near $v = 0$:

$$\sigma_{\bar{A}}^0(s,s')\bar{H}_A^{int}(v,\cos\vartheta) = \sigma_{\bar{A}}^0(s,s')H_A^{int}(v,\cos\vartheta) - \frac{\sigma_{\bar{A}}^0(s)}{v}D_{\bar{A}}(\cos\vartheta)H_{sing}^{int}(\cos\vartheta), \tag{1.4.43}$$

with:

$$H_{sing}^{int}(\cos\vartheta) = 4\ln\frac{C_-}{C_+}. \tag{1.4.44}$$

The subtraction in Eq. (1.4.43) makes the hard corrections finite at $v = 0$. It has to be added (after integration) to the soft photonic correction $S_A(\cos\vartheta,\epsilon)$ of Eq. (93) in [9], which has the same singularity with opposite sign:

$$D_{\bar{A}}(\cos\vartheta)\bar{S}^{int}(\Delta,\cos\vartheta) = S_A(\cos\vartheta,\epsilon) + D_{\bar{A}}(\cos\vartheta)H_{sing}^{int}(\cos\vartheta)\int_\epsilon^\Delta\frac{dv}{v}. \tag{1.4.45}$$

The subroutine COSCUT calls subroutine SOFTIN with argument SFTI for the calculation of the soft photon corrections, subroutine BOXIN with argument BOXI for the box corrections, and performs a numerical integration over function HARD (with variable $R = 1 - v$) in order to determine the hard photonic corrections HRD. Their sum is then transferred to subroutine ZANCUT. In terms of the variables of ZFITTER, the differential cross-section contribution from the initial-final state interference is:

$$\begin{aligned} \frac{d\sigma^{int}}{d\cos\vartheta} &= \texttt{SIGQED} \\ &= \frac{3}{8}\frac{\texttt{CSIGNB}}{s}[(\texttt{SFTI} + \texttt{BOXI})\texttt{CORINT} - \texttt{HRD}]. \end{aligned} \tag{1.4.46}$$

The factor

$$\texttt{CORINT} = \texttt{RQCDV} \tag{1.4.47}$$

is taken from subroutine `EWCOUP`, see Section 3.7. Further, we have to notice that the Born factors in the box terms are composed not in subroutine `BORN` but in subroutine `BOXIN`.

Now we give the explicit expressions for the various contributions and begin with $\bar{S}^{int}$ = `SFTI`[8]:

$$\bar{S}^{int}(\Delta, \cos\vartheta) = 2\left[2\ln\Delta\ln\frac{C_-}{C_+} + \mathrm{Li}_2(C_+) - \mathrm{Li}_2(C_-) - \frac{1}{2}\left(\ln^2 C_+ - \ln^2 C_-\right)\right], \tag{1.4.48}$$

with $C_\pm$ from Eq. (1.4.18).

We now come to the calculations of the photonic box contributions from Section 4.1 of [9], used in Eq. (1.4.38) and Eq. (1.4.42).

Up to the normalization factor `(3/8)·CSIGNB/S`, they are calculated completely inside the subroutine `BOXIN`. It suffices to derive the pure γ and the pure Z exchange function; then the γZ interference is also known from Eq. (1.4.41). The box functions for $A = T$ and $A = FB$ are related:

$$B_{T,FB}(\cos\vartheta, n, n) = \left[b(\cos\vartheta, n, n) \pm b(-\cos\vartheta, n, n)\right]. \tag{1.4.49}$$

Thus, only two different box functions remain to be calculated[9]:

$$\begin{aligned} b(\cos\vartheta, \gamma, \gamma) &= C_+^2 \ln\frac{C_+}{C_-}\left[-2\pi i\right] - \frac{1}{2}\ln C_-\Big[-2C_+ + \cos\vartheta(\ln C_- + 2\pi i)\Big] \\ &\quad + \pi i C_+, \end{aligned} \tag{1.4.50}$$

$$\begin{aligned} b(\cos\vartheta, Z, Z) &= 2C_+(1-R_Z)\left\{\ln\frac{C_-}{R_Z} - (1-R_Z)L_Z + \right. \\ &\quad \left. \frac{1}{C_+}(1-R_Z-2C_+)\left[l(1) - l(C_-) - L_Z\ln C_-\right]\right\} \\ &\quad + C_+^2\left\{\left[4L_Z + \ln(C_+C_-)\right]\ln\frac{C_+}{C_-} + 2l(C_+) - 2l(C_-)\right\}. \end{aligned} \tag{1.4.51}$$

The following abbreviations are used:

$$l(a) = \mathrm{Li}_2\left(1 - aR_Z^{-1}\right), \tag{1.4.52}$$

$$L_Z = \ln\left(1 - R_Z^{-1}\right), \tag{1.4.53}$$

[8] A dependence on the infrared pole has been already cancelled between the box and soft photon functions used. To control them, consult Section 4.1 of [9].

[9] In [9], the overall signs in Eqs. (95) and (96) are wrong. To control the divergent terms, consult Section 4.1 of [9]. There, the divergent term in Eq. (96) is by a factor 2 too small.

and $R_Z =$ `XR` is:

$$R_Z \;=\; \frac{m_Z^2}{s}. \tag{1.4.54}$$

The complex mass m_Z is defined in Eq. (1.1.10).

To state it correctly: In `ZFITTER` the programming of the box contributions to the angular distribution deviates slightly from the conventions used in this description so far. In subroutine `BOXIN`, the real and imaginary parts of $B_{A}(n,n)$ in Eq. (1.4.49) are calculated explicitely:

$$\Re e\, B_{T}(\cos\vartheta;\gamma,\gamma) \;=\; -\texttt{REF4BX}, \tag{1.4.55}$$
$$\Im m\, B_{T}(\cos\vartheta;\gamma,\gamma) \;=\; -\texttt{AMF4BX}, \tag{1.4.56}$$
$$\Re e\, B_{FB}(\cos\vartheta;\gamma,\gamma) \;=\; \texttt{REF1BX}, \tag{1.4.57}$$
$$\Im m\, B_{FB}(\cos\vartheta;\gamma,\gamma) \;=\; \texttt{AMF1BX}, \tag{1.4.58}$$
$$B_{T}(\cos\vartheta;Z,Z) \;=\; -\texttt{XH4BX}, \tag{1.4.59}$$
$$B_{FB}(\cos\vartheta;Z,Z) \;=\; \texttt{XH1BX}. \tag{1.4.60}$$

Further, the box corrections do not take the overall factors with coupling constants, $\sigma^0_{A}(s,s')$, from subroutine `BORN`.

These factors are constructed in `BOXIN` directly out of the building blocks of subroutine `EWCOUP`. As an example, we give the cross-section contribution from the pure photonic boxes:

$$\frac{d\sigma^{int,box}}{d\cos\vartheta}(\gamma,\gamma) \;=\; \frac{\alpha}{\pi}Q_eQ_f\left[\sigma^0_{FB}(s,s;\gamma,\gamma)\,B_{T}(\cos\vartheta,\gamma,\gamma)+\sigma^0_{T}(s,s;\gamma,\gamma)\,B_{FB}(\cos\vartheta,\gamma,\gamma)\right]. \tag{1.4.61}$$

This is the (γ,γ) part of the variable `BOXI = BOXIS + BOXIA`. In terms of the variables used in `ZFITTER`[10]:

$$\frac{d\sigma^{int,box}}{d\cos\vartheta}(\gamma,\gamma) \;=\; -\texttt{ALQEF}\cdot\texttt{VPOL2}\cdot(\texttt{AEFA}\cdot\texttt{REF4BX}+\texttt{VEFA}\cdot\texttt{REF1BX})\cdot\texttt{CORINT}. \tag{1.4.62}$$

We see that besides the box functions there is an explicit dependence on the combinations of couplings like `AEFA, VEFA, VPOL2`.

Explicitely,

$$\texttt{REF4BX} \;=\; -\left[\cos\vartheta\ln\frac{C_+}{C_-}\left[\ln(C_+C_-)-1\right]+\ln(C_+C_-)\right], \tag{1.4.63}$$
$$\texttt{AMF4BX} \;=\; 2\pi\left(\cos\vartheta\ln\frac{C_+}{C_-}-1\right), \tag{1.4.64}$$
$$\texttt{REF1BX} \;=\; -\cos\vartheta\left[\ln^2C_+ + \ln^2C_- - \ln\left(C_+C_-\right)\right]-\ln\frac{C_+}{C_-}, \tag{1.4.65}$$
$$\texttt{AMF1BX} \;=\; -2\pi\left[\cos\vartheta\left[\ln\left(C_+C_-\right)-1\right]+\left(1+\cos^2\vartheta\right)\ln\frac{C_+}{C_-}\right]. \tag{1.4.66}$$

[10]The imaginary parts of the pure photonic boxes contribute through the γZ interference.

The hard radiator parts H_T^{int} = H4 and H_{FB}^{int} = H1 are independent of the gauge boson exchanged. They are calculated as arguments of subroutine HCUT, called by function HARD:

$$H_{T,FB}^{int}(v,\cos\vartheta) = \left[h_{T,FB}^{int}(v,\cos\vartheta) \pm h_{T,FB}^{int}(v,-\cos\vartheta)\right]. \tag{1.4.67}$$

While the box terms for $A = FB$ and $A = T$ are expressed by one and the same function, this is not the case for H_T^{int} and H_{FB}^{int}. They are composed as symmetric and anti-symmetric combinations of variables h_T^{int} = H4M, h_{FB}^{int} = H1M (Eqs. (100) and (101), respectively, in [9]). This is done in ZFITTER by two subsequent calls of subroutine HINTFM:

$$\begin{aligned} h_T^{int}(v,\cos\vartheta) &= 2C_+\left\{\left[\frac{4}{v}-3-R(2+R)\right]\ln\frac{C_-}{C_+}-(1+R)^2\ln\frac{\bar\gamma}{\gamma}\right\} \\ &\quad +2\left[-\frac{4}{v}+4+R(2+\ln R)\right]+\frac{4}{\gamma}\left[\frac{2}{v}-2-R(1+R)\right], \end{aligned} \tag{1.4.68}$$

$$\begin{aligned} h_{FB}^{int}(v,\cos\vartheta) &= 2\left(1+\cos^2\vartheta\right)\ln C_-\left(\frac{2}{v}-1-R-R^2\right) \\ &\quad +4C_+\left[-\frac{4}{v}+4+2R-R(1-R)\ln R\right]+\frac{4}{\gamma}\left(-\frac{2}{v^2}+\frac{5}{v}-3-R\right) \\ &\quad +\frac{2}{\gamma^2}\left(-\frac{2}{v^2}+\frac{6}{v}-4-2R-R^2\right)+2(R^2-1)C_+\ln C_+C_- \\ &\quad +2\left[(1-R+R^2)+\cos\vartheta(1-R^2)+\cos^2\vartheta(1+R+R^2)\right]\ln\gamma. \end{aligned} \tag{1.4.69}$$

Here, γ is defined in Eq. (1.4.19)) and $\bar\gamma = \gamma(C_\pm \to C_\mp)$.

Integrated cross-sections

The radiator functions in Eq. (1.4.39) and Eq. (1.4.40) are:

$$R_A^{int}(v,c,m,n) = \frac{\alpha}{\pi}Q_eQ_f\left\{\delta(v)\left[\bar S_A^{int}(c)+B_A(c,m,n)\right]+\bar H_A^{int}(v,c)\right\}. \tag{1.4.70}$$

In ZFITTER, the soft photon corrections are $\bar S_T^{int}(c)$ = - SFTI4 and $\bar S_{FB}^{int}(c)$ = SFTI1, and their contributions to cross-sections are then SFTIS = - SFTI4 · ABORN0 · ALQEF and SFTIA = SFTI1 · SBORN0 · ALQEF. They are used in all calculational chains and are calculated in subroutine SFTINT, which is called by subroutine SFAST or, alternatively, by SCUT. Their explicit expressions are derived from the functions $S_A^{int}(c,\epsilon)$, Eqs. (20) and (25) of [10], with a regularization:

$$\bar S_A^{int}(c) = S_A^{int}(c,\epsilon)+H_{sing,A}^{int}(c)\int_\epsilon^\Delta\frac{dv}{v}, \tag{1.4.71}$$

while at the same time compensating terms contribute to functions SHARD and AHARD:

$$\sigma_{\bar A}^0(s,s')\bar H_A^{int}(v,c) = \sigma_{\bar A}^0(s,s')H_A^{int}(v,c)-\frac{\sigma_{\bar A}^0(s)}{v}H_{sing,A}^{int}(c). \tag{1.4.72}$$

Functions $H_{sing,A}^{int}(c)$ are the angular integrals of functions $D_{\bar A}(\cos\vartheta)H_{sing}^{int}(\cos\vartheta)$:

$$H_{sing,T}^{int}(c) = -4\left[\left(c^2-1\right)\ln\frac{c_+}{c_-}+2c\right], \tag{1.4.73}$$

$$H_{sing,FB}^{int}(c) = \frac{4}{3}\left[-8\ln 2-4\ln(c_+c_-)-3C_T(c)\ln\frac{c_+}{c_-}-c^2\right]. \tag{1.4.74}$$

Then, we may write with $\ln\Delta = \texttt{ALDEL}$:

$$\begin{aligned}\bar{S}_T^{int}(c) &= H_{sing,T}^{int}(c)\ln\Delta + 2\left(c^2-1\right)\left[\mathrm{Li}_2(c_+) - \mathrm{Li}_2(c_-)\right] \\ &- \left(c^2-1\right)\ln\left(c_+c_-\right)\ln\frac{c_+}{c_-} - 4c\ln(c_+c_-) - 4\ln\frac{c_+}{c_-} + 8c, \end{aligned} \tag{1.4.75}$$

$$\begin{aligned}\frac{3}{4}\bar{S}_{FB}^{int}(c) &= H_{sing,FB}^{int}(c)\ln\Delta \\ &+ \frac{3}{2}C_T(c)\left[\mathrm{Li}_2(c_+) - \mathrm{Li}_2(c_-)\right] + 2\left[\mathrm{Li}_2(c_+) + \mathrm{Li}_2(c_-)\right] \\ &- \frac{3}{4}C_T(c)\ln(c_+c_-)\ln\frac{c_+}{c_-} - \left(\ln^2 c_+ + \ln^2 c_-\right) + 4\ln^2 2 + \ln 2 \\ &-\frac{1}{2}\ln(c_+c_-)(c^2-1) + \frac{c^2}{2} - 2\mathrm{Li}_2(1). \end{aligned} \tag{1.4.76}$$

For $c = 1$, the expressions simplify considerably: $\bar{S}_T^{int}(1) = -8(\ln\Delta - 1)$ and $\bar{S}_{FB}^{int}(1) = -(1+8\ln 2)\ln\Delta + 2\mathrm{Li}_2(1) + 4\ln^2 2 + \ln 2 + 1/2$. Though, this is not used in ZFITTER.

The net box contributions to the integrated cross-sections are called BOXIS and BOXIA. They are calculated in subroutine BOXINT, which itself is called by either subroutine SFAST or subroutine SCUT. For the integrated box functions apply the correspondences Eq. (1.4.55) to Eq. (1.4.60). The box functions have an explicit dependence on the kind of exchanged vector boson and are written in (anti-)symmetrised form (see Eqns. (21), (22), (26), (27) of [10])[11]:

$$B_{T,FB}(c;n,n) = b_{T,FB}(c;n,n) \mp b_{T,FB}(-c;n,n), \tag{1.4.77}$$

with

$$b_T(c;\gamma,\gamma) = \frac{1}{2}\left(c^2-1\right)\ln^2 c_+ + \left(-c^2+2c-3\right)\ln c_+ - 3c - i\pi(c^2-1)\ln c_+, \tag{1.4.78}$$

$$\begin{aligned} b_{FB}(c;\gamma,\gamma) &= -\frac{1}{2}\left(c^2-1\right)\ln^2 c_+ - \left(-c^2+2c-3\right)\ln c_+ - \frac{1}{2}\left(\ln^2 2 + 6\ln 2 + c^2\right) \\ &- \frac{i\pi}{3}\left[5\ln 2 + \left(2c^3+3c^2+6c+5\right)\ln c_+ - \frac{2}{3}c^2\right], \end{aligned} \tag{1.4.79}$$

$$\begin{aligned} b_T(c;Z,Z) &= -2\Big\{-2cR_Z(1-R_Z)\ln c_+ \\ &- \left[-2R_Z^2 + R_Z\left(c^2+1\right) + c^2 - 1\right]\ln c_+ - cR_Z(R_Z+1)\Big\}L_Z \\ &+ 4cR_Z(R_Z-1)l(1) - 2c\ln R_Z + \left(c^2-1\right)\ln^2 c_+ \\ &+ 2\left[R_Z\left(c^2-1\right) - c^2 + 2c + 3\right]\ln c_+ \\ &- 2\left[2R_Z^2 + 2cR_Z(R_Z-1) - R_Z\left(c^2+1\right)\right]l(c_+) + 2R_Z c - 6c, \qquad n \neq 0, \end{aligned} \tag{1.4.80}$$

[11] ZFITTER calculates the expressions $B_{T,FB}$. We remark here that in Eq. (19) of [10] the $\pm$ has to be a $\mp$ and that in Eq. (22) the first term in the curly bracket has a wrong sign. Further, in Eq. (18) the factor σ^0 is superfluous.

$$
\begin{aligned}
b_{FB}(c;Z,Z) &= \left[C_T(c)+\frac{4}{3}\right]\ln^2 c_+ \\
&+ \left\{\left(4R_Z^2-2R_Z+\frac{10}{3}\right)\ln 2\right. \\
&+ \left[4R_Z^2-2R_Z\left(c^2+1\right)+2c^2+\frac{10}{3}\right]\ln c_+ \\
&\left.+ 4\left[cR_Z(R_Z-1)+C_T(c)\right]\ln c_+ + c^2\left(-R_Z^2+3R_Z-\frac{4}{3}\right)\right\}L_Z \\
&+ c^2\left(\frac{4}{3}R_Z-\frac{5}{3}\right)\ln R_Z + \left(\frac{16}{3}R_Z^3-4R_Z^2+2R_Z-\frac{2}{3}\right)l\left(\frac{1}{2}\right) \\
&+ 2c^2(R_Z-1)l(1) - \frac{4}{3}\ln^2 2 + \left(\frac{8}{3}R_Z^2+\frac{8}{3}R_Z-6\right)\ln 2 \\
&+ \left[\frac{8}{3}R_Z^2+R_Z\left(-\frac{4}{3}c^2+\frac{8}{3}\right)+2\left(c^2-3\right)\right]\ln c_+ \\
&+ \left(\frac{8}{3}R_Z^2+\frac{4}{3}R_Z-4\right)c\ln c_+ \\
&+ 2\left[-\frac{8}{3}R_Z^3+2R_Z^2-R_Z\left(c^2+1\right)+c^2+\frac{1}{3}\right]l(c_+) \\
&+ 2\left[2c\left(R_Z^2-R_Z\right)+C_T(c)\right]l(c_+)+\left(\frac{2}{3}R_Z-1\right)c^2, \;\; n\neq 0.
\end{aligned}
\tag{1.4.81}
$$

For $l(a)$, L_Z, and R_Z we use Eqs. (1.4.52)–(1.4.54). Both the soft photon and the box corrections simplify considerably if no acceptance cut is applied. For this case, the latter are given in [47,48], where also the completely integrated corrections $\sigma_{T,FB}^{QED,int}(1)$ (i.e. with no cut) may be found in a rather compact form which is, though, not realized in subroutine `SFAST` of `ZFITTER`.

The hard radiator functions $\bar{H}_A^{int}$ in Eq. (1.4.72) are calculated in functions `SHARD` and `AHARD`. They are explicitely regulated there at $v\to 0$, while the functions H_A^{int} = `H4, H1` are taken from Eqs. (24) and (28) of [10] and called from subroutines `SHFULL, AHFULL`:

$$
H_T^{int}(v,c) = 4c_+c_-\left[\frac{r_1r_2}{v}\ln\frac{c_+}{c_-}+\left(\frac{c^2}{c_+c_-}R-v^2\right)\ln\frac{\gamma_+}{\gamma_-}\right]+4cR\left(-\frac{r_1}{v}+\ln R\right), \tag{1.4.82}
$$

$$
\begin{aligned}
H_{FB}^{int}(v,c) &= \frac{2c^2R}{\gamma_+\gamma_-}\left(\frac{1}{3}v^2-\frac{2}{3v}+\frac{2R}{r_1}+\frac{1}{3}c^2vr_1\right) \\
&- 2c^2Rv\ln R - 4\frac{r_1}{v}c_+c_-r_2\ln(c_+c_-) \\
&- \frac{16}{3}\frac{r_3}{v}\left(c_-^3\ln c_- + c_+^3\ln c_+\right)+\frac{2}{3}\left(2R-5r_2\right)\frac{r_1}{v}\ln r_1 \\
&- 4\ln\gamma_-\left[2cc_-^2-\gamma_-\left(v+\frac{4}{3}\frac{\gamma_-^2}{v}-4c_-^2+\gamma_-\right)\right] \\
&+ 4\ln\gamma_+\left[2cc_+^2+\gamma_+\left(v+\frac{4}{3}\frac{\gamma_+^2}{v}-4c_+^2+\gamma_+\right)\right],
\end{aligned}
\tag{1.4.83}
$$

with $r_n, c_\pm, \gamma_\pm$ defined in Eq. (1.4.17), Eq. (1.4.25), Eq. (1.4.26).

1.5. Photonic Corrections with Acollinearity Cut

The calculational chain with cuts on angular acceptance, acollinearity, and minimal energy of the final state fermions was originally implemented in ZFITTER by M. Bilenky and A. Sazonov (1989) [45] (flag ICUT=0). The present default treatment of photonic $\mathcal{O}(\alpha)$ corrections with the package acol.f is chosen with flag ICUT=2 or ICUT=3 in the call of subroutine ZUCUTS; see also Section 4.2.4. It is based on [11,43,49]. The phase space parameterisation derived in [50] is applied. Higher order QED corrections depend on the flag FOT2, see Section 1.6 and Appendix 4.2.2.

In this approach, the cross-sections σ_T and σ_{FB} are calculated with formulae that assume the following cuts on the production angle $\cos\vartheta$ of one fermion (*acceptance cut*), on the final state fermions' energies $E_{\bar{f}}, E_f$, and on the fermions' acollinearity angle ξ:

$$\begin{array}{ccccc} c_1 & \leq & \cos\vartheta & \leq & c_2, \\ E_f^{min} & \leq & E_{\bar{f}}, E_f & \leq & \frac{\sqrt{s}}{2}\ , \\ 0 & \leq & \xi & \leq & \xi^{max}. \end{array} \tag{1.5.1}$$

The equality of the lower fermion energy limits is not essential but simplifies some formulae and is assumed to be valid in ZFITTER. Some technical restrictions of the cut boundaries will be mentioned later. The cut conditions do not explicitly depend on fermion masses in the approximations assumed, but there is an influence of the acollinearity cut on the scattering angle, see remark after Eq. (1.5.26).

ZFITTER returns the cross-section with QED corrections SIGQED, the asymmetry AFBQED, and the effective Born quantities SIGBRN and AFBBRN from subroutine ZCUT. The angular distributions over $\cos\vartheta$ are calculated by subroutine ZANCUT (see e.g. Eq. (1.2.6) and Eqs. (1.2.18)–(1.2.23) and the flowcharts in Figs. I.3–I.4). Technicalities of the calculation are described in Section 1.2.

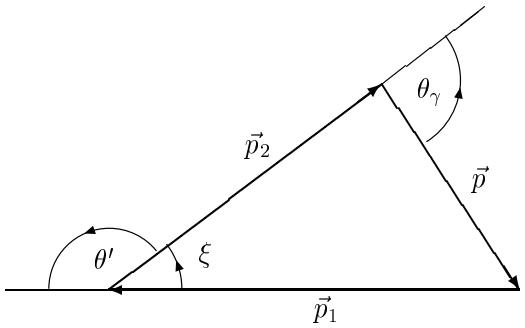

Figure 1.6. *Acollinearity angle* ξ

1.5.1. Kinematics

A three-fold analytical integration of the squared matrix elements had to be performed over three angles of phase space: $\varphi_\gamma, v_2(\cos\theta_\gamma)$ and $\cos\vartheta$, with $\varphi_\gamma, \theta_\gamma$ as photon angles (in the fermion-photon restframe) and v_2 as invariant mass of photon and antifermion. The last integration, that over $R = s'/s$, is then performed numerically by `ZFITTER`.

The three variables $\cos\theta_\gamma$, v_2, and R may be related to the three final state momenta $p_f, p_{\bar{f}}, p_\gamma$ in the centre of mass system (cms) where the three-momenta form a triangle: $\vec{p}_f + \vec{p}_{\bar{f}} + \vec{p}_\gamma = 0$ with $v_2 = 2p_\gamma p_{\bar{f}}$ and $s' = (p_f + p_{\bar{f}})^2$ (see Fig. 1.6 with $\vec{p}_1 = \vec{p}_f, \vec{p}_2 = \vec{p}_{\bar{f}}, \vec{p} = \vec{p}_\gamma$). This triangle is characterized by two angles, besides θ_γ also by $\theta' = \pi - \xi$, where ξ is the acollinearity angle (the deviation of the fermions' opening angle from π).

Conditions on the two angles,

$$\sin^2\theta_\gamma \geq 0, \tag{1.5.2}$$
$$\sin^2(\xi/2) \leq \sin^2(\xi^{max}/2), \tag{1.5.3}$$

are related to the moduli of the three-momenta in the triangle in the cms [51]. These moduli may be expressed by s, $R = s'/s$ and v_2 so that the photon angle θ_γ as variable can be substituted by v_2 which simplifies the analytical integrations substantially. This chain of relations gives an access to the boundary conditions of the physically allowed region:

$$v_{2_m}^{min}(R) \leq v_2 \leq v_{2_m}^{max}(R), \tag{1.5.4}$$
$$R_E - R \leq v_2 \leq 1 - R_E, \tag{1.5.5}$$

and

$$v_2 \leq v_{2_\xi}^{min}(R), \tag{1.5.6}$$

or

$$v_{2_\xi}^{max}(R) \leq v_2, \tag{1.5.7}$$

where

$$v_{2_m}^{max,min}(R) = \frac{1}{2}(1-R)\left(1 \pm \sqrt{1 - \frac{4m_f^2}{s'}}\right), \tag{1.5.8}$$
$$v_{2_\xi}^{max,min}(R) = \frac{1}{2}(1-R)\left[1 \pm \sqrt{1 - \frac{R}{R_\xi}\frac{(1-R_\xi)^2}{(1-R)^2}}\right], \tag{1.5.9}$$
$$R_E = \frac{2E_f^{min}}{\sqrt{s}}, \tag{1.5.10}$$
$$R_\xi = \frac{1-\sin(\xi^{max}/2)}{1+\sin(\xi^{max}/2)}. \tag{1.5.11}$$

The Dalitz plot given in Fig. 1.7 may help to understand the relation between a simple s' cut (just region I) and the cuts applied here (regions I with II and III).

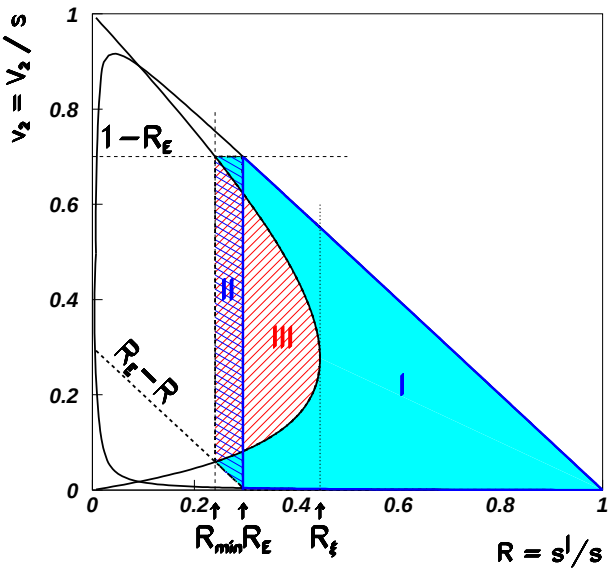

Figure 1.7. *Dalitz plot with cuts on ξ and E_f (I)*

As Fig. 1.7 shows, we have to determine the cross-sections in three phase-space regions with different boundary values of v_2 at given R:

$$\frac{d\sigma}{d\cos\vartheta} = \left[\int_{\rm I} + \int_{\rm II} - \int_{\rm III}\right] dR\; dv_2 \frac{d\sigma}{dR dv_2 d\cos\vartheta}. \tag{1.5.12}$$

Region I corresponds to the simple s' cut. The integration over R extends from R_{min} to 1:

$$R_{min} \;=\; R_E\left(1 - \frac{\sin^2(\xi^{max}/2)}{1 - R_E\cos^2(\xi^{max}/2)}\right). \tag{1.5.13}$$

The soft-photon corner of the phase space is at $R = 1$. Thus, the additional contributions related to the acollinearity cut are exclusively due to hard photons. The boundaries for the integration over v_2 can now be summarized with one general parameter $A = A(R)$ to:

$${v_2}^{max,min}(R) \;=\; \frac{1}{2}(1-R)\;\left[1 \pm A(R)\right], \tag{1.5.14}$$

where in every region $A = A(R)$ depends on only one of the applied cuts:

$$A_{\rm I}(R) \;=\; \sqrt{1 - \frac{R_m}{R}} \approx 1, \tag{1.5.15}$$

$$A_{\rm II}(R) \;=\; \frac{1 + R - 2R_E}{1 - R}, \tag{1.5.16}$$

$$A_{\rm III}(R) \;=\; \sqrt{1 - \frac{R(1-R_\xi)^2}{R_\xi(1-R)^2}}, \tag{1.5.17}$$

with

$$R_m = \frac{4m_f^2}{s}, \tag{1.5.18}$$

$$R_E = \frac{2E_{min}}{\sqrt{s}}, \tag{1.5.19}$$

$$R_\xi = \frac{1-\sin(\xi^{max}/2)}{1+\sin(\xi^{max}/2)}. \tag{1.5.20}$$

The turning point P_t of the acollinearity bound is given by

$$P_t \equiv [R_t; v_{2,t}] = \left[R_\xi; \frac{1}{2}(1-R_\xi)\right]. \tag{1.5.21}$$

The upper and lower fermion energy cuts of Eq. (1.5.5) are straight lines meeting at a value $\tilde{R}_E$ of R:

$$\tilde{R}_E = R_E^f + R_E^{\bar{f}} - 1. \tag{1.5.22}$$

Two qualitatively different cases may arise. In the first case, $\tilde{R}_E < R_\xi$, the acollinearity cut affects the integration region and the absolute minimum of R is given by

$$R_{min} = R_E\left(1 - \frac{\sin^2(\xi^{max}/2)}{1-R_E\cos^2(\xi^{max}/2)}\right). \tag{1.5.23}$$

The complete integration region to be used in Eq. (1.2.24) and Eq. (1.2.25) can then be split into three different parts where the kinematical bound by m_f, the linear bounds by the energy cuts, and the curved acollinearity bound are considered separately:

$$\begin{aligned}\Gamma &= \Gamma_I + \Gamma_{II} - \Gamma_{III} \\ &= \int_{\bar{R}_E}^1 dR \int_{v_{2m}^{min}(R)}^{v_{2m}^{max}(R)} dv_2 + \int_{R_{min}}^{\bar{R}_E} dR \int_{R_E-R}^{1-R_E} dv_2 - \int_{R_{min}}^{R_\xi} dR \int_{v_{2\xi}^{min}(R)}^{v_{2\xi}^{max}(R)} dv_2.\end{aligned} \tag{1.5.24}$$

In the other case, $\tilde{R}_E \geq R_\xi$, the energy cuts are so stringent that the acollinearity cut has no effect. The minimum value of R is $R_{min} = \tilde{R}_E$ and the integration region is simplified to a trapezoid:

$$\Gamma = \Gamma_I + \Gamma_{II} = \int_{\bar{R}_E}^1 dR \int_{v_{2m}^{min}(R)}^{v_{2m}^{max}(R)} dv_2 + \int_{R_{min}}^{\bar{R}_E} dR \int_{R_E-R}^{1-R_E} dv_2. \tag{1.5.25}$$

The cut value $\bar{R}_E$ in Eq. (1.5.24) and Eq. (1.5.25),

$$\bar{R}_E = \frac{2\frac{m_f^2}{s} + (1-R_E)\left(R_E + \sqrt{R_E^2 - 4\frac{m_f^2}{s}}\right)}{2(1-R_E+\frac{m_f^2}{s})}, \tag{1.5.26}$$

can safely be set to R_E neglecting m_f here, as is done in ZFITTER (see also Eq. (1.5.28)). The two corresponding Dalitz plots are shown in Fig. 1.8.

In subroutine ZCUT the distinction of the two situations Eq. (1.5.24) and Eq. (1.5.25) is organized in a straightforward manner where the hard acollinearity cut corrections

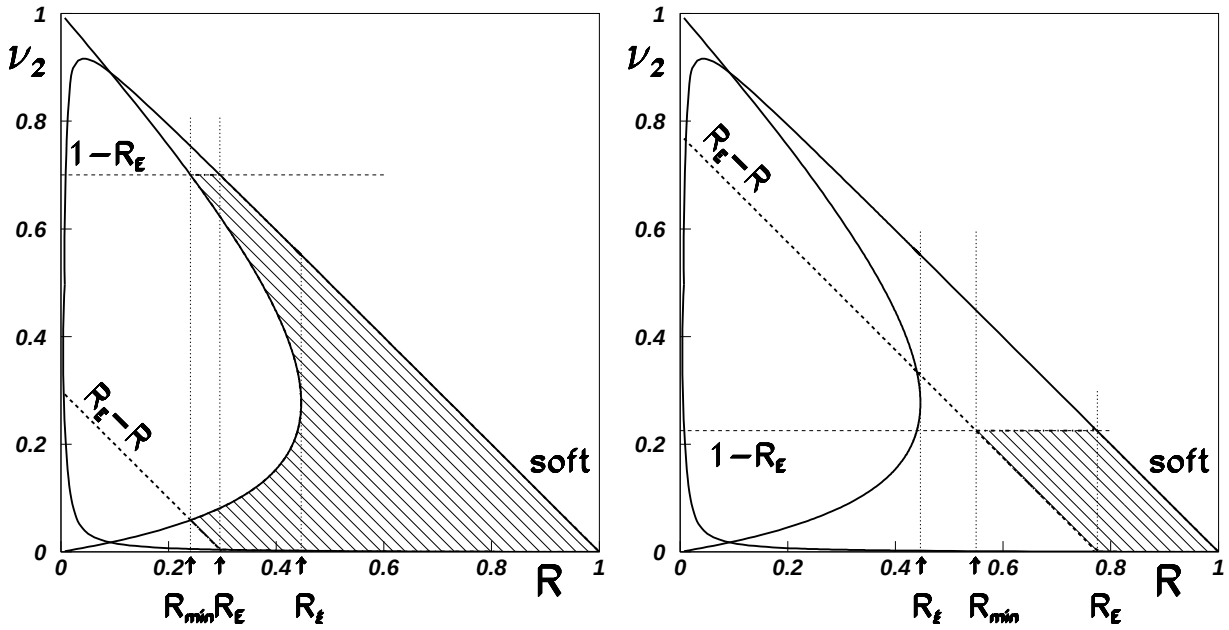

Figure 1.8. *Dalitz plots with cuts on ξ and E_f (II); the two cases are discussed in the text*

are calculated by subtractions from the s' cut result, in subroutine `SCUT` including all angular cuts (by functions `SHARD` and `AHARD`), and in `SFAST` with acollinearity, but without acceptance cut (by functions `FCROS` and `FASYM`). The corresponding hard corrections to the angular distributions are treated in an analogous way in `ZANCUT` (see subroutines `COSCUT` and `HARD`).

The above relations are independent of the scattering angle and thus, as mentioned, compatible with the angular acceptance cut defined in Eq. (1.4.4). Though, we would like to point out that the acollinearity cut has an indirect influence on the acceptance cut. It is easy to see that the maximal scattering angle of the second fermion (which is unrestricted by the user's acceptance cut) becomes limited by an acollinearity cut, i.e. the scattering angle of the second fermion is limited to $[-(\xi^{max}+\vartheta^{max}),(\xi^{max}+\vartheta^{max})]$.

The user may apply a sometimes reasonable approximation of the acollinearity cut in terms of the simpler Δ cut ($\equiv s'$ cut); this can be achieved by using Δ_ξ for the definition of the integration limit Eq. (1.4.2) in Section 1.4:

$$\Delta_\xi \equiv 1 - R_\xi = \frac{2\sin(\xi^{max}/2)}{1+\sin(\xi^{max}/2)} \approx \xi^{max}. \tag{1.5.27}$$

The quality of such an approximation depends critically on the values of the E_{min} cut and the ξ^{max} cut; for loose cuts it improves. Because of the approximations that have been implemented in the code for this calculational chain, the user must be cautious when

applying severe cuts. Since the approximation is ultra-relativistic one should restrict oneself to the following region of the phase space:

$$E^{min} \gg m_f, \tag{1.5.28}$$

$$\xi^{max} \ll \left(1 - \frac{8m_f}{\sqrt{s}}\right)\pi. \tag{1.5.29}$$

On the other hand, the validity of inclusive soft-photon exponentiation (see Section 1.4.2 and Section 1.4.2) comes into question if the kinematical region shrinks to the soft photon corner either due to too stringent energy cuts or if the turning point P_t introduced in Eq. (1.5.21) is moved too far to the right:

$$E^{min} < 0.95\, E_{\rm beam}, \tag{1.5.30}$$

$$\xi^{max} > 2^\circ. \tag{1.5.31}$$

In this Section, we discussed the *final state kinematics* and the resulting physical phase space boundaries. In Section 1.5.3, we will discuss yet the influence of the *initial state kinematics* on the singularity structure of the squared radiative matrix elements and the resulting peculiarities of the integrated radiator functions; see discussion around Eq. (1.5.37).

1.5.2. Cross-sections

The cross-sections with acollinearity cut calculated finally in ZFITTER may be written generically in close analogy to those given in Section 1.4, e.g. Eq. (1.4.9) and Eq. (1.4.20):

$$\frac{d\sigma^a}{d\cos\vartheta} = \sum_{B=T,FB}\left[\int_{R_E}^{1} + \int_{R_{min}}^{R_E} - \theta_R \int_{R_{min}}^{R_\xi}\right] dR\; \sigma_B^0(s') R^a_{B,reg}(R,\cos\vartheta), \tag{1.5.32}$$

$$\sigma_B^a(c) = \left[\int_{R_E}^{1} + \int_{R_{min}}^{R_E} - \theta_R \int_{R_{min}}^{R_\xi}\right] dR\; \sigma_B^0(s') R^a_{B,reg}(R,c), \quad B = T, FB, \tag{1.5.33}$$

with

$$\theta_R = \theta\left(R_\xi - (2R_E - 1)\right). \tag{1.5.34}$$

The subindex *reg* indicates that the expressions for the radiators R depend on the region, *reg = I,II,III*. In region I, the usual decomposition of the radiators into hard and soft+virtual components holds as was described in much detail in Section 1.4. Further, soft photon exponentiation may be performed there. If it is performed, then not necessarily from R_E to the upper integration bound in R, but starting from $\max(R_E, R_\xi)$. In the other two regions, there are only hard radiatior parts to be considered.

For later reference, we give here also the generic formula for common exponentiation of initial and final state photons:

$$\frac{d\sigma^{ini+fin}}{d\cos\vartheta} = \sum_{B=T,FB}\left[\int_{R_E}^{1} + \int_{R_{min}}^{R_E} - \theta_R \int_{R_{min}}^{R_\xi}\right] dR\sigma_B^0(s') R^{ini}_{B,reg}(R,\cos\vartheta)\bar{R}^{fin}_B(R), \tag{1.5.35}$$

$$\sigma_B^{ini+fin}(c) = \left[\int_{R_E}^{1} + \int_{R_{min}}^{R_E} - \theta_R \int_{R_{min}}^{R_\xi}\right] dR\sigma_B^0(s') R^{ini}_{B,reg}(R,c)\bar{R}^{fin}_B(R), \quad B = T, FB. \tag{1.5.36}$$

We will not give here the various hard radiator expressions to be used in ZFITTER. Instead, after some introduction to their treatment we will quote as an instrucive example the rather compact formulae for the integrated cross-sections without acceptance cut ($c = 1$). Further, the explicit expressions for $\bar{R}_B^{fin}(R)$ will be given in Section 1.5.4. With these two examples at hand, the expert user will be able to find any further information needed from the Fortran code itself.

1.5.3. Hard radiator parts. Package acol.f

In presence of an acollinearity cut, the hard radiator parts have to be calculated differently in three regions of the Dalitz shown in Fig. 1.7. For regions II and III, they are calculated with the package acol.f.

Flags and subroutines

In ZFITTER the calculation of cross-sections and asymmetries is done through subroutine ZCUT which either calls subroutine SCUT (formulae with all cuts) or SFAST (formulae for special cases). The corresponding angular distributions can be calculated by subroutine ZANCUT which calls COSCUT for the hard flux functions. Flag ICUT from subroutine ZUCUTS decides in both cases which cuts are being applied:

- ICUT=2 : Cuts on acollinearity, minimal energies, but no acceptance cut. Subroutine SFAST calls FCROS and FUNFIN for σ_T and FASYM and FUNFIN for σ_{FB}
- ICUT=3 : Cuts on acollinearity, minimal energies, and acceptance. Subroutine SCUT calls SHARD and FUNFIN for σ_T and AHARD and FUNFIN for σ_{FB}

The flag value ICUT=2 also sets the flag IFAST=1 in ZUCUTS, so subroutine SFAST is called in ZCUT. We call ICUT=2 in the calculational chain related to subroutine SFAST since it is a generalization of the numerically fastest case with no cuts but on s'. In all other cases, the calculations are done by subroutine SCUT (with IFAST=0)[12].

The hard flux functions H_B^a for the acollinearity cut are called from essentially five different functions in ZFITTER: SHARD, AHARD, FCROS, FASYM, and FUNFIN. Functions SHARD and AHARD call the hard corrections for the integrated cross-sections from subroutines SHFULL, AHFULL (integration region I) and SHCUTACOL, AHCUTACOL (integration regions II and III) from the linked package acol.f. The complete hard corrections with all cuts are then further defined by subroutines RADTIN, RTFUN0, RTFUN1 and RADFBIN, RFBFUN0, RFBFUN1. Similarly, functions FCROS and FASYM call SHACOL, AHACOL for the shorter expressions without acceptance cut ($c = 1$).

The angular distributions $d\sigma_{T,FB}/d\cos\vartheta$ are calculated via subroutine ZANCUT, and the acollinearity cut is chosen with flag ICUT=2 (or equivalently, ICUT=3). The hard flux functions $H_B^a(R, A(R), \cos\vartheta)$ are derived by function HARD. In HARD, subroutine HCUT is called which itself uses subroutines HINIM for the initial state contributions H_B^{ini} and HINTFM for the initial-final state interference contributions H_B^{int}. Final state corrections are again provided by subroutine FUNFIN. One should mention that FUNFIN is always

[12]In order to maintain compatibility with earlier releases, the branch ICUT=0 (corresponding to the old coding for general cuts) also calculates with the old coding of the final state corrections (flag IFUNFIN=0), while all other branches use the newly corrected final state contributions (flag IFUNFIN=1).

called in subroutine BORN so final state corrections are always considered together with the (effective) Born observables.

Phase space splitting with acollinearity cut

At this point one has to note that the treatment of mass singularities in the hard initial state and initial-final state interference contributions (when setting the initial state mass m_e to zero) necessitates a splitting of the remaining phase space of $\cos\vartheta$ and s' into different regions of phase space with different analytical expressions. This is due to the fact that squared matrix elements contain, from initial state radiation and the initial-final state interference, the electron (positron) propagator after radiation of a photon, and these terms are proportional to

$$\frac{1}{Z_{1(2)}} = -\frac{1}{(k_{1(2)}-p)^2-m_e^2} = \frac{1}{2k_{1(2)}p} \tag{1.5.37}$$

up to the second power of this expression. In the course of the analytical integration over the first two angles of phase space (φ_γ and θ_γ) they generate logarithmic expressions with vanishing arguments when neglecting the electron mass m_e. This happens for certain values of $\cos\vartheta$ depending on the remaining kinematical variable R and the applied cuts. One has to distinguish four different regions of phase space for $\cos\vartheta$ and R, each region with different analytical expressions for the radiators $H_B^{ini,int}(R, A(R), \cos\vartheta)$ of the angular distribution. In turn, four (or respectively six) different expressions for the integrated results $H_T^{ini,int}(R, A(R), c)$ ($H_{FB}^{ini,int}$) have to be used in ZFITTER. For a detailed analysis on this issue see [43]. The phase space splitting for the initial state and interference terms is organized by subroutine PHASEREGC. PHASEREGC decides which phase space region and which correponding formulae have to be chosen depending on c (or $\cos\vartheta$), R, ξ^{max}, and E_{min}.

Without acceptance cut ($c = 1$), the number of different cases and analytical expressions for $H_T^{ini,int}(R, A(R), C)$ in phase space boil down to one, and for $H_{FB}^{ini,int}(R, A(R), C)$ down to two ($C = \cos\vartheta, c$) [11]. These results are very compact and attached to the SFAST branch of ZFITTER.

Hard radiators without acceptance cut ($c = 1$)

The hard corrections H_B^a for $c = 1$ to the integrated flux functions [11] are written below. They are defined – as stated above – in subroutines SHACOL and AHACOL. For brevity we set everywhere $A \equiv A(R)$. The hard contributions to $\sigma_T(R)$ are:

$$H_T^{ini}(R;A) = \frac{3\alpha}{4\pi}Q_e^2 \cdot \left[\left(A+\frac{A^3}{3}\right)\frac{1+R^2}{1-R}\left(\ln\frac{s}{m_e^2}-1\right)+(A-A^3)\frac{2R}{1-R}\right], \tag{1.5.38}$$

$$H_T^{int}(R;A) = -\frac{\alpha}{\pi}Q_eQ_f \cdot \frac{4AR(1+R)}{1-R}, \tag{1.5.39}$$

$$H_T^{fin}(R;s,A) = \frac{\alpha}{\pi}Q_f^2 \cdot \left[\frac{1+R^2}{1-R}\ln\frac{1+A}{1-A} - \frac{8A\cdot m_f^2/s}{(1-A^2)(1-R)} - A(1-R)\right]. \tag{1.5.40}$$

For $\sigma_{FB}^{ini,int}(R)$, two cases have to be distinguished depending on the parameter A_0:

$$A_0(R) = \frac{1-R}{1+R}. \tag{1.5.41}$$

For $A > A_0$ (as is the case in the entire region I with $A = 1$):

$$\begin{aligned} H_{FB}^{ini}(R; A \geq A_0) &= \frac{\alpha}{\pi} Q_e^2 \cdot \frac{1+R^2}{1-R} \left[\frac{4R}{(1+R)^2} \left(\ln \frac{s(1+R)^2}{4m_e^2 R} - 1 \right) \right. \\ &\quad - \frac{1}{(1+R)^2} \left[y_+ y_- \ln |y_+ y_-| + 4R \ln(4R) \right] \\ &\quad \left. - (1-A^2) \left(\ln \frac{s}{4m_e^2 (1+A)^2 R} - 1 \right) \right] \\ &\quad + \frac{4A(1-A)R}{1-R}, \end{aligned} \tag{1.5.42}$$

$$\begin{aligned} H_{FB}^{int}(R, A \geq A_0) &= \frac{\alpha}{\pi} Q_e Q_f \cdot \left\{ \frac{3R}{2} \left[\ln \frac{z_+}{z_-} + \frac{2 - R + \frac{5}{3}R^2}{1-R} \ln R \right] \right. \\ &\quad - \frac{1+R}{2(1-R)} (5 - 2R + 5R^2) \ln \frac{(1+R)(1+A)}{2} \\ &\quad + \frac{1}{4(1-R)} \left[\frac{(1 - 4R + R^2)[A(1+R)^2 - (1-R)^2]}{1+R} \right. \\ &\quad \left. \left. + 2A(1-A)(1+R^3) \right] \right\}. \end{aligned} \tag{1.5.43}$$

While, for $A < A_0$:

$$\begin{aligned} H_{FB}^{ini}(R; A < A_0) &= \frac{\alpha}{\pi} Q_e^2 \cdot \frac{1+R^2}{1-R} \left[-\frac{y_+ y_-}{(1+R)^2} \ln \left| \frac{y_+}{y_-} \right| + (1-A^2) \ln \frac{1+A}{1-A} \right] \\ &\quad + \frac{8AR^2}{(1+R)(1-R)}, \end{aligned} \tag{1.5.44}$$

$$H_{FB}^{int}(R, A < A_0) = \frac{3\alpha}{2\pi} Q_e Q_f \cdot \; R \left\{ \ln \frac{z_+}{z_-} - \frac{2 - R + \frac{5}{3}R^2}{1-R} + A(1-R) \right\}. \tag{1.5.45}$$

The hard contribution to σ_{FB}^{fin} is in both cases:

$$H_{FB}^{fin}(R; s, A) = H_T^{fin}(R; s, A) + \frac{\alpha}{\pi} Q_f^2 \cdot \left[A(1-R) - (1+R) \ln \frac{z_+}{z_-} \right]. \tag{1.5.46}$$

The abbreviations used are

$$y_\pm = (1-R) \pm A(1+R), \tag{1.5.47}$$

$$z_\pm = (1+R) \pm A(1-R). \tag{1.5.48}$$

We just mention that the final state mass m_f must be included for the final state contributions H_B^{fin} in region I, where $A = \sqrt{1 - 4m_f^2/s'}$. For this case, the formulae from Eq. (1.5.38) to Eq. (1.5.41) deliver the already well known results from [10,15,9] (with acceptance cut) or [52] (no cuts) and are therefore calculated by subroutines `SHFULL` and `AHFULL` for region I in `SHARD` or are directly inserted in `FCROS` and `FASYM` for region I in `SFAST`.

Finally, soft and virtual corrections $S^{ini,int}_{T,FB}$ are taken care of as was the case for the s' cut (see Section 1.4). Subtractions from the hard corrections $H^{ini,int}_{T,FB}$, so that the overall radiators $R^{ini,int}_B$ in `SHARD`, `AHARD`, `FCROS`, and `FASYM` are finite at $v \to 0$, affect only region I.

The complete hard radiator functions $\bar{H}^{ini,fin}_{T,FB}(R, A(R), \cos\vartheta)$ for the angular distributions to order $\mathcal{O}(\alpha)$ with all cuts, as well as their integrals over $\cos\vartheta$, will be given elsewhere [49].

1.5.4. Common soft photon exponentiation of initial and final state radiation

The final state correction factor is needed both for the calculation of the soft+virtual initial state corrections (integration of functions `SSOFT, ASOFT` which delivers the terms `SSFT, ASFT` in `SCUT`) and the hard one (attached to `SHINI, AHINI` and calculated in `SHARD, AHARD` in `SCUT`). This treatment of final state effects is done in a completely analogous way in subroutine `COSCUT` (angular distributions) and similarly in subroutine `SFAST` (special cuts). Thus, the final state factors are calculated by several calls to subroutine `FUNFIN`, which itself is called from subroutine `BORN`:

$$\texttt{SFIN} = \bar{R}^{fin}_T(R), \tag{1.5.49}$$

$$\texttt{AFIN} = \bar{R}^{fin}_{FB}(R). \tag{1.5.50}$$

In case of common initial and final state soft photon exponentiation, final state radiation is taken into account in Eq. (1.5.35) and Eq. (1.5.36) as follows [9]:

$$\begin{aligned}\bar{R}^{fin}_B(R) &= \int_{R_{min}/R}^1 du \left[[1+\bar{S}^{fin}(\beta'_f)]\beta'_f(1-u)^{\beta'_f-1}\theta(u-R_{max}) + \bar{H}^{fin}_B(u)\right] \\ &= [1+\bar{S}^{fin}(\beta'_f)](1-R_{max})^{\beta'_f} + \bar{G}_B(R),\end{aligned} \tag{1.5.51}$$

with

$$R_{max} = max\left(\frac{R_{min}}{R}, R_E\right), \tag{1.5.52}$$

$$\bar{G}_B(R) = \int_{R_{min}/R}^1 du\ \bar{H}^{fin}_B(u). \tag{1.5.53}$$

The $\bar{S}^{fin}(\beta'_f)$ and β'_f are defined in Eq. (1.4.30) and Eq. (1.4.31). For region I, the hard radiator part $\bar{G}_B(v)$ was introduced in Eq. (1.4.29) and an analytical expression was given there. For the other two regions, one has to perform the integration of H^{fin}_B over u taking into account the dependence of $A(u)$ on the integration variable u. So the hard contributions $\bar{G}_B(R)$ are explicitly integrated in the following way:

$$\begin{aligned}\bar{G}_B(R) &= \left\{\int_{R_{min}/R}^1 du\theta\,(u-R_E) + \ \theta\left(R_E - \frac{R_{min}}{R}\right)\int_{R_{min}/R}^{R_E} du\right. \\ &\quad \left. - \theta\left(R_\xi - \frac{R_{min}}{R}\right)\int_{R_{min}/R}^{R_\xi} du\right\}\bar{H}^{fin}_B(u) \\ &= \left\{\int_{R_{min}/R}^1 du\theta\,(u-R_E) + \ \theta\left(R - \frac{R_{min}}{R_E}\right)\int_{R_{min}/R}^{R_E} du\right. \\ &\quad \left. - \theta\left(R - \frac{R_{min}}{R_\xi}\right)\int_{R_{min}/R}^{R_\xi} du\right\}\bar{H}^{fin}_B(u).\end{aligned} \tag{1.5.54}$$

Further, for regions II and III – with the soft-photon corner being in region I – ZFITTER adds or subtracts the integrals over the unregularized hard flux functions:

$$\bar{H}_B^{fin}(u) = H_B^{fin}(u), \tag{1.5.55}$$

while in region I the regularized hard radiator is integrated for $R > R_{max}$ and added.

These results are included in the terms SHRD and AHRD1 which arise from integation of functions SHARD, AHARD over R in subroutine SCUT, as indicated in Eq. (1.5.54). These final state corections SFIN, AFIN are contained in subroutine BORN (which is called in SHARD,AHARD) as factors to the effective Born cross-sections. In a similar fashion the acollinearity options of subroutines SFAST and COSCUT are organized with terms SHRD, AHRD1 substituted by term HRD, or by terms CROS,ASYM respectively, and functions SHARD, AHARD replaced by function HARD, or by functions FCROS, FASYM respectively. This dependence of $A(u)$ on the integration variable u presents an additional complication compared to region I with $A = 1$. Nevertheless, the integrations have been done analytically with exclusion of two logarithms. The results of the hard integration over u for region II are found in subroutine FUNFIN ($R_{II} \equiv R_E$):

$$\begin{aligned}
\bar{G}_{T,II}(R) &= \frac{\alpha Q_f^2}{\pi} \int_{R_{min}/R}^{R_{II}} du \left[\frac{1+u^2}{1-u} \ln \frac{1+A_{II}(u)}{1-A_{II}(u)} - A_{II}(u)(1-u) \right] \\
&= \frac{\alpha Q_f^2}{\pi} \left[\texttt{ALE1I} + D_1 \left(\frac{1}{2} D_1 - D_2 \right) \right], \qquad (1.5.56) \\
\bar{G}_{FB,II}(R) &= \frac{\alpha Q_f^2}{\pi} \int_{R_{min}/R}^{R_{II}} du \left[\frac{1+u^2}{1-u} \ln \frac{1+A_{II}(u)}{1-A_{II}(u)} \right. \\
&\quad \left. + (1+u) \ln \frac{(1+u) + A_{II}(u)(1-u)}{(1+u) - A_{II}(u)(1-u)} \right] \\
&= \frac{\alpha Q_f^2}{\pi} \left[\texttt{ALE1I} + \texttt{ALE2I} \right], \qquad (1.5.57)
\end{aligned}$$

with

$$\begin{aligned}
D_1 &= \texttt{ALIM} - \texttt{RECUT2} = \frac{R_{min}}{R} - R_{II}, \qquad (1.5.58) \\
D_2 &= \texttt{RECUT2} - 1 = R_{II} - 1, \qquad (1.5.59)
\end{aligned}$$

and $A_{II}(u)$ defined in Eq. (1.5.16). The electromagnetic coupling is defined in Section 3.6.2. Functions ALE1I and ALE2I are the integrals over the logarithms. In ZFITTER, they are obtained from an interpolation of tabulated values of these integrals (over region II) of:

$$\begin{aligned}
\texttt{FAL1(u)} &= \frac{1+u^2}{1-u} \ln \frac{1+A(u)}{1-A(u)}, \qquad (1.5.60) \\
\texttt{FAL2(u)} &= -(1+u) \ln \frac{N_+(u)}{N_-(u)}, \qquad (1.5.61) \\
N_\pm(u) &= (1+u) \pm A(u)(1-u). \qquad (1.5.62)
\end{aligned}$$

In fact, the two logarithms are integrated numerically. This is done using SIMPS, for predefined small, and rising intervals of u inside the integration region, thus forming a table

with 20 entries (NP=20), the fields being called ALEi and ALAi ($i = 1, 2$) for regions II and III, repectively. This table then is used for the truly needed integrations ALAiI, ALEiI, $i = 1, 2$, by interpolation with subroutine INTERP, called in FUNFIN for the calculation of factors SFIN and AFIN. The factors are calculated in three steps, in the following order: II + I – III.

For equidistant points, fulfilling $x_1 < x_2 < x_3$ and distance Δ, the interpolation is done with the Lagrange interpolation formula:

$$f(x) = \frac{1}{2\Delta^2}\left[(x-x_1)(x-x_2)y_3 - 2\,(x-x_1)(x-x_3)y_2 + (x-x_2)(x-x_3)y_1\right]. \tag{1.5.63}$$

This formula is realized in INTERP and makes a quadratic interpolation of the integral over u of the two logarithms mentioned using tables. The tables are prepared by SETFIN using SIMPS for selected values of R_{min}/R, covering the full regions II and III.

Analogously, for region III (to be subtracted) ($R_{III} \equiv R_\xi$):

$$\begin{aligned}
\texttt{SFIN}^{III} &= \frac{\alpha Q_f^2}{\pi}\int_{R_{min}/R}^{R_{III}} du\left[\frac{1+u^2}{1-u}\ln\frac{1+A_{III}(u)}{1-A_{III}(u)} - A_{III}(u)(1-u)\right] && (1.5.64)\\
&= \frac{\alpha Q_f^2}{\pi}\left[\texttt{ALA1I} + \frac{1}{2}\left((R_{min}/R+B)\texttt{SQR} - (1-B^2)\ln\left|\frac{\texttt{RACUT}+B}{\texttt{SQR}+R_{min}/R+B}\right|\right)\right],\\
\texttt{AFIN}^{III} &= \frac{\alpha Q_f^2}{\pi}\int_{R_{min}/R}^{R_{III}} du\left[\frac{1+u^2}{1-u}\ln\frac{1+A_{III}(u)}{1-A_{III}(u)}\right.\\
&\quad \left. + (1+u)\ln\frac{(1+u)+A_{III}(u)(1-u)}{(1+u)-A_{III}(u)(1-u)}\right]\\
&= \frac{\alpha Q_f^2}{\pi}\left[\texttt{ALA1I} + \texttt{ALA2I}\right], && (1.5.65)
\end{aligned}$$

with $A_{III}(u)$ defined in Eq. (1.5.17) and

$$\begin{aligned}
\texttt{SQR} &= \sqrt{\max\left[0, (R_{min}/R)^2 + 2BR_{min}/R + 1\right]}, && (1.5.66)\\
B &= -\frac{1+\sin^2(\xi^{max}/2)}{\cos^2(\xi^{max}/2)}, && (1.5.67)\\
\texttt{RACUT} &= R_{III}. && (1.5.68)
\end{aligned}$$

Functions ALE1I and ALE2I are again the integrals over the logarithms, obtained from an interpolation of tabulated values of these integrals (over region III now) of Eq. (1.5.60) and Eq. (1.5.61).

1.6. Higher Order QED Corrections

1.6.1. Virtual and soft photonic and fermion pair production corrections

There are two classes of ISR QED corrections: *photonic* and *fermion pair production* corrections. Photonic corrections are governed by flag FOT2 and pair production corrections by flag ISPP.

For the photonic corrections in ZFITTER three different radiators are accessible:

- FOT2=0,3 – additive radiator of the Kuraev-Fadin type [53]
- FOT2=4 – the QED-E radiator, Eqs. (3.31) and (3.32) of [54] (F. Berends and W. van Neerven, unpublished)
- FOT2=5 – "pragmatic" factorized radiator, Eq. (63) of [55]

For fermion pair production corrections the following options are accessible:

- ISPP=–1 – a "fudge" implementation using formulae of [56]
- ISPP=0 – pair corrections are switched off
- ISPP=1 – an implementation fully consistent with [56], supplemented by a naive reweighting procedure; option used in [57][13]
- ISPP=2 – allows to include the singlet channel and higher orders according to [37]
- ISPP=3 – according to [58]
- ISPP=4 – as ISPP=3, but supplemented by an extended treatment of hadronic pairs [37]

Photonic corrections

Higher order photonic corrections are applied up to the third order leading log contribution of order $\mathcal{O}\left((\alpha L)^3\right)$.

All the higher order virtual and soft photonic corrections are determined in subroutine SETFUN.

The second order virtual and soft pure photonic corrections $S^{(2)}$ in Eq. (1.3.9) are calculated following Eq. (2.30) of [59]; for the third order correction we follow [60]:

$$S^{(2+3)} = \left(\frac{\alpha}{\pi}\right)^2 \delta_2^{V+S} + \left(\frac{\alpha}{\pi}\right)^3 \delta_3^{V+S} \tag{1.6.1}$$

$$\begin{aligned}\delta_2^{V+S} &= \left(\frac{9}{8} - 2\zeta(2)\right) L_e^2 + \left[-\frac{45}{16} + \frac{11}{2}\zeta(2) + 3\zeta(3)\right] L_e \\ &\quad + \left[-\frac{6}{5}\zeta(2)^2 - \frac{9}{2}\zeta(3) - 6\zeta(2)\ln 2 + \frac{3}{8}\zeta(2) + \frac{19}{4}\right],\end{aligned} \tag{1.6.2}$$

$$\delta_3^{\mathrm{V+S}} = (L_e - 1)^3 \left[\frac{9}{16} - 3\zeta(2) + \frac{8}{3}\zeta(3)\right]. \tag{1.6.3}$$

The terms proportional to L_e^2 are taken into account for setting FOT2=0 (or higher), those to L_e for FOT2=1 (or higher), the non-logarithmic ones for FOT2=2 (or higher).

[13] This option produces reasonable numbers below and at the Z resonance and begins to quickly deteriorate above the resonance; for this reason it is considered now as obsolete option.

Pair production corrections

The virtual and soft corrections from initial state fermion pair production $\delta^{V+S,p}$ are included following Eq. (21) of [56]:

$$\delta^{V+S,p} = \left(\frac{\alpha}{\pi}\right)^2 \sum_{n=e,\mu,\tau,h} P_n^{V+S}, \tag{1.6.4}$$

$$\begin{aligned} P_n^{V+S} &= \left[R(\infty)\left(\frac{1}{2}L_n^2 - \zeta(2)\right) + R_0 L_n + R_1\right]\left(\frac{2}{3}l + \frac{1}{2}\right) \\ &\quad + [R(\infty)l + R_0]\left(\frac{2}{3}l^2 - \frac{7}{12}\right) + R(\infty)\left[\frac{4}{9}L_n^3 + \frac{2}{3}\zeta(3) + \frac{5}{8}\right], \end{aligned} \tag{1.6.5}$$

where:

$$L_n = \ln\frac{s}{m_n^2} \quad \text{for leptons,} \tag{1.6.6}$$

$$L_h = \ln\frac{s}{4m_\pi^2} \quad \text{for hadrons,} \tag{1.6.7}$$

$$m_\pi = 0.1396 \ \text{GeV}, \tag{1.6.8}$$

$$l = \ln\frac{2\delta}{\sqrt{s}}, \tag{1.6.9}$$

$$\frac{\delta}{\sqrt{s}} = \begin{cases} 0.0055 & \texttt{ISPP} = -1 \\ 10^{-6} & \texttt{ISPP} = 1 \end{cases}. \tag{1.6.10}$$

The constant PAIRDL=$\delta/\sqrt{s}$ is an auxiliary parameter used to adjust a smooth connection of soft and hard radiation parts, with $2m/\sqrt{s} \ll \delta/\sqrt{s} \ll (1-\sqrt{R})$.

The additional constants are for hadrons:

$$R(\infty) = 4.0, \tag{1.6.11}$$

$$R_0 = -8.31, \tag{1.6.12}$$

$$R_1 = 13.1, \tag{1.6.13}$$

and for leptons:

$$R(\infty) = 1, \tag{1.6.14}$$

$$R_0 = -\frac{5}{3}, \tag{1.6.15}$$

$$R_1 = \frac{28}{9} - \zeta(2). \tag{1.6.16}$$

Further abbreviations are:

$$\zeta(2) = \frac{\pi^2}{6}, \tag{1.6.17}$$

$$\zeta(3) = 1.202\,056\,903\,159\,6. \tag{1.6.18}$$

For ISPP =–1, pairs are treated like photons, i.e. their $V+S$ contributions are added to the photonic ones. In this way an interplay of pairs with photons is realized.

1.6.2. Hard corrections for the total cross-section

The higher order hard corrections consist of hard photonic corrections and of hard contributions due to real initial state fermion pair production. The influence of flags `FOT2` and `ISPP` is described in Section 1.6.1.

For σ_T and for `ISPP` = –1, both photonic and pair production contributions are calculated in function `SH2`, which is called by function `FCROS` for the cross-sections without cuts, by function `SHFULL` for the integrated cross-sections, and by function `HARD` for the differential cross-section:

$$H_T^{(2+3)}(v) \;=\; h_T^{(2+3)} + h_T^p. \tag{1.6.19}$$

We remind that $v = 1 - z,\ z = R$.

For `ISPP` ≥ 1, the pair production contribution is calculated in function `PH2`. For `ISPP` = 1, instead of Eq. (1.6.19) one applies a "reweighting" procedure, which may be described as follows:

$$\sigma^{\rm QED} = \sigma^{\rm photonic}\left(1 + \delta^{V+S,p} + \delta^{H,p}\right), \tag{1.6.20}$$

where $\delta^{V+S,p}$ is given by Eq. (1.6.5) and

$$\delta^{H,p} = \frac{\sigma^{H,p}}{\sigma^{\rm Born}}\,. \tag{1.6.21}$$

Finally, for the implementation of pairs for `ISPP` ≥ 2 we refer the reader to [37].

Photonic corrections

The hard photonic corrections are calculated according to $\tilde{\delta}_2^H$ (Eq. (2.30) of [59]):

$$h_T^{(2+3)} \;=\; \left(\frac{\alpha}{\pi}\right)^2 \tilde{\delta}_2^H + \left(\frac{\alpha}{\pi}\right)^3 \tilde{\delta}_3^H, \tag{1.6.22}$$

$$\tilde{\delta}_2^H \;=\; h_2 L_e^2 + h_1 L_e + h_0, \tag{1.6.23}$$

$$h_2 \;=\; -\frac{1+z^2}{1-z}\ln z + (1+z)\left[-2\ln(1-z) + \frac{1}{2}\ln z\right] - \frac{5}{2} - \frac{z}{2}\,, \tag{1.6.24}$$

$$\begin{aligned} h_1 \;=\; & \frac{1+z^2}{1-z}\left[{\rm Li}_2(1-z) + \ln z \ln(1-z) + \frac{7}{2}\ln z - \frac{1}{2}\ln^2 z\right] \\ & +(1+z)\left[\frac{1}{4}\ln^2 z + 4\ln(1-z) - 2\zeta(2)\right] - \ln z + 7 + \frac{z}{2}\,, \end{aligned} \tag{1.6.25}$$

$$\begin{aligned} h_0 \;=\; & \frac{1+z^2}{1-z}\left[-\frac{1}{6}\ln^3 z + \frac{1}{2}\ln z {\rm Li}_2(1-z) + \frac{1}{2}\ln^2 z \ln(1-z)\right. \\ & \left. -\frac{3}{2}{\rm Li}_2(1-z) - \frac{3}{2}\ln z \ln(1-z) + \zeta(2)\ln z - \frac{17}{6}\ln z - \ln^2 z\right] \\ & +(1+z)\left[\frac{3}{2}{\rm Li}_3(1-z) - 2S_{1,2}(1-z) - \ln(1-z){\rm Li}_2(1-z) - \frac{5}{2}\right] \\ & -\frac{1}{4}(1-5z)\ln^2(1-z) + \frac{1}{2}(1-7z)\ln z \ln(1-z) \end{aligned}$$

$$
\begin{aligned}
&-\frac{25}{6}z\mathrm{Li}_2(1-z)+\left(1+\frac{19}{3}z\right)\zeta(2)-\left(\frac{1}{2}+3z\right)\ln(1-z)\\
&+\frac{1}{6}(11+10z)\ln z+\frac{2}{(1-z)^2}\ln^2 z-\frac{25}{11}z\ln^2 z\\
&-\frac{2z}{3(1-z)}\left[1+\frac{2}{1-z}\ln z+\frac{1}{(1-z)^2}\ln^2 z\right] \qquad (1.6.26)
\end{aligned}
$$

$$
\begin{aligned}
\delta_3^H &= (L_e-1)^3\frac{1}{6}\Big\{-\frac{27}{2}+\frac{15}{4}v+4\left(1-\frac{v}{2}\right)\left[6\zeta(2)-6\ln^2 v+3\mathrm{Li}_2 2\,(v)\right]\\
&+3\left(-\frac{6}{v}+7-\frac{3}{2}v\right)\ln(1-v)+\left(\frac{4}{v}-7+\frac{7}{2}v\right)\ln^2(1-v)\\
&-6\,(6-v)\ln v+6\left(-\frac{4}{v}+6-3v\right)\ln(1-v)\ln v\Big\}. \qquad (1.6.27)
\end{aligned}
$$

Pair production corrections

The hard part of the initial state corrections due to fermion pair creation is according to Eqs. (22) and (23) of [56]:

$$
h_T^p = \theta(R-z_{\min})\theta\left[(1-\sqrt{R})^2-\delta^2\right]\left[h_e^p+h_\mu^p+h_\tau^p+h_{had}^p\right], \qquad (1.6.28)
$$

$$
\begin{aligned}
h_{had}^p &= \left(\frac{\alpha}{\pi}\right)^2\frac{1}{3}\Bigg\{\frac{1+z^2}{(1-z)}\left[R(\infty)\left(\frac{1}{2}\ln^2\frac{s(1-z)^2}{4m_\pi^2 z}-\zeta(2)\right)+R_0\ln\frac{s(1-z)^2}{4m_\pi^2 z}+R_1\right]\\
&-(1-z)\left[R(\infty)\left(2\ln\frac{s(1-z)^2}{4m_\pi^2 z}-3\right)+2R_0\right]\\
&-R(\infty)\left[\frac{z^2}{1-z}\left(\frac{1}{2}\ln^2 z+\mathrm{Li}_2(1-z)\right)+\ln z\right]\Bigg\}, \qquad (1.6.29)
\end{aligned}
$$

$$
\begin{aligned}
h_\mu^p &= \left(\frac{\alpha}{\pi}\right)^2\frac{1}{3}\Bigg\{\frac{1+z^2}{2(1-z)}\bar{L}_\mu^2+\left[\frac{1+z^2}{1-z}\left(\ln\frac{(1-z)^2}{z}-\frac{5}{3}\right)-2(1-z)\right]\bar{L}_\mu\\
&+\frac{1+z^2}{1-z}\left(\frac{1}{2}\ln^2\frac{(1-z)^2}{z}-\frac{5}{3}\ln\frac{(1-z)^2}{z}-2\zeta(2)+\frac{28}{9}\right)\\
&-(1-z)\left(2\ln\frac{(1-z)^2}{z}-\frac{19}{3}\right)-\frac{z^2}{1-z}\left[\frac{1}{2}\ln^2 z+\mathrm{Li}_2(1-z)\right]-\ln z\Bigg\}, \qquad (1.6.30)
\end{aligned}
$$

with $\bar{L}_\mu=\ln(s/m_\mu^2)$, etc., and

$$
z_{\min} = \frac{s'_{\min}}{s}\,. \qquad (1.6.31)
$$

We use further:

$$
\mathrm{Li}_3(y)\equiv S_{2,1}(y) = \int_0^1\frac{dx}{x}\ln x\ln(1-xy)=\int_0^y\frac{dx}{x}\mathrm{Li}_2(x), \qquad (1.6.32)
$$

$$
S_{1,2}(y) = \frac{1}{2}\int_0^1\frac{dx}{x}\ln^2(1-xy)=\frac{1}{2}\int_0^y\frac{dx}{x}\ln^2(1-x). \qquad (1.6.33)
$$

For their numerical calculation in the routines `TRILOG` and `S12` we use [25].

In order to get a better agreement with the pair production correction shown in Figure 4, bottom dotted curve of [58], we somewhat arbitrarily multiplied the soft and hard muonic corrections by a correction factor,

$$\texttt{CORFAC} = 2.6. \tag{1.6.34}$$

This factor is set in subroutine `SETFUN` and used for `ISPP`=–1 only; an outdated option, which is retained for backward compatiblity.

1.6.3. Hard corrections for the forward-backward asymmetry

The corresponding corrections for σ_{FB} are calculated in function `AH2`, which is called by function `FASYM` for the cross-sections without cuts, by function `AHFULL` for the integrated cross-sections, and by function `HARD` for the differential cross-section:

$$H_{FB}^{(2)}(v) \;=\; h_T^{(2)} + \delta h_{FB}^{(2)}\,, \tag{1.6.35}$$

where the $h_T^{(2)}$ is taken over from Eq. (1.6.19), and the additional correction in leading logarithmic approximation is:

$$\begin{aligned}\delta h_{FB}^{(2)} \;=\; & \frac{1}{4}\left(\frac{\alpha}{\pi}\right)^2 L_e^2\Bigg[\frac{(1-z)^3}{2z} + \frac{(1-z)^2}{\sqrt{z}}\left(\arctan\frac{1}{\sqrt{z}} - \arctan\sqrt{z}\right) \\ & -(1+z)\ln z + 2(1-z)\Bigg] + \mathcal{O}(\alpha^3).\end{aligned} \tag{1.6.36}$$

The correction $\delta h_{FB}^{(2)}$ is coded according to $\tilde{\Phi}_{FB}$ from Eq. (2.35) of [61], where it was calculated for the total forward-backward asymmetry without cuts.

The initial state fermion pair production correction h_{FB}^{p} is unknown and set equal to zero.

Chapter 2

Pseudo-Observables

2.1. Introduction

In this Section we describe the calculation of the so-called *pseudo-observables*, PO, which are used for the combination of LEP data from the four LEP Collaborations [62,63], and which are also needed for the calculation of the cross-sections within the Standard Model. The various cross-sections, asymmetries, or polarizations are called *realistic observables*.

Pseudo-observables, which may derived from them, are usually definition dependent quantities. Typical examples of pseudo-observables are partial Z-decay widths, Γ_f, effective sinuses of weak mixing angles, $\sin^2\theta^f_{\rm eff}$, the parameter Δr, or more general — amplitude form factors. In some renormalization schemes the W-boson mass, M_W, may be also considered as a PO.

For the calculations of POs `ZFITTER` uses the `DIZET` package which relies on the so-called *on-mass-shell (OMS)* renormalization scheme [3,4].

2.2. Input Parameters

2.2.1. Input parameter set

A very important notion is the notion of an *input parameter set*, IPS, i.e. the choice of the input parameters of a given renormalization scheme.

Our OMS uses the masses of all fundamental particles, both fermions and bosons, and two coupling constants: $\alpha(0)$ and $\alpha_s(M_Z^2)$. There is the exception of the ill-defined masses of light quarks u, d, c, s and b: they are excluded and replaced by $\alpha(M_Z^2)$ by making use of a dispersion relation Eq. (2.2.39) between the real and imaginary parts of the hadronic vacuum polarization $\Pi^{\rm R}(s)$ Eq. (2.2.40) and the optical theorem relating the imaginary part with the total cross-section $\sigma_{\rm tot}\left(e^+e^-\to\gamma^*\to{\rm hadrons}\right)$ [27]. More details are given in Subsection 2.2.3.

More rigorously, in this way we exclude mass singular logarithmic terms like $\ln(m_q^2/s)$, while power suppressed terms of order $\mathcal{O}\left(m_q^2/M_Z^2\right)$ are either totally ignored for light quarks (u, d and s), or are kept only in FSR QCD corrections for heavy quarks (c and b), or are treated within the language of effective quark masses (see Subsection 3.6.3). For the description of the FSR QCD corrections we use the notion of running masses in the $\overline{MS}$ scheme. This introduces into the IPS the pole masses of c and b quarks. They are

set inside subroutine QCDCOF and are not supposed to be varied by the user.

The knowledge about the hadronic vacuum polarization is contained in the quantity $\Delta\alpha_h^{(5)}(M_Z^2)$, which is treated as one of the input parameters and used in parallel to $\alpha(0)$ since the latter is also needed at least for the ISR corrections.

The $\Delta\alpha_h^{(5)}(M_Z^2)$ can be either computed from quark masses or, preferrably, fitted to experimental annihilation data. In the DIZET package both treatments are foreseen; see the description of user option ALEM in Appendix 4.1.3.

Nowadays, the mass of the W boson is experimentally known with a precision of about 60 MeV both from $p\bar{p}$ and e^+e^- measurements, that is, with a combined precision of about 40 MeV. Although this precision is supposed to be reduced further with future LEP2 data taking and analysis and with forthcoming improvements from FNAL, still M_W can be calculated with a better theoretical error exploiting the very precise knowledge of the Fermi constant in μ-decay, G_μ. For this reason, M_W is usually replaced in the IPS by G_μ, see Subsection 2.2.2.

The following parameters are passed to subroutine DIZET by its argument list:

$$\texttt{AMW} = M_W, \tag{2.2.1}$$
$$\texttt{AMZ} = M_Z, \tag{2.2.2}$$
$$\texttt{AMT} = m_t, \tag{2.2.3}$$
$$\texttt{DAL5H} = \Delta\alpha_h^{(5)}(M_Z^2), \tag{2.2.4}$$
$$\texttt{ALSTR} = \alpha_s(M_Z^2). \tag{2.2.5}$$

G_μ is set inside subroutine CONST1 for DIZET together with all the other numerical input for the calculation of POs. Two important constants are:

$$\texttt{ALFAI} = 1/\alpha(0) = 137.0359895, \tag{2.2.6}$$
$$\alpha(0) = \alpha, \tag{2.2.7}$$
$$\texttt{GMU} = G_\mu = 1.16639\,10^{-5}\ \mathrm{GeV}^{-2}; \tag{2.2.8}$$

see also the description of flag GFER, see Subsection 4.1.3. At present they both are also set in subroutine EWINIT. A special auxiliary constant A_0,

$$\texttt{A0} = A_0 = \sqrt{\frac{\pi\alpha(0)}{\sqrt{2}G_\mu}} = 37.28052\ , \tag{2.2.9}$$

is also computed in subroutine CONST1.

Note that Eqs. (2.2.1)–(2.2.5) together with G_μ is over-complete; only two of the three parameters

$$G_\mu, \quad M_W, \quad \text{and} \quad M_Z \tag{2.2.10}$$

are independent. This is exploited by option IMOMS = NPAR(4), see Subsection 2.2.2.

The definition of the *effective quark masses* is initialized in subroutine CONST1 by flag MQ. Effective quark masses are some fitted values which allow to reproduce in the one-loop order the quantity $\Delta\alpha_h^{(5)}(M_Z^2)$. They are also used in power suppressed mass dependent terms of self-energies and in the calculation of various imaginary parts. The power dependence of POs on effective quark masses is very weak (in contrast to the logarithmic

mass singularities) and as far as the effective masses are compatible with a chosen value of $\Delta\alpha_h^{(5)}(M_Z^2)$ the residual theoretical uncertainty is totally ignorable.

For imaginary parts the situation is even better since we usually are well above the thresholds of light quarks where the imaginary parts are equal to $i\pi$ and the precise values of effective masses are irrelevant.

The preferred setting is `MQ`=1 (`MQ` = `ITQ`=2–`IHVP`), and for `IHVP`=1 one uses a set of effective masses, which is compatible with the fit of [27].

All lepton and effective quark masses are set in subroutine `CONST1`.

The lepton masses are taken from [64]:

$$m_\nu = 0, \tag{2.2.11}$$
$$m_e = 0.510\,999\,07 \times 10^{-3}\,\mathrm{GeV}, \tag{2.2.12}$$
$$m_\mu = 0.105\,658\,389\,\mathrm{GeV}, \tag{2.2.13}$$
$$m_\tau = 1.777\,05\,\mathrm{GeV}. \tag{2.2.14}$$

The scheme of determination of quark masses for all applications but QCD final state corrections is as follows. We describe it in some detail since an expert user could like to change the preset values for some reasons. One of three foreseen sets `AMQ(I)` of quark masses is selected. The default setting is:

$$m_u = 0.062\,\mathrm{GeV}, \tag{2.2.15}$$
$$m_d = 0.083\,\mathrm{GeV}, \tag{2.2.16}$$
$$m_c = 1.50\,\mathrm{GeV}, \tag{2.2.17}$$
$$m_s = 0.215\,\mathrm{GeV}, \tag{2.2.18}$$
$$m_t = \texttt{TMASS}, \tag{2.2.19}$$
$$m_b = 4.7\,\mathrm{GeV}. \tag{2.2.20}$$

For the alternative choices of the flag, `IHVP`=2,3, it is chosen:

$$m_u = 0.04145\,\mathrm{GeV}, \tag{2.2.21}$$
$$m_d = 0.04146\,\mathrm{GeV}, \tag{2.2.22}$$
$$m_c = 1.5\,\mathrm{GeV}, \tag{2.2.23}$$
$$m_s = 0.15\,\mathrm{GeV}, \tag{2.2.24}$$
$$m_t = \texttt{TMASS}, \tag{2.2.25}$$
$$m_b = 4.7\,\mathrm{GeV}. \tag{2.2.26}$$

`DIZET` returns the following quantities which are described in this section:

$$\texttt{ALQED} = \alpha(M_Z^2), \tag{2.2.27}$$

the running QED coupling at M_Z^2; further:

$$\texttt{ALSTRT} = \alpha_s(m_t^2), \tag{2.2.28}$$

the running QCD coupling at m_t^2; further:

`ZPAR` – array of useful quantities,

`PARTZ` – array of partial Z-widths,

`PARTW` – array of partial W-widths.

The last three arrays are described in Section 4.1.

The conversion factor, making cross-sections to be measured in nanobarn when energies are used in GeV, is `CONHC`. The settings in subroutine `EWINIT` are:

$$\texttt{CONHC} \;=\; 0.389\,379\,66 \times 10^6\,\mathrm{GeV}^2\mathrm{nbarn}, \tag{2.2.29}$$

and cross-sections are normalized with the factor

$$\texttt{CSIGNB} \;=\; \frac{4}{3}\pi\alpha^2\texttt{CONHC}. \tag{2.2.30}$$

In the OMS renormalization scheme the weak mixing angle is defined uniquely through the gauge-boson masses:

$$\sin^2\theta_W \equiv s_W^2 = 1 - \frac{M_W^2}{M_Z^2}\ . \tag{2.2.31}$$

We should mention here that the calculations of electroweak corrections have been done in `DIZET` in the unitary gauge. The pseudo-observables (the weak form factors in particular) are independent of the gauge since they are (if only in principle) measurable quantities.

2.2.2. Further specification of input quantities

As soon as the IPS is specified, one may calculate some potentially measurable quantity taking into account as many orders of the perturbative series as are available in the literature.

First of all, after a call of `CONST1`, `DIZET` computes by function `XFOTF3` the running QED coupling $\alpha(M_Z^2)$. For the leptonic part, $\Delta\alpha_l$, up to three-loop QED corrections are taken. For $\Delta\alpha_h^{(5)}(M_Z^2)$ the parameterization depends on flag `VPOL`, see Subsection 2.2.3. By call of subroutine `QCDCOF`, FSR QCD corrections include up to four loops, see Subsection 3.6.

Then, `DIZET` offers three opportunities in subroutine `SETCON`, depending on flag `IMOMS`:

- The default is `IMOMS`=1; the W boson mass is calculated iteratively from the equation:

$$M_W = \frac{M_Z}{\sqrt{2}}\sqrt{1+\sqrt{1-\frac{4A_0^2}{M_Z^2\,(1-\Delta r)}}}\ , \tag{2.2.32}$$

  using the standard IPS Eqs. (2.2.1)–(2.2.5).

- The alternative, chosen with `IMOMS`=2 and foreseen for expert users only, calculates iteratively M_Z from G_μ, M_W and other input parameters:

$$M_Z = \frac{M_W}{\sqrt{1-\dfrac{A_0^2}{M_W^2\,(1-\Delta r)}}}\ . \tag{2.2.33}$$

- A third setting, IMOMS=3, was foreseen for the calculation of G_μ from M_W, M_Z by means of iterations of the equation

$$G_\mu = \frac{\alpha\pi}{\sqrt{2}M_W^2(1-M_W^2/M_Z^2)(1-\Delta r)} \tag{2.2.34}$$

  with respect to G_μ. However, this is not realized in the code.

Eq. (2.2.34) follows from the calculation of one-loop EWRC for μ-decay, followed by the renormalization group re-summation of Δr, governed by $\Delta\alpha$:

$$\Delta r = \Delta\alpha(M_Z^2) + \Delta r_{\rm EW}. \tag{2.2.35}$$

The re-summation of $\Delta r_{\rm EW}$ is not justified by renormalization group arguments, it simply 'accompanies' $\Delta\alpha$ in Eq. (2.2.34). The only correct generalization of Eq. (2.2.34) is to compute the next perturbative order and to write an expression which is consistent with higher order calculations. More details about Δr may be found in Subsection 2.3.1.

Eqs. (2.2.32)–(2.2.33) are nothing but algebraic solutions of Eq. (2.2.34) with respect to M_W and M_Z, correspondingly. However, since Δr also depends implicitely on M_W and M_Z, one has to solve them iteratively.

These equations establish interdependences between input parameters using the precisely known quantity G_μ. Actually only IMOMS=1 is meaningful for the analysis of Z-resonance data. That's why IMOMS is fixed in subroutine ZDIZET (a CPU time saving interface to DIZET) and is not accessible to changes by users.

After execution of SETCON, the M_W is computed and the IPS becomes fully specified.

2.2.3. The running QED coupling

The running QED coupling $\alpha(s)$ appears in many places in calculations.

Fermion one-loop insertions to the photon propagator are summed together with the photonic Born diagram to form the matrix element A_γ^{OLA}:

$$A_\gamma^{OLA} = i\chi_\gamma(s)\alpha(s)\gamma_\mu \otimes \gamma_\mu\,. \tag{2.2.36}$$

Dyson summation leads to the change of α into $\alpha(s)$:

$$\alpha(s) = \frac{\alpha(0)}{1-\Delta\alpha^{\rm fer}(s)} = \frac{\alpha(0)}{1-\Delta\alpha^{(5)}(s)-\Delta\alpha^{t}(s)-\Delta\alpha^{\alpha\alpha_S}(s)}\,, \tag{2.2.37}$$

where we explicitly disentangled the one-loop top-quark contribution $\Delta\alpha^t(s)$ and the two-loop irreducible higher-order correction $\Delta\alpha^{\alpha\alpha_S}(s)$.

The function XFOTF3, belonging to the DIZET package, is used to calculate $\alpha(s)$.

In function XFOTF3('ALEM','ALE2','VPOL','QCDC',ITOP,DAL5H,Q2) we use the convention that Q2=$-s$ in the s channel and Q2=t in the t channel.

Important user options are ALEM, ALE2, VPOL, QCDC, described in Section 4.2.2), while ITOP is an internal flag switching on/off for ITOP=1/0 the two last terms in Eq. (2.2.37).

The 5-flavor part is a sum of leptonic and hadronic contributions:

$$\Delta\alpha^{(5)} = \Delta\alpha_l + \Delta\alpha_h^{(5)}. \tag{2.2.38}$$

The leptonic part is assigned to the variable `XCHQ21`, and the hadronic part to `UDCSB`. $\Delta\alpha_h^{(5)}$ might be also treated as an input parameter for the fit.

The $\Delta\alpha^{\alpha\alpha_S}$ correction is given by $\alpha/(4\pi)$ `ALFQCD`.

The result for $\Delta\alpha_h^{(5)}(s)$ was obtained in [27] by making use of a dispersion relation:

$$\Delta\alpha_h^{(5)}(s) = -\frac{\alpha}{3\pi} s \,\mathrm{Re}\int_{4m_\pi^2}^{\infty} ds' \frac{R_\gamma(s')}{s'(s'-s-i\epsilon)}\,, \tag{2.2.39}$$

with

$$R_\gamma(s) = \frac{\sigma(e^+e^- \to \gamma^* \to \text{hadrons})}{\sigma(e^+e^- \to \gamma^* \to \mu^+\mu^-)} \tag{2.2.40}$$

as an experimental input. For the hadronic contribution at M_Z it gives:

$$\Delta\alpha_h^{(5)}(M_Z^2) = 0.0280398. \tag{2.2.41}$$

The parameterization of [27] is chosen with `VPOL`=1 and $\Delta\alpha_h^{(5)}(s)$ is calculated by a call to subroutine `hadr5` [26].

The leptonic one-loop contribution, $\Delta\alpha_l(s)$, is defined by

$$\alpha(s) = \frac{\alpha}{1 - \frac{\alpha}{4\pi}\left[\Pi_{\gamma\gamma}^{\text{fer}}(s) - \Pi_{\gamma\gamma}^{\text{fer}}(0)\right]}\,, \tag{2.2.42}$$

with

$$\Pi_{\gamma\gamma}^{\text{fer}}(s) = 4\sum_f c_f Q_f^2 B_f(-s; m_f, m_f)\,, \tag{2.2.43}$$

$$\begin{aligned} B_f\left(p^2; M_1, M_2\right) &= 2\left[B_{21}\left(p^2; M_1, M_2\right) + B_1\left(p^2; M_1, M_2\right)\right] \\ &= -\frac{1}{\bar{\varepsilon}} + 2\int_0^1 dx x(1-x)\ln\frac{p^2x(1-x) + M_1(1-x) + M_2 x}{\mu^2}\,. \end{aligned} \tag{2.2.44}$$

For the two-loop corrections we use [65] and for the three-loop terms [66]. The contributions in `ZFITTER` are:

$$\Delta\alpha_l = 314.97637\cdot 10^{-4} = [314.18942_{1-\text{loop}} + 0.77616_{2-\text{loop}} + 0.01079_{3-\text{loop}}]\cdot 10^{-4}. \tag{2.2.45}$$

These numbers were derived with leptonic masses taken from [64] and with $M_Z = 91.1867$ GeV. The leptonic contribution is calculated by function `DALPHL`.

The top contribution is given by Eq. (2.3.35), it depends on the mass of the top quark, and we present its numerical value for $m_t = 173.8$ GeV:

$$\Delta\alpha^t(M_Z^2) = -0.585844\cdot 10^{-4}. \tag{2.2.46}$$

The mixed two-loop $\mathcal{O}(\alpha\alpha_s)$ correction arising from $t\bar{t}$ loops with gluon exchange is calculated using formulae from [38]. For more details see Subsection 3.4.2. Its numerical value at $m_t = 173.8$ and $\alpha_s = 0.119$ is

$$\Delta\alpha^{\alpha\alpha_S}(M_Z^2) = -0.103962\cdot 10^{-4}. \tag{2.2.47}$$

All numerical results presented in Chapter 2 are derived with `DIZET` v.6.05 as were those shown in [57].

2.3. Electroweak Renormalization, Parameters $\Delta\rho$ and Δr

In this Subsection we discuss two important ingredients of the renormalization scheme: parameters Δr and $\Delta\rho$.

2.3.1. Δr at one loop

Sirlin's parameter Δr [67] is calculated in subroutine `SEARCH`. There are several user options, depending on the flags `BARB`, `QCDC`, `VPOL`, `MASS`, `ALEM`, `AFMT`, `AMT4`, `HIGS`, `SCRE`, which influence its calculation; see the description of flags in Section 4.2.2.

The one-loop expression for Δr is given by

$$\Delta r = \frac{g^2}{16\pi^2}\left\{-\frac{2}{3} - \Pi^{\rm fer,F}_{\gamma\gamma}(0) + \frac{c_W^2}{s_W^2}\Delta\rho^F + \frac{1}{s_W^2}\left[\Delta\rho_W^F + \frac{11}{2} - \frac{5}{8}c_W^2(1+c_W^2) + \frac{9}{4}\frac{c_W^2}{s_W^2}\ln c_W^2\right]\right\}, \tag{2.3.1}$$

The expression given in our old, short description in [14] and coded in `DIZET` differs from Eq. (2.3.1) only by notations. We give the dictionary:

$$c_W^2 = \texttt{R}, \tag{2.3.2}$$

$$\Pi^{\rm fer,F}_{\gamma\gamma}(0) = \frac{4}{3}\sum_f Q_f^2 \ln\frac{m_f^2}{M_W^2} = \frac{4}{3}\texttt{(SL2+SQ2)}, \tag{2.3.3}$$

$$\Sigma^F_{VV}(x) = V(x), \qquad \text{with} \quad V = W, Z, \tag{2.3.4}$$

$$\Delta\rho^F = W(M_W^2) - Z(M_Z^2) = s_W^2\texttt{(XDWZ1F+XWZ1R1)} \tag{2.3.5}$$

$$\begin{aligned}\Delta\rho_W^F &= W(0) - W(M_W^2) = \texttt{W0F+W0-DREAL(XWM1F+XWM1)} \\ &= \frac{1}{M_W^2}\left[\Sigma^F_{WW}(0) - \Sigma^F_{WW}(M_W^2)\right].\end{aligned} \tag{2.3.6}$$

The one-loop Δr in this form was introduced in appendices (E.8) and (F.3) of [3,4], with the t mass dependent terms being given in the appendix of [8].

In Eq. (2.3.1) are certain combinations of self-energy functions. One of them, appearing in every amplitude form factors, is a gauge invariant quantity which plays a special role in all calculations:

$$\Delta\rho = \frac{1}{M_W^2}\left[\Sigma_{WW}(M_W^2) - \Sigma_{ZZ}(M_Z^2)\right], \tag{2.3.7}$$

2.3.2. The parameter $\Delta\rho$

$\Delta\rho$ is closely related to the well-known Veltman parameter ρ defined in [68,69] as the ratio of neutral and charged current effective coupling constants in neutrino scattering for very low transferredd momentum squares q^2:

$$\rho = \frac{M_W^2}{M_Z^2\cos^2\theta_W^0}, \tag{2.3.8}$$

where

$$\cos^2\theta_W^0 \tag{2.3.9}$$

depends on a weak mixing angle θ_W^0 measured at low q^2. If all radiative corrections (RC) are ignored, then it is equal to

$$c_W^2 = M_W^2/M_Z^2\,. \tag{2.3.10}$$

RCs induce some difference between c_W^2 and $\cos^2\theta_W^0$. To evaluate this difference, let us consider both masses and $\cos^2\theta_W^0$ to be the running quantities (because of RCs) and differentiate Eq. (2.3.8) in the vicinity of $q^2 = 0$:

$$\delta\rho(0) = \frac{\delta M_W^2(0)}{M_Z^2\cos^2\theta_W^0} - \frac{\delta M_Z^2(0) M_W^2}{M_Z^4\cos^2\theta_W^0}\,, \tag{2.3.11}$$

where we made use of the fact that $\delta\cos^2\theta_W^0(0) = 0$. Noting that all *derivatives* δ are of order $\mathcal{O}(\alpha)$ and that the difference between Eqs. (2.3.9) and (2.3.10) is also of order $\mathcal{O}(\alpha)$, we have in the one-loop approximation

$$\delta\rho(0) = \frac{\delta M_W^2(0)}{M_W^2} - \frac{\delta M_Z^2(0)}{M_Z^2} = \frac{g^2}{16\pi^2 M_W^2}\Big[\Sigma_{WW}(0) - \Sigma_{ZZ}(0)\Big]. \tag{2.3.12}$$

For Z resonance observables more relevant is the quantity defined as the difference of two complete one-loop self-energies taken at their physical masses, Eq. (2.3.7):

$$\delta\rho = \frac{\alpha}{4\pi s_W^2}\Delta\rho, \tag{2.3.13}$$

$$\Delta\rho = \frac{1}{M_W^2}\Big[\Sigma_{WW}(M_W^2) - \Sigma_{ZZ}(M_Z^2)\Big], \tag{2.3.14}$$

which is closely related to Eq. (2.3.8) and which arises naturally within the OMS scheme.

Although Eq. (2.3.14) implies the use of self-energies computed at one-loop level, it may be considered as generalized to higher perturbative order in coupling constants α and α_s. For this reason it is convenient to include the coupling constant in the superscript of $\delta\rho$. At the one-loop order we introduce:

$$\delta\rho^{\alpha} = \frac{\alpha}{4\pi s_W^2}\Delta\rho. \tag{2.3.15}$$

Now we proceed by presenting $\delta\rho$ as a sum of terms which are known in the literature:

$$\delta\rho = \delta\rho^{\alpha} + \delta\rho^{\alpha\alpha_S} + \delta\rho^{\alpha^2} + \delta\rho_L^{\alpha\alpha_S^2}. \tag{2.3.16}$$

We note that only for the first two terms the complete calculations are available [70, 13,38,71]. For the two-loop electroweak correction, $\delta\rho^{\alpha^2}$, only the two first terms in an expansion in m_t^2 are known ([34,35]):

$$\delta\rho^{\alpha^2} = \delta\rho_L^{\alpha^2} + \delta\rho_{NL}^{\alpha^2}. \tag{2.3.17}$$

For the three-loop correction $\texttt{AFMT} \sim \delta\rho^{\alpha\alpha_S^2}$ [72,73], only the leading in m_t^2 term is known. The flag `AFMT` is explained in Subsection 4.1.3.

Below we discuss briefly each term.

By examining the one-loop $\delta\rho^\alpha$ it is easy to verify that it is enhanced *quadratically* with the top quark mass, i.e. if one expands the complete one-loop expression for the fermionic component of $\delta\rho^\alpha$ into a series and retains only the first term one gets:

$$\delta\rho^\alpha \approx \delta\rho^\alpha_{L} \equiv -N_c \frac{\alpha}{16\pi s_W^2 c_W^2}\frac{m_t^2}{M_Z^2} = -\texttt{DRHO1}. \tag{2.3.18}$$

Eq. (2.3.18) introduces on passing the notion of *leading* term. Actually, in many cases a radiative correction may be split into two parts: *leading* part and *remainder*.

This splitting should satisfy the following requirements:

1. There is a guiding principle of splitting: Usually a splitting is undertaken in order to re-sum the leading term to all orders in perturbation theory.

2. The leading term should be bigger than the remainder.

3. Splitting should respect gauge invariance. For instance, if we define

$$\delta\rho = \delta\rho_{L} + \delta\rho_{\rm rem}\,, \tag{2.3.19}$$

both $\delta\rho_{L}$ and $\delta\rho_{\rm rem}$ must be separately gauge invariant. The $\delta\rho_{L}$ is re-summed to all orders, while $\delta\rho_{\rm rem}$ is treating in a fixed order of perturbation theory.

The splitting (2.3.19) is gauge invariant because $\Delta\rho$, as defined by Eq. (2.3.14), is a gauge invariant object, and the leading term (2.3.18) is apparently gauge-invariant.

However, since the top quark mass is only two times bigger than the Z boson mass, the quadratic enhancement is not so pronounced and the second condition is not fulfilled in a strict sense. A way out could be found observing that the complete $\Delta\rho$ is a good candidate for re-summation because it is gauge invariant. In [74] the following quantity was introduced:

$$\delta\hat\rho^\alpha \equiv \frac{\alpha}{4\pi s_W^2}\frac{1}{M_W^2}\Big[\Sigma_{WW}(M_W^2) - \Sigma_{ZZ}(M_Z^2)\Big]\Big|_{\overline{MS},\,\mu=M_Z}, \tag{2.3.20}$$

$$\delta\hat\rho^\alpha = \frac{s_W^2}{c_W^2}\left[-\texttt{AL4PI}*\texttt{DWZ1AL} + \texttt{SCALE}\right]. \tag{2.3.21}$$

Since this quantity is divergent it is understood as regularized in the $\overline{MS}$ sense, that means dropping out the pole term $1/\bar\varepsilon$. All divergences cancel for physical observables, therefore we may simply drop them all for every ingredient of calculations.After that we are left with the residual dependence on the t'Hooft scale parameter μ in the individual components, again cancelling in the sum [1]. It became customary to define all scale dependent quantities at $\mu = M_Z$, which is conventionally considered to be the natural scale not only for the Z-resonance, but also for all electroweak observables.

We note that the two separately gauge invariant terms in Eq. (2.3.19) may be considered with different coupling constants: α or G_μ. As was proven in [75], the leading term

[1] In fact, every divergence $1/\bar\varepsilon$ is accompanied by $-\ln M^2/\mu^2$.

should be considered with coupling constant G_μ , i.e. one should perform a *conversion* of couplings:

$$\alpha \to G_\mu \,. \tag{2.3.22}$$

This may be achieved by multiplying Eq. (2.3.18) by the conversion factor

$$f = \frac{\sqrt{2} G_\mu M_Z^2 s_W^2 c_W^2}{\pi \alpha} \,. \tag{2.3.23}$$

As a result, $\delta\rho_L$ becomes:

$$\delta\rho_L^G = -N_c x_t = -\texttt{DRIRR} + 3x_t^2 \texttt{AMT4C} \,, \tag{2.3.24}$$

with

$$x_t = \frac{G_\mu m_t^2}{8\sqrt{2}\pi^2} = \texttt{AXF} \,. \tag{2.3.25}$$

Here the superscript G emphasizes the use of the scale G_μ.

For a discussion about $\delta\rho^{\alpha\alpha_S}$ we refer to Subsection 3.4.2 and about $\delta\rho^{\alpha^2}$ to Subsection 3.5.

The sum of the two leading terms is:

$$-\left(\delta\rho_L^{G\alpha_S} + \delta\rho_L^{G\alpha_S^2}\right) = 3x_t \texttt{TBQCD0}, \tag{2.3.26}$$

where the second term is the `AFMT` correction:

$$\delta\rho_L^{G\alpha_S^2} = \texttt{AFMT}. \tag{2.3.27}$$

It is accessed through variable `TBQCD0`.

2.3.3. Δr beyond one loop

We begin with a rearrangement of terms in Eq. (2.3.1):

$$\begin{aligned} \Delta r &= \Delta\alpha^{(5)}(M_Z^2) + \frac{\alpha}{4\pi s_W^2}\left\{ s_W^2 \left[-\frac{2}{3} - \Pi_{\gamma\gamma}^{t,F}(0) - \Pi_{\gamma\gamma}^{l+5q,F}\left(M_Z^2\right)\right] + \frac{c_W^2}{s_W^2}\Delta\rho^F \right. \\ &\quad \left. + \Delta\rho_W^F + \frac{11}{2} - \frac{5}{8}c_W^2\left(1 + c_W^2\right) + \frac{9c_W^2}{4s_W^2}\ln c_W^2 \right\}. \end{aligned} \tag{2.3.28}$$

Here the superscript $l + 5q$ denotes a summation over leptons and five light quarks. Remember now that any self-energy function in Eq. (2.3.28) is defined at the scale $\mu = M_W$ as an artifact of the definition:

$$\begin{aligned} B_0\left(p^2; M_1, M_2\right) &= \frac{1}{\bar{\varepsilon}} - \ln\frac{M_1 M_2}{\mu^2} + \frac{\Lambda}{p^2}\ln\frac{-p^2 - i\epsilon + M_1^2 + M_2^2 - \Lambda}{2M_1 M_2} \\ &\quad + \frac{M_1^2 - M_2^2}{2p^2}\ln\frac{M_1^2}{M_2^2} + 2 \qquad (2.3.29) \\ &= \frac{1}{\bar{\varepsilon}} - \ln\frac{M_W^2}{\mu^2} + B_0^F\left(p^2; M_1, M_2\right), \qquad (2.3.30) \end{aligned}$$

where $\Lambda^2 = \lambda\left(p^2, M_1^2, M_2^2\right)$ is the Källen λ-function:

$$\lambda(x,y,z) = x^2 + y^2 + z^2 - 2xy - 2xz - 2yz. \tag{2.3.31}$$

However, we need them being defined at scale $\mu = M_Z$ in the $\overline{MS}$ spirit. For instance, $\Delta\rho^F$ re-scales as follows:

$$\frac{c_W^2}{s_W^4}\Delta\rho^F\Big|_{\mu=M_W} = \frac{c_W^2}{s_W^4}\Delta\rho^F\Big|_{\mu=M_Z} + \frac{1}{s_W^2}\left[\frac{1}{6}N_f - \frac{4}{3}s_W^2\sum_f c_f Q_f^2 - \frac{1}{6} - 7c_W^2\right]\ln c_W^2. \tag{2.3.32}$$

That explains the definition of variable `SCALE`:

$$\texttt{SCALE} = -\frac{\alpha}{4\pi s_W^2}\left[\frac{1}{6}N_f - \frac{4}{3}s_W^2\sum_f c_f Q_f^2 - \frac{1}{6} - 7c_W^2\right]\ln c_W^2. \tag{2.3.33}$$

After rescaling to $\mu = M_Z$ one gets:

$$\begin{aligned}\Delta r &= \Delta\alpha^{(5)}(M_Z^2) + \Delta\alpha^t(M_Z^2) + \frac{\alpha}{4\pi s_W^2}\left\{\left[\frac{c_W^2}{s_W^2}\Delta\rho^F + \Delta\rho_W^F - s_W^2\Pi_{\gamma\gamma}\left(M_Z^2\right)\right]\right|_{\mu=M_Z} \\ &\quad -\frac{2}{3}s_W^2 + \left(\frac{1}{6}N_f - \frac{1}{6} - 7c_W^2\right)\ln c_W^2 + \frac{11}{2} - \frac{5}{8}c_W^2\left(1 + c_W^2\right) + \frac{9c_W^2}{4s_W^2}\ln c_W^2\Bigg\},\end{aligned} \tag{2.3.34}$$

with

$$\Delta\alpha^t(M_Z^2) = \frac{\alpha}{4\pi}\left[\Pi_{\gamma\gamma}^{t,F}\left(M_Z^2\right) - \Pi_{\gamma\gamma}^{t,F}(0)\right]. \tag{2.3.35}$$

In Eq. (2.3.34) we disentangled the pure QED contributions $\Delta\alpha^{(5)}(M_Z^2)$ and $\Delta\alpha^t(M_Z^2)$, the parameter $\Delta\rho$, and the rest.

The one-loop result for Δr contains two *large* terms: the running coupling $\Delta\alpha^{(5)}(M_Z^2)$ (*logarithmically* enhanced by fermionic mass singularities, $\ln(m_f/s)$), and the parameter $\Delta\rho$ (enhanced *quadratically* by m_t^2). In the spirit of leading/remainder splittings it may be presented in two ways:

$$\Delta r = \Delta\alpha(M_Z^2) + \frac{c_W^2}{s_W^2}\Delta\rho_L^\alpha + \Delta r_{\rm rem} \equiv \Delta\alpha(M_Z^2) + \frac{c_W^2}{s_W^2}\Delta\hat{\rho}^\alpha + \Delta\hat{r}_{\rm rem}. \tag{2.3.36}$$

The first term is:

$$\Delta\alpha(M_Z^2) = \Delta\alpha^{(5)}(M_Z^2) + \Delta\alpha^t(M_Z^2), \tag{2.3.37}$$

and the second term is the *leading* electroweak part of Δr.

In Eq. (2.3.36) all three terms are separately gauge invariant. The full Δr is gauge invariant, being the physical amplitude of μ-decay. The $\Delta\alpha^{(5)}(M_Z^2)$ is gauge invariant since it contains only fermionic loops. Then, the second terms (Eq. (2.3.18) for the first choice or Eq. (2.3.21) for the second choice) are gauge invariant as discussed above. As a consequence, both $\Delta r_{\rm rem}$ and $\Delta\hat{r}_{\rm rem}$ are also gauge invariant.

Different variants of leading/remainder splitting are governed by the user option `AMT4`, see Subsection 4.1.3. We define:

$$\Delta r = \Delta\alpha(M_Z^2) - \Delta r_{_L} + \Delta r_{\rm rem}\,, \tag{2.3.38}$$

where $\Delta r_{_L}$ (and consequently $\Delta r_{\rm rem}$) depends on `AMT4`:

$$\Delta r_{_L}^{(\alpha)} = -\frac{c_W^2}{s_W^2} \times \left\{ \begin{array}{ll} \delta\rho_{_L}^{\alpha} + \delta\rho_{_L}^{\alpha^2} & \text{for} \quad \texttt{AMT4} = 1, \\ \delta\rho_{_L}^{\alpha} + \delta\rho_{_L}^{\alpha^2} + \delta\rho_{_L}^{\alpha\alpha_S} & \text{for} \quad \texttt{AMT4} = 2, \\ \delta\hat{\rho}^{\alpha} + \delta\rho_{_L}^{\alpha^2} + \delta\rho_{_L}^{\alpha\alpha_S} & \text{for} \quad \texttt{AMT4} = 3. \end{array} \right. \tag{2.3.39}$$

Moreover, superscript α emphasizes the use of scale α. Here we indicated also some higher order terms in order to show the difference between different settings of `AMT4`. The *re-summed* version used in `ZFITTER` for `AMT4`=1,2,3 is

$$\frac{1}{1-\Delta r} \;=\; \frac{1}{\Big[1-\Delta\alpha(M_Z^2)\Big]\Big[1+f\Delta r_{_L}^{(\alpha)}\Big] - \Delta r_{\rm rem}^{(\alpha)}}\,, \tag{2.3.40}$$

where f is the conversion factor of Eq. (2.3.23). This old implementation (before the advent of next-to-leading two-loop electroweak corrections) was described in [14]. These options are not supported beginning with `ZFITTER` v.5.10. We remind that the re-summation of $\Delta\alpha(M_Z^2)$ is dictated by the renormalization group. The re-summation of m_t enhanced terms comprises to special factorization in Eq. (2.3.40) and to *conversion* of the scale of $\Delta r_{_L}^{(\alpha)}$ from α to G_μ with the conversion factor (2.3.23). An alternative notion is useful:

$$\frac{1}{1-\Delta r} \;=\; \frac{1}{\Big[1-\Delta\alpha(M_Z^2)\Big]\left[1-\dfrac{c_W^2}{s_W^2}\delta\hat{\rho}^{(G)}\right] - \Delta r_{\rm rem}^{(\alpha)}}\,, \tag{2.3.41}$$

where the superscript G denotes the conversion to the scale G_μ in all terms, see Eq. (2.3.39).

When [14] was written it was not clear where to place $\Delta r_{\rm rem}$, either as in Eq. (2.3.41) or as in rows of Eq. (99) of [14], and which scale to use for it. That's why various *options* were considered, depending on flag `EXPR`. It may be easily seen that these options differ by terms of order $\mathcal{O}(G_\mu^2 m_t^2 M_Z^2)$.

This uncertainty is removed now by a calculation of order $\mathcal{O}(G_\mu^2 m_t^2 M_Z^2)$ two-loop electroweak corrections enhanced by the top quark mass [34,35]. The leading term of order $\mathcal{O}(G_\mu^2 m_t^4)$, which was known since 1992 [76,77] was also re-calculated in [34,35].

The implementation of terms of $\mathcal{O}(G_\mu^2 m_t^2 M_Z^2)$ into `ZFITTER` is realized by option `AMT4`=4 which is by now the default. The other options became obsolete.

In [34,35] it was shown that one should place the one-loop $\Delta r_{\rm rem}$ as follows:

$$\frac{1}{1-\Delta r} \;=\; \frac{1}{\Big[1-\Delta\alpha(M_Z^2)-\Delta r_{\rm rem}^{(G)}\Big]\left[1-\dfrac{c_W^2}{s_W^2}\delta\hat{\rho}^{(G)}\right]}\,. \tag{2.3.42}$$

Irreducible higher order corrections are applied by means of a simple modification of the leading and remainder terms

$$\delta\hat{\rho} \;\to\; \delta\hat{\rho} + \delta\hat{\rho}^{ho}, \tag{2.3.43}$$

$$\Delta r_{\rm rem} \;\to\; \Delta r_{\rm rem} + \Delta r_{\rm rem}^{ho}\,. \tag{2.3.44}$$

A higher order (ho) term is a sum of known corrections:

$$\delta\hat{\rho}^{ho} \;=\; \delta\hat{\rho}^{G\alpha_S} + \delta\hat{\rho}^{G\alpha_S^2} + \delta\hat{\rho}^{G^2}, \tag{2.3.45}$$

$$\Delta r_{\rm rem}^{ho} \;=\; \Delta r_{\rm rem}^{G\alpha_S} + \Delta r_{\rm rem}^{G^2}\,. \tag{2.3.46}$$

Terms of the orders $\mathcal{O}(G_\mu^2 m_t^4)$ and $\mathcal{O}(G_\mu^2 m_t^2 M_Z^2)$ are calculated in subroutine `GDEGNL`, an interface to the package `m2tcor.f` [30,78]; see Subsection 3.5 for more details. Complete two-loop mixed EW⊗QCD corrections may be calculated by two packages: with `bcqcdl5_14.f` for `QCDC=1,2` [13], and with `bkqcdc5_14.f` for `QCDC=3` (based on formulae of [38], presented in Subsection 3.4.2). They produce equal results within the accuracy of integration. However, `QCDC=3` is much faster since it uses analytically integrated expressions, while `QCDC=2` relies on a numerical integration.

We supply a dictionary:

for $\Delta\rho$:

$$-\delta\hat{\rho}^{G} = \texttt{DROBLO}, \tag{2.3.47}$$

$$-(\delta\hat{\rho}_L^{G\alpha_S} + \delta\hat{\rho}_L^{G\alpha_S^2}) = 3x_t\texttt{TBQCDO}, \tag{2.3.48}$$

$$-\delta\hat{\rho}^{G^2} = \texttt{DRHOD}, \tag{2.3.49}$$

$$-\delta\hat{\rho}^{(G)} = \texttt{DROBAR}; \tag{2.3.50}$$

for $\Delta r_{\rm rem}$:

$$\Delta r_{\rm rem}^{\alpha} + \Delta r_{\rm rem}^{\alpha\alpha_S} + \Delta\alpha^{\alpha\alpha_S}(M_Z^2) = \texttt{DRREM} - \texttt{DRHIG1}, \tag{2.3.51}$$

$$\Delta r_{\rm rem}^{\alpha\alpha_S} = \texttt{TBQCD} + 2\texttt{CLQQCD} - \texttt{TBQCDL}, \tag{2.3.52}$$

$$\Delta r_{\rm rem}^{\alpha^2} = \texttt{DRDREM}, \tag{2.3.53}$$

$$\Delta\alpha^{(5)}(M_Z^2) + \Delta\alpha^{t}(M_Z^2) = \texttt{DALFA}, \tag{2.3.54}$$

$$\Delta\alpha^{\alpha\alpha_S}(M_Z^2) = \frac{\alpha}{4\pi}\texttt{ALQCD}; \tag{2.3.55}$$

and finally for the complete Δr:

$$\Delta r = \texttt{DRBIG} = 1 - \left(1 + \frac{R}{1-R}\texttt{DROBAR} - \texttt{DRHIGS}\right)(1 - \texttt{DALFA} - \texttt{DRREM} - \texttt{DRDREM}). \tag{2.3.56}$$

2.3.4. Simulation of theoretical uncertainties

After the advent of next-to-leading two-loop electroweak corrections, the options developed to simulate the theoretical uncertainties as described in [14] became obsolete and were critically revisited. In this subsection we discuss new realizations.

With the aid of the option `EXPR` we select different `EXP`ansions of Δr:

$$\Delta r = \begin{cases} 1 - \left(1 - \dfrac{c_W^2}{s_W^2}\delta\bar{\rho} - \Delta r_{\rm res}^{H,G}\right)\left[1 - \Delta\alpha - \Delta r_{\rm rem} - \left(\Delta r_{\rm rem}^{ho} + \Delta r_L^{H,\alpha^2}\right)K_{\rm scale}\right], \\ 1 - \left(1 - \dfrac{c_W^2}{s_W^2}\delta\bar{\rho} - \Delta r_{\rm res}^{H,G}\right)(1 - \Delta\alpha - \Delta r_{\rm rem}) + \left(\Delta r_{\rm rem}^{ho} + \Delta r_L^{H,\alpha^2}\right)K_{\rm scale}, \\ 1 - \left(1 - \dfrac{c_W^2}{s_W^2}\delta\bar{\rho} - \Delta r_{\rm res}^{H,G}\right)(1 - \Delta\alpha) \\ \qquad\qquad + \left(1 - \dfrac{c_W^2}{s_W^2}\delta\rho^{G}\right)\Delta r_{\rm rem} + \left(\Delta r_L^{H,\alpha^2} + \Delta r_{\rm rem}\right)K_{\rm scale}. \end{cases} \tag{2.3.57}$$

We note that the first row (EXPR=0) realizes the so-called OMS-I renormalization scheme [34,35], while the third row approaches the spirit of the OMS-II renormalization scheme – a fully expanded option – with the second row being an intermediate step on the road from OMS-I to OMS-II.

In Eqs. (2.3.50), (2.3.55) and (2.3.57) are two terms, which optionally affect the resummation of the leading Higgs contribution to Δr:

$$\Delta r_{\rm res}^{H,G} = \frac{\sqrt{2}G_\mu M_W^2}{4\pi^2}\frac{11}{12}\left(\ln\frac{M_H^2}{M_W^2}-\frac{5}{6}\right) = \texttt{DRHIGS}, \tag{2.3.58}$$

$$\Delta r_{\rm res}^{H,\alpha} = \frac{\alpha}{4\pi s_W^2}\frac{11}{12}\left(\ln\frac{M_H^2}{M_W^2}-\frac{5}{6}\right) = \texttt{DRHIG1}. \tag{2.3.59}$$

We assume here:

$$\ln\frac{M_H^2}{M_W^2}-\frac{5}{6} \geq 0. \tag{2.3.60}$$

For flag IHIGS=1, the $\Delta r_{\rm res}^H$ is extracted from the remainder with scale α/s_W^2 and added to the leading term with scale G_μ, as in Eq. (2.3.59). We observe that 10/12 of $\Delta r_{\rm res}^H$ is contained in $\delta\hat{\rho}$. Therefore, for AMT4=4 only 1/12 of it is additionally re-summed. The influence of this option on theoretical errors was found to be tiny. For this reason, this re-summation has been implemented only for Δr and not for other POs.

With the options HIG2=1/0 it is possible to switch on/off the quadratically enhanced two-loop Higgs contribution [79,80]:

$$\texttt{DRHHS} = \Delta r_L^{H,\alpha^2} = -0.005832\frac{\alpha^2}{\pi^2 s_W^4}\frac{M_H^2}{M_W^2}\,. \tag{2.3.61}$$

With the choices SCRE=0,1,2 one changes the scale in the two-loop remainder terms as in the following three rows

$$K = \begin{cases} 1, \\ f^2, \\ f^{-2}. \end{cases} \tag{2.3.62}$$

The default is SCRE=0. Then one uses the scale as suggested by the author of m2tcor.f. For more details see Subsection 3.5. With conversion factor f^{-2} it is converted back to the scale α/s_W^2 and this operation is symmetrized in order to have symmetric errors due to change of scale of remainders.

The option SCAL=0,1,2,3,4 is the only QCD option. At the default, SCAL=0, we implemented the exact AFMT correction. For SCAL=1,2,3 we implemented the ξ-factor as given in [81]. Finally, for SCAL=4, Sirlin's scale $\xi = 0.248$ (see [82]) was implemented. Only SCAL=0,4 are left among the working options.

The last step in subroutine SEARCH is the calculation of a factor A,

$$A = \frac{A_0}{\sqrt{1-\Delta r}} = \texttt{AAFAC}, \tag{2.3.63}$$

that is used for various options IMOMS, see the iterations in Eqs. (2.2.32) and (2.2.33).

2.4. Partial and Total Z Decay Widths

The one-loop electroweak corrections to the Z boson width are calculated in ZFITTER following [12], higher orders are treated as described in [14], and the QCD corrections follow [83], and references therein.

2.4.1. Notations

We recall the amplitude of the decay $Z \to f\bar{f}$ in one-loop approximation and in the approximation of vanishing external fermion masses [12,8], given by:

$$V_\mu^{Zf\bar{f}}\left(M_Z^2\right) = (2\pi)^4\, i\, i\, \sqrt{\sqrt{2}G_\mu M_Z^2}\sqrt{\rho_Z^f} I_f^{(3)} \gamma_\mu \left[(1+\gamma_5) - 4|Q_f| s_W^2 \kappa_Z^f\right], \tag{2.4.1}$$

where ρ_Z^f and κ_Z^f are called *effective couplings* of Z-decay; they are some complex-valued constants.

The two effective couplings for each fermionic partial width of the Z boson are computed in subroutine FOKAPP. The relations between variables of the code and the notations used in Eq. (2.4.1) are:

$$\texttt{XRO1} \;=\; \rho_Z^f \equiv \rho_Z^{f,\alpha}, \tag{2.4.2}$$

$$\texttt{XAK1} \;=\; \kappa_Z^f \equiv \kappa_Z^{f,\alpha}, \tag{2.4.3}$$

where the superscript α is introduced in order to emphasize the perturbative order and scale. For their ingredients (on top of dictionary Eq. (2.3.6)) we have:

$$\texttt{XZFM1A} \;=\; \Sigma'_{ZZ}(M_Z^2), \tag{2.4.4}$$

$$\texttt{XZM1A-W0A} \;=\; -\Delta\rho_Z^F, \tag{2.4.5}$$

$$\texttt{XAMM1A} \;=\; \Pi_{Z\gamma}^F(M_Z^2), \tag{2.4.6}$$

$$\texttt{XV1ZZ} \;=\; \mathcal{F}_Z\left(M_Z^2\right), \tag{2.4.7}$$

$$\texttt{UFF} \;=\; u_f. \tag{2.4.8}$$

We use two expressions for the partial decay widths of the Z boson. One for decays into a pair of leptons, $l = e, \mu, \tau$:

$$\begin{aligned}\Gamma_l \equiv \Gamma\left(Z \to l\bar{l}\right) \;=\; & \Gamma_0 |\rho_Z^l| \sqrt{1 - \frac{4m_l^2}{M_Z^2}} \left[\left(1 + \frac{2m_l^2}{M_Z^2}\right)\left(|g_Z^l|^2 + 1\right) - \frac{6m_l^2}{M_Z^2}\right] \\ & \times \left[1 + \frac{3}{4}\frac{\alpha(M_Z^2)}{\pi} Q_f^2\right],\end{aligned} \tag{2.4.9}$$

and another one for decays into a pair of quarks, $f = u, d, c, s, b$:

$$\Gamma_f \equiv \Gamma\left(Z \to f\bar{f}\right) = \Gamma_0\, c_f\, |\rho_Z^f| \left[|g_Z^f|^2\, R_V^f(M_Z^2) + R_A^f(M_Z^2)\right] + \Delta_{\text{EW/QCD}}\,. \tag{2.4.10}$$

Here,

$$\Gamma_0 = \frac{G_\mu M_Z^3}{24\sqrt{2}\,\pi} = 82.945(7)\,\text{MeV} \tag{2.4.11}$$

is the 'standard' partial width. The complex-valued variable

$$g_Z^f = \frac{v_f}{a_f} = 1 - 4|Q_f|(\kappa_Z^f s_W^2 + I_f^2) \tag{2.4.12}$$

is the ratio of effective vector and axial couplings[2],

$$v_f \;=\; I_f^{(3)} - 2Q_f(\kappa_Z^f s_W^2 + I_f^2)\,, \tag{2.4.13}$$

$$a_f \;=\; I_f^{(3)}. \tag{2.4.14}$$

Finally, $c_f = 3$ is the color factor.

One should note the appearance of the order $\mathcal{O}(\alpha^2)$ term I_f^2 which denotes a real-valued contribution originating from the product of two imaginary parts of finite parts of polarization operators:

$$I_f^2 = \left(\frac{\alpha(s)}{4\,\pi}\right)^2 \mathrm{Im}\Pi_{\gamma\gamma}(s)\;\mathrm{Im}\Pi_{Z\gamma}(s) = \alpha^2(s)\frac{35}{18}\left[1 - \frac{8}{3}\mathrm{Re}(\kappa_Z^f)s_W^2\right], \tag{2.4.15}$$

giving a sometimes non-negligible contribution due to the enhancement by the factor π^2. Note that it bears the channel index f.

The radiator factors

$$R_{V,A}^f(M_Z^2) \tag{2.4.16}$$

describe the final state QED and QCD vector and axial vector corrections for quarkonic decay modes. They are described in Subsection 3.6.

The combinations

$$\sin^2\theta_{\rm eff}^f = \mathrm{Re}(\kappa_Z^f)s_W^2 + I_f^2 \tag{2.4.17}$$

define the flavor dependent *effective weak mixing angles*.

The Eqs. (2.4.9)defzwidthq differ by the treatment of final state corrections and finite mass effects originating from the Born amplitude and from the final state QCD corrections. For leptonic decay modes, Eq. (2.4.9), the mass effects are separated from the final state QED correction factor since only Born-induced mass effects are taken into account. For quarkonic decay modes, QED, QCD, mixed QED⊗QCD corrections and finite mass corrections (the latter are accounted for in terms of *running* masses) are included all together by means of radiator factors $R_{V,A}^f$. Another important feature of quarkonic widths, Γ_f, is the presence of the *non-factorizable* EW⊗QCD corrections $\Delta_{\rm EW/QCD}$ [84,85], which will be referred to as `CKHSS` corrections. Their handling is governed by the flag `CZAK`.

Since these corrections have a relative order of magnitude of less than one per mill, they are implemented in `ZFITTER` as fixed numbers taken from [84,85]:

$$\Delta_{\rm EW/QCD} = \texttt{ARCZAK} = \begin{cases} -0.113 & \text{MeV, for } u \text{ and } c \text{ quarks,} \\ -0.160 & \text{MeV, for } d \text{ and } s \text{ quarks,} \\ -0.040 & \text{MeV, for } b \text{ quark.} \end{cases} \tag{2.4.18}$$

[2]Beware of two different definitions of v_f and a_f used in this description. We use here the definitions Eq. (2.4.14), while in `ZFITTER` and everywhere else in the description we use instead Eqs. (1.1.12)–(1.1.14), i.e. quantities normalized by $I_f^{(3)}$.

The form factors comprise one-loop and higher order virtual electroweak and *internal* QCD corrections, see Subsection 3.4. Their implementation relies on the notion of leading and remainder terms.

Here we present only the realization for `AMT4`=4, i.e. that with next-to-leading two-loop electroweak corrections. First of all we have to rewrite identically the one-loop expressions in Eq. (2.4.1) in order to introduce a *leading-remainder splitting*:

$$\rho_Z^f = 1 - \delta\hat{\rho}^\alpha + \delta\rho_{\rm rem}^{f,\alpha}\,, \tag{2.4.19}$$

$$\kappa_Z^f = 1 - \frac{c_W^2}{s_W^2}\delta\hat{\rho}^\alpha + \delta\kappa_{\rm rem}^{f,\alpha}\,. \tag{2.4.20}$$

These expressions uniquely define leading terms containing $\delta\hat{\rho}^\alpha$ and remainder terms containing the rest.

2.4.2. Simulation of theoretical uncertainties

In a complete analogy with Eq. (2.3.57) one may develop options to simulate theoretical errors for ρ_Z^f and κ_Z^f due to non-calculated orders. They are governed by the flag `EXPF`=0,1,2, correspondingly. For ρ_Z^f one has

$$\rho_Z^f = \begin{cases} \dfrac{1+\delta\rho_{\rm rem}^{f,[G]}+\delta\rho_{\rm rem}^{f,G^2}K_{\rm scale}}{1+\delta\hat{\rho}^{(G)}\left(1-\Delta\bar{r}_{\rm rem}^{[G]}\right)}\,, \\ \dfrac{1+\delta\rho_{\rm rem}^{f,[G]}}{1+\delta\hat{\rho}^{(G)}\left(1-\Delta\bar{r}_{\rm rem}^{[G]}\right)} + \delta\rho_{\rm rem}^{f,G^2}K_{\rm scale}\,, \\ 1-\delta\hat{\rho}^{(G)} + \left(\delta\hat{\rho}^G\right)^2 + \delta\hat{\rho}^G\Delta\bar{r}_{\rm rem}^{[G]} + \delta\rho_{\rm rem}^{f,[G]}\left(1-\delta\hat{\rho}^G\right) + \delta\rho_{\rm rem}^{f,G^2}K_{\rm scale}\,. \end{cases} \tag{2.4.21}$$

Here superscript (G) stands for the inclusion of all known terms, as in the first Eq. (2.3.44), while superscript $[G]$ denotes the inclusion of one-loop EW corrections together with all known orders in α_s, i.e. $[G] = G + G\alpha_s + \ldots$ We also note that the ρ and κ-remainders are channel-dependent quantities (f-dependent).

Moreover, it is:

$$\Delta\bar{r}_{\rm rem}^{[G]} = \Delta\bar{r}_{\rm rem}^{G} + \Delta r_{\rm rem}^{G\alpha_S}, \tag{2.4.22}$$

with the one-loop remainder [78]:

$$\begin{aligned}\Delta\bar{r}_{\rm rem}^{G} &= \frac{\sqrt{2}G_\mu M_Z^2 s_W^2 c_W^2}{4\pi^2}\Big\{-\frac{2}{3}+\frac{1}{s_W^2}\Big[\frac{1}{6}N_f-\frac{1}{6}-7c_W^2\Big]\ln c_W^2 \\ &\quad +\frac{1}{s_W^2}\Big[\Delta\rho_W^F+\frac{11}{2}-\frac{5}{8}c_W^2\left(1+c_W^2\right)+\frac{9c_W^2}{4s_W^2}\ln c_W^2\Big]\Big\}.\end{aligned} \tag{2.4.23}$$

Finally, we note that all rows for user options `EXPF` are analogously as for `EXPR`, Eq. (2.3.57).

Similarly, for κ_Z^f (realized also by flag `EXPF`):

$$\kappa_Z^f = \begin{cases} \left(1+\delta\kappa_{\rm rem}^{f,[G]}+\delta\kappa_{\rm rem}^{f,G^2}K_{\rm scale}\right)\left[1-\dfrac{c_W^2}{s_W^2}\delta\hat{\rho}^{(G)}\left(1-\Delta\bar{r}_{\rm rem}^{[G]}\right)\right], \\ \left(1+\delta\kappa_{\rm rem}^{f,[G]}\right)\left[1-\dfrac{c_W^2}{s_W^2}\delta\hat{\rho}^{(G)}\left(1-\Delta\bar{r}_{\rm rem}^{[G]}\right)\right]+\delta\kappa_{\rm rem}^{f,G^2}K_{\rm scale}\,, \\ 1-\dfrac{c_W^2}{s_W^2}\delta\hat{\rho}^{(G)}+\dfrac{c_W^2}{s_W^2}\delta\hat{\rho}^{G}\Delta\bar{r}_{\rm rem}^{[G]}+\delta\kappa_{\rm rem}^{f,[G]}\left(1-\dfrac{c_W^2}{s_W^2}\delta\hat{\rho}^{G}\right)+\delta\kappa_{\rm rem}^{f,G^2}K_{\rm scale}\,. \end{cases} \tag{2.4.24}$$

In Subsection 3.5 we will show how the quantities introduced in Eqs. (2.4.21) and (2.4.24) are related to variables supplied by the package `m2tcor.f` [30].

Since the next-to-leading two-loop EW corrections are not known for the $Z \to b\bar{b}$ channel, the code internally realizes `AMT4`=3 for this channel. That's why we refer the reader to old publications for the description of the implementation of higher orders and theoretical options [14,6]. The one-loop corrections for the $Z \to b\bar{b}$ channel are fully described elsewhere.

The Z decay rate is calculated in subroutine `ZWRATE`, where also the W decay rate is calculated [86].

2.4.3. Weak form factors for $Z \to b\bar{b}$

Due to the large mass splitting between the t and b quarks, there are two one-loop vertex diagrams for the Z decay into b quarks and also higher order vertex corrections, which contribute additional *non-universal* m_t-dependent terms that are absent in the cases of light quarks [12,87] (see also [88–90]). Their leading term and the corresponding higher order corrections are taken into account with the correction τ_b:

$$\tau_b = -2x_t\left[1-\frac{\pi}{3}\alpha_{_S}(m_t^2)+x_t\tau^{(2)}\left(\frac{m_t^2}{M_H^2}\right)\right] = \texttt{TAUBB1}+\texttt{TAUBB2}. \tag{2.4.25}$$

For the first term, $tau_b = -2x_t$, defined in Eq. (2.3.25), we refer to [6], for the second term – which will be called `FTJR` correction – to [91–94], and for the last one to [76].

Since the first term represents a one-loop correction with scale G_μ, one has to subtract it with scale α from the $Zb\bar{b}$ decay amplitude form factor $F_{_L}$:

$$V_\mu^{Zf\bar{f}}(s) = (2\pi)^4\, i\frac{ig^3}{16\pi^2 2c_W}\gamma_\mu\left[I_f^{(3)}F_{Z_L}(s)\,(1+\gamma_5)-2Q_f s_W^2 F_{ZQ}(s)\right], \tag{2.4.26}$$

$$F_{_L} \to F_{_L}-\left(-\frac{\alpha}{8\pi s_W^2}\frac{m_t^2}{M_W^2}\right). \tag{2.4.27}$$

If ρ_b and κ_b denote couplings based on the subtracted quantity Eq. (2.4.27), then τ_b has to be accounted for by means of the following replacements:

$$\rho_b \to \rho_b\,(1+\tau_b)^2\,, \tag{2.4.28}$$

$$\kappa_b \to \frac{\kappa_b}{(1+\tau_b)}\,, \tag{2.4.29}$$

as was proven in [76].

A compact form of the function $\tau^{(2)}$ may be taken from [77].

At the end we give the two leading terms of the unsubtracted F_L in the limit of large t-quark masses [12]:

$$F_L \approx -\frac{\alpha}{8\pi s_W^2}\,|V_{tb}|^2\left[\frac{m_t^2}{M_W^2}+\left(\frac{8}{3}+\frac{1}{6c_W^2}\right)\ln\frac{m_t^2}{M_W^2}\right]. \tag{2.4.30}$$

2.5. Table of Pseudo-Observables

We complete the section about pseudo-observables with a full list of their *definitions*, with indication of their locations in `COMMON` blocks, and with a Table of all POs accessible in `ZFITTER`.

In order to compute POs, only a part of the `ZFITTER` package is needed. POs may be computed with a main routine `zfmain_PO.f` which has to be compiled together with the following packages: `dizet6_21.f`, `zf514_aux.f`, `m2tcor5_11.f`, `bkqcdl5_14.f`, and `bcqcdl5_14.f`.

All accessible POs are listed in Tab. 2.1. In the first two rows we see the W boson mass and $s_W^2 = 1 - M_W^2/M_Z^2$. Given the discussion in the previous Section about the calculation of M_W in `ZFITTER`, these quantities need not be defined. Further, all partial Z widths are shown, then the invisible width, simply equal to $3\Gamma_\nu$, then the total hadronic width, equal to the sum of all quarkonic widths, and finally the total width.

Then there is a group of quantities straightforwardly derived from widths: first the ratios

$$R_l = \frac{\Gamma_h}{\Gamma_e}, \tag{2.5.1}$$

$$R_f^0 = \frac{\Gamma_f}{\Gamma_h}, \tag{2.5.2}$$

and then the hadronic and leptonic pole cross-sections

$$\sigma_h^0 = 12\pi\,\frac{\Gamma_e\Gamma_h}{M_Z^2\Gamma_Z^2}, \tag{2.5.3}$$

$$\sigma_\ell^0 = 12\pi\,\frac{\Gamma_e\Gamma_l}{M_Z^2\Gamma_Z^2}. \tag{2.5.4}$$

Next there follow three effective weak mixing angles defined by Eq. (2.4.17) and three ρ_Z^f parameters ($f = e, b, c$) defined by the first of Eq. (2.4.21). The so-called *coupling factors* are trivially made out of the *real parts* of the ratios of effective couplings Eq. (2.4.14):

$$\mathcal{A}_f = \frac{2\,\mathrm{Re}\,g_Z^f}{\left(\mathrm{Re}\,g_Z^f\right)^2+1}. \tag{2.5.5}$$

They are also known as *left-right flavor asymmetries*. Finally, *forward-backward peak asymmetries* are mere combinations of these coupling factors:

$$A_{\rm FB}^{0f} = \frac{3}{4}\,\mathcal{A}_e\,\mathcal{A}_f. \tag{2.5.6}$$

Observable	minimal	preferred	maximal	interval
M_W [GeV]	80.3669	80.3738	80.3742	0.73 MeV
s^2_W	0.22309	0.22310	0.22323	0.00013
Γ_ν [MeV]	167.215	167.234	167.239	0.024 MeV
Γ_e [MeV]	83.983	83.995	83.999	0.016 MeV
Γ_μ [MeV]	83.982	83.995	83.998	0.016 MeV
Γ_τ [MeV]	83.793	83.805	83.808	0.015 MeV
Γ_u [MeV]	300.092	300.154	300.168	0.076 MeV
Γ_d [MeV]	382.928	382.996	383.012	0.084 MeV
Γ_c [MeV]	300.031	300.092	300.106	0.075 MeV
Γ_b [MeV]	375.886	375.993	375.995	0.109 MeV
$\Gamma_{\rm inv}$ [GeV]	0.50165	0.50170	0.50172	0.071 MeV
Γ_h [GeV]	1.74187	1.74223	1.74227	0.40 MeV
Γ_z [GeV]	2.49527	2.49573	2.49578	0.51 MeV
R_l	20.7406	20.7420	20.7421	0.0015
R^0_b	0.215786	0.215811	0.215813	0.000027
R^0_c	0.172243	0.172246	0.172252	0.000009
σ^0_h [nb]	41.4777	41.4777	41.4785	0.8 pb
σ^0_l [nb]	1.9997	1.9997	1.9999	0.2 pb
$\sin^2\theta^{\rm lept}_{\rm eff}$	0.231594	0.231601	0.231653	0.000059
$\sin^2\theta^{b}_{\rm eff}$	0.232941	0.232950	0.233004	0.000063
$\sin^2\theta^{c}_{\rm eff}$	0.231488	0.231495	0.231547	0.000059
ρ_e	1.00516	1.00528	1.00532	0.00016
ρ_b	0.99403	0.99424	0.99424	0.00021
ρ_c	1.00586	1.00598	1.00601	0.00015
$\mathcal{A}_e$	0.145988	0.146396	0.146452	0.000464
$\mathcal{A}_b$	0.934573	0.934607	0.934613	0.000040
$\mathcal{A}_c$	0.667416	0.667595	0.667620	0.000204
$A^{0,l}_{\rm FB}$	0.015984	0.016074	0.016086	0.000102
$A^{0,b}_{\rm FB}$	0.102327	0.102617	0.102657	0.000330
$A^{0,c}_{\rm FB}$	0.073076	0.073300	0.073331	0.000255

Table 2.1
Predictions for pseudo-observables from ZFITTER

2.5.1. Pseudo-Observables in common blocks of DIZET

Channel dependent quantities are stored in the common block COMMON/CDZRKZ/ and in the array PARTZ(0:11); we quote from the code:

```
*
      COMMON/CDZRKZ/ARROFZ(0:10),ARKAFZ(0:10),ARVEFZ(0:10),ARSEFZ(0:10)
     &             ,AROTFZ(0:10),AIROFZ(0:10),AIKAFZ(0:10),AIVEFZ(0:10)
*---
      DIMENSION NPAR(21),ZPAR(31),PARTZ(0:11),PARTW(3)
*---
      CALL DIZET
     &(NPAR,AMW,AMZ,AMT,AMH,DAL5H,ALQED,ALPHST,ALPHTT,ZPAR,PARTZ,PARTW)
*
```

The correspondences are as follows:

$$\texttt{ARROFZ(0:10)} = (\rho_Z^f)', \tag{2.5.7}$$
$$\texttt{AROTFZ(0:10)} = \mathrm{Re}\,\rho_Z^f, \tag{2.5.8}$$
$$\texttt{ARKAFZ(0:10)} = \mathrm{Re}\,\kappa_Z^f, \tag{2.5.9}$$
$$\texttt{ARVEFZ(0:10)} = \mathrm{Re}\,g_Z^f, \tag{2.5.10}$$
$$\texttt{AIROFZ(0:10)} = \mathrm{Im}\,\rho_Z^f, \tag{2.5.11}$$
$$\texttt{AIKAFZ(0:10)} = \mathrm{Im}\,\kappa_Z^f, \tag{2.5.12}$$
$$\texttt{AIVEFZ(0:10)} = \mathrm{Im}\,g_Z^f, \tag{2.5.13}$$
$$\texttt{ARSEFZ(0:10)} = \sin^2\theta_{\rm eff}^f, \tag{2.5.14}$$
$$\texttt{PARTZ(0:11)} = \Gamma_f, \tag{2.5.15}$$

with the usual ZFITTER channel assignments (see Fig. I.5), and with all quantities but $(\rho_Z^f)'$ already defined. The quantity $(\rho_Z^f)'$ absorbs imaginary parts of g_Z^f. Namely, if one defines the partial widths Eqs. (2.4.9) and (2.4.10) using $(g_Z^f)^2$ instead of $|g_Z^f|^2$ one has to use the pre-factor $(\rho_Z^f)'$ instead of $|\rho_Z^f|$. Both options MISC=1/0 (with $(\rho_Z^f)'/|\rho_Z^f|$) are used in the so-called *Model Independent interfaces* of ZFITTER, see Appendix 4.3.

In view of the potential use of quantities $(\rho_Z^f)'$, another common block, COMMON /CDZAUX/, deserves an explanation. We again quote from the code:

```
*
      COMMON /CDZAUX/PARTZA(0:10),PARTZI(0:10),RENFAC(0:10),SRENFC(0:10)
*
```

It is:

$$R_f = \texttt{RENFAC}(0:10) = \frac{\Gamma_Z \text{ computed with Im parts of effective couplings}}{\Gamma_Z \text{ computed without Im parts of effective couplings}}, \tag{2.5.16}$$

$$\sqrt{R_f} = \texttt{SRENFC}(0:10). \tag{2.5.17}$$

The vectors PARTZA(0:10) and PARTZI(0:10) are for expert use only.

Chapter 3

Improved Born Cross-Section

3.1. Introduction

Having discussed POs, we have to make the next step towards *realistic observables*, i.e. various cross-sections and asymmetries with experimental cuts. We have to construct the so-called *improved Born approximations*, IBAs. They are also called sometimes doubly deconvoluted observables [57] since they are made free of initial state QED and final state QED⊗QCD corrections. The latter two groups of corrections form two separately gauge invariant sub-sets of diagrams. All remaining diagrams contribute to the IBA: purely EW and *internal* QCD corrections.

In the first three Sections of this Chapter we introduce some of the ingredients needed to construct the IBA. First we discuss the Z boson parameter transformation, then the one-loop EW form factors, and finally the two classes of higher order corrections: internal, mixed EW⊗QCD corrections and two-loop EW corrections.

The calculation of the IBA from these ingredients does not belong to the `DIZET` package and will be discussed in Sections 3.7 and 3.8.

3.2. The Z Propagator

The Z boson propagator in the Breit-Wigner form appears already at the level of the Born cross-sections. It ensures the finiteness of the Born cross-section.

In general, the imaginary part depends on s:

$$\mathcal{K}_z(s) = \frac{s}{s-m_z^2}\,, \tag{3.2.1}$$

$$m_z^2 = M_z^2 - iM_z\Gamma_z(s). \tag{3.2.2}$$

At LEP, it is common to use the following definition for the Z width function (default, for flag `GAMS`=1):

$$\Gamma_z(s) = \frac{s}{M_z^2}\Gamma_z\,. \tag{3.2.3}$$

This is an approximation, valid far away from production thresholds. In the Standard Model the Z boson width Γ_z is predicted as a result of quantum corrections and calculated in `ZFITTER` according to the formulae of Section 2.4.

In another approach the Z width function is treated as a constant (chosen with flag GAMS=0):

$$\bar{\Gamma}_Z(s) = \bar{\Gamma}_Z, \tag{3.2.4}$$

$$\bar{\mathcal{K}}_Z(s) = \frac{s}{s-\bar{m}_Z^2}, \tag{3.2.5}$$

$$\bar{m}_Z^2 = \bar{M}_Z^2 - i\bar{M}_Z\Gamma_Z. \tag{3.2.6}$$

The following equality holds [42]:

$$G_\mu \mathcal{K}_Z(s) \equiv \bar{G}_\mu \bar{\mathcal{K}}_Z(s), \tag{3.2.7}$$

with:

$$\bar{M}_Z = \frac{1}{\sqrt{1+\Gamma_Z^2/M_Z^2}} M_Z \approx M_Z - \frac{1}{2}\frac{\Gamma_Z^2}{M_Z} \approx M_Z - 34 \text{ MeV}, \tag{3.2.8}$$

$$\bar{\Gamma}_Z = \frac{1}{\sqrt{1+\Gamma_Z^2/M_Z^2}} \Gamma_Z \approx \Gamma_Z - \frac{1}{2}\frac{\Gamma_Z^3}{M_Z} \approx \Gamma_Z - 1 \text{ MeV}, \tag{3.2.9}$$

$$\bar{G}_\mu = \frac{G_\mu}{1+i\Gamma_Z/M_Z}. \tag{3.2.10}$$

The choice of the definition of the Z mass and width is left to the user, see flag GAMS, defined in Appendix 4.2.2. Additional literature on the definition of the Z boson parameters may be found in [14,95].

3.3. One-Loop Electroweak Form Factors

The amplitude of the process $e^+e^- \to f\bar{f}$ in the Standard Model gets in the one-loop approximation contributions from self-energy insertions, vertex corrections, box diagrams, and bremsstrahlung diagrams. We divide these diagrams into several gauge invariant subsets.

We recall that first of all we disentangle a QED subset: QED-vertices and fermionic self-energies, $\gamma\gamma$ and $Z\gamma$ boxes and bremsstrahlung, see Section 1.2.

Then, we divide the remaining diagrams into two more gauge-invariant subsets, giving rise to two *improved (or dressed)* amplitudes: i) improved γ exchange amplitude with running QED-coupling where only fermion loops contribute (see Eq. (2.2.36)), and ii) improved Z exchange amplitude with four, in general complex-valued *EW form factors* $\rho_{ef}, \kappa_e, \kappa_f, \kappa_{ef}$:

$$\begin{aligned}\mathcal{A}_Z^{OLA}(s,t) = {} & i\,e^2\,4\,I_e^{(3)}I_f^{(3)}\frac{\chi_Z(s)}{s}\rho_{ef}(s,t)\Big\{\gamma_\mu(1+\gamma_5)\otimes\gamma_\mu(1+\gamma_5) \\ & -4|Q_e|s_W^2\kappa_e(s,t)\gamma_\mu\otimes\gamma_\mu(1+\gamma_5) - 4|Q_f|s_W^2\kappa_f(s,t)\gamma_\mu(1+\gamma_5)\otimes\gamma_\mu \\ & +16|Q_eQ_f|s_W^4\kappa_{e,f}(s,t)\gamma_\mu\otimes\gamma_\mu\Big\}.\end{aligned} \tag{3.3.1}$$

The form factors are simply related to the one-loop form factors

$$\rho_{ef} = 1 + F_{LL}(s,t) - s_W^2 \Delta r, \tag{3.3.2}$$
$$\kappa_e = 1 + F_{QL}(s,t) - F_{LL}(s,t), \tag{3.3.3}$$
$$\kappa_f = 1 + F_{LQ}(s,t) - F_{LL}(s,t), \tag{3.3.4}$$
$$\kappa_{ef} = 1 + F_{QQ}(s,t) - F_{LL}(s,t). \tag{3.3.5}$$

This set of form factors corresponds to an equivalent Born-like ansatz:

$$\begin{aligned}\mathcal{A}_Z^{OLA} = {} & i\frac{g^2}{16\pi^2}\, e^2\, 4\, I_e^{(3)} I_f^{(3)} \frac{\chi_Z(s)}{s} \\ & \times\Big\{\gamma_\mu(1+\gamma_5)\otimes\gamma_\mu(1+\gamma_5)F_{LL}(s,t) - 4|Q_e|s_W^2\gamma_\mu\otimes\gamma_\mu(1+\gamma_5)F_{QL}(s,t) \\ & -4|Q_f|s_W^2\gamma_\mu(1+\gamma_5)\otimes\gamma_\mu F_{LQ}(s,t) + 16|Q_eQ_f|s_W^4\gamma_\mu\otimes\gamma_\mu F_{QQ}(s,t)\Big\}.\end{aligned} \tag{3.3.6}$$

These form factors are functions of two Mandelstam invariants (s,t) due to the remaining WW and ZZ box contributions. The Mandelstam variables are defined such that they satisfy the identity :

$$s + t + u = 0, \qquad t = -\frac{s}{2}(1-\cos\vartheta). \tag{3.3.7}$$

3.3.1. Subroutine `ROKANC`

The weak form factors in the one-loop approximation are calculated in subroutine `ROKANC`. The four Eqs. (3.3.2)–(3.3.5) are assigned to the complex-valued array `XROK(4)`:

$$\texttt{XROK(1)} = \rho_{ef}^{\alpha}(s,t), \tag{3.3.8}$$
$$\texttt{XROK(2)} = \kappa_e^{\alpha}(s,t), \tag{3.3.9}$$
$$\texttt{XROK(3)} = \kappa_f^{\alpha}(s,t), \tag{3.3.10}$$
$$\texttt{XROK(4)} = \kappa_{ef}^{\alpha}(s,t). \tag{3.3.11}$$

The four form factors Eqs. (3.3.2)–(3.3.5) are split into leading and remainder parts following exactly the same philosophy as described in Subsection 2.4. The analogs of first rows of Eqs. (2.4.21) and (2.4.24) are used, for instance:

$$\rho_{ef} = \frac{1+\delta\rho_{\rm rem}^{ef,(G)}}{1+\delta\hat{\rho}^{(G)}\left(1-\Delta\bar{r}_{\rm rem}^{[G]}\right)}, \tag{3.3.12}$$

etc., with a trivial generalization concerning the treatment of next-to-leading order two-loop EW remainder terms, $\delta\rho_{\rm rem}^{f,G^2}$ and $\delta\kappa_{\rm rem}^{f,G^2}$. For κ_e one uses the κ remainder for the $Z\to e^+e^-$ channel, for κ_f the κ remainder for the $Z\to f\bar{f}$ channel, and for κ_{ef} both. For ρ_{ef} one uses $1/2(\delta\rho_{\rm rem}^{e,G^2}+\delta\rho_{\rm rem}^{f,G^2})$. However, an emulation of the theoretical uncertainties as it is done in the second and third rows of Eqs. (2.4.21) and (2.4.24) was not realized. The imaginary parts of EW form factors are attributed to remainders.

When [96] was written, `ZFITTER` had yet a simplified treatment of the additional terms in m_t for the $e^+e^-\to b\overline{b}$ channel. They were contained in three constant terms contributing to the $Zb\overline{b}$-vertex [12] and vanishing in the limit $m_t\to 0$: $V_{1W}^t(M_Z^2)$, $V_{2W}^t(M_Z^2)$, and

$\delta^t_{ct,b}$ (see also Eqs.(268)–(271) of [96] and the description in [6]). Now, we take into account in these terms the complete kinematical dependencies, arising from diagrams with virtual W boson exchange (see for details [97]): $\mathcal{F}_{Wa}(s)$, $\overline{\mathcal{F}}_{Wa}(s)$, $\hat{\mathcal{F}}_{Wn}(s)$, $\hat{\mathcal{F}}_{W}(s)$ and $\hat{\mathcal{B}}^d_{WW}(s,t)$. These *additions* form a gauge invariant subset of terms. They are supplied with a call to subroutine `VTBANA(NUNI,S,WWv2,WWv11,WWv12)`:

$$\mathcal{F}_{Wa}(s) = \texttt{WWv11}, \tag{3.3.13}$$
$$\overline{\mathcal{F}}_{Wa}(s) = \texttt{WWv12}, \tag{3.3.14}$$
$$\hat{\mathcal{F}}_{Wn}(s) = \texttt{WWv2}, \tag{3.3.15}$$
$$\hat{\mathcal{F}}_{W}(s) = \texttt{VTBX1}. \tag{3.3.16}$$

The last variable and another one,

$$\texttt{VTBX2} = \left(\frac{M_Z^2}{s} - 1\right) c_W^2 \left[\hat{\mathcal{F}}_{Wn}(s) - (1 - |Q_b|)\,\mathcal{F}_{Wa}(s)\right], \tag{3.3.17}$$

are used in the calculation of two corrections:

$$\texttt{DVTBB1} = \frac{\alpha}{4\pi s_W^2}\left[\texttt{VTBX1} - \left(-\frac{m_t^2}{2M_W^2}\right)\right], \tag{3.3.18}$$
$$\texttt{DVTBB2} = \frac{\alpha}{4\pi s_W^2}\texttt{VTBX2}. \tag{3.3.19}$$

In the first one we subtracted the leading asymptotic term of $\texttt{VTBX1} = -m_t^2/M_W^2/2$, (see Eq. (2.4.27)), which is shifted to the leading term with the scale G_μ and accounted for by the substitutions Eq. (2.4.29). The non-box m_t-additions are applied by

$$\delta\rho^{ef}_{\rm rem} \to \delta\rho^{ef}_{\rm rem} + \texttt{DVTBB1}, \tag{3.3.20}$$
$$\kappa^{e}_{\rm rem} \to \kappa^{e}_{\rm rem} + \texttt{DVTBB2}, \tag{3.3.21}$$
$$\kappa^{f}_{\rm rem} \to \kappa^{f}_{\rm rem} - \texttt{DVTBB1}, \tag{3.3.22}$$
$$\kappa^{ef}_{\rm rem} \to \kappa^{ef}_{\rm rem} - \texttt{DVTBB1}. \tag{3.3.23}$$

The WW box contributes to the EW form factor $F_{LL}(s,t)$. It is written as a sum of two terms, corresponding to a zero t mass part and an additional one vanishing at $m_t \to 0$. The additional terms also contain non-unitary contributions, which have to be cancelled analytically. Otherwise the treatment with `BOXD=1` may induce heavy gauge violations, see [97]. After this cancellation some remnant arises in Eqs. (3.3.2)–(3.3.5):

$$\frac{r_t}{4}\left[B_0^F(-s; M_W, M_W) + 1\right] = \texttt{XROBT}. \tag{3.3.24}$$

It is present only in the $Z \to b\overline{b}$ channel.

In Subsection 3.3.2 we will describe the implementation of the EW boxes in `ROKANC` in more detail.

3.3.2. Treatment of electroweak boxes in DIZET

Every weak form factor gets a contribution from the purely weak boxes, the WW and ZZ diagrams. They are vanishingly small at the Z peak but very important at higher energies. For the LEP2 case see [98].

Calculation and treatment of these boxes deserve a dedicated discussion. There are three options governed by the flag BOXD:

- BOXD=0, the box contributions are ignored. Strictly speaking such a *truncation* of form factors is not a gauge invariant procedure and it is more or less justified only in the vicinity of the Z resonance where the net box contribution is small anyway since it is suppressed by a factor $(s - M_Z^2)/s$.

- BOXD=1, the boxes are calculated as additive separate contribution to the cross-section. Since box contributions depend on the scattering angle it should be integrated over an angular interval. This is done by a numerical integration of the differential distribution supplied by the function DZEWBX(RACOS), where RACOS is the cms scattering angle. This treatment is gauge invariant only for deconvoluted quantities. If one subsequently convolutes an IBA part with ISR, but without boxes, and adds the boxes without convolution instead, then an apparent violation of gauge invariance is being introduced. This procedure is applicable only near the resonance.

- BOXD=2, box contributions are added to the four form factors in subroutine ROKANC. This is the only gauge invariant treatment. However, it may be done only via interface ZANCUT, which is differential in the scattering angle, followed by a subsequent numerical integration over the scattering angle if integrated quantities are needed.

The box additions $\rho_{ef}^{\rm box}(s,t)$, $\kappa_{e,f}^{\rm box}(s,t)$ and $\kappa_{ef}^{\rm box}(s,t)$ to the form factors are functions of two Mandelstam variables:

$$\rho_{ef}^{\rm box}(s,t) = \rho_{ZZ}^{\rm box}(s,t) + \rho_{WW}^{\rm box}(s,t), \tag{3.3.25}$$

$$\kappa_{e,f}^{\rm box}(s,t) = \kappa_{e,fZZ}^{\rm box}(s,t) - \rho_{ZZ}^{\rm box}(s,t) - \rho_{WW}^{\rm box}(s,t), \tag{3.3.26}$$

$$\kappa_{ef}^{\rm box}(s,t) = \kappa_{efZZ}^{\rm box}(s,t) - \rho_{ZZ}^{\rm box}(s,t) - \rho_{WW}^{\rm box}(s,t). \tag{3.3.27}$$

For the WW contributions the dictionary is:

$$\begin{aligned}
\rho_{WW}^{\rm box}(s,t) &= \frac{\alpha}{4\pi s_W^2}\texttt{XWWRO} \qquad (3.3.28)\\
&= -s_e s_f c_W^2 \left(\frac{M_Z^2}{s} - 1\right)\left(\frac{s}{s-t}\right)^2 \begin{cases} \mathcal{B}_{WW}^{(+)} = \texttt{XWWP} \\ \mathcal{B}_{WW}^{(-)} = \texttt{XWWM} \end{cases} \\
&= \begin{cases} -c_W^2\,(R_Z - 1)\, s\hat{\mathcal{B}}_{WW}^{d}\,(s,t) \\ +c_W^2\,(R_Z - 1)\, s\hat{\mathcal{B}}_{WW}^{c}\,(s,t) \end{cases},
\end{aligned}$$

with $s_f = 2I_f^{(3)}$, and $\hat{\mathcal{B}}_{WW}^{d}\,(s,t)$ given by the "unitarized" direct box and $\hat{\mathcal{B}}_{WW}^{c}\,(s,t)$ given by the crossed one, which has to be "unitarized" by dropping out two terms with $1/R_W$.

Contributions to the weak form factors from ZZ boxes

The ZZ box contribution forms a separate gauge invariant sub-set of terms:

$$\rho^{\rm box}_{ZZ}(s,t) = \texttt{XZZRO} = \frac{s_e s_f}{32R}\frac{s-M_Z^2}{s}\Bigg\{\left[(v_e^2+a_e^2)(v_f^2+a_f^2)+4v_e v_f\right]\left(\frac{s}{I_1}\right)^2\mathcal{B}^{(+)}_{ZZ} - \left[(v_e^2+a_e^2)(v_f^2+a_f^2)-4v_e v_f\right]\left(\frac{s}{I_2}\right)^2\mathcal{B}^{(-)}_{ZZ}\Bigg\}, \tag{3.3.29}$$

$$\kappa^{\rm box}_{e,f_{ZZ}}(s,t) = \texttt{XZZJ} = \frac{s_e s_f}{32R}\frac{s-M_Z^2}{s}(v_{e,f}-a_{e,f})\Bigg[(v_{e,f}+a_{e,f})^2\left(\frac{s}{I_2}\right)^2\mathcal{B}^{(-)}_{ZZ} -(v_{e,f}-a_{e,f})^2\left(\frac{s}{I_1}\right)^2\mathcal{B}^{(+)}_{ZZ}\Bigg], \tag{3.3.30}$$

$$\kappa^{\rm box}_{ef_{ZZ}}(s,t) = \texttt{XZZIJ} = \frac{s_e s_f}{16R}\frac{s-M_Z^2}{s}(v_e-a_e)(v_f-a_f)\left(\frac{s}{I_1}\right)^2\mathcal{B}^{(+)}_{ZZ}, \tag{3.3.31}$$

where

$$\mathcal{B}^{(+)}_{ZZ} = \texttt{XZZP} = +\mathcal{B}(s,I_1,I_2,M_Z^2) - 2\left(\frac{I_1}{s}\right)^3\mathcal{F}_4(s,I_1,M_Z^2), \tag{3.3.32}$$

$$\mathcal{B}^{(-)}_{ZZ} = \texttt{XZZM} = -\mathcal{B}(s,I_2,I_1,M_Z^2) - 2\left(\frac{I_2}{s}\right)^3\mathcal{F}_4(s,I_2,M_Z^2), \tag{3.3.33}$$

with the angular dependent invariants:

$$I_1 = -u, \qquad I_2 = -t, \qquad t = -\frac{s}{2}(1-\cos\vartheta). \tag{3.3.34}$$

In this and the next Subsections the usual ZFITTER conventions Eqs. (1.1.12)–(1.1.14) are used. The genuine box-function $\mathcal{B}(s,I_1,I_2,M_V^2)$ is calculated by function XBOX:

$$\begin{aligned}\mathcal{B}(s,I_1,I_2,M_V^2) = \texttt{XBOX} &= 2\frac{I_1}{s}\ln\frac{I_2}{M_V^2} + \frac{I_1}{s}\left(1-4\frac{M_V^2}{s}\right)s\mathcal{F}(-s,M_V^2,M_V^2)\\ &+2\frac{I_2-I_1-2M_V^2}{s}\left[\mathrm{Li}_2(1)-\mathrm{Li}_2\left(1-\frac{I_2}{M_V^2}\right)+\mathcal{F}_3(s,M_V^2)\right]\\ &+\left\{2\frac{M_V^2}{s}\left[M_V^2\,(2s-I_1)-2I_2^2\right]+\frac{I_2}{s}\left(I_1^2+I_2^2\right)\right\}\frac{1}{s^2}\mathcal{F}_4(s,I_1,M_V^2).\end{aligned} \tag{3.3.35}$$

The functions $\mathcal{F}(-s,M_V^2,M_V^2)$, $\mathcal{F}_3(s,M_V^2)$ and $\mathcal{F}_4(s,I_1,M_V^2)$ were introduced in [8].

The box-contribution as an additive part of the cross-section

For BOXD=1 the box-contribution is treated differently – as an extra piece of the cross-section. The corresponding formulae were presented in [8]. Here we repeat them again[1]. The angular distribution is returned by function DZEWBX($\cos\vartheta$):

$$\frac{d\sigma^{\rm box}}{d\cos\vartheta} = \frac{\alpha G_\mu^2 M_W^4}{8s\pi^2}\Bigg\{\lambda^L h^L \mathcal{R}e\left[\left(Q_e Q_f F_A^* + s_e s_f \chi v_e^L v_f^L\right)\left(\mathcal{B}^{(+)}_{WW}+\mathcal{B}^{(-)}_{WW}\right)\right]$$

[1] Actually the expressions for the differential weak box terms in [8] contained some misprints.

$$+\frac{1}{64}\mathcal{R}e\Bigg[\Bigg(Q_eQ_fF_A^*\left[\lambda^Lh^L(v_e^L)^2(v_f^L)^2+\lambda^Rh^R(v_e^R)^2(v_f^R)^2\right]$$
$$+s_es_f\chi^*\left[\lambda^Lh^L(v_e^L)^3(v_f^L)^3+\lambda^Rh^R(v_e^R)^3(v_f^R)^3\right]\Bigg)\mathcal{B}_{ZZ}^{(+)}$$
$$+\Bigg(Q_eQ_fF_A^*\left[\lambda^Lh^R(v_e^L)^2(v_f^R)^2+\lambda^Rh^L(v_e^R)^2(v_f^L)^2\right]$$
$$+s_es_f\chi^*\left[\lambda^Lh^R(v_e^L)^3(v_f^R)^3+\lambda^Rh^L(v_e^R)^3(v_f^L)^3\right]\Bigg)\mathcal{B}_{ZZ}^{(-)}\Bigg]\Bigg\}. \tag{3.3.36}$$

Here we use:

$$F_A=\alpha(s)/\alpha, \tag{3.3.37}$$

with $\alpha(s)$ defined by Eq. (2.2.42)), and:

$$v_e^L = v_e+a_e, \tag{3.3.38}$$
$$v_e^R = v_e-a_e, \tag{3.3.39}$$
$$v_f^L = v_f+a_f, \tag{3.3.40}$$
$$v_f^R = v_f-a_f, \tag{3.3.41}$$
$$\lambda^L = \lambda_1+\lambda_2 = (1+\lambda_+)(1-\lambda_-), \tag{3.3.42}$$
$$\lambda^R = \lambda_1-\lambda_2 = (1-\lambda_+)(1+\lambda_-), \tag{3.3.43}$$
$$h^L = h_1+h_2 = \frac{1}{4}(1+h_+)(1-h_-), \tag{3.3.44}$$
$$h^R = h_1-h_2 = \frac{1}{4}(1-h_+)(1+h_-). \tag{3.3.45}$$

3.4. Mixed Electroweak and QCD Corrections

Mixed $\mathcal{O}(\alpha\alpha_s)$ corrections originate from gluon insertions to the fermionic components of bosonic self-energies. It is easy to derive the $\mathcal{O}(\alpha\alpha_s)$ contributions to Δr, ρ, and κ simply by replacing every self-energy contribution of order $\mathcal{O}(\alpha)$ by a contribution of order $\mathcal{O}(\alpha\alpha_s)$. In this way we get:

$$\Delta\Delta r = \frac{\alpha\alpha_s}{12\pi^2}\Big[-\Pi_{\gamma\gamma}^{t,F}(0)-\Pi_{\gamma\gamma}^{l+5q,F}\left(M_Z^2\right)+\frac{c_W^2}{s_W^4}\Delta\rho^{\mathrm{fer},F}+\frac{1}{s_W^2}\Delta\rho_W^{\mathrm{fer},F}\Big], \tag{3.4.1}$$
$$\Delta\rho_{ef} = \frac{\alpha\alpha_s}{12\pi^2}\frac{1}{s_W^2}\Big[-\Delta\rho_Z^{\mathrm{fer},F}+\mathcal{D}_Z^{\mathrm{fer},F}(s)\Big], \tag{3.4.2}$$
$$\Delta\kappa_e = \Delta\kappa_f=\frac{1}{2}\kappa_{ef}=\frac{\alpha\alpha_s}{12\pi^2}\frac{1}{s_W^2}\Big[-\frac{c_W^2}{s_W^2}\Delta\rho^{\mathrm{fer},F}-\Pi_{ZA}^{\mathrm{fer},F}(s)\Big]. \tag{3.4.3}$$

3.4.1. Package `bcqcdl.f`

The implementation of internal QCD corrections is governed by flag `QCDC`. If `QCDC`=0, they are not implemented. The options `QCDC`=1,2 are based on [99] and [70] where the two-loop self-energy functions of order $\mathcal{O}(\alpha\alpha_s)$ were reduced to two numerically treated integrals. In [13] all these corrections, Eqs. (3.4.1)–(3.4.3), were computed in terms of three

self-energy functions $\Pi^{V,A,W}$ and Taylor expansions in powers of s/m_t^2 were developed. These expansions, accessible with `QCDC`=1, ensured sufficient precision in the beginning of LEP1 running and allowed a very fast computing compared to the exact, but CPU time consuming option `QCDC`=2. The relevant functions are supplied by the package `bcqcdl.f`. Both options are fully described in [96,13]. We do not repeat their description here since a better option is available.

3.4.2. Package `bkqcdl.f`

With the option `QCDC`=3 we implemented analytic results for $\Pi^{V,A,W}$ derived in [38] in the dimensional regularization scheme. A `FORTRAN` code for their calculations was provided by B. Kniehl.

From Eqs. (3.4.1)–(3.4.3) it is easy to derive two sets of equations:

(i) for a light quark u–d doublet;

(ii) for the heavy quark t–b doublet.

The expressions for a light quark doublet are very short:

$$\Delta r^{ud} = \texttt{CLQQCD} = -\frac{\alpha\alpha_S}{\pi^2}\frac{1}{4}\frac{c_W^2 - s_W^2}{s_W^4}\ln c_W^2, \tag{3.4.4}$$

$$\Delta\rho^{ud} = \texttt{ROQCD} = -\frac{\alpha\alpha_S}{\pi^2}\frac{1}{16}\frac{1}{s_W^2 c_W^2}\Big[2 + (\sigma_t^a)^2 + (\sigma_b^a)^2\Big]\frac{s}{s - M_Z^2}\ln R_Z, \tag{3.4.5}$$

$$\Delta\kappa^{ud} = \texttt{AKQCD} = \frac{\alpha\alpha_S}{\pi^2}\frac{1}{4s_W^4}\Big\{c_W^2\ln c_W^2 + s_W^2\Big[1 - 4s_W^2\left(Q_u^2 + Q_f^2\right)\Big]\ln R_Z\Big\}. \tag{3.4.6}$$

Here and below we use the ratios:

$$c_W^2 = \frac{M_W^2}{M_Z^2}, \tag{3.4.7}$$

$$s_W^2 = 1 - c_W^2, \tag{3.4.8}$$

$$r_W = \frac{M_H^2}{M_W^2}, \tag{3.4.9}$$

$$r_Z = \frac{M_H^2}{M_Z^2}, \tag{3.4.10}$$

$$R_W = \frac{M_W^2}{s}, \tag{3.4.11}$$

$$R_Z = \frac{M_Z^2}{s}, \tag{3.4.12}$$

and:

$$\sigma_f^a = |v_f + a_f| = 1 - 4|Q_f|s_W^2. \tag{3.4.13}$$

For a heavy quark doublet one derives:

$$\Delta r^{tb} = \texttt{XTBQCD} = \frac{\alpha\alpha_S}{\pi^2}\Big\{Q_t^2 V_1'(0) + \frac{c_W^2}{s_W^4}\frac{r_t}{4}\left[\zeta(2) + \frac{1}{2}\right] - \frac{z_t}{4s_W^4}\mathrm{Re}\Big[(\sigma_t^a)^2 V_1(r_Z) + A_1(r_Z)$$

$$-A_1(0)\Big] + \frac{c_W^2 - s_W^2}{s_W^4} r_t \Big[\mathrm{Re}F_1(x) - \mathrm{Re}F_1(0)\Big] - \frac{1}{8s_W^4}\sigma_b^a \ln z_t \Big\}, \tag{3.4.14}$$

$$\Delta\rho^{tb} = \texttt{ROQCD} = \frac{\alpha\alpha_s}{\pi^2}\frac{1}{4s_W^2 c_W^2}\Big\{ z_t\Big[(\sigma_t^a)^2 V_1(r_z) + A_1(r_z)\Big]$$
$$+\frac{m_t^2}{M_Z^2 - s}\Big\{(\sigma_t^a)^2\Big[V_1(r) - V_1(r_z)\Big] + A_1(r) - A_1(r_z)\Big\}$$
$$-\frac{1}{4}\Big[1 + (\sigma_b^a)^2\Big]\frac{s}{s - M_Z^2}\ln R_Z - 2z_f\left[\frac{23}{8} - \zeta(2) - 3\zeta(3)\right]\Big\}, \tag{3.4.15}$$

$$\Delta\kappa^{tb} = \texttt{AKQCD} = \frac{\alpha\alpha_s}{\pi^2}\Big\{\frac{c_W^2}{4s_W^4} r_t\Big[(\sigma_t^a)^2 V_1(r_z) + A_1(r_z)\Big] - \frac{c_W^2}{s_W^4} r_t F_1(x)$$
$$+\frac{\sigma_t^a}{s_W^2}|Q_t| r_t V_1(r) - \frac{1}{16 s_W^4}\Big[-(1 + \sigma_b^a)\ln z_t - 4\sigma_b^a |Q_b| s_W^2 \ln R_Z\Big]\Big\}, \tag{3.4.16}$$

where

$$r_t = \frac{m_t^2}{M_W^2}, \tag{3.4.17}$$

$$r = \frac{s + i\epsilon}{4m_t^2}, \tag{3.4.18}$$

$$r_Z = \frac{M_Z^2 + i\epsilon}{4m_t^2}, \tag{3.4.19}$$

$$x = \frac{M_W^2 + i\epsilon}{4m_t^2}. \tag{3.4.20}$$

They are returned by complex-valued functions:

$$V_1(r) = \texttt{CV1(CR)}, \tag{3.4.21}$$

$$A_1(r) = \texttt{CA1(CR)}, \tag{3.4.22}$$

$$F_1(x) = \texttt{CF1(CX)}. \tag{3.4.23}$$

3.5. Two-Loop Electroweak Corrections. Package `m2tcor.f`

The two-loop EW corrections are supplied by the package `m2tcor.f` [30]. It is based on [34–36]. The package is interfaced to `ZFITTER` by subroutine `GDEGNL`:

```
GDEGNL(GMU,MZ,MT,AMH,MW,PI3QF,SMAN,DRDREM,DRHOD,DKDREM,DROREM)
```

In the argument list, the following variables are `INPUT`:

$$\texttt{GMU} = G_\mu, \tag{3.5.1}$$

$$\texttt{MZ} = M_Z, \tag{3.5.2}$$

$$\texttt{MT} = m_t, \tag{3.5.3}$$

$$\texttt{AMH} = M_H, \tag{3.5.4}$$

$$\texttt{MW} = M_W, \tag{3.5.5}$$

$$\texttt{PI3QF} = Q_f, \tag{3.5.6}$$

$$\texttt{SMAN} = s; \tag{3.5.7}$$

and the following ones are `OUTPUT`:

$$\texttt{DRDREM} = \Delta r^{\alpha^2}_{\rm rem}\,, \tag{3.5.8}$$

$$\texttt{DRHOD} = -\delta\hat{\rho}^{G^2}\,, \tag{3.5.9}$$

$$\texttt{DKDREM} = \delta\kappa^{f,G^2}_{\rm rem}\,, \tag{3.5.10}$$

$$\texttt{DROREM} = \delta\rho^{f,G^2}_{\rm rem}\,. \tag{3.5.11}$$

The various two-loop corrections consist of two pieces. One is derived in the $\overline{MS}$ framework and the other one, with the superscript OMS, contains the additional corrections coming from the expansion of the OMS sine of weak mixing angle in the one-loop result. The OMS result is a sum: $\texttt{something} + \texttt{something}_{\rm OMS}$, with the coupling constant being expressed in terms of OMS quantities.

Typically, every correction has two branches: $h_t < 1/4$ — the *light Higgs case*, and $h_t > 4$ — the *heavy Higgs case*, with an interpolation in between. The expressions are rather lengthy in spite of expansions in positive powers of m_t^2. The two-loop level is quite involved and since the Higgs mass is unknown we would like to have an expression valid for any mass of the Higgs.

In what follows we use the short hand notations:

$$w_t = \frac{M_W^2}{m_t^2}\,, \tag{3.5.12}$$

$$z_t = \frac{M_Z^2}{m_t^2}\,, \tag{3.5.13}$$

$$h_t = \frac{M_H^2}{m_t^2}\,. \tag{3.5.14}$$

The leading two-loop term in the calculation of Δr is accounted for by the following substitutions:

$$f\Delta r_{_L} \rightarrow f\Delta r_{_L} + \frac{c_W^2}{s_W^2} N_c x_t^2 \left(\Delta\rho^{(2)} + \Delta\rho^{(2)}_{\rm OMS}\right), \tag{3.5.15}$$

$$-\Delta\hat{\rho} = \Delta\rho^{(2)} + \Delta\rho^{(2)}_{\rm OMS}\,. \tag{3.5.16}$$

For the leading contributions to $\rho^f_{_L}$ and $\kappa^f_{_L}$ they are [36]:

$$f\rho^f_{_L} \rightarrow \Delta\hat{\rho}\,(1 - \Delta\bar{r}_{\rm rem})\,, \tag{3.5.17}$$

$$f\kappa^f_{_L} \rightarrow -\frac{c_W^2}{s_W^2}\Delta\hat{\rho}\,(1 - \Delta\bar{r}_{\rm rem})\,, \tag{3.5.18}$$

where f is the conversion factor Eq. (2.3.23) and $\Delta\bar{r}_{\rm rem} = \texttt{DF1BAR}$ is defined by Eq. (2.4.23).

The $\Delta\rho^{(2)}$ is the two-loop irreducible contribution to Veltman's ρ-parameter, as defined by Eq. (2.3.21):

$$\Delta\hat{\rho} = \frac{\alpha}{4\pi s_W^2}\frac{1}{M_W^2}\Big[\Sigma_{WW}(M_W^2) - \Sigma_{ZZ}(M_Z^2)\Big]\Big|_{\overline{MS},\,\mu=M_Z}\,, \tag{3.5.19}$$

but now to orders $\mathcal{O}\left(G_\mu^2 m_t^4\right)$ and $\mathcal{O}\left(G_\mu^2 m_t^2 M_Z^2\right)$.

All results for $\Delta\rho^{(2)}$ are returned by the subroutines `ew2ltobf` and `ew2ltobfOS`. The subroutine `ew2ltobf` computes the two-loop expression of Eq. (3.5.19) in units of $N_c\alpha^2/(16\pi s_W^2 z_t c_W^2)^2$:

$$\Delta\rho^{(2)} \;=\; \texttt{tobf2lew}. \tag{3.5.20}$$

The subroutine `ew2ltobfOS` computes the additional term to be added to the $\overline{MS}$ two-loop expression of Eq. (3.5.19) in units of $N_c\alpha^2/[(4\pi s_W^2)^2 4 z_t c_W^2]$:

$$\Delta\rho^{(2)}_{\rm OMS} \;=\; 4 z_t c_W^2 \cdot \texttt{tobf2ewOS}. \tag{3.5.21}$$

The three *remainders* are modified as follows:

$$\Delta r_{\rm rem} \;\to\; \Delta r_{\rm rem} + \Delta r^{(2)}_{\rm rem}, \tag{3.5.22}$$

$$\rho^f_{\rm rem} \;\to\; f\rho^f_{\rm rem} + \rho^{f(2)}_{\rm rem}, \tag{3.5.23}$$

$$\kappa^f_{\rm rem} \;\to\; f\kappa^f_{\rm rem} + \kappa^{f(2)}_{\rm rem}. \tag{3.5.24}$$

However, contrary to the leading term Eq. (3.5.16), the remainders contain also contributions from vertex diagrams. That's why they are channel dependent and bear the superscript f. Now we list all terms entering Eq. (3.5.24):

- $\Delta r^{(2)}_{\rm rem}$:

$$\Delta r^{(2)}_{\rm rem} \;=\; \texttt{DRDREM} = N_c \left(\frac{\alpha}{4\pi s_W}\right)^2 \left(\frac{m_t^2}{M_W^2}\right)^2 \left[\Delta r^{(2)}_W + \Delta r^{(2)}_{W,\rm OMS} - \left(\frac{\delta e}{e}\right)^{(2)}\right]. \tag{3.5.25}$$

The $\Delta r^{(2)}_W$ is made of the two-loop contribution to

$$\Delta\hat\rho_W = \frac{1}{M_W^2}\left[\Sigma^F_{WW}(0) - \Sigma^F_{WW}\left(M_W^2\right)\right]\Big|_{\overline{MS},\,\mu=M_Z}, \tag{3.5.26}$$

and a vertex correction V_r:

$$\Delta r^{(2)}_W = -\Delta\rho^{(2)}_W + V_r\,. \tag{3.5.27}$$

The $(\delta e/e)^{(2)}$ is the two-loop contribution to the electric charge renormalization.
The Subroutine `ew2ldeltarw` returns these two-loop expressions in the variable `drs2lew`:

$$\Delta r^{(2)}_W \;=\; \texttt{drs2lew}, \tag{3.5.28}$$

$$-\Delta\rho^{(2)}_W \;=\; \texttt{aww}, \tag{3.5.29}$$

$$V_r \;=\; \texttt{vertex1}. \tag{3.5.30}$$

The (`aww` and `vertex1` are internal variables. Subroutine `ew2ldeltarwOS` computes the term to be added to the $\overline{MS}$ two-loop expression of $\Delta\rho^{(2)}_W$ in units of $N_c\alpha^2/[(4\pi s_W^2)^2 4 z_t c_W^2]$:

$$\Delta\rho^{(2)}_{W,\rm OMS} = \frac{1}{4} z_t c_W \texttt{drs2ewOS}. \tag{3.5.31}$$

The subroutine `ew2ltwodel` computes the two-loop contribution to the electric charge renormalization in units of $N_c\alpha^2/(4\pi s_W^2 z_t c_W^2)^2$:

$$\left(\frac{\delta e}{e}\right)^{(2)} = \texttt{deleoe2lew}. \tag{3.5.32}$$

- $\rho_{\rm rem}^{f(2)}(s)$:

$$\rho_{\rm rem}^{f(2)}(s) = \texttt{DROREM} = N_c\,(4x_t)^2\left[w_t\Big(\eta^{(2)}+\eta_{\rm OMS}^{f(2)}(s)-2c_W^2\log c_W^2\Big)-\Big(\Delta r_W^{(2)}+\Delta r_{W,\rm OMS}^{(2)}\Big)\right]. \quad (3.5.33)$$

The $\eta^{(2)}$ is the two-loop contribution to

$$\mathrm{Re}\left[\frac{\Sigma_{ZZ}(s)-\Sigma_{ZZ}(M_Z^2)}{s-M_Z^2}\right]\Bigg|_{s=M_Z^2}. \quad (3.5.34)$$

The subroutine `ew2leta` returns its two-loop expression in units of $N_c\alpha^2/[(4\pi s_W^2)^2 z_t c_W^2]$:

$$\eta^{(2)} = \texttt{eta2lew}. \quad (3.5.35)$$

The additional piece to be added to the $\overline{MS}$ two-loop contribution `eta2lewOS`, Eq. (3.5.34), is returned by subroutine `ew2letaOS` in units of $N_c\alpha^2/[(4\pi s_W^2)^2 4 z_t c_W^2]$:

$$\eta_{\rm OMS}^{f(2)}(s) = \frac{1}{4}\texttt{eta2lewOS}. \quad (3.5.36)$$

- $\kappa_{\rm rem}^{f(2)}(s)$:

$$\kappa_{\rm rem}^{f(2)}(s) = \texttt{DKDREM} = N_c x_t^2\Big[k^{(2)}+k_{\rm OMS}^{f(2)}(s)\Big]. \quad (3.5.37)$$

The $k^{(2)}$ is the two-loop contribution to

$$\Pi_{Z\gamma}(M_Z^2)+V_m\,, \quad (3.5.38)$$

i.e. the two-loop expressions for the $Z\gamma$-mixing and the relevant vertex correction.

The subroutine `kappacur2l` returns it in units of $N_c\alpha^2/(16\pi s_W^2 z_t c_W^2)^2$:

$$k^{(2)} = \texttt{k2lew}. \quad (3.5.39)$$

The additional piece to be added to the $\overline{MS}$ two-loop contribution is calculated in subroutine `kappacur2lOS` in units of $N_c\alpha^2/[(4\pi s_W^2)^2 4 z_t]$:

$$k_{\rm OMS}^{f(2)}(s) \;=\; -4c_W^2 z_t\texttt{k2lewOS}. \quad (3.5.40)$$

3.6. Final State QCD and QED Corrections

This subsection is devoted to the detailed description of the corrections $R_V^f(s)$ and $R_A^f(s)$ introduced in the expressions for the Z width Eq. (2.4.9) and Eq. (2.4.10).

3.6.1. Case of leptons

In Eq. (2.4.9), for the Z decays into leptons the QED FSR for an inclusive setup are described by a simple factor $R_{\rm QED}(M_Z^2)$:

$$R_{\rm QED}(s) = 1+\frac{3}{4}\frac{\alpha(s)}{\pi}Q_f^2\,, \quad (3.6.1)$$

$$R_{\rm QED}(M_Z^2) = 1+0.0017Q_f^2\,. \quad (3.6.2)$$

The same factor is used for the total cross-section of lepton pair production for the case `FINR`=0. For lepton pair production with a proper treatment of final state radiation with cuts (`FINR`=1) this factor is replaced by different formulae, see Chapter 1.

3.6.2. Case of quarks

In Eq. (2.4.10) for the Z decays into quarks the radiator factors $R^f_{V,A}(M_Z^2)$ introduced in Eq. (2.4.10) are used. For quark production cross-sections these radiator factors get s-dependent. They will be given in this section. When cuts are applied, the QED is treated properly. This means that the one-loop QED pieces of the radiator factors Eqs. (3.6.3)–(3.6.4) are left out. Then, the higher order QCD and mixed QCD⊗QED pieces are applied in an approximate way since they are known only for the total cross-section.

For A_{FB}, the one-loop QED and QCD corrections vanish in massless approximation. These factors are applied only for the $c\overline{c}$ and $b\overline{b}$ channels to first order in $\mathcal{O}\left(m_q/\sqrt{s}\right)$ [100].

Subroutine `QCDCOF` computes the inclusive $R_{V,A}$-factors:

$$
\begin{aligned}
R^q_V(s) &= 1+\frac{3}{4}Q_q^2\frac{\alpha(s)}{\pi}+\frac{\alpha_S(s)}{\pi}-\frac{1}{4}Q_q^2\frac{\alpha(s)}{\pi}\frac{\alpha_S(s)}{\pi} \\
&+\left[C_{02}+C_2^t\left(\frac{s}{m_t^2}\right)\right]\left(\frac{\alpha_S(s)}{\pi}\right)^2+C_{03}\left(\frac{\alpha_S(s)}{\pi}\right)^3 \\
&+\frac{m_c^2(s)+m_b^2(s)}{s}C_{23}\left(\frac{\alpha_S(s)}{\pi}\right)^3 \\
&+\frac{m_q^2(s)}{s}\left[C_{21}^V\frac{\alpha_S(s)}{\pi}+C_{22}^V\left(\frac{\alpha_S(s)}{\pi}\right)^2+C_{23}^V\left(\frac{\alpha_S(s)}{\pi}\right)^3\right] \\
&+\frac{m_c^4(s)}{s^2}\left[C_{42}-\ln\frac{m_c^2(s)}{s}\right]\left(\frac{\alpha_S(s)}{\pi}\right)^2+\frac{m_b^4(s)}{s^2}\left[C_{42}-\ln\frac{m_b^2(s)}{s}\right]\left(\frac{\alpha_S(s)}{\pi}\right)^2 \\
&+\frac{m_q^4(s)}{s^2}\left\{C_{41}^V\frac{\alpha_S(s)}{\pi}+\left[C_{42}^V+C_{42}^{V,L}\ln\frac{m_q^2(s)}{s}\right]\left(\frac{\alpha_S(s)}{\pi}\right)^2\right\} \\
&+12\frac{m_q'^4(s)}{s^2}\left(\frac{\alpha_S(s)}{\pi}\right)^2-\frac{m_q^6(s)}{s^3}\left\{8+\frac{16}{27}\left[155+6\ln\frac{m_q^2(s)}{s}\right]\frac{\alpha_S(s)}{\pi}\right\}, \qquad (3.6.3)
\end{aligned}
$$

$$
\begin{aligned}
R^q_A(s) &= 1+\frac{3}{4}Q_q^2\frac{\alpha(s)}{\pi}+\frac{\alpha_S(s)}{\pi}-\frac{1}{4}Q_q^2\frac{\alpha(s)}{\pi}\frac{\alpha_S(s)}{\pi} \\
&+\left[C_{02}+C_2^t\left(\frac{s}{m_t^2}\right)-\left(2I_q^{(3)}\right)\mathcal{I}^{(2)}\left(\frac{s}{m_t^2}\right)\right]\left(\frac{\alpha_S(s)}{\pi}\right)^2 \\
&+\left[C_{03}-\left(2I_q^{(3)}\right)\mathcal{I}^{(3)}\left(\frac{s}{m_t^2}\right)\right]\left(\frac{\alpha_S(s)}{\pi}\right)^3 \\
&+\frac{m_c^2(s)+m_b^2(s)}{s}C_{23}\left(\frac{\alpha_S(s)}{\pi}\right)^3+\frac{m_q^2(s)}{s}\left[C_{20}^A+C_{21}^A\frac{\alpha_S(s)}{\pi}+C_{22}^A\left(\frac{\alpha_S(s)}{\pi}\right)^2\right. \\
&\left.+6\left(3+\ln\frac{m_t^2}{s}\right)\left(\frac{\alpha_S(s)}{\pi}\right)^2+C_{23}^A\left(\frac{\alpha_S(s)}{\pi}\right)^3\right] \\
&-10\frac{m_q^2(s)}{m_t^2}\left[\frac{8}{81}+\frac{1}{54}\ln\frac{m_t^2}{s}\right]\left(\frac{\alpha_S(s)}{\pi}\right)^2 \\
&+\frac{m_c^4(s)}{s^2}\left[C_{42}-\ln\frac{m_c^2(s)}{s}\right]\left(\frac{\alpha_S(s)}{\pi}\right)^2+\frac{m_b^4(s)}{s^2}\left[C_{42}-\ln\frac{m_b^2(s)}{s}\right]\left(\frac{\alpha_S(s)}{\pi}\right)^2
\end{aligned}
$$

$$+\frac{m_q^4(s)}{s^2}\left\{C_{40}^A + C_{41}^A\frac{\alpha_s(s)}{\pi} + \left[C_{42}^A + C_{42}^{A,L}\ln\frac{m_q^2(s)}{s}\right]\left(\frac{\alpha_s(s)}{\pi}\right)^2\right\}$$
$$-12\frac{m_q'^4(s)}{s^2}\left(\frac{\alpha_s(s)}{\pi}\right)^2. \tag{3.6.4}$$

Eqs. (3.6.2)–(3.6.4) are strictly valid only in the inclusive setup, i.e. when no cuts are applied in the final state. For this setup the appearance of $\alpha_s(s)$ and $\alpha(s)$ is strictly proved, see [101] for the QED case and [83] for the QCD case.

However, in the case of QCD FSR corrections to the hadronic total cross-section, the feasibility of the inclusive formulae is justified not only for rather loose cuts by the fact that hadrons are always inclusive with respect to gluon bremsstrahlung.

For QED corrections with loose cuts, when we apply nevertheless formulae depending on cuts, it is reasonable to use the running QED coupling at scale $\alpha(s)$ rather than at scale $\alpha(0)$ in order to have a smooth transition to the case of inclusive setup.

Moreover, it is understood that:

- only c-and b-quark finite mass corrections are retained, i.e. $m_q = 0$ for $q = u, d, s$. Therefore, these corrections are valid slightly above the $b\overline{b}$-threshold, say $\sqrt{s} \geq 13$ GeV, and below the $t\bar{t}$-threshold, say $\sqrt{s} < 350$ GeV;
- m_q' denotes *the other* mass in a quark doublet, i.e. it is m_b if $q = c$ and it is m_c if $q = b$; quark masses with the argument (s) are $\overline{MS}$ *running* masses, while M_q stands for *pole* masses. The numerical coefficients in Eq. (3.6.3) and Eq. (3.6.4) are listed here:

Massless non-singlet corrections [102–105]:

$$C_{02} = \texttt{COEF02} = \frac{365}{24} - 11\zeta(3) + \left[-\frac{11}{12} + \frac{2}{3}\zeta(3)\right]n_f, \tag{3.6.5}$$

$$C_{03} = \texttt{COEF03} = \frac{87029}{288} - \frac{121}{8}\zeta(2) - \frac{1103}{4}\zeta(3) + \frac{275}{6}\zeta(5)$$
$$+\left[-\frac{7847}{216} + \frac{11}{6}\zeta(2) + \frac{262}{9}\zeta(3) - \frac{25}{9}\zeta(5)\right]n_f$$
$$+\left[\frac{151}{162} - \frac{1}{18}\zeta(2) - \frac{19}{27}\zeta(3)\right]n_f^2; \tag{3.6.6}$$

Quadratic massive corrections [83]:

$$C_{23} = \texttt{COEFL3} = -80 + 60\zeta(3) + \left[\frac{32}{9} - \frac{8}{3}\zeta(3)\right]n_f, \tag{3.6.7}$$

$$C_{21}^V = \texttt{COEFV1} = 12, \tag{3.6.8}$$

$$C_{22}^V = \texttt{COEFV2} = \frac{253}{2} - \frac{13}{3}n_f, \tag{3.6.9}$$

$$C_{23}^V = \texttt{COEFV3} = 2522 - \frac{855}{2}\zeta(2) + \frac{310}{3}\zeta(3) - \frac{5225}{6}\zeta(5)$$

$$+\left[-\frac{4942}{27}+34\zeta(2)-\frac{394}{27}\zeta(3)+\frac{1045}{27}\zeta(5)\right]n_f+\left[\frac{125}{54}-\frac{2}{3}\zeta(2)\right]n_f^2, \tag{3.6.10}$$

$$C_{20}^A = \texttt{COEFA0} = -6, \tag{3.6.11}$$

$$C_{21}^A = \texttt{COEFA1} = -22, \tag{3.6.12}$$

$$C_{22}^A = \texttt{COEFA2} = -\frac{8221}{24}+57\zeta(2)+117\zeta(3)+\left[\frac{151}{12}-2\zeta(2)-4\zeta(3)\right]n_f, \tag{3.6.13}$$

$$\begin{aligned} C_{23}^A = \texttt{COEFA3} &= -\frac{4544045}{864}+1340\zeta(2)+\frac{118915}{36}\zeta(3)-127\zeta(5)\\ &+\left[\frac{71621}{162}-\frac{209}{2}\zeta(2)-216\zeta(3)+5\zeta(4)+55\zeta(5)\right]n_f\\ &+\left[-\frac{13171}{1944}+\frac{16}{9}\zeta(2)+\frac{26}{9}\zeta(3)\right]n_f^2; \end{aligned} \tag{3.6.14}$$

Quartic massive corrections:

$$C_{42} = \frac{13}{3}-4\zeta(3), \tag{3.6.15}$$

$$\texttt{R4LC} = \frac{m_c^4(s)}{s^2}\left(C_{42}-\ln\frac{m_c^4(s)}{s}\right)\frac{\alpha_s^2(s)}{\pi^2}, \tag{3.6.16}$$

$$C_{40}^V = -6, \tag{3.6.17}$$

$$C_{41}^V = -22, \tag{3.6.18}$$

$$C_{42}^V = -\frac{3029}{12}+162\zeta(2)+112\zeta(3)+\left[\frac{143}{18}-4\zeta(2)-\frac{8}{3}\zeta(3)\right]n_f, \tag{3.6.19}$$

$$\texttt{RV40} = C_{40}^V+C_{41}^V\frac{\alpha_s(s)}{\pi}+C_{42}^V\frac{\alpha_s^2(s)}{\pi^2}, \tag{3.6.20}$$

$$C_{42}^{V,L} = -\frac{11}{2}+\frac{1}{3}n_f, \tag{3.6.21}$$

$$\texttt{RV4L} = C_{42}^{V,L}\frac{\alpha_s^2(s)}{\pi^2}, \tag{3.6.22}$$

$$C_{40}^A = 6, \tag{3.6.23}$$

$$C_{41}^A = 10, \tag{3.6.24}$$

$$C_{42}^A = \frac{3389}{12}-162\zeta(2)-220\zeta(3)+\left[-\frac{41}{6}+4\zeta(2)+\frac{16}{3}\zeta(3)\right]n_f, \tag{3.6.25}$$

$$\texttt{RA40} = C_{40}^A + C_{41}^A \frac{\alpha_S(s)}{\pi} + C_{42}^A \frac{\alpha_S^2(s)}{\pi^2}, \tag{3.6.26}$$

$$C_{42}^{A,L} = \frac{77}{2} - \frac{7}{3} n_f, \tag{3.6.27}$$

$$\texttt{RA4L} = C_{42}^{A,L} \frac{\alpha_S^2(s)}{\pi^2}; \tag{3.6.28}$$

Power suppressed t-mass correction:

$$C_2^t(x) = x\left(\frac{44}{675} - \frac{2}{135}\ln x\right); \tag{3.6.29}$$

Singlet axial corrections:

$$\mathcal{I}^{(2)}(x) = -\frac{37}{12} + \ln x + \frac{7}{81}x + \texttt{0.0132}x^2, \tag{3.6.30}$$

$$\mathcal{I}^{(3)}(x) = -\frac{5075}{216} + \frac{23}{6}\zeta(2) + \zeta(3) + \frac{67}{18}\ln x + \frac{23}{12}\ln^2 x; \tag{3.6.31}$$

Singlet vector correction:

$$R_V^h(s) = \left(\sum_f v_f\right)^2 (\texttt{-0.41317}) \left(\frac{\alpha_S(s)}{\pi}\right)^3; \tag{3.6.32}$$

ABL corrections for A_{FB} [100]:

$$R_{FB}^q = f_1 \frac{m_q}{\sqrt{s}}, \tag{3.6.33}$$

$$f_1 = \frac{16}{3}\frac{\alpha_S(s)}{\pi}. \tag{3.6.34}$$

3.6.3. Running masses

The running c-quark mass is calculated by function `ZRMCMC`:

$$\begin{aligned} M_c = m_c(M_c^2)\Bigg\{1 &+ \left[\frac{4}{3} + \ln\frac{M_c^2}{m_c^2(M_c^2)}\right]\frac{\alpha_S(M_c^2)}{\pi} \\ &+ \left[K_c + \left(\frac{173}{24} - \frac{13}{36}n_f\right)\ln\frac{M_c^2}{m_c^2(M_c^2)} + \left(\frac{15}{8} - \frac{1}{12}n_f\right)\ln^2\frac{M_c^2}{m_c^2(M_c^2)}\right. \\ &\left. + \frac{4}{3}\Lambda\left(\frac{m_s(M_c^2)}{m_c(M_c^2)}\right)\right]\left(\frac{\alpha_S(M_c^2)}{\pi}\right)^2\Bigg\}, \end{aligned} \tag{3.6.35}$$

with

$$K_c = \texttt{AKC} = \frac{2905}{288} + \frac{1}{3}\left[7 + 2\ln(2)\right]\zeta(2) - \frac{1}{6}\zeta(3) - \frac{1}{3}\left[\frac{71}{48} + \zeta(2)\right]n_f, \tag{3.6.36}$$

$$\Lambda(r) \approx \frac{\pi^2}{8}r - 0.597r^2 + 0.230r^3, \tag{3.6.37}$$

which is solved numerically with respect to $m_c(M_c^2)$ at $n_f = 4$, followed by a RG-evolution (in subroutine `QCDCOF`) with two scales: 1) $M_c^2 \to M_b^2$, 2) $M_b^2 \to s$:

$$\begin{aligned} m_c(s) &= \texttt{AMQRUN} = m_c(M_c^2)\left[\frac{\alpha_s(M_b^2)}{\alpha_s(M_c^2)}\right]^{\gamma_0^{(4)}/\beta_0^{(4)}}\left\{1 + C_1(4)\left[\frac{\alpha_s(M_b^2)}{\pi} - \frac{\alpha_s(M_c^2)}{\pi}\right]\right. \\ &+\frac{1}{2}C_1^2(4)\left[\frac{\alpha_s(M_b^2)}{\pi} - \frac{\alpha_s(M_c^2)}{\pi}\right]^2 + \frac{1}{2}C_2(4)\left[\left(\frac{\alpha_s(M_b^2)}{\pi}\right)^2 - \left(\frac{\alpha_s(M_c^2)}{\pi}\right)^2\right]\Bigg\} \\ &\times\left[\frac{\alpha_s(s)}{\alpha_s(M_b^2)}\right]^{\gamma_0^{(5)}/\beta_0^{(5)}}\left\{1 + C_1(5)\left[\frac{\alpha_s(s)}{\pi} - \frac{\alpha_s(M_b^2)}{\pi}\right]\right. \\ &+\frac{1}{2}C_1^2(5)\left[\frac{\alpha_s(s)}{\pi} - \frac{\alpha_s(M_b^2)}{\pi}\right]^2 + \frac{1}{2}C_2(5)\left[\left(\frac{\alpha_s(s)}{\pi}\right)^2 - \left(\frac{\alpha_s(M_b^2)}{\pi}\right)^2\right]\Bigg\}. \end{aligned} \tag{3.6.38}$$

The running b-quark mass is calculated by an analogous chain with the first step similar to Eq. (3.6.35) with the obvious replacements $c \to b$, $s \to s$ *and* c at $n_f = 5$, followed by a 'one step' RG-evolution: $M_b^2 \to s$. We note that $m_s(\mu)$ and $m_c(\mu)$ *inside* Δ in turn evolve as appropriate[2].

In the equations above:

$$C_1(n_f) = \frac{\gamma_1^{(n_f)}}{\beta_0^{(n_f)}} - \frac{\beta_1^{(n_f)}\gamma_0^{(n_f)}}{\left(\beta_0^{(n_f)}\right)^2}, \tag{3.6.39}$$

$$C_2(n_f) = \frac{\gamma_2^{(n_f)}}{\beta_0^{(n_f)}} - \frac{\beta_1^{(n_f)}\gamma_1^{(n_f)}}{\left(\beta_0^{(n_f)}\right)^2} - \frac{\beta_2^{(n_f)}\gamma_0^{(n_f)}}{\left(\beta_0^{(n_f)}\right)^2} + \frac{\left(\beta_1^{(n_f)}\right)^2\gamma_0^{(n_f)}}{\left(\beta_0^{(n_f)}\right)^3}. \tag{3.6.40}$$

The Beta function coefficients are:

$$\beta_0^{(n_f)} = \texttt{BETA0} = \frac{1}{4}\left(11 - \frac{2}{3}n_f\right), \tag{3.6.41}$$

$$\beta_1^{(n_f)} = \texttt{BETA1} = \frac{1}{16}\left(102 - \frac{38}{3}n_f\right), \tag{3.6.42}$$

$$\beta_2^{(n_f)} = \texttt{BETA2} = \frac{1}{64}\left(\frac{2857}{2} - \frac{5033}{18}n_f + \frac{325}{54}n_f^2\right). \tag{3.6.43}$$

The Gamma function coefficients are:

$$\gamma_0^{(n_f)} = \texttt{GAMA0} = 1, \tag{3.6.44}$$

$$\gamma_1^{(n_f)} = \texttt{GAMA1} = \frac{1}{16}\left(\frac{202}{3} - \frac{20}{9}n_f\right), \tag{3.6.45}$$

$$\gamma_2^{(n_f)} = \texttt{GAMA2} = \frac{1}{64}\left\{1249 - \left[\frac{2216}{27} + \frac{160}{3}\zeta(3)\right]n_f - \frac{140}{81}n_f^2\right\}. \tag{3.6.46}$$

[2]It should also be noted that Eq. (3.6.35)) has a very bad perturbative convergence for the case of c-quark, like $1 + 0.253 + 0.228$.This is due to the large numerical value of K_c and $\alpha_s(M_c^2) = 0.375$. For the b-quark it looks a bit better: $1 + 0.119 + 0.059$ due to a smaller value of $\alpha_s(M_b^2) = 0.225$ (we used $\alpha_s(M_z^2) = 0.1204$ in this evaluation).

The running α_s follows:

$$\frac{\alpha_s\left(s,\Lambda_{\overline{\rm MS}}^{(n_f)}\right)}{\pi} = \frac{1}{\beta_0 L}\left\{1-\frac{\beta_1}{\beta_0^2 L}\ln L+\frac{\beta_1^2}{\beta_0^4 L^2}\left[\ln^2 L-\ln L-1+\frac{\beta_2\beta_0}{\beta_1^2}\right]\right\}, \tag{3.6.47}$$

$$L = \ln\frac{s}{\left(\Lambda_{\overline{\rm MS}}^{(n_f)}\right)^2}\,. \tag{3.6.48}$$

Actually the code calculates $\Lambda_{\overline{\rm MS}}^{(5)}$ for an input value of $\bar{\alpha_s}(M_Z^2)$, solving numerically the RG-equation:

$$\frac{\alpha_s\left(M_Z^2,\Lambda_{\overline{\rm MS}}^{(5)}\right)}{\pi}-\frac{1}{\beta_0 L}\left\{1-\frac{\beta_1}{\beta_0^2 L}\ln L+\frac{\beta_1^2}{\beta_0^4 L^2}\left[\ln^2 L-\ln L-1+\frac{\beta_2\beta_0}{\beta_1^2}\right]\right\} = 0. \tag{3.6.49}$$

Then $\Lambda_{\overline{\rm MS}}^{(4)}$ and $\Lambda_{\overline{\rm MS}}^{(3)}$ are calculated using the matching condition:

$$\begin{aligned}\ln\left(\frac{\Lambda_{\overline{\rm MS}}^{(n_f)}}{\Lambda_{\overline{\rm MS}}^{(n_f-1)}}\right)^2 = {}& \beta_0^{(n_f-1)}\left\{\left(\beta_0^{(n_f)}-\beta_0^{(n_f-1)}\right)L_M+\left(\frac{\beta_1^{(n_f)}}{\beta_0^{(n_f)}}-\frac{\beta_1^{(n_f-1)}}{\beta_0^{(n_f-1)}}\right)\ln L_M\right.\\ & -\frac{\beta_1^{(n_f-1)}}{\beta_0^{(n_f-1)}}\ln\frac{\beta_0^{(n_f)}}{\beta_0^{(n_f-1)}}+\frac{\beta_1^{(n_f)}}{\left(\beta_0^{(n_f)}\right)^2}\left(\frac{\beta_1^{(n_f)}}{\beta_0^{(n_f)}}-\frac{\beta_1^{(n_f-1)}}{\beta_0^{(n_f-1)}}\right)\frac{\ln L_M}{L_M}\\ & \left.+\frac{1}{\beta_0^{(n_f)}}\left[\left(\frac{\beta_1^{(n_f)}}{\beta_0^{(n_f)}}\right)^2-\left(\frac{\beta_1^{(n_f-1)}}{\beta_0^{(n_f-1)}}\right)^2-\frac{\beta_2^{(n_f)}}{\beta_0^{(n_f)}}+\frac{\beta_2^{(n_f-1)}}{\beta_0^{(n_f-1)}}-\frac{7}{72}\right]\frac{1}{L_M}\right\},\end{aligned} \tag{3.6.50}$$

where

$$L_M = \ln\frac{M_q^2}{\left(\Lambda_{\overline{\rm MS}}^{(n_f)}\right)^2}\,. \tag{3.6.51}$$

The parameters $\Lambda_{\overline{\rm MS}}^{(n_f)}$ for different flavor numbers are used then where appropriate in the Eq. (3.6.48) in order to calculate the running $\alpha_s(s)$.

3.7. Subroutine EWCOUP

Subroutine EWCOUP(INTRF,INDF,S) prepares coupling functions dressed with EW and QCD corrections. For the Born case they were introduced in Section 1.1.

In the argument list of subroutine EWCOUP(INTRF,INDF,S) all parameters are INPUT. For the default setting it is run for every s and produces EW COUPlings for requested values of INTeRFace and INDF of a process. If it is called from ZUATSM, the angular distribution branch, and if EW boxes are added to EW form factors, it will be called for every t.

3.7.1. Helicities and polarizations

First, we introduce the longitudinal polarizations of the electron (λ_-) and positron (λ_+) and the helicities of the final state fermions $h_\pm$ in the following combinations for polarizations:

$$\lambda_1 \;=\; \texttt{COMB1} = 1 - \lambda_+\lambda_- \,, \tag{3.7.1}$$

$$\lambda_2 \;=\; \texttt{COMB2} = \lambda_+ - \lambda_- \,, \tag{3.7.2}$$

and for helicities, assuming that helicity may have only three values $(0, -1, +1)$[3]:

$$h_+ \neq 0 \;\texttt{.and.}\; h_- \neq 0 \quad \begin{cases} h_1 = \texttt{HOMB1} = \dfrac{1}{4}(1 - h_+h_-), \\ h_2 = \texttt{HOMB2} = \dfrac{1}{4}(h_+ - h_-), \end{cases}$$

$$h_+ = 0 \;\texttt{.and.}\; h_- = 0 \quad \begin{cases} h_1 = \texttt{HOMB1} = 1, \\ h_2 = \texttt{HOMB2} = 0, \end{cases}$$

$$h_+ = 0 \;\texttt{.and.}\; h_- \neq 0 \quad \begin{cases} h_1 = \texttt{HOMB1} = \dfrac{1}{2}, \\ h_2 = \texttt{HOMB2} = \dfrac{1}{2}(-h_-), \end{cases} \tag{3.7.3}$$

$$h_+ \neq 0 \;\texttt{.and.}\; h_- = 0 \quad \begin{cases} h_1 = \texttt{HOMB1} = \dfrac{1}{2}, \\ h_2 = \texttt{HOMB2} = \dfrac{1}{2}(+h_+). \end{cases}$$

[3]The helicity values $(-1, +1)$ correspond to eigenvalues and may be used for the determination of final state helicity asymmetries while the value (0) reflects helicity averaging.

Then, if we neglect masses, Eqs. (1.1.15)–(1.1.22) for the coupling functions (or alternatively *coupling factors*) change to:

$$\begin{aligned}
K_T^f(\gamma) &\to K_T^f(\gamma,\lambda_{1,2},h_{1,2}) &&= \lambda_1 h_1 Q_e^2 Q_f^2 c_f,\\
0 &\to K_{FB}^f(\gamma,\lambda_{1,2},h_{1,2}) &&= \lambda_2 h_2 Q_e^2 Q_f^2 c_f,\\
K_T^f(I) &\to K_T^f(I,\lambda_{1,2},h_{1,2}) &&= 2|Q_eQ_f|(\lambda_1 v_e+\lambda_2 a_e)(h_1 v_f+h_2 a_f)c_f,\\
K_{FB}^f(I) &\to K_{FB}^f(I,\lambda_{1,2},h_{1,2}) &&= 2|Q_eQ_f|(\lambda_1 a_e+\lambda_2 v_e)(h_1 a_f+h_2 v_f)c_f,\\
K_T^f(Z) &\to K_T^f(Z,\lambda_{1,2},h_{1,2}) &&= \Big[\lambda_1(v_e^2+a_e^2)+2\lambda_2 v_e a_e\Big]\Big[h_1(v_f^2+a_f^2)+2h_2 v_f a_f\Big]c_f,\\
K_{FB}^f(Z) &\to K_{FB}^f(Z,\lambda_{1,2},h_{1,2}) &&= \Big[2\lambda_1 v_e a_e+\lambda_2\Big(v_e^2+a_e^2\Big)\Big]\Big[2h_1 v_f a_f+h_2\Big(v_f^2+a_f^2\Big)\Big]c_f.
\end{aligned} \tag{3.7.4}$$

One may see that the vector- and axial-vector couplings v_e, a_e and their squares v_e^2, a_e^2 merely have to be substituted by "new" couplings depending linearly on the polarization λ (the same is true in an analogous manner for couplings and polarization of the final-state).

If $m_f \neq 0$, a_f has to be substituted in the above formulae by $a_f\beta_f$, with β_f given by Eq. (1.1.8).

Then, one has for $K_T^f(I)$, $K_T^f(Z)$:

$$K_T^f(I,\lambda_{1,2},h_{1,2}) \to K_T^f(I,\lambda_{1,2},h_{1,2},\beta_f(s)) = 2|Q_eQ_f|[\lambda_1 v_e+\lambda_2 a_e][h_1 v_f+h_2 a_f\beta_f(s)], \tag{3.7.5}$$

$$\begin{aligned}
K_T^f(Z,\lambda_{1,2},h_{1,2}) \to\ & K_T^f(Z,\lambda_{1,2},h_{1,2},\beta_f(s)) = \Big[\lambda_1(v_e^2+a_e^2)+2\lambda_2 v_e a_e\Big]\\
&\times\Big[h_1\Big(v_f^2+a_f^2\beta_f^2(s)\Big)+2h_2 v_f a_f\beta_f(s)\Big].
\end{aligned} \tag{3.7.6}$$

There are further contributions $K_T^m(\gamma)$, $K_T^m(I)$ and $K_T^m(Z)$ in the total cross-section σ_T:

$$K_T^m(\gamma,\lambda_{1,2},h_{1,2}) = \lambda_1(2-h_1)Q_e^2Q_f^2, \tag{3.7.7}$$

$$K_T^m(I,\lambda_{1,2},h_{1,2}) = 2|Q_eQ_f|(\lambda_1 v_e+\lambda_2 a_e)(2-h_1)v_f, \tag{3.7.8}$$

$$K_T^m(Z,\lambda_{1,2},h_{1,2}) = \Big[\lambda_1(v_e^2+a_e^2)+2\lambda_2 v_e a_e\Big](2-h_1)v_f^2. \tag{3.7.9}$$

3.7.2. Preparation of effective couplings for various interfaces

In the beginning `EWCOUP` calculates the running electromagnetic coupling $\alpha(s)$ by a call of `XFOTF3` and the four complex-valued effective couplings by a call of `ROKANC`, see Fig. I.5:

$$\rho_{ef} = \texttt{XRO}, \tag{3.7.10}$$

$$G_e = \texttt{XVEZ} = 1-4|Q_e|\Big(\kappa_e s_W^2+I_e^2\Big), \tag{3.7.11}$$

$$G_f = \texttt{XVFZ} = 1-4|Q_f|\Big(\kappa_f s_W^2+I_f^2\Big), \tag{3.7.12}$$

$$G_{ef} = \texttt{XVEFZ} = -1+G_e+G_f+16|Q_e||Q_f|\Big[s_W^4\kappa_{ef}+s_W^2\Big(\kappa_e I_f^2+\kappa_f I_e^2\Big)\Big]. \tag{3.7.13}$$

In general, they are functions of two Mandelstam variables (s,t). These four complex-valued form factors are generalizations of the effective Z decay constants ρ_Z^f and g_Z^f for the case of the scattering process $e^+e^- \to f\bar{f}$.

At the Z resonance, some approximations and factorizations are fulfilled:

$$\rho^2_{ef}(M_Z^2,t) \approx \rho^e_Z\rho^f_Z\,, \tag{3.7.14}$$
$$\kappa_{ef}(M_Z^2,t) \approx \kappa^e_Z\kappa^f_Z\,, \tag{3.7.15}$$
$$\kappa_{e}(M_Z^2,t) \approx \kappa^e_Z\,, \tag{3.7.16}$$
$$\kappa_{f}(M_Z^2,t) \approx \kappa^f_Z\,. \tag{3.7.17}$$

We note that the t-dependence switches off at $s = M_Z^2$.

If the factorization property were fulfilled we would have

$$G_{ef} = G_eG_f, \tag{3.7.18}$$

which, in turn, would greatly simplify all subsequent formulae. Although factorization holds with rather good precision at the Z resonance, it deteriorates on the wings and the very high precision of LEP1 data demands to refuse from an application of this approximation even at resonance.

Then EWCOUP calculates s-dependent QCD corrections by a call to QCDCOF, providing the array QCDCOR(0:14), see Eq. (4.1.1). From QCDCOR(13) one constructs three vector singlet contributions $R_V^{S,\{\gamma,Z\gamma,Z\}}(s)$:

$$R_V^{S,\gamma}(s) = \texttt{VSNGAA} = \frac{1}{9}R_V^S(s), \tag{3.7.19}$$
$$R_V^{S,Z\gamma}(s) = \texttt{VSNGZA} = \left(\frac{7}{3} - \frac{44}{9}s_W^2\right)R_V^S(s), \tag{3.7.20}$$
$$R_V^{S,Z}(s) = \texttt{VSNGZZ} = \left(1 + \frac{4}{3}s_W^2\right)R_V^S(s), \tag{3.7.21}$$

which are shared 'democratically' over five open quark channels: u, d, c, s, b.

Depending on the flag FINR the final state QCD⊗QED correction factors $R^f_{V,A}$ and R^S_V are modified as follows:

FINR=–1: $R^f_{V,A} = 1$, $R_V^{S,\{\gamma,Z\gamma,Z\}} = 0$;

FINR=0: full expressions are used as given in Section 3.6;

FINR=1: from $R^f_{V,A}$ one subtracts the inclusive $\mathcal{O}(\alpha)$ QED correction $3\alpha Q_f^2/(4\pi)$ avoiding double counting in the case of a proper treatment of cuts with the aid of function FUNFIN, see Subsection 3.8; the factors R^S_V remain unchanged.

Further, EWCOUP provides non-factorized EW⊗QCD corrections, governed by flag CZAK.

This all is done for every of the ten values of INTRF and of the twelf values of INDF (see Fig. I.5 for the meaning of INDF and for the correspondence between interface name and its number INTERF).

Then the calculations proceed in different streams for different interfaces providing seven *coupling factors* $K^f_{T,FB}(\gamma, I, Z)$, Eq. (3.7.4), and $\bar{K}^{f,m}_T(Z)$, see Eq. (1.1.22).

We note that they bear also the process index f = INDF.

3.7.3. Standard Model interfaces ZUTHSM, ZUTPSM, ZULRSM, ZUATSM. INTRF=1

In the SM, the coupling factors take into account EW and QCD RC by means of EWFF (Eqs. (3.3.2)–(3.3.5)) and mixed QEQ⊗QCD FSR corrections by means of radiator factors (Eq. (2.4.16) and Section 3.6). The Born formulae Eq. (3.7.4) change to:

$$K_T^f(\gamma,\lambda_{1,2},h_{1,2}) = \texttt{VEFA} = \lambda_1 h_1 Q_e^2\left[Q_f^2 R_V^f(s)+\frac{1}{5}R_V^{S,\gamma}(s)\right]c_f, \tag{3.7.22}$$

$$K_{FB}^f(\gamma,\lambda_{1,2},h_{1,2}) = \texttt{AEFA} = \lambda_2 h_2 Q_e^2 Q_f^2 c_f, \tag{3.7.23}$$

$$\begin{aligned}\frac{1}{2}K_T^f(I,\lambda_{1,2},h_{1,2}) &= \texttt{XVEFI} = \rho_{ef}\Bigg\{\lambda_1 h_1|Q_e|\left[|Q_f|G_{ef}R_V^f(s)+G_e\frac{1}{5}R_V^{S,Z\gamma}(s)\right]\\ &\quad +|Q_e||Q_f|\Big[\lambda_2 h_1 G_f+\lambda_1 h_2 G_e+\lambda_1 h_2\Big]\Bigg\}c_f,\end{aligned} \tag{3.7.24}$$

$$\begin{aligned}\frac{1}{2}K_{FB}^f(I,\lambda_{1,2},h_{1,2}) &= \texttt{XAEFI} = \rho_{ef}|Q_e||Q_f|\Big\{\lambda_1 h_1 R_{FB}^q(s)\\ &\quad +\lambda_2 h_1 G_e+\lambda_1 h_2 G_f+\lambda_2 h_2 G_{ef}\Big\}c_f,\end{aligned} \tag{3.7.25}$$

$$\bar{K}_T^{f,m}(Z,\lambda_{1,2},h_{1,2}) = \texttt{VEEZ} = |\rho_{ef}|^2\lambda_1 h_1(|G_e|^2+1)R_A^f(s)c_f, \tag{3.7.26}$$

$$K_T^f(Z,\lambda_{1,2},h_{1,2}) = \texttt{VEFZ} = |\rho_{ef}|^2\Big[\lambda_1 h_1 V_{Z1}+\lambda_2 h_1 V_{Z2}\lambda_1 h_2 A_{Z2}+\lambda_2 h_2 A_{Z1}\Big]c_f, \tag{3.7.27}$$

$$K_{FB}^f(Z,\lambda_{1,2},h_{1,2}) = \texttt{AEFZ} = |\rho_{ef}|^2\Big[\lambda_1 h_1 A_{Z1}+\lambda_2 h_1 A_{Z2}\lambda_1 h_2 V_{Z2}+\lambda_2 h_2 V_{Z1}\Big]c_f. \tag{3.7.28}$$

The vector and axial combinations are:

$$V_{Z1} = \Big(|G_{ef}|^2+|G_f|^2\Big)R_V^f(s)+\Big(|G_e|^2+1\Big)\left[R_A^f(s)+\frac{1}{5}R_V^{S,Z}(s)\right], \tag{3.7.29}$$

$$V_{Z2} = 2\mathrm{Re}\Big[G_{ef}^* G_f R_V^f(s)+G_e R_A^f(s)\Big], \tag{3.7.30}$$

$$A_{Z1} = 2\mathrm{Re}\Big(G_e G_f^*+G_{ef}\Big)R_{FB}^q(s)\,, \tag{3.7.31}$$

$$A_{Z2} = 2\mathrm{Re}\Big(G_{ef}^* G_e+G_f\Big). \tag{3.7.32}$$

For a proper account of non-factorized corrections one needs also vector factors without QCD corrections:

$$V_{Z1}^0 = |G_{ef}|^2+|G_f|^2+|G_e|^2+1, \tag{3.7.33}$$

$$V_{Z2}^0 = 2\mathrm{Re}\Big(G_{ef}^* G_f+G_e\Big), \tag{3.7.34}$$

and a corresponding $K_T^{f,0}$ (without helicities and polarizations) made of $V_{Z1,2}^0$ by an expression similar to Eq. (3.7.27).

It is instructive to see that without QCD corrections and if the factorization properties Eqs. (3.7.14)–(3.7.17) are fulfilled the K_A factors reduce to familiar expressions Eq. (3.7.4) up to trivial substitutions of couplings:

$$v_f \to G_f, \tag{3.7.35}$$

$$a_f \to 1, \tag{3.7.36}$$

and with corresponding prefactors made of ρ_{ef}.

The coupling factors are used in subroutines ZANCUT and ZCUT in order to calculate differential or integrated observables. This is done in Subroutines COSCUT, or SFAST and SCUT respectively, which call BORN for the calculation of the IBA cross-section σ_T^0 and forward-backward difference σ_{FB}^0. These couplings are also used in those parts of the code which calculate contributions from the initial-final interference, IFI.

3.7.4. Interface ZUXSEC. INTRF=2

Here we discuss the parameter release scheme used in the interface ZUXSEC. It calculates only the cross-section, without initial or final state polarizations. This corresponds to the internal flag INTRF=2 set in Subroutine EWCOUP which provides the coupling functions for the subsequent use in BORN within a scheme where one wants to have partial Z widths to be released for a fit to experimental data. Let us denote the partial width to be released by $\overline{\Gamma}_f$.

Within this scheme γ exchange and $Z\gamma$ interference are simply taken from the SM:

$$K_T^f(\gamma) = \texttt{VEFA} = Q_e^2\left[Q_f^2 R_V^f(s) + \frac{1}{5}R_V^{S,\gamma}(s)\right]c_f, \tag{3.7.37}$$

$$K_{FB}^f(\gamma) = \texttt{AEFA} = 0, \tag{3.7.38}$$

$$\frac{1}{2}K_T^f(I) = \texttt{XVEFI} = \rho_{ef}\left\{|Q_e|\left[|Q_f|G_{ef}R_V^f(s) + G_e\frac{1}{5}R_V^{S,Z\gamma}(s)\right]\right\}c_f, \tag{3.7.39}$$

$$\frac{1}{2}K_{FB}^f(I) = \texttt{XAEFI} = \rho_{ef}|Q_e||Q_f|R_{FB}^q(s)c_f, \tag{3.7.40}$$

$$K_{FB}^f(Z) = \texttt{AEFZ} = |\rho_{ef}|^2 2\mathrm{Re}\Big(G_e G_f^* + G_{ef}\Big)R_{FB}^q(s)c_f. \tag{3.7.41}$$

Therefore, they all should be understood as SM remnants.

The release of $\overline{\Gamma}_f$ is realized through the Z-couplings by the following set of equations:

$$\bar{K}_T^{f,m}(Z) = \texttt{VEEZ} = \left[\frac{\overline{\Gamma}_e}{A_N c_{ee}} - \frac{\Gamma_e}{A_N c_{ee}} + |\rho_{ef}|^2(|G_e|^2+1)\right]R_A^f(s)c_f, \tag{3.7.42}$$

$$\begin{aligned} K_T^f(Z) = \texttt{VEFZ} &= \frac{\overline{\Gamma}_e}{A_N c_{ee}}\left[\frac{\overline{\Gamma}_f}{A_N\beta_f} + 6\rho_f r(m_f)R_A^f(s)c_f\right]\frac{1}{c_2(m_f)} \\ &- \frac{\Gamma_e}{A_N c_{ee}}\left[\frac{\Gamma_f}{A_N\beta_f} + 6\rho_f r(m_f)R_A^f(s)c_f\right]\frac{1}{c_2(m_f)} \\ &+ |\rho_{ef}|^2\left\{\Big(|G_{ef}|^2+|G_f|^2\Big)R_V^f(s) + |G_e|^2 + 1\left[R_A^f(s) + \frac{1}{5}R_V^{S,Z}(s)\right]\right\}c_f. \end{aligned} \tag{3.7.43}$$

The ρ_f is a short hand notation for the real part of the Z decay form factor $\mathrm{Re}\,\rho_Z^f$:

$$\rho_f = \mathrm{Re}\,\rho_Z^f, \tag{3.7.44}$$

see also the discussion in Subsection 3.7.5 and Eq. (3.7.61). Here we also introduced the notations:

$$r(m_f) = \frac{m_f^2}{M_Z^2}, \tag{3.7.45}$$

$$c_2(m_f) = 1 + 2r(m_f), \tag{3.7.46}$$

$$A_N = \frac{G_\mu M_Z^3}{24\sqrt{2}\pi}, \tag{3.7.47}$$

$$c_{ee} = 1 + \frac{3}{4}\frac{\alpha(s)}{\pi}Q_e^2, \tag{3.7.48}$$

where c_{ee} is a QED correction factor and Γ_e and Γ_f stand for partial Z-boson decay widths calculated within the SM by the `DIZET` package. Finally, again for a proper account of non-factorized corrections one needs a coupling function $K_T^{f,0}(Z)$ without QCD corrections:

$$K_T^{f,0}(Z) = \texttt{VEFZ0}. \tag{3.7.49}$$

Let us define the *SM-trajectory* by the set of equations

$$\overline{\Gamma}_f = \Gamma_f. \tag{3.7.50}$$

We note that Eqs. (3.7.42)–(3.7.43) at the SM-trajectory are identically equal to their SM analogs Eqs. (3.7.26)–(3.7.27). This is the reason for the invention of the terminology "a Semi–Model-Independent Approach, SMIA" for releases of such kind. Everything what makes coupling factors in Eqs. (3.7.42)–(3.7.43) deviate from their *released* values will be called *SM-remnants*.

The scheme which has been just described is realized for `INTRF`=2 and `INDF`=0,9. For the calculation of the total hadronic cross-section special chains exist in subroutines `EWCOUP` and `BORN`. For these chains, for the sake of CPU time saving the coupling functions are stored in arrays:

$$K_T^{f=\mathrm{J}}(\gamma) = \texttt{AVEFA(J)}, \tag{3.7.51}$$

$$K_{FB}^{f=\mathrm{J}}(\gamma) = \texttt{AAEFA(J)} = 0, \tag{3.7.52}$$

$$\frac{1}{2}K_T^{f=\mathrm{J}}(I) = \texttt{XXVEFI(J)}, \tag{3.7.53}$$

$$\frac{1}{2}K_{FB}^{f=\mathrm{J}}(I) = \texttt{XXAEFI(J)}, \tag{3.7.54}$$

$$K_{FB}^{f=\mathrm{J}}(Z) = \texttt{AAEFZ(J)}, \tag{3.7.55}$$

$$\bar{K}_T^{f=\mathrm{J},m}(Z) = \texttt{AVEEZ(J)}, \tag{3.7.56}$$

where J counts the flavor index f from u- to b-quarks. The couplings are super-indexed with f. It is worth mentioning that the EW form factors were calculated by means of a call to `ROKANC` not five times, for every $f = u, d, c, s, d$, but only three times, for $f = u, d, b$. This also saves CPU time.

The coupling functions Eqs. (3.7.51)–(3.7.56) are similar to Eqs. (3.7.37)–(3.7.42), while $K_T^f(Z)$ gets a special treatment:

$$\begin{aligned} K_T^{f=\mathrm{J}}(Z) &= \texttt{AVEFZ(J)} = \frac{\overline{\Gamma}_h}{\Gamma_h}\left\{\frac{\overline{\Gamma}_e}{A_N c_{ee}}\frac{\Gamma_f}{A_N} - \frac{\Gamma_e}{A_N c_{ee}}\frac{\Gamma_f}{A_N}\right. \\ &+ \left.|\rho_{ef}|^2\left\{\left(|G_{ef}|^2 + |G_f|^2\right)R_V^f(s) + |G_e|^2 + 1\left[R_A^f(s) + \frac{1}{5}R_V^{S,Z}(s)\right]\right\}c_f\right\}, \end{aligned} \tag{3.7.57}$$

and also the corresponding coupling function $K_T^{f=\mathrm{J},0}(Z)$ without QCD corrections.

The arrays Eqs. (3.7.51)–(3.7.57) are needed not only for a use in subroutine BORN. They are also used in subroutine BOXINT as a part of the calculation of the IFI corrections to order $\mathcal{O}(\alpha)$. In order to save further CPU time, EWCOUP prepares *summed* coupling functions weighted with Q_f, since $\sigma^{\rm IFI} \propto Q_e Q_f$:

$$K_{_T}(\gamma) = \sum_{J=1}^{5} Q_f K_{_T}^{f=\mathtt{J}}(\gamma), \tag{3.7.58}$$

etc.

3.7.5. Interfaces ZUXSA and ZUTAU. INTRF=3

Now we introduce a family of SMIA interfaces (ZUXSA, ZUTAU), which use the language of *effective couplings release*. The effective couplings may then be fitted to experimental data. Let us introduce short-hand notations for the real parts of on-resonance couplings calculated within the SM (see Eqs. (2.4.12) and (2.5.15)):

$$\rho_f = \mathrm{Re}\,\rho_{_Z}^f\,, \tag{3.7.59}$$
$$\rho'_f = \left(\rho_{_Z}^f\right)'\,, \tag{3.7.60}$$
$$g_f = \mathrm{Re}\,g_{_Z}^f\,. \tag{3.7.61}$$

Let $\bar\rho_e$, $\bar\rho_f$, $\bar g_e$, $\bar g_f$, $\bar a_e$ and $\bar a_f$ denote constant, real valued couplings to be fitted to the experimental data.

In all MI subroutines using the language of effective couplings we have two modes:

> MODE=0: the $\bar g_f$ and $\bar a_f$ have the meaning of vector and axial vector effective coupling constants in the decay $Z \to f\bar f$ and the $\bar\rho_f$ are set equal to one;
>
> MODE=1: the $\bar g_f$ have the meaning of the ratio of vector and axial vector couplings and instead of $\bar a_f^2$ one uses $\bar\rho_f$.

For MISC=0 we use the "barred" quantities together with the SM values ρ_e and ρ_f directly. If instead one chooses MISC=1, a scaling is performed first. For a discussion of this scaling and the definition of the R_f factors see at the end of Subsection 2.5.1. We will use the abbreviation OSCAL for such a scaling:

$$\bar\rho_e \to \bar\rho_e/R_e\,, \tag{3.7.62}$$
$$\bar\rho_f \to \bar\rho_f/R_f\,, \tag{3.7.63}$$
$$\bar g_e \to \bar g_e/\sqrt{R_e}\,, \tag{3.7.64}$$
$$\bar g_f \to \bar g_f/\sqrt{R_f}\,, \tag{3.7.65}$$
$$\bar a_e \to \bar a_e/\sqrt{R_e}\,, \tag{3.7.66}$$
$$\bar a_f \to \bar a_f/\sqrt{R_f}\,, \tag{3.7.67}$$
$$\rho_e \to \rho'_e/R_e\,, \tag{3.7.68}$$
$$\rho_f \to \rho'_f/R_f. \tag{3.7.69}$$

For this case we define the *SM trajectory* by another set of equalities, which are `MODE` dependent. We give it for the example of `MODE`=0:

$$\bar{\rho}_e = \rho_e\,, \tag{3.7.70}$$
$$\bar{\rho}_f = \rho_f, \tag{3.7.71}$$
$$\bar{g}_e = g_e\,, \tag{3.7.72}$$
$$\bar{g}_f = g_f. \tag{3.7.73}$$

Z resonance approximation and SM-remnants

In the vicinity of the Z resonance the following approximations hold with rather high accuracy:

$$\rho_{ef} \approx \sqrt{\rho_e\rho_f}, \tag{3.7.74}$$
$$G_e \approx g_e\,, \tag{3.7.75}$$
$$G_f \approx g_f\,, \tag{3.7.76}$$
$$G_{ef} \approx g_e g_f\,. \tag{3.7.77}$$

This allows us to define a new set of couplings, which at the *SM trajectory* exactly coincides with the SM analog:

$$\hat{\rho}_{ef} = \sqrt{\bar{\rho}_e\bar{\rho}_f} - \sqrt{\rho_e\rho_f} + \rho_{ef}\,, \tag{3.7.78}$$
$$\hat{G}_e = \bar{g}_e - g_e + G_e\,, \tag{3.7.79}$$
$$\hat{G}_f = \bar{g}_f - g_f + G_e\,, \tag{3.7.80}$$
$$\hat{G}_{ef} = \bar{g}_e\bar{g}_f - g_e g_f + G_{ef}\,. \tag{3.7.81}$$

They are an example of a parameter release with *exact s-dependent SM remnants* since at the SM trajectory:

$$\hat{\rho}_{ef} = \rho_{ef}\,, \tag{3.7.82}$$

etc.

We only mention that the quantities, accompanying the barred release quantities in Eqs. (3.7.78)–(3.7.81),

$$-\sqrt{\rho_e\rho_f} + \rho_{ef}\,, \tag{3.7.83}$$

etc., are another class of SM remnants compared to those appearing in Eqs. (3.7.42)–(3.7.43).

For the photonic coupling factors `VEFI` and `AEFI`, we use their SM values of Eqs. (3.7.22)–(3.7.23), because they have nothing to do with effective Z couplings. For the γZ interference and Z exchange coupling factors we use expressions similar to those of the SM, Eqs. (3.7.24)–(3.7.28), but with two modifications:

- use $\hat{\rho}_{ef}$, $\hat{G}_f$, etc. instead of ρ_{ef}, G_f, etc.;
- proper restoration of axial couplings having in mind the two options of `MODE` described above.

It is sufficient to show the modifications of V, A and those of the γZ interference and of the $\bar{K}_T^{f,m}$ coupling functions. The former are:

$$V_{Z1} = \Big(|\hat{G}_{ef}|^2 + \bar{a}_e^2|\hat{G}_f|^2\Big)R_V^f(s) + \Big(|\hat{G}_e|^2 + \bar{a}_e^2\Big)\bar{a}_f^2\left[R_A^f(s) + \frac{1}{5}R_V^{S,Z}(s)\right], \tag{3.7.84}$$

$$V_{Z2} = 2\mathrm{Re}\Big[\bar{a}_e\hat{G}_{ef}^* G_f R_V^f(s) + \hat{G}_e\bar{a}_e\bar{a}_f^2 R_A^f(s)\Big], \tag{3.7.85}$$

$$A_{Z1} = 2\mathrm{Re}\Big(\hat{G}_e\hat{G}_f^* + \hat{G}_{ef}\Big)\bar{a}_e\bar{a}_f R_{FB}^q(s)\,, \tag{3.7.86}$$

$$A_{Z2} = 2\mathrm{Re}\Big(\hat{G}_e\hat{G}_{ef}^* + \bar{a}_e^2\hat{G}_f\Big)\bar{a}_f, \tag{3.7.87}$$

$$V_{Z1}^0 = |\hat{G}_{ef}|^2 + \bar{a}_e^2|\hat{G}_f|^2 + \Big(|\hat{G}_e|^2 + \bar{a}_e^2\Big)\bar{a}_f^2, \tag{3.7.88}$$

$$V_{Z2}^0 = 2\mathrm{Re}\Big(\bar{a}_e\hat{G}_{ef}^* G_f + \bar{a}_e\hat{G}_e\bar{a}_f^2\Big), \tag{3.7.89}$$

and the latter:

$$\begin{aligned}\frac{1}{2}K_T^f(I,\lambda_{1,2},h_{1,2}) &= \texttt{XVEFI} = \hat{\rho}_{ef}\Bigg\{\lambda_1 h_1|Q_e|\left[|Q_f|\hat{G}_{ef}R_V^f(s) + \hat{G}_e\frac{1}{5}R_V^{S,Z^\gamma}(s)\right]\\ &\quad +|Q_e||Q_f|\Big[\lambda_2 h_1\bar{a}_e\hat{G}_f + \lambda_1 h_2\hat{G}_e\bar{a}_f + \lambda_1 h_2\bar{a}_e\bar{a}_f\Big]\Bigg\}c_f,\end{aligned} \tag{3.7.90}$$

$$\begin{aligned}\frac{1}{2}K_{FB}^f(I,\lambda_{1,2},h_{1,2}) &= \texttt{XAEFI} = \hat{\rho}_{ef}|Q_e||Q_f|\Big\{\lambda_1 h_1\bar{a}_e\bar{a}_f R_{FB}^q(s)\\ &\quad +\lambda_2 h_1\hat{G}_e\bar{a}_f + \lambda_1 h_2\bar{a}_e\hat{G}_f + \lambda_2 h_2\hat{G}_{ef}\Big\}c_f,\end{aligned} \tag{3.7.91}$$

$$\bar{K}_T^{f,m}(Z,\lambda_{1,2},h_{1,2}) = \texttt{VEEZ} = |\rho_{ef}|^2\lambda_1 h_1(|\hat{G}_e|^2 + \bar{a}_e^2)\bar{a}_f^2 R_A^f(s)c_f. \tag{3.7.92}$$

3.7.6. Interface ZUXSA2. INTRF=4

The interface ZUXSA2 is very similar to interface ZUXSA. It was invented only for a study of leptonic channels assuming lepton universality and was designed ignoring polarizations and helicities. The formulae are particularly compact due to these limitations. In ZUXSA2, the quantities released for the fit are $\rho_l^2, \bar{g}_l^2, \bar{a}_l^2$. If MISC=0 they are used directly. For MISC=1, the rescaling OSCAL (introduced in Subsection 3.7.5) is performed:

$$\rho_l^2 \to \rho_l^2/R_e^2\,, \tag{3.7.93}$$

$$\sqrt{\bar{g}_l^2} \to \sqrt{\bar{g}_l^2}/\sqrt{R_e}\,, \tag{3.7.94}$$

$$\sqrt{\bar{g}_l^2} \to \sqrt{\bar{g}_l^2}/\sqrt{R_e}\,, \tag{3.7.95}$$

$$\bar{a}_l^2 \to \bar{a}_l^2/R_e\,, \tag{3.7.96}$$

$$\bar{g}_l^2 \to \bar{g}_l^2/R_e\,, \tag{3.7.97}$$

$$\rho_e \to \rho_e'/R_e\,, \tag{3.7.98}$$

$$\rho_f \to \rho_f'/R_f. \tag{3.7.99}$$

The parameter release with exact s-dependent SM remnants is realized by:

$$\hat{\rho}_{ef} = \sqrt{\rho_l^2} - \sqrt{\rho_e\rho_f} + \rho_{ef}\,, \tag{3.7.100}$$

$$\hat{G}_e = \sqrt{\bar{g}_l^2} - g_e + G_e\,, \tag{3.7.101}$$

$$\hat{G}_f = \sqrt{\bar{g}_l^2} - g_f + G_f\,, \tag{3.7.102}$$

$$\hat{G}_{ef} = \bar{g}_l^2 - g_e g_f + G_{ef}\,. \tag{3.7.103}$$

The coupling functions for this interface are written down without auxiliary functions since they are compact:

$$\begin{aligned}
\texttt{VEFA} &= Q_e^2 Q_f^2, && (3.7.104)\\
\texttt{AEFA} &= 0, && (3.7.105)\\
\texttt{XVEFI} &= \hat{\rho}_{ef}|Q_e Q_f|\hat{G}_{ef}, && (3.7.106)\\
\texttt{XAEFI} &= \hat{\rho}_{ef}|Q_e Q_f|\bar{a}_l^2, && (3.7.107)\\
\texttt{VEEZ} &= |\hat{\rho}_{ef}|^2\Big(|\hat{G}_e|^2 + \bar{a}_l^2\Big)\bar{a}_l^2, && (3.7.108)\\
\texttt{VEFZ} &= |\hat{\rho}_{ef}|^2\Big[\Big(|\hat{G}_{ef}|^2 + \bar{a}_l^2|\hat{G}_f|^2\Big) + (|\hat{G}_e|^2 + \bar{a}_l^2)\bar{a}_l^2\Big], && (3.7.109)\\
\texttt{VEFZO} &= \texttt{VEFZ}, && (3.7.110)\\
\texttt{AEFZ} &= |\hat{\rho}_{ef}|^2\bar{a}_l^2 2\mathrm{Re}\Big(\hat{G}_e\hat{G}_f^* + \hat{G}_{ef}\Big). && (3.7.111)
\end{aligned}$$

3.7.7. Interface ZUXAFB. INTRF=5

Interface ZUXAFB uses as parameters for release three combinations of couplings: $(\bar{g}_e^2 + \bar{a}_e^2)$, $(\bar{g}_f^2+\bar{a}_f^2)$ and $\bar{g}_e\bar{a}_e\bar{g}_f\bar{a}_f$. Like the previous one, it is also intended only for an application to leptonic channels ignoring polarizations and helicities. However, it doesn't make use of lepton universality. Moreover, it doesn't have MODE=1; therefore, $\bar{g}_f$ should be treated as $\bar{v}_f$.

If MISC=0 these three parameters are used directly. For MISC=1 the scaling OSCAL (introduced in Subsection 3.7.5) looks as follows:

$$\begin{aligned}
(\bar{g}_e\bar{a}_e\bar{g}_f\bar{a}_f) &= (\bar{g}_e\bar{a}_e\bar{g}_f\bar{a}_f)/R_e/R_f, && (3.7.112)\\
(\bar{g}_e^2 + \bar{a}_e^2) &= (\bar{g}_e^2 + \bar{a}_e^2)/R_e\,, && (3.7.113)\\
(\bar{g}_f^2 + \bar{a}_f^2) &= (\bar{g}_f^2 + \bar{a}_f^2)/R_f, && (3.7.114)\\
\rho_e &= \rho_e'/R_e\,, && (3.7.115)\\
\rho_f &= \rho_f'/R_f. && (3.7.116)
\end{aligned}$$

Again, γ-exchange and γZ interference couplings are taken from the SM:

$$\begin{aligned}
\texttt{VEFA} &= Q_e^2 Q_f^2, && (3.7.117)\\
\texttt{AEFA} &= 0, && (3.7.118)\\
\texttt{XVEFI} &= \rho_{ef}|Q_e Q_f|G_{ef}, && (3.7.119)\\
\texttt{XAEFI} &= \rho_{ef}|Q_e Q_f|, && (3.7.120)
\end{aligned}$$

and the release is performed for the Z-couplings only:

$$\begin{aligned}
\texttt{VEEZ} &= (\bar{g}_e^2 + \bar{a}_e^2) - \rho_e(g_e^2+1) + |\rho_{ef}|^2(|G_e|^2+1), && (3.7.121)\\
\texttt{VEFZ} &= (\bar{g}_e^2 + \bar{a}_e^2)(\bar{g}_f^2 + \bar{a}_f^2) - \rho_e(g_e^2+1)\rho_f(g_f^2+1)\\
&\quad +|\rho_{ef}|^2(|G_{ef}|^2 + |G_f|^2 + |G_e|^2 + 1), && (3.7.122)\\
\texttt{VEFZO} &= \texttt{VEFZ}, && (3.7.123)\\
\texttt{AEFZ} &= 4[(\bar{g}_e\bar{a}_e\bar{g}_f\bar{a}_f) - g_e g_f\rho_e\rho_f] + 2|\rho_{ef}|^2\mathrm{Re}(G_e G_f^* + G_{ef}). && (3.7.124)
\end{aligned}$$

3.7.8. Interface ZUALR. INTRF=6

The interface ZUALR is presently empty. It is foreseen for the analysis of A_{LR}.

3.8. Subroutine BORN

3.8.1. Cross-sections and forward-backward asymmetry

Subroutine BORN delivers the two IBA cross-sections $\sigma_T^{\rm IBA}$ and $\sigma_{FB}^{\rm IBA}$ for the production of leptons or quarks in the final-state (determined by flag INDF) or only one $\sigma_T^{\rm IBA}$ for the total hadronic cross-section (for INDF=10 and INTRF=2):

$$\begin{aligned}\sigma_T^{\rm IBA}(R_1,R_2)=\texttt{SBORN} &= \frac{1}{R_1}\beta_f\Big\{S^f_{\rm QED}c_2(m_f)\Big[K_T^f(\gamma)|V_{pol}|^2+\frac{1}{2}\Re e\Big(K_T^f(I)\chi(R_1,R_2)V^*_{pol}\Big)\Big]\\ &+\Big[c_2(m_f)\Big(K_T^f(Z)+\Big(S^f_{\rm QED}-1+S^f_{\rm CKHSS}\Big)K_T^{f,0}(Z)\Big)\\ &+c_3(m_f)\bar{K}_T^{f,m}(Z)\Big]\Re e\Big(\chi_Z(R_1)\chi_Z^*(R_2)\Big)\Big\},\end{aligned} \tag{3.8.1}$$

$$\begin{aligned}\sigma_{FB}^{\rm IBA}(R_1,R_2)=\texttt{ABORN} &= \frac{1}{R_1}\beta_f^2A^f_{\rm QED}\Big\{K_{FB}^f(\gamma)|V_{pol}|^2+\frac{1}{2}\Re e\Big(K_{FB}^f(I)\chi(R_1,R_2)V^*_{pol}\Big)\\ &+K_{FB}^f(Z)\Re e\Big(\chi_Z(R_1)\chi_Z^*(R_2)\Big)\Big\}.\end{aligned} \tag{3.8.2}$$

Now we explain all ingredients of Eqs. (3.8.1)–(3.8.2). It may be helpful to compare the IBA cross-section formulae with those introduced in Section 1.1 for the Born cross-sections and in Section 3.2 for the Z propagator. The mass-factors $\beta_f\equiv\beta_f(s),c_1(m_f),c_2(m_f)$ are defined in Eqs. (1.1.32)–(1.1.34). They are basically used only for leptonic channels; for some exceptions see the descriptions of flags FINR and POWR in Appendix 4.2.2.

The γ and Z propagator ratios are:

$$\chi(R_1,R_2) = \chi_Z(R_1)+\chi_Z(R_2), \tag{3.8.3}$$

$$\chi_Z(s') = \begin{cases} A_\kappa\dfrac{s'}{s'-M_Z^2+iM_Z\Gamma_Z} & \text{if} \quad \texttt{GAMS}=\texttt{0}\\[2ex] \kappa\dfrac{s'}{s'-\bar{M}_Z^2+i\bar{M}_Z\bar{\Gamma}_Z} & \text{if} \quad \texttt{GAMS}=\texttt{1}, \end{cases} \tag{3.8.4}$$

where

$$\kappa = \frac{A_\kappa}{1+i\Gamma_Z/M_Z}\,, \tag{3.8.5}$$

$$A_\kappa = G_\mu\frac{M_Z^2}{8\sqrt{2}\pi\alpha}\,, \tag{3.8.6}$$

$$\bar{M}_Z = \frac{M_Z}{c_\kappa}\,, \tag{3.8.7}$$

$$\bar{\Gamma}_Z = \frac{\Gamma_Z}{c_\kappa}\,, \tag{3.8.8}$$

$$c_\kappa = \sqrt{1+\Gamma_Z^2/M_Z^2}\,, \tag{3.8.9}$$

$$R_1 = \frac{s_1'}{s}\,, \tag{3.8.10}$$

$$R_2 = \frac{s_2'}{s}\,. \tag{3.8.11}$$

The default setting is GAMS=1. In this approach, the mass and width of the Z boson are considered to be M_Z and Γ_Z, although in the propagator the scaled parameters are used. This leads to the well-known phenomenon that fits to the Z resonance line lead to different numerical rsults for mass and width if in Eq. (3.8.4) either the upper or lower definition is used (see also Section 3.2 and references quoted therein).

The quantity V_{pol} stands for the contributions to the running $\alpha(s)$ from QED vacuum polarization by fermions, see Eq. (2.2.42). Here it is a complex valued quantity calculated by function XFOTF3:

$$V_{pol} = \alpha(s)/\alpha = \frac{1}{1 - \dfrac{\alpha}{4\pi}(\texttt{XFOTF3}(\texttt{IALEM}, \texttt{IALE2}, \texttt{IHVP}, \texttt{IQCD}, 1, \texttt{DAL5H}, -\texttt{S}))} \,. \tag{3.8.12}$$

The calculation of V_{pol} depends on flags ALEM, ALE2 and CONV. Their interplay is thoroughly described in Appendix 4.2.2 and shown in Fig. I.5 and Fig. I.6. Here we only explain why both EWCOUP and BORN compute $\alpha(s)$. In regular use (CONV=0,1), EWCOUP is supposed to deliver s dependent quantities. However, the results of BORN, Eqs. (3.8.1)–(3.8.2), are in general convoluted and, as known, $\alpha(s)$ has to be convoluted too. That's why BORN calculates first of all $\alpha(s')$. We briefly mention a special option CONV=2 when BORN calls EWCOUP from inside and then not only $\alpha(s)$, but also all coupling functions supplied by EWCOUP are convoluted. It is a very CPU time consuming option. It was used once in [57] to show that at LEP1 energies it is not necessary to convolute EWRC. This deserves however a dedicated study for LEP2 energies.

The factors $S^f_{\rm QED}$ and $A^f_{\rm QED}$ are QED FSR correction factors which are calculated depending on flag FINR. If FINR=–1, there are no QED-corrections, i.e.

$$S^f_{\rm QED} = A^f_{\rm QED} = 1. \tag{3.8.13}$$

If FINR=0, their inclusive values are used:

$$S^f_{\rm QED} = 1 + \frac{3}{4}\frac{\alpha(s')}{\pi}Q_f^2\,, \tag{3.8.14}$$

$$A^f_{\rm QED} = 0. \tag{3.8.15}$$

For FINR=1, the $S^f_{\rm QED}$ and $A^f_{\rm QED}$ are supplied by subroutine FUNFIN. In this case the returned values depend on the cuts that are used; see the description of ZUCUTS in Appendix 4.2.4 and in Fig. I.2 and Fig. I.3.

Finally, the factors $S^f_{\rm CKHSS}$ describe non-factorized mixed QCD⊗EW corrections of order $\mathcal{O}\left(\alpha\alpha_s\right)$ [84,85], which are assumed to be equal to their on-resonance values, Eq. (2.4.18).

Another option in BORN is the calculation of the total hadronic cross section σ_h. This is done in an extra chain for INDF=10 and INTRF=2. The corresponding term SBORN, proportional to σ_h, is:

$$\begin{aligned}
\texttt{SBORN} \;=\; & \sum_{J=1}^{5}\frac{1}{R_1}\beta_f\Big\{S^f_{\rm QED}c_2(m_f)\Big[K_T^{f=J}(\gamma)|V_{pol}|^2 + \frac{1}{2}\Re e\Big(K_T^{f=J}(I)\chi(R_1,R_2)V^*_{pol}\Big)\Big] \\
& + \Big[c_2(m_f)\Big(K_T^{f=J}(Z) + \Big(S^f_{\rm QED} - 1 + S^f_{\rm CKHSS}\Big)K_T^{f=J,0}(Z)\Big) \\
& + c_3(m_f)\bar{K}_T^{f=J,m}(Z)\Big]\Re e\Big(\chi_Z(R_1)\chi^*_Z(R_2)\Big)\Big\}.
\end{aligned} \tag{3.8.16}$$

Further, BORN computes two additional objects:

$$\texttt{SBORNS} = \frac{1}{R_1}\Big[K_{\scriptscriptstyle T}(\gamma)|V_{pol}|^2 + \frac{1}{2}\Re e\Big(K_{\scriptscriptstyle T}(I)\chi(R_1,R_2)V_{pol}^*\Big) + K_{\scriptscriptstyle T}(Z)\Re e\Big(\chi_{\scriptscriptstyle Z}(R_1)\chi_{\scriptscriptstyle Z}^*(R_2)\Big)\Big], \tag{3.8.17}$$

$$\texttt{ABORNS} = \frac{1}{R_1}\Big[K_{\scriptscriptstyle FB}(\gamma)|V_{pol}|^2 + \frac{1}{2}\Re e\Big(K_{\scriptscriptstyle FB}^f(I)\chi(R_1,R_2)V_{pol}^*\Big) + K_{\scriptscriptstyle FB}^f(Z)\Re e\Big(\chi_{\scriptscriptstyle Z}(R_1)\chi_{\scriptscriptstyle Z}^*(R_2)\Big)\Big], \tag{3.8.18}$$

composed with the summed couplings given in Eq. (3.7.58). They are used at MISD=1 in order to restore the SM remnants for IFI completely.

The Eqs. (3.8.1)–(3.8.2) and Eqs. (3.8.16)–(3.8.18) represent the complete set of objects used for the subsequent convolution with ISR (see Chapter 1) and for construction of realistic observables: total and differential cross-sections and forward-backward asymmetries with cuts[4].

3.8.2. More asymmetries

In addition to the forward-backward asymmetry, several other asymmetries are interesting. It is useful to define a generic 'spin' asymmetry, $A(h)$:

$$A(h) = \frac{\sigma(h) - \sigma(-h)}{\sigma(h) + \sigma(-h)}\,, \tag{3.8.19}$$

where h can denote the polarization of an incoming fermion or the helicity of an outgoing one.

Choosing h to be $h_+ = +1$ the helicity of a final-state τ^+ and $\sigma(h)$ to be $\sigma_{\scriptscriptstyle T}(h_+)$, $A(h)$ becomes the τ polarization, $\lambda_\tau \equiv A^{\rm pol}$. Similarly, one can define: $A_{\scriptscriptstyle F}^{\rm pol}$, $A_{\scriptscriptstyle B}^{\rm pol}$ from (3.8.19) with $\sigma(h) = \sigma_{\scriptscriptstyle A}(h_+),\ A = F, B, FB$, respectively. The subscript $F(B)$ is used to indicate that only data from the forward (backward) hemisphere are in the measurement; the corresponding theoretical relations are given by Eqs. (I.3)–(I.8). The forward-backward polarization asymmetry $A_{\scriptscriptstyle FB}^{\rm pol}$ may be defined as follows:

$$A_{\scriptscriptstyle FB}^{\rm pol} = \frac{\sigma_{\scriptscriptstyle FB}(h) - \sigma_{\scriptscriptstyle FB}(-h)}{\sigma_{\scriptscriptstyle T}}\,. \tag{3.8.20}$$

The τ polarization $\lambda_\tau \equiv A^{\rm pol}$ and asymmetry Eq. (3.8.20) are constructed in interfaces ZUTPSM and ZUTAU, and left-right asymmetries Eq. (3.8.19) – in ZULRSM.

3.8.3. Bhabha scattering

The present ZFITTER package contains BHANG version 4.67 (May 1991). We restrict ourselves to a description of effective Born cross-sections although with the package BHANG also photonic corrections may be calculated. A sketch of the photonic corrections may be found in Section 2.4 of [6]. Early comparisons of the October 1990 version with other Fortran programs indicated to deviations at the per cent level [106,107]. Since then, we have not performed a detailed study of the accuracy of the numerical output.

[4]If at least one incoming and one outgoing fermion are polarized, then the contribution to the forward-backward anti-symmetric Standard Model cross section from pure photon exchange does *not* vanish as in Eq. (1.1.16). This can be seen from formulae Eqs. (3.7.3)–(3.7.4).

Concerning the effective Born cross-section, the situation is better. For INDF=11, the Bhabha cross-section is calculated. Then, instead of subroutine ZCUT, subroutine BHANG is selected. The first call is for subroutine BHAINI. Flag IPART=0 selects the Bhabha cross-section and e.g. IPART=1 the s channel terms only. Depending on the pre-selected flag INTRF, different interfaces are chosen: 1 – Standard Model, 2 – partial widths, 3 – couplings, 4 – squared couplings. This flag is active in subroutine BHACOU where the actual couplings are calculated. After BHAINI, BHANG calls subroutine BHATOT. After this call, the variables CROSB (the integrated effective Born cross-section) and ASYB (forward-backward asymmetry) are determined in BHATOT. The angular integrations are done analytically. In fact, for the determination of effective Born results BHATOT calls subroutine BHABBB which returns expressions integrated from $\cos\vartheta = 0$ to a cut value. Two calls suffice then to treat an arbitrary angular interval. Alternatively, the calculation of QED corrections is performed with the numerical integration subroutine SIMPS and calls the differential cross-section function BHAFUN(THET), with THET the scattering angle.

If a polarization asymmetry is to be calculated, the (expert) user has to select the beam polarizations ALAMP and ALAMM in subroutine BHAINI. When instead of BHATOT the subroutine BHADIF is called, a differential cross-section is returned, also using function BHAFUN. Though, for this the interface has to be written by the user; so we recommend such an option only to the expert user.

For the Standard Model interface, the following approximations were done in order to simplify and speed up calculations. The complex valued s channel form factors $\alpha(s)$, $\rho(s)$, $\kappa_e(s)$, $\kappa_{ee}(s)$ are calculated during the initialization phase when s is set; they depend through the weak box diagrams also on t and u:

$$\texttt{T} = \frac{s}{2}(1-\cos\vartheta) = -t, \tag{3.8.21}$$

$$\texttt{U} = s + t = -u. \tag{3.8.22}$$

For the Bhabha process, it is set arbitrarily

$$|t| = |u| = \frac{s}{2} \tag{3.8.23}$$

for the following call of subroutine ROKANC (the exclusion is the calculation of ZZ and WW box contributions when it is set IBOX=1). In the t channel, $\alpha(t)$ is calculated with function XFOTF1 while the other t channel form factors are set:

$$\rho(t) = \kappa_e(t) = \kappa_{ee}(t) = 1. \tag{3.8.24}$$

At LEP1 this was a good approximation for years, since there the s channel dominates, and the form factors are not too dependent on s, t, u. When the s channel looses its dominance and, additionally, the weak box diagrams are less suppressed, one should give up this approximation.

The weak couplings are prepared in subroutine BHACOU. The effective Born cross-section functions returned are SBORN0, ABORN0. Further functions in use are BHABNS, BHABNT; the former with pure s channel terms, the latter with st interferences and the t channel exchange contributions.

The weak form factors are calculated with the package DIZET. The formulae to be used for the cross-sections are described in [16]. The numbers presented there have been produced with the Fortran program BHASHA [108][5].

The form factors $\kappa_e, \kappa_{ee}, \rho_{ee}$ are calculated in subroutine ROKANC. which depend on s,t,u and the charges of the initial and final state fermions (here minus one). In the s channel, one calls with QE=–1, QF=–1:

$$\texttt{ROKANC}(\ldots, u, -s, t, \texttt{QE}, \texttt{QF}, \texttt{XFZ}, \ldots), \tag{3.8.25}$$

and in the t channel

$$\texttt{ROKANC}(\ldots, s, -t, u, \texttt{QE}, \texttt{QF}, \texttt{XFZ}, \ldots), \tag{3.8.26}$$

and sets:

$$\begin{aligned} \rho_{ee} &= \texttt{XFZ}(1), \\ v_e &= 1 - 4 * \texttt{SW2} * \texttt{XFZ}(2), \\ v_{ee} &= 1 - 8 * \texttt{SW2} * \texttt{XFZ}(2) + 16 * \texttt{SW2} * \texttt{SW2} * \texttt{XFZ}(4). \end{aligned} \tag{3.8.27}$$

These corrections are switched on and off with flag WEAK. They introduce in the weak corrections to the s channel a dependence on the scattering angle. In the t channel, correspondingly, the weak corrections will depend not only on the scattering angle, but also on s – if WW and ZZ boxes are not switched off. The complex valued s channel corrections from the fermionic vacuum polarization are contained in $F_{\scriptscriptstyle A}(s)$,

$$F_{\scriptscriptstyle A}(s) = \frac{\alpha(-|s|)}{\alpha}, \tag{3.8.28}$$

and in the t channel:

$$F_{\scriptscriptstyle A}(t) = \frac{\alpha(|t|)}{\alpha}. \tag{3.8.29}$$

This is described in Section 2.2.3.

In what follows, we give the explicit expressions for the differential cross-section in the Standard Model approach. It is trivial then for the expert user to understand the other interfaces.

The improved Born approximation for the Bhabha differential cross-section consists of the sum of contributions with t channel and s channel exchange of the photon and Z boson and their interferences:

$$\frac{d\sigma^{SM}}{d\cos\vartheta} = \frac{\pi\alpha^2}{2s} \sum_A \sum_a T_a(A) \quad A = \gamma, \gamma Z, Z, \quad a = s, st, t. \tag{3.8.30}$$

We introduce the notation:

$$\lambda_1 = 1 - \lambda_+\lambda_-, \tag{3.8.31}$$

$$\lambda_2 = \lambda_+ - \lambda_-, \tag{3.8.32}$$

$$\lambda_3 = 1 + \lambda_+\lambda_-, \tag{3.8.33}$$

[5] BHASHA was derived from a 1990 version of DIZET.

where ALAMP=λ_+, ALAMM=λ_- are the degree of longitudinal polarization of the positron or electron beam.

The s channel cross-section contributions are ($c = \cos\vartheta$):

$$T_s(\gamma) = |F_A(s)|^2 \left[\lambda_1 \left(1+c^2\right)\right], \tag{3.8.34}$$

$$\begin{aligned} T_s(\gamma Z) = {} & 2\Re e\Big\{\rho_{ee}(s)\chi(s)F_A^*(s)\Big[[\lambda_1 v_{ee}(s)+\lambda_2 v_e(s)](1+c^2) \\ & + [\lambda_1+\lambda_2 v_e(s)]2c\Big]\Big\}, \end{aligned} \tag{3.8.35}$$

$$\begin{aligned} T_s(Z) = {} & |\rho_{ee}(s)\chi(s)|^2 \Bigg\{\Big[\lambda_1\left(1+2|v_e(s)|^2+|v_{ee}(s)|^2\right) \\ & + 2\lambda_2 \Re e\left(v_e(s)[1+v_{ee}(s)^*]\right)\Big](1+c^2) \\ & + 2\Re e\left[\lambda_1\left(|v_e(s)|^2+v_{ee}(s)\right)+\lambda_2 v_e(s)\left(1+v_{ee}^*(s)\right)\right]2c\Bigg\}. \end{aligned} \tag{3.8.36}$$

We now describe the t channel contributions:

$$T_t(\gamma) = F_A(t)^2\left[2\lambda_1\frac{(1+c)^2}{(1-c)^2}+8\lambda_3\frac{1}{(1-c)^2}\right], \tag{3.8.37}$$

$$\begin{aligned} T_t(\gamma Z) = {} & 2\rho_{ee}(t)\chi(t)F_A(t) \\ & \times\left\{2\left[\lambda_1\left(1+v_{ee}(t)\right)-\lambda_2 v_e(t)\right]\frac{(1+c)^2}{(1-c)^2}-8\lambda_3\left(1-v_{ee}(t)\right)\frac{1}{(1-c)^2}\right\}, \end{aligned} \tag{3.8.38}$$

$$\begin{aligned} T_t(Z) = {} & [\rho_{ee}(t)\chi(t)]^2\Bigg\{2\Bigg[\lambda_1\left(1+4v_e(t)^2+2v_{ee}(t)+v_{ee}(t)^2\right) \\ & + 4\lambda_2 v_e(t)\left(1+v_{ee}(t)\right)\Bigg]\frac{(1+c)^2}{(1-c)^2}+\ 8\lambda_3\left(1-v_{ee}(t)\right)^2\frac{1}{(1-c)^2}\Bigg\}. \end{aligned} \tag{3.8.39}$$

The following additional abbreviation is used:

$$\chi(t) = \frac{G_\mu M_Z^2}{\sqrt{2}8\pi\alpha}\frac{t}{t+M_Z^2}. \tag{3.8.40}$$

The form factors $F_A(t), v_e(t), v_{ee}(t), \rho(t)$ are real valued.

Finally, we describe in this Section the contributions from the γZ interference:

$$T_{st}(\gamma) = -2\Re e\left[F_A^*(s)F_A(t)\right]\lambda_1\frac{(1+c)^2}{(1-c)}, \tag{3.8.41}$$

$$T_{st}(\gamma Z) = -2\Re e\left\{\chi(t)\rho_{ee}(t)F_A^*(s)\left[\lambda_1\left(1+v_{ee}(t)\right)-2\lambda_2 v_e(t)\right]+(t\leftrightarrow s)\right\}\frac{(1+c)^2}{(1-c)}, \tag{3.8.42}$$

$$\begin{aligned} T_{st}(Z) = {} & -2\Re e\left\{\chi(s)\rho_{ee}(s)\chi(t)\rho_{ee}(t)\left[\lambda_1\left([1+v_{ee}(s)][1+v_{ee}(t)]\right.\right.\right. \\ & \left.\left.\left.+4v_e(s)v_e(t)\right)-\lambda_2\left(v_e(s)[1+v_{ee}(t)]+v_e(t)[1+v_{ee}(s)]\right)\right]\right\}\frac{(1+c)^2}{(1-c)}. \end{aligned} \tag{3.8.43}$$

It is straightforward to improve the weak corrections for the Bhabha channel.

In view of the recent update of the photonic corrections with acollinearity cut for fermion pair production, we have to assume that the photonic corrections for Bhabha scattering deserve also a complete (and quite involved) re-calculation. This is planned to be done.

Chapter 4

Technical Description of the ZFITTER package

4.1. DIZET User Guide

4.1.1. Structure of DIZET

The package DIZET is a library that calculates electroweak (EW), internal mixed QCD⊗-EW and QCD⊗QED final state radiative corrections for several processes in the Standard Model. A first call of subroutine DIZET returns various pseudo-observables, the W-boson mass, weak mixing angles, the Z-boson width, the W-boson width and other quantities. After the first call to DIZET, several subroutines of DIZET might be used for the calculation of:

- weak form factors and running $\alpha(s)$ for two-fermion into two-fermion neutral current processes – call subroutine ROKANC, see Subsection 3.3.1;
- weak form factors for two-fermion into two-fermion charged current processes – call subroutine RHOCC;
- weak form factors for $\nu_e e$ elastic and deep inelastic NC and CC neutrino-nucleon scattering (earlier versions were interfaced with the codes NUFITTER [110] and NUDIS2 [111]);
- weak form factors and running $\alpha(s)$ for $l - N$ NC and CC deep inelastic scattering – call from package HECTOR [112] and [113]).

4.1.2. Input and Output of DIZET

The DIZET argument list contains Input, Output, and Mixed (I/O) types of arguments:

```
CALL DIZET(NPAR,AMW,AMZ,AMT,AMH,DAL5H,ALQED,ALSTR,ALSTRT,ZPAR,PARTZ,PARTW)
```

Input and I/O parameters to be set by the user

Input:

NPAR(1:21), INTEGER*4 vector of flags, see Subsection 4.1.3 and Subsection 4.2.2

AMT = m_t – t-quark mass

AMH = M_H – Higgs boson mass

ALSTR = $\alpha_s(M_Z^2)$ – strong coupling at $s = M_Z^2$

I/O:

AMW = M_W, W boson mass, input if NPAR(4) = 2,3, but is being calculated for NPAR(4) = 1

AMZ = M_Z, Z boson mass, input if NPAR(4) = 1,3, but is being calculated for NPAR(4) = 2

DAL5H = $\Delta\alpha_h^{(5)}(M_Z^2)$, see Subsection 2.2.1

The M_Z^2, M_W^2, and $\Delta\alpha_h^{(5)}(M_Z^2)$ cannot be assigned by a parameter statement (input/output variables).

Output of the DIZET package

ALQED = $\alpha(M_Z^2)$, calculated from $\Delta\alpha_h^{(5)}(M_Z^2)$, see description of flag ALEM in Subsection 4.1.3

ALSTRT = $\alpha_s(m_t^2)$

ZPAR(1) = DR=Δr, the loop corrections to the muon decay constant G_μ, see Section 2.3.1

ZPAR(2) = DRREM = $\Delta r_{\rm rem}$, the remainder contribution $\mathcal{O}(\alpha)$

ZPAR(3) = SW2 = s_W^2, squared of sine of the weak mixing angle defined by weak boson masses

ZPAR(4) = GMUC = G_μ, muon decay constant, if NPAR(4) = 1,2, is set in CONST1 depending on flag NPAR(20), see Subsection 4.1.3 (It should be calculated if NPAR(4)=3 from M_Z, M_W, but then it will deviate from the experimental value.)

ZPAR(5-14) – stores effective sines for all partial Z-decay channels:

- 5 – neutrino
- 6 – electron
- 7 – muon
- 8 – tau
- 9 – up
- 10 – down
- 11 – charm
- 12 – strange
- 13 – top (presently equal to up)
- 14 – bottom

ZPAR(15) = ALPHST $\equiv \alpha_s(M_Z^2)$

ZPAR(16-30) = QCDCOR(0-14), QCDCOR(I) – array of QCD correction factors for quark production processes and/or Z boson partial width (channel i) into quarks. Enumeration as follows:

$$
\begin{array}{lcll}
\texttt{QCDCOR(0)} & = & 1 & \\
\texttt{QCDCOR(1)} & = & R_V^u(M_Z^2) & \\
\texttt{QCDCOR(2)} & = & R_A^u(M_Z^2) & \\
\texttt{QCDCOR(3)} & = & R_V^d(M_Z^2) & \\
\texttt{QCDCOR(4)} & = & R_A^d(M_Z^2) & \\
\texttt{QCDCOR(5)} & = & R_V^c(M_Z^2) & \\
\texttt{QCDCOR(6)} & = & R_A^c(M_Z^2) & \\
\texttt{QCDCOR(7)} & = & R_V^s(M_Z^2) & \\
\texttt{QCDCOR(8)} & = & R_A^s(M_Z^2) & \\
\texttt{QCDCOR(9)} & = & R_V^u(M_Z^2) & \text{foreseen for} \\
\texttt{QCDCOR(10)} & = & R_A^u(M_Z^2) & t\bar{t}\text{-channel} \\
\texttt{QCDCOR(11)} & = & R_V^b(M_Z^2) & \\
\texttt{QCDCOR(12)} & = & R_A^b(M_Z^2) & \\
\texttt{QCDCOR(13)} & = & R_V^S\text{–singlet vector correction, see Section 3.6} & \\
\texttt{QCDCOR(14)} & = & f_1, \quad \text{ABL–correction, Eq. (3.6.34), [100]} &
\end{array}
\tag{4.1.1}
$$

PARTZ(I) – array of partial decay widths of the Z-boson (see definitions in Eqs. (2.4.9) and (2.4.10)) for the channels:

I = 0 neutrino
I = 1 electron
I = 2 muon
I = 3 tau
I = 4 up
I = 5 down
I = 6 charm
I = 7 strange
I = 8 top (foreseen, not realized)
I = 9 bottom
I = 10 hadrons
I = 11 total

PARTW(I) – array of partial decay widths of the W-boson[1] for the channels:

I = 1 one leptonic
I = 2 one quarkonic
I = 3 total

[1]The calculation of the W width [86] follows the same principles as that of the Z width and is realized in subroutine ZWRATE of DIZET. Since the W width is not that important for the description of fermion pair production, we do not go into details.

4.1.3. The flags used by DIZET

Since the DIZET package may be used as stand-alone in order to compute POs and since it is being used by other codes (e.g. KORALZ [114], BHAGENE3 [115], HECTOR [112,113]), we present here a short description of all flags in DIZET. The flag values must be filled in vector NPAR(1:21) by the the user. Most of these flags overlap with the flags set in user subroutine ZUFLAG called by ZFITTER, however, in the stand-alone mode ZUFLAG need not be called. In order to explcitely show the correspondence between the flag names called with ZUFLAG and the flags used inside DIZET we will provide boxes:

ZUFLAG('CHFLAG', IVALUE-inside DIZET).

The description is given in the order of vector NPAR(1:21). Flag values marked as **presently not supported** are not recommended. For instance, they may be chosen for backward compatibility with respect to earlier versions of the code.

NPAR(1) = IHVP → ZUFLAG('VPOL',IHVP) – Handling of hadronic vacuum polarization:

IHVP = **1** (default) by the parameterization of [27]

IHVP = **2** by effective quark masses of [116,117] **presently not**

IHVP = **3** by the parameterization of [29] **supported**

NPAR(2) = IAMT4 → ZUFLAG('AMT4',IAMT4) – Re-summation of the leading $\mathcal{O}(G_\mu m_t^2)$ electroweak corrections, see Subsection 2.3.3:

IAMT4 = **0** no re-summation

IAMT4 = **1** with re-summation recipe of [75] **presently**

IAMT4 = **2** with re-summation recipe of [71] **not**

IAMT4 = **3** with re-summation recipe of [74] **supported**

IAMT4 = **4** (default) with two-loop sub-leading corrections and re-summation recipe of [31–34,30,36]

NPAR(3) = IQCD → ZUFLAG('QCDC',IQCD) – Handling of internal QCD corrections of order $\mathcal{O}(\alpha\alpha_s)$, see Subsection 3.4:

IQCD = **0** no internal QCD corrections

IQCD = **1** by Taylor expansions (fast option) of [13]

IQCD = **2** by exact formulae of [13]

IQCD = **3** (default) by exact formulae of [38]

NPAR(4) = IMOMS – Choice of two input/output parameters from the three parameters $\{G_\mu, M_Z, M_W\}$, see Subsection 2.2.1:

IMOMS = **1** (default) input G_μ, M_Z (output: M_W), see Eq. (2.2.32)

IMOMS = **2** input G_μ, M_W (output: M_Z), see Eq. (2.2.33)

IMOMS = **3** input M_Z, M_W (output: G_μ), **foreseen, not realized**, see Eq. (2.2.34)

NPAR(5) = IMASS – Handling of hadronic vacuum polarization in Δr; for tests only:

IMASS = **0** (default) uses a fit to data

IMASS = **1** uses effective quark masses, see Subsection 2.2.1

NPAR(6) = ISCRE → ZUFLAG('SCRE',ISCRE) – Choice of the scale of the two-loop remainder terms of Δr with the aid of a conversion factor f, see Eq. (2.3.23) and discussion in the beginning of Subsection 2.3.4:

ISCRE = **0** scale of the remainder terms is $K_{\rm scale} = 1$

ISCRE = **1** scale of the remainder terms is $K_{\rm scale} = f^2$

ISCRE = **2** scale of the remainder terms is $K_{\rm scale} = \dfrac{1}{f^2}$

NPAR(7) = IALEM → ZUFLAG('ALEM',IALEM) – Controls the usage of $\alpha(M_Z^2)$, see flowchart Fig. I.6. Inside DIZET, however, its meaning is limited:

IALEM = **0 or 2** $\Delta\alpha_h^{(5)}(M_Z^2)$ must be supplied by the user as input to the DIZET package

IALEM = **1 or 3** $\Delta\alpha_h^{(5)}(M_Z^2)$ is calculated by the program using a parameterization IHVP

For details see the complete discussion about this flag in Section 3.8 and Subsection 4.2.2.

NPAR(8) = IMASK – Historical relict of earlier versions. **Presently unused.**

NPAR(9) = ISCAL → ZUFLAG('SCAL',ISCAL) – Choice of the scale of $\alpha_s(\xi m_t)$:

ISCAL = **0** (default) exact AFMT correction [72]

ISCAL = **1,2,3** options used in [81], **presently not supported**

ISCAL = **4** Sirlin's scale $\xi = 0.248$ [82]

NPAR(10) = IBARB → ZUFLAG('BARB',IBARB) – Handling of leading $\mathcal{O}\left(G_\mu^2 m_t^4\right)$ corrections:

IBARB = **0** corrections are not included

IBARB = **1** corrections are applied in the limiting case: Higgs mass negligible with respect to the top mass, [118]

IBARB = **2** (default) analytic results of [119] approximated by a polynomial [120]

These options are inactive for AMT4 = 4.

NPAR(11) = IFTJR → ZUFLAG('FTJR',IFTJR) – Treatment of $\mathcal{O}\left(G_\mu \alpha_s m_t^2\right)$ FTJR corrections [92], see Eq. (2.4.25) in Subsection 2.4.3

IFTJR = **0** without FTJR corrections

IFTJR = **1,2** with FTJR corrections

Inside DIZET its meaning is limited. See complete discussion about this flag in Subsection 4.2.2.

NPAR(12) = IFACR → ZUFLAG('EXPR',IFACR) – Realizes different expansions of Δr:

IFACR = **0** first row
IFACR = **1** second row
IFACR = **2** third row
} of Eq. (2.3.57)

NPAR(13) = IFACT → ZUFLAG('EXPF',IFACT) – Realizes different expansions of ρ and κ:

IFACT = **0** first row
IFACT = **1** second row
IFACT = **2** third row
} of Eqs. (2.4.21) and (2.4.24)

NPAR(14) = IHIGS → ZUFLAG('HIGS',IHIGS) – Switch on/off resummation of the leading Higgs contribution, see discussion around Eq. (2.3.59):

IHIGS = **0** leading Higgs contribution is not re-summed

IHIGS = **1** leading Higgs contribution is re-summed

NPAR(15) = IAFMT → ZUFLAG('AFMT',IAFMT) – AFMT corrections [72], see discussion after Eq. (2.3.17) in Subsection 2.3.2 and also Eq. (2.3.26):

IAFMT = **0** without AFMT correction

IAFMT = **1** with AFMT correction (see also description of flag SCAL)

NPAR(16) = IEWLC – Treatment of the remainder terms of ρ and κ (used in ROKAPP together with obsolete option AMT4 = 1-3):

IEWLC = **0** all remainders are set equal to zero

IEWLC = **1** (default) standard treatment

NPAR(17) = ICZAK → ZUFLAG('CZAK',ICZAK) – CKHSS non-factorized $\mathcal{O}(\alpha\alpha_s)$ corrections, [84,85], see Eq. (2.4.18) in Subsection 2.4.1 and Fig. I.6:

ICZAK = **0** without CKHSS corrections

ICZAK = **1,2** with CKHSS corrections

Inside DIZET its meaning is limited. See complete discussion about this flag in Subsection 4.2.2.

NPAR(18) = IHIG2 → ZUFLAG('HIG2',IHIG2) – Handling of the leading Higgs contribution, Eq. (2.3.61) and [79,80]:

IHIG2 = **0** without Higgs corrections

IHIG2 = **1** with Higgs corrections

NPAR(19) = IALE2 → ZUFLAG('ALE2',IALE2) – Treatment of leptonic corrections for $\Delta\alpha$, Fig. I.5:

IALE2 = **0** for backward compatibility with versions up to v.5.12

IALE2 = **1** with one-loop corrections Eq. (2.2.42)

IALE2 = **2** with two-loop corrections [65]

IALE2 = **3** with three-loop corrections [66]

NPAR(20) = IGFER → ZUFLAG('GFER',IGFER) – Handling of QED corrections to the Fermi constant:

IGFER = **0** for backward compatibility with versions up to v.5.12

IGFER = **1** one-loop QED corrections for Fermi constant [121–123]

IGFER = **2** two-loop QED corrections for Fermi constant [124,125]

NPAR(21) = IDDZZ – Used in ZWRATE for internal tests:

IDDZZ = **0** RQCDV(A) are set to 0

IDDZZ = **1** (default) standard treatment of FSR QCD corrections

4.1.4. Calculation of $\alpha(s)$. Function XFOTF3

the running QED coupling at scale s is calculated with function XFOTF3 as follows:

$$\alpha(s) = \frac{\alpha}{1 - \frac{\alpha}{4\pi}\mathtt{DREAL}(\mathtt{XFOTF3}(\mathtt{IALEM}, \mathtt{IALE2}, \mathtt{IHVP}, \mathtt{IQCD}, 1, \mathtt{DAL5H}, -\mathtt{S}))} \,. \tag{4.1.2}$$

4.2. ZFITTER User Guide

ZFITTER is coded in FORTRAN 77 and it has been implemented on different computers with different operating systems: IBM, IBM PC, VMS, APOLLO, HP, SUN, and PC-linux. Double-precision variables have been used throughout the program in order to obtain maximum accuracy, which is especially important for resonance physics. The

package consists of eleven FORTRAN files with the number of lines as shown below, giving a total of 23671 lines:

zf514_aux.f	1616
zfbib6_21.f	4790
zfmai6_21.f	20
zfusr6_21.f	3344
acol6_1.f	3610
bcqcdl5_14.f	727
bhang4_67.f	2054
bkqcdl5_14.f	484
dizet6_21.f	5653
m2tcor5_11.f	848
pairho.f	525

Some flowcharts, which may help to understand the internal organization of ZFITTER are shown in Fig. I.2, Fig. I.3, Fig. I.4, Fig. I.5, Fig. I.6.

The following routines are normally called in the initialization phase of programs using the ZFITTER package. Normally they are called in the order listed below. See, however, an example of different use as described in Subsection 2.5.

4.2.1. Subroutine ZUINIT

Subroutine ZUINIT is used to initialize variables with their default values. This routine *must* be called before any other ZFITTER routine.

```
CALL ZUINIT
```

4.2.2. Subroutine ZUFLAG

Subroutine ZUFLAG is used to modify the default values of flags which control various ZFITTER options.

```
CALL ZUFLAG(CHFLAG,IVALUE)
```

Input Arguments:

CHFLAG is the character identifier of a ZFITTER flag.

IVALUE is the value of the flag. See Tab. I.1 for a list of the defaults.

Sixteen flags that may be modified by ZUFLAG overlap with flags used by DIZET package. They are described in Subsection 4.1. Here we describe 21 flags: the remaining 18 flags and 3 overlapping ones, whose meaning is broader than described in Subsection 4.1. Possible combinations of CHFLAG and IVALUE for these 21 flags are listed below:[2]

AFBC – Controls the calculation of the forward backward asymmetry for interfaces ZUTHSM, ZUXSA, ZUXSA2, and ZUXAFB:

[2]It is worth noting that not for all flags the default value is necessarily the preferred value. A typical example is flag FINR, distinguishing two different treatments of FSR, which are relevant in different experimental setups.

IVALUE = **0** asymmetry calculation is inhibited (can speed up the program if asymmetries are not desired)

IVALUE = **1** (default) both cross-section and asymmetry calculations are done

AFMT – see NPAR(15) in subsection 4.1.3

ALEM – Controls the treatment of the running QED coupling $\alpha(s)$:

IVALUE = **0 or 2** $\Delta\alpha_h^{(5)}(M_Z^2)$ must be supplied by the user as input to the DIZET package; using this input DIZET calculates ALQED = $\alpha(M_Z^2)$

IVALUE = **1 or 3** $\Delta\alpha_h^{(5)}(M_Z^2)$ and $\alpha(M_Z^2)$ are calculated by the program using a parameterization IHVP.

The scale of α(scale) is governed in addition by the flag CONV, see description below and the flowchart Fig. I.6. Values ALEM = 0,1 are accessible only at CONV = 0. Then for ALEM = 0,1 $\alpha(M_Z^2)$ and for ALEM = 2,3 $\alpha(s)$ are calculated. Values ALEM = 2,3 are accessible for CONV = 0,1,2. Then for CONV = 0 $\alpha(s)$ and for CONV = 1,2 $\alpha(s')$ are calculated. Recommended values: ALEM = 2,3.

ALE2 – see NPAR(19) in subsection 4.1.3

AMT4 – see NPAR(2) in subsection 4.1.3

BARB – see NPAR(10) in subsection 4.1.3

BORN – Controls calculation of QED and Born observables:

IVALUE = **0** (default) QED convoluted observables

IVALUE = **1** electroweak observables corrected by Improved Born Approximation

BOXD – Determines calculation of ZZ and WW box contributions, (see Section 3.3.2):

IVALUE = **0** no box contributions are calculated

IVALUE = **1** (default) the boxes are calculated as additive separate contribution to the cross-section

IVALUE = **2** box contributions are added to all four form factors

CONV – Controls the energy scale of running α and EWRC, see Fig. I.6:

IVALUE = **0** $\alpha(s)$

IVALUE = **1** (default) $\alpha(s')$ convoluted

IVALUE = **2** both electroweak radiative correction and α_s are convoluted

CZAK – Treatment of CKHSS non-factorized corrections, [84], [85], see Fig. I.6:

IVALUE = **0** without CKHSS corrections

IVALUE = **1** (default) with CKHSS corrections everywhere

IVALUE = **2** CKHSS corrections are taken into account only in POs, the option is used for tests only

DIAG – Selects type of diagrams taken into account:

IVALUE = **−1** only Z- exchange diagrams are taken into account

IVALUE = **0** Z and γ - exchange diagrams are taken into account

IVALUE = **1** (default) Z and γ exchange and $Z\gamma$ interference are included

EXPF – see NPAR(13) in subsection 4.1.3

EXPR – see NPAR(12) in subsection 4.1.3

FINR – Controls the calculation of final-state radiation, see Fig. I.5:

IVALUE = **−1** final-state QED and QCD correction are not applied;

IVALUE = **0** by s' cut, final-state QED correction is described with the factor $1 + 3\alpha(s)/(4\pi)Q_f^2$

IVALUE = **1** (default) M_{ff}^2 cut, includes complete treatment of final-state radiation with common soft-photon exponentiation

FOT2 – Controls second-order leading log and next-to-leading log QED corrections:

IVALUE = **−1** no initial state radiation QED convolution at all

IVALUE = **0** complete α additive radiator

IVALUE = **1** with logarithmic hard corrections

IVALUE = **2** complete α^2 additive radiator

IVALUE = **3** (default) complete α^3 additive radiator

IVALUE = **4** optional α^3 additive radiator for estimation of theoretical errors: QED-E radiator, Eqs. (3.31) to (3.32) [54]

IVALUE = **5** "pragmatic" LLA third order corrections in a factorized form [55]

FSRS – Final state radiation scale:

IVALUE = **0** $\alpha(0)$, preferred for tight cuts

IVALUE = **1** (default) $\alpha(s)$, preferred for loose cuts

FTJR – Treatment of FTJR corrections [92], see Fig. I.6:

IVALUE = **0** without FTJR corrections

IVALUE = **1** (default) with FTJR corrections everywhere

IVALUE = **2** FTJR corrections are taken into account only in POs, the option is used for tests only

GAMS – Controls the s dependence of $\mathcal{G}_Z$, the Z-width function, see Section 3.2:

IVALUE = **0** forces $\mathcal{G}_Z$ to be constant

IVALUE = **1** (default) allows $\mathcal{G}_Z$ to vary as a function of s [42].

GFER – see NPAR(20) in subsection 4.1.3

HIGS – see NPAR(14) in subsection 4.1.3

HIG2 – see NPAR(18) in subsection 4.1.3

INTF – Determines if the $\mathcal{O}(\alpha)$ initial-final state QED interference (IFI) is calculated:

IVALUE = **0** the interference term is ignored

IVALUE = **1** (default) with IFI in the $\mathcal{O}(\alpha)$

IPFC – Pair flavour content for the pair production corrections:

IVALUE = **1** only electron pairs

IVALUE = **2** only muon pairs

IVALUE = **3** only tau-lepton pairs

IVALUE = **4** only hadron pairs

IVALUE = **5** (default) all channels summed

IVALUE = **6** leptonic pairs (without hadrons)

IPSC – Pair production singlet-channel contributions (works with ISPP = 2):

IVALUE = **0** (default) only non-singlet pairs

IVALUE = **1** LLA singlet pairs according to [59]

IVALUE = **2** complete $O(\alpha^2)$ singlet pairs, *ibid*

IVALUE = **3** singlet pairs up to order $(\alpha L)^3$, *ibid*

IPTO – Third (and higher) order pair production contributions [37] (works with ISPP = 2):

IVALUE = **0** only $O(\alpha^2)$ contributions

IVALUE = **1** $O(\alpha^3)$ pairs

IVALUE = **2** some "non-standard" $O(\alpha^3)$ LLA pairs added

IVALUE = **3** (default) $O(\alpha^4)$ LLA electron pairs added

ISPP – Treatment of ISR pairs:

IVALUE = **−1** pairs are treated with a "fudge" factor as in versions up to v.5.14

IVALUE = **0** without ISR pairs

IVALUE = **1** with ISR pairs, [56] with a re-weighting, see Section 1.6

IVALUE = **2** (default) with ISR pairs according to [37]

IVALUE = **3** with ISR pairs according to [58]

IVALUE = **4** with ISR pairs [58] with extended treatment of hadron pair production

MISC – Controls the treatment of scaling of ρ in the Model Independent approach, see discussion in Subsection 2.5.1:

IVALUE = **0** (default) non-scaled ρ's are used, AROTFZ-array

IVALUE = **1** scaled ρ's, absorbing imaginary parts, are used, ARROFZ-array

MISD – Controls the s dependence of the Model Independent approach, see Section 3.7:

IVALUE = **0** fixed $s = M_Z^2$ in EWRC, old treatment

IVALUE = **1** (default) ensures equal numbers from all interfaces and for all partial channelds but INDF=10 for all $\sqrt{s}$ and for INDF=10 up to 100 GeV[3]

PART – Controls the calculation of various parts of Bhabha scattering:

IVALUE = **0** (default) calculation of full Bhabha cross-section and asymmetry

IVALUE = **1** only s channel

IVALUE = **2** only t channel

IVALUE = **3** only $s - t$ interference

POWR – Controls inclusion of final-state fermion masses in kinematical factors, see Fig. I.6. It acts differently for quarks and leptons. For leptons:

IVALUE = **0** final state lepton masses are set equal to zero

IVALUE = **1** (default) final state lepton masses are retained in all kinematical factors

For quarks it is active only for FINR = –1 and then:

IVALUE = **0** final state quark masses are set equal to zero

IVALUE = **1** (default) final state quark masses are set to their running values (that is, for $c\overline{c}$ and $b\overline{b}$ channels) and retained in all kinematical factors

PREC – is an integer number which any precision governing any numerical integration is divided by, increasing thereby the numerical precision of computation:

IVALUE = **10** (default)

[3]The reason of that will be investigated while working on the LEP2 version of ZFITTER.

IVALUE = **1 − 99** in some cases when some numerical instability while running v.5.10 was registered, it was sufficient to use PREC = 3, in some other cases (e.g. with P_τ) only PREC = 30 solved the instability

PRNT – Controls ZUWEAK printing:

IVALUE = **0** (default) printing by subroutine ZUWEAK is suppressed

IVALUE = **1** each call to ZUWEAK produces some output

QCDC – see NPAR(3) in subsection 4.1.3

SCAL – see NPAR(9) in subsection 4.1.3

SCRE – see NPAR(6) in subsection 4.1.3

VPOL – see NPAR(1) in subsection 4.1.3

WEAK – Determines if the weak loop calculations are to be performed

IVALUE = **0** no weak loop corrections to the cross-sections are calculated and weak parameters are forced to their Born values, i.e. $\rho_{ef} = \kappa_{e,f,ef} = 1$

IVALUE = **1** (default) weak loop corrections to the cross-sections are calculated

In Tab. I.3 an overview over all flags used in DIZET and ZFITTER is given. The internal flag names and their default values are listed as well as their corresponding positions in the vectors NPAR(1:21) in DIZET (or NPARD(1:21) in ZFITTER) and NPAR(1:30) in ZFITTER.

4.2.3. Subroutine ZUWEAK

Subroutine ZUWEAK is used to perform the weak sector calculations. These are done internally with DIZET, see Section 4.1. The routine calculates a number of important electroweak parameters which are stored in common blocks for later use (see Section 2.5). If any ZFITTER flag has to be modified this must be done before calling ZUWEAK.

```
CALL ZUWEAK(ZMASS,TMASS,HMASS,DAL5H,ALFAS)
```

Input Arguments:

ZMASS is the Z mass M_Z in GeV.

TMASS is the top quark mass m_t in GeV, [10-400].

HMASS is the Higgs mass M_H in GeV, [10-1000].

DAL5H is the value of $\Delta\alpha_h^{(5)}(M_Z^2)$.

ALFAS is the value of the strong coupling constant α_s at $q^2 = M_Z^2$ (see factors QCDCOR in Tab. 4.1.1).

Computing time may be saved by performing weak sector calculations only once during the initialization of the ZFITTER package. This is possible since weak parameters are nearly independent of s near the Z peak, e.g. $\sim \ln s/M_Z^2$. However, the incredible precision of LEP1 data forced us to give up this option, see description of flag MISD.

4.2.4. Subroutine ZUCUTS

Subroutine ZUCUTS is used to define kinematic and geometric cuts for each fermion channel: it selects the appropriate QED calculational *chain*.

```
CALL ZUCUTS(INDF,ICUT,ACOL,EMIN,S_PR,ANG0,ANG1,SIPP)
```

Input Arguments:

INDF is the fermion index (see Tab. I.2 and Fig. I.5).

ICUT controls the kinds of cuts (*chain*) to be used.

ICUT = –1: (default) allows for an s' cut (a cut on $M^2_{f\bar{f}}$, the fermion and antifermion invariant mass); the fastest branch based on [10]

ICUT = 0: **not recommended**; branch is known to contain bugs. It allows for a cut on the acollinearity ACOL of the $f\bar{f}$ pair, on the minimum energy EMIN of both fermion and antifermion, and for a geometrical acceptance cut [45][4]

ICUT = 1: s' or $M^2_{f\bar{f}}$ cuts and geometrical acceptance cut, based on [9]

ICUT = 2: new branch, replaces ICUT = 0 for realistic cuts ACOL and EMIN, based on [11]

ICUT = 3: the same branch, using ACOL cut and EMIN cut but also with possibility to impose an additional acceptance cut [43]

ACOL is the maximum acollinearity angle $\xi^{\max}$ of the $f\bar{f}$ pair in degrees (ICUT = 0,2,3).

EMIN is the minimum energy $E_f^{\min}$ of the fermion and antifermion in GeV (ICUT = 0,2,3).

S_PR is the minimum allowed invariant $f\bar{f}$ mass $M^2_{f\bar{f}}$ in GeV (ICUT = –1,1) or, with some approximations, the minimum allowed invariant mass of the propagator after ISR[5] (This is related to the maximum photon energy by Eq. (1.3.3), Eq. (1.4.2). See also description of FINR flag.).

ANG0 (default = 0°) is the minimum polar angle ϑ in degrees of the final-state antifermion.

ANG1 (default = 180°) is the maximum polar angle ϑ in degrees of the final-state antifermion.

SIPP a cut parameter governing the calculation of corrections due to initial pairs, actually it should be chosen equal to s'.

[4] As was shown recently [11,126,43], the old results of [45] contained bugs which occasionally didn't show up in comparisons as e.g. in [14]. The option is retained for back-compatibility with older versions only.
[5] The invariant mass of the propagator is not an observable quantity unless specific assumptions on ISR and FSR are made.

4.2.5. Subroutine ZUINFO

Subroutine ZUINFO prints the values of ZFITTER flags and cuts.

```
CALL ZUINFO(MODE)
```

Input Argument:

MODE controls the printing of ZFITTER flag and cut values.

MODE = 0: Prints all flag values.

MODE = 1: Prints all cut values.

4.3. Interface Routines of ZFITTER

The calculational chains of ZFITTER can be combined with several interfaces. These interfaces will be described here. For the Standard Model branch the cross-section and asymmetry interface is subroutine ZUTHSM, while for the tau polarization it is subroutine ZUTPSM. Subroutine ZUATSM allows to calculate the differential cross-section, $d\sigma/d\cos\theta$, predicted by the Standard Model. With subroutine ZULRSM the left-right asymmetry is determined within the Standard Model. Subroutines ZUXSA, ZUXSA2, ZUXAFB, and ZUTAU are interfaces using effective couplings. The interface for the partial widths is ZUXSEC. The interface using an S-matrix inspired language is realized with the SMATASY package [19,20,17,18].

Note that subroutine ZUWEAK must be called prior to any of the interfaces to be described below. As a consequence, flags used in this subroutine can influence the calculation of cross-sections and asymmetries in the interfaces described now.

All subroutines need the following input arguments:

INDF is the fermion index (see Tab. I.2).

SQRS is the centre-of-mass energy $\sqrt{s}$ in GeV.

ZMASS is the Z mass M_Z in GeV.

4.3.1. Subroutine ZUTHSM

Subroutine ZUTHSM is used to calculate Standard Model cross-sections and forward-backward asymmetries as described in Section 3.7.3.

```
CALL ZUTHSM(INDF,SQRS,ZMASS,TMASS,HMASS,DAL5H,ALFAS,XS*,AFB*)
```

Input Arguments:

TMASS is the top quark mass m_t in GeV, [10-400].

HMASS is the Higgs mass M_H in GeV, [10-1000].

DAL5H is the value of $\Delta\alpha_h^{(5)}(M_Z^2)$.

ALFAS is the value of the strong coupling constant α_s at $q^2 = M_Z^2$ (see also flag QCDC and factors QCDCOR).

Output Arguments[6]:

XS is the total cross-section σ_T in nb.

AFB is the forward-backward asymmetry A_{FB}.

Output Internal Flag:

INTRF=1

4.3.2. Subroutine ZUATSM

Subroutine ZUATSM is used to calculate differential cross-sections, $d\sigma/d\cos\theta$, in the Standard Model as described in Section 3.7.3.

```
CALL ZUATSM(INDF,SQRS,ZMASS,TMASS,HMASS,DAL5H,ALFAS,CSA*,DXS*)
```

Input Arguments:

TMASS is the top quark mass m_t in GeV, [10-400].

HMASS is the Higgs mass M_H in GeV, [10-1000].

ALQED is the value of the running electromagnetic coupling constant.

ALFAS is the value of the strong coupling constant α_s at $q^2 = M_Z^2$ (see factors QCDCOR).

CSA is the cosine of the scattering angle.

Output Arguments:

DXS is the theoretical differential cross-section.

Output Internal Flag:

INTRF=1

4.3.3. Subroutine ZUTPSM

Subroutine ZUTPSM is used to calculate the tau polarization and tau polarization asymmetry in the Standard Model as described in Section 3.7.3.

```
CALL ZUTPSM(SQRS,ZMASS,TMASS,HMASS,DAL5H,ALFAS,TAUPOL*,TAUAFB*)
```

Input Arguments:

HMASS is the Higgs mass M_H in GeV, [10-1000].

[6] An asterisk (*) following an argument in a calling sequence is used to denote an output argument.

DAL5H is the value of $\Delta\alpha_h^{(5)}(M_Z^2)$.

ALFAS is the value of the strong coupling constant α_s at $q^2 = M_Z^2$ (see factors QCDCOR).

Output Arguments:

TAUPOL is the tau polarization $A_{\rm pol}$ of (Eq. (3.8.19)).

TAUAFB is the tau polarization forward-backward asymmetry $A_{FB}^{\rm pol}$ as defined in (Eq. (3.8.20)).

Output Internal Flag:

INTRF=1

4.3.4. Subroutine ZULRSM

Subroutine ZULRSM is used to calculate the left-right asymmetry in the Standard Model as described in Section 3.7.3.

```
CALL ZULRSM(INDF,SQRS,ZMASS,TMASS,HMASS,DAL5H,ALFAS,POL,XSPL*,XSMI*)
```

Input Arguments:

TMASS is the top quark mass m_t in GeV, [40-300].

HMASS is the Higgs mass M_H in GeV, [10-1000].

DAL5H is the value of $\Delta\alpha_h^{(5)}(M_Z^2)$.

ALFAS is the value of the strong coupling constant α_s at $q^2 = M_Z^2$ (see also flag ALST).

POL is the degree of longitudinal polarization of electrons.

Output Arguments:

XSPL is the cross-section for POL > 0

XSMI is the cross-section for POL < 0

Output Internal Flag:

INTRF=1

4.3.5. Subroutine ZUXSA

Subroutine ZUXSA is used to calculate cross-section and forward-backward asymmetry as described in Section 3.7.5 as functions of $\sqrt{s}$, M_Z, Γ_Z.

```
CALL ZUXSA(INDF,SQRS,ZMASS,GAMZ0,MODE,GVE,XE,GVF,XF,XS*,AFB*)
```

Input Arguments:

GAMZ0 is the total Z width Γ_Z in GeV.

MODE determines which weak couplings are used:

MODE = 0: XE (XF) are effective axial-vector couplings $\bar{a}_{e,f}$ for electrons (final-state fermions).

MODE = 1: XE (XF) are the effective weak neutral-current amplitude normalizations $\bar{\rho}_{e,f}$ for electrons (final-state fermions).

GVE is the effective vector coupling for electrons $\bar{g}_e$.

XE is the effective axial-vector coupling $\bar{a}_e$ or weak neutral-current amplitude normalization $\bar{\rho}_e$ for electrons (see MODE).

GVF is the effective vector coupling for the final-state fermions $\bar{g}_f$.

XF is the effective axial-vector coupling $\bar{a}_f$ or the weak neutral-current amplitude normalization $\bar{\rho}_f$ for the final-state fermions (see MODE).

Output Arguments:

XS is the cross-section σ_T in nb.

AFB is the forward-backward asymmetry A_{FB}.

Output Internal Flag:

INTRF=3

4.3.6. Subroutine ZUXSA2

Subroutine ZUXSA2 is used to calculate lepton cross-section and forward-backward asymmetry as functions of $\sqrt{s}$, M_Z, Γ_Z, and of the weak couplings *assuming lepton universality* as introduced in Section 3.7.6. This routine is similar to ZUXSA except that the couplings are squared.

```
CALL ZUXSA2(INDF,SQRS,ZMASS,GAMZ0,MODE,GV2,X2,XS*,AFB*)
```

Input Arguments:

GAMZ0 is the total Z width Γ_Z in GeV.

MODE determines which weak couplings are used:

MODE = 0: X2 is the square of the effective axial-vector coupling $\bar{a}_l$ for leptons.

MODE = 1: X2 is the square of the effective neutral-current amplitude normalization $\bar{\rho}_l$ for leptons.

GV2 is the square of the effective vector coupling $\bar{g}_l$ for leptons.

X2 is the square of the effective axial-vector coupling $\bar{a}_l$ or neutral-current amplitude normalization $\bar{\rho}_l$ for leptons (see MODE).

Output Arguments:

XS is the cross-section σ_T in nb.

AFB is the forward-backward asymmetry A_{FB}.

Output Internal Flag:

INTRF=4

4.3.7. Subroutine ZUTAU

Subroutine ZUTAU is used to calculate the τ^+ polarization as a function of $\sqrt{s}$, M_Z, Γ_Z, and the weak couplings, see Section 3.7.5.

```
CALL ZUTAU(SQRS,ZMASS,GAMZ0,MODE,GVE,XE,GVF,XF,TAUPOL*,TAUAFB*)
```

Input Arguments:

GAMZ0 is the total Z width Γ_Z in GeV.

MODE determines which weak couplings are used:

MODE = 0: XE (XF) is the effective axial-vector coupling $\bar{a}_{e,f}$ for electrons (final-state fermions).

MODE = 1: XE (XF) is the effective weak neutral-current amplitude normalization $\bar{\rho}_{e,f}$ for electrons (final-state fermions).

GVE is the effective vector coupling for electrons $\bar{g}_e$.

XE is the effective axial-vector coupling $\bar{a}_e$ or weak neutral-current amplitude normalization $\bar{\rho}_e$ for electrons (see MODE).

GVF is the effective vector coupling for the final-state fermions $\bar{g}_f$.

XF is the effective axial-vector coupling $\bar{a}_f$ or weak neutral-current amplitude normalization $\bar{\rho}_f$ for the final-state fermions (see MODE).

Output Arguments:

TAUPOL is the τ-lepton polarization λ_τ defined in (Eq. (3.8.19)).

TAUAFB is the forward-backward asymmetry for polarized τ-leptons $A_{FB}^{\rm pol}$ as defined in (Eq. (3.8.20)).

Output Internal Flag:

INTRF=3

4.3.8. Subroutine ZUXSEC

Subroutine ZUXSEC is used to calculate the cross section as a function of $\sqrt{s}$, M_Z, Γ_Z, Γ_e and Γ_f as described in Section 3.7.4.

```
CALL ZUXSEC(INDF,SQRS,ZMASS,GAMZ0,GAMEE,GAMFF,XS*)
```

Input Arguments:

GAMZ0 is the total Z width Γ_Z in GeV.

GAMEE is the partial Z decay width Γ_e in GeV.

GAMFF is the partial Z decay width Γ_f in GeV; if INDF=10, GAMFF=Γ_h.

Output Internal Flag:

INTRF=2

4.3.9. Subroutine ZUXAFB

Subroutine ZUXAFB is used to calculate the cross section as a function of $\sqrt{s}$, M_Z, Γ_Z, Γ_e and Γ_f as described in Section 3.7.7.

```
CALL ZUXAFB(INDF,SQRS,ZMASS,GAMZ0,PFOUR,PVAE2,PVAF2,XS*,AFB*)
```

Input Arguments:

GAMZ0 is the total Z width Γ_Z in GeV.

PFOUR is the product of vector and axial-vector couplings $\bar{g}_e\bar{a}_e\bar{g}_f\bar{a}_f$.

PVAE2 is $\bar{g}_e^2 + \bar{a}_e^2$.

PVAF2 is $\bar{g}_f^2 + \bar{a}_f^2$.

Output Argument:

XS is the cross-section σ_T in nb.

AFB is the forward-backward asymmetry A_{FB}.

Output Internal Flag:

INTRF=5

4.3.10. Subroutine ZUALR

Subroutine ZUALR is reserved for the fit of A_{LR}, see Section 3.7.8.

```
CALL ZUALR(SQRS,ZMASS,GAMZ0,MODE,GVE,XE,GVF,XF,TAUPOL,TAUAFB)
```

Output Internal Flag:

INTRF=6

4.4. ZFITTER Common Blocks

Only a few ZFITTER common blocks are of potential interest. to the user. They are documented here.

```
COMMON /ZUPARS/QDF,QCDCOR(0:14),ALPHST,SIN2TW,S2TEFF(0:11),WIDTHS(0:11)
```

The common block /ZUPARS/ contains some ZFITTER parameters:

QDF is the final-state radiation factor $3\alpha/(4\pi)$

QCDCOR is an array of QCD corrections, defined in Eq. (4.1.1)

ALPHST is $\alpha_{_S}(M_Z^2)$.

SIN2TW is s_W^2, Sirlin's weak mixing angle as defined in Eq. (2.2.31).

S2TEFF are the values of $\kappa_f s_W^2$ at $s = M_Z^2$ for each fermion channel f (see Tab. I.2). They are some auxiliary quantities, which do not coincide with the *effective weak mixing angles* defined by Eq. (2.4.17) and may be of interest for experts only. Note that S2TEFF(10:11) are set to zero.

WIDTHS are the partial decay widths Eqs. (2.4.9)–(2.4.10) of the Z for all fermion channels enumerated as in Tab. I.2. WIDTHS(11) is the total Z width.

```
COMMON/ZFCHMS/ALLCH(0:11),ALLMS(0:11)
```

The common block ZFCHMS contains the charges ALLCH and masses ALLMS of the fermions. See Tab. I.2 for enumeration.

Note that ALLCH(10) = 1 for technical reasons and ALLCH(11) is undefined. Also, ALLMS(10) = 0 and ALLMS(11) again is undefined.

We would also like to mention that the variables FAA, FZA, FZZ, which are introduced as DATA in subroutine EWCOUP allow us to switch on/off the $\gamma\gamma$, γZ, ZZ parts of the cross-sections, respectively.

Chapter 5

ZFITTER availability

The Fortran files composing the ZFITTER package, this description, and also related information may be found at the following locations:

```
/afs/cern.ch/user/b/bardindy/public/

http://www.ifh.de/~riemann/Zfitter/zf.html
```

E-mail addresses of the authors of this description:

D. Bardin	bardin@nusun.jinr.ru
	Dmitri.Bardin@cern.ch
P. Christova	penchris@nusun.jinr.ru
	penka@ifh.de
M. Jack	jack@ifh.de
L. Kalinovskaya	kalinov@nusun.jinr.ru
	Lidia.Kalinovskaia@cern.ch
A. Olshevsky	Alexander.Olchevski@cern.ch
S. Riemann	Sabine.Riemann@ifh.de
T. Riemann	Tord.Riemann@ifh.de

Acknowledgments

We would like to thank the colleagues who joined us for longer or shorter periods: A. Chizhov, O. Fedorenko, M. Sachwitz, A. Sazonov, Yu. Sedykh, I. Sheer, and L. Vertogradov. Without their contributions the ZFITTER package would not be what it is.

We acknowledge the contributions to the first description of the package, ref. [6], from A. Chizhov, O. Fedorenko, S. Ganguli, A. Gurtu, M. Lokajicek, K. Mazumdar, G. Mitselmakher, J. Ridky, M. Sachwitz, A. Sazonov, D. Schaile, Yu. Sedykh, I. Sheer, and L. Vertogradov.

In the process of package development we profited heavily from the fruitful discussions with G. Altarelli, S. Arkadova, W. Hollik, E. Kuraev, A. Leike, L. Maiani, L. Okun and D. Shirkov.

The implementation of higher order corrections into the package was supported by A. Arbuzov, R. Barbieri, F. Berends, K. Chetyrkin, G. Degrassi, P. Gambino, F. Jegerlehner, R. Harlander, A. Kataev, H. Kühn, S. Larin, M. Steinhauser, and O. Tarasov.

Without the dedicated comparisons with other programs performed in close collaboration with A. Borrelli, W. Hollik, S. Jadach, L. Maiani, M. Martinez, G. Passarino, B. Pietrzyk, A. Rozanov, F. Teubert, and Z. Was the package would not be as reliable as it is.

Special thanks goes to the users of ZFITTER, who were constantly providing us with critical commments and ideas for improvements: M. Grünewald, T. Kawamoto, C. Pauss, and G. Quast.

We would like to acknowledge also the contributions of: D. Bourilkov, I. Boyko, R. Clare, P. Clarke, G. Duckeck, F. Filthaut, D. Haidt, J. Holt, J. Kellogg, M. Kobel, K. Mazumdar, J. Mnich, K. Mönig, P. Renton, D. Schaile, M. Winter, and of many others for useful discussions and suggestions, which were constantly stimulating the ZFITTER package development.

The authors are grateful to the JINR and LNP directorates, in particular: V. Kadyshevsky, A. Sissakian, N. Rusakovitch, and A. Kurilin for their constant interest and support.

D.B., P.C., and L.K. are very much indebted to DESY Zeuthen for financial support and hospitality extended to them during several stays in 1994–1998 when a notable part of the stays was devoted to this project. They are indebted for the generous help of DESY Zeuthen, especially to Paul Söding, for strengthening their computing equipments.

D.B. is indebted to the Theory Division of CERN for financial support and hospitality extended to him during several short stays in 1996–1999 when part of the time was devoted to this project, in particular for the stay in May–June 1999, when it was completed.

D.B. would like to express special thanks to Giampiero Passarino for the numerous selfless comparisons of ZFITTER and TOPAZ0 results during several workshops on LEP1 and LEP2 physics and in collaboration with the LEP Electroweak Working Group.

Appendix A

One-Loop Core of ZFITTER

A.1. Introduction to One-Loop EWRC

The aim of this Appendix is to give a condensed presentation of the one-loop core of ZFITTER. It outlines the way from Feynman diagrams to the amplitude form factors; the latter are the main building blocks of the code.

This Appendix consists of three Sections. Section A.2 introduces the Passarino-Veltman functions [109] used in ZFITTER, Section A.3 contains the building blocks for the construction of the one-loop electroweak *amplitudes*, and Section A.4 contains the **amplitudes** themselves. A complete presentation of the OMS renormalization scheme, on which the electroweak core of ZFITTER is based upon, was presented recently in [39]. This Appendix is not a plane extraction from there, but contains some minimum of formulae needed to understand the amplitude form factors for the process $e^+e^- \to f\overline{f}$.

A.2. Passarino–Veltman Functions

Here we present scalar integrals over Feynman parameters which one meets in the calculation of $\mathcal{O}(\alpha)$ electroweak radiative corrections, EWRC. We use the Passarino-Veltman functions $A_0,\ B_0,\ C_0$ and D_0. The defining integrals and the answers in the dimensional regularization are given.

One-point function

Defining integral:

$$i\pi^2 A_0\left(M\right) = \mu^{4-n}\int \frac{d^n q}{q^2+M^2-i\epsilon}\,. \tag{A.2.1}$$

Here and below μ is the so-called t'Hooft scale, an arbitrary quantity with mass dimensionality which is introduced in order to make the dimensionality of the integral of Eq. (A.2.1) independent of the variation of space-time dimension n. Its answer is

$$A_0\left(M\right) = M^2\left(-\frac{1}{\bar{\varepsilon}} + \ln\frac{M^2}{\mu^2} - 1\right). \tag{A.2.2}$$

Two-point functions

Defining integral:

$$i\pi^2 B_0\left(p^2;M_1,M_2\right) = \mu^{4-n}\int\frac{d^nq}{d_0d_1}, \tag{A.2.3}$$

$$d_0 = q^2+M_1^2-i\epsilon, \tag{A.2.4}$$

$$d_1 = (q+p)^2+M_2^2-i\epsilon. \tag{A.2.5}$$

The most general answer reads

$$B_0\left(p^2;M_1,M_2\right) = \frac{1}{\bar\varepsilon}-\ln\frac{M_1M_2}{\mu^2}+\frac{\Lambda}{p^2}\ln\frac{-p^2-i\epsilon+M_1^2+M_2^2-\Lambda}{2M_1M_2} + \frac{M_1^2-M_2^2}{2p^2}\ln\frac{M_1^2}{M_2^2}+2, \tag{A.2.6}$$

where $\Lambda^2=\lambda\left(p^2,M_1^2,M_2^2\right)$ is the Källen λ-function:

$$\lambda(x,y,z)=x^2+y^2+z^2-2xy-2xz-2yz. \tag{A.2.7}$$

Several particular cases are needed. The case of equal masses:

$$B_0\left(p^2;M,M\right)=\frac{1}{\bar\varepsilon}-\ln\frac{M^2}{\mu^2}+2-\beta\ln\frac{\beta+1}{\beta-1}, \tag{A.2.8}$$

with

$$\beta^2=1+4\frac{M^2}{p^2-i\epsilon}. \tag{A.2.9}$$

Cases with some vanishing arguments:

$$B_0(0;M_1,M_2) = \frac{A_0(M_2)-A_0(M_1)}{M_1^2-M_2^2}, \tag{A.2.10}$$

$$B_0(0;0,M) = -\frac{A_0(M)}{M^2}, \tag{A.2.11}$$

$$B_0\left(p^2;0,0\right) = \frac{1}{\bar\varepsilon}-\ln\frac{p^2-i\epsilon}{\mu^2}+2. \tag{A.2.12}$$

It is convenient to split A_0- and B_0-functions into two parts: (i) one containing the ultraviolet (UV) singularity and the μ-dependent part, i.e. the *pole* part, and (ii) the *finite* rest. For A_0 this is already achieved in Eq. (A.2.1), while for B_0 we define in addition a B_0^F function:

$$B_0\left(p^2;M_1,M_2\right)=\frac{1}{\bar\varepsilon}-\ln\frac{M_W^2}{\mu^2}+B_0^F\left(p^2;M_1,M_2\right), \tag{A.2.13}$$

with an artificial scale M_W.

Higher-rank B-functions, B_1 and B_{21}, are also needed. We simply list for them the integral representations with separated UV-poles:

$$B_1\left(p^2;M_1,M_2\right) = -\frac{1}{2}\frac{1}{\bar\varepsilon}+\int_0^1 dx\,x\ln\frac{p^2x(1-x)+M_1(1-x)+M_2x}{\mu^2} = \frac{1}{2p^2}\Big[A_0(M_1)-A_0(M_2)+\left(\Delta M_{12}^2-p^2\right)B_0\left(p^2;M_1,M_2\right)\Big], \tag{A.2.14}$$

and

$$\begin{aligned} B_{21}\left(p^2;M_1,M_2\right) &= \frac{1}{3}\frac{1}{\bar{\varepsilon}} - \int_0^1 dx x^2 \ln\frac{p^2x(1-x)+M_1(1-x)+M_2x}{\mu^2} \\ &= \frac{3\left(M_1^2+M_2^2\right)+p^2}{18p^2} + \frac{\Delta M_{12}^2-p^2}{3p^4}A_0\left(M_1\right) - \frac{\Delta M_{12}^2-2p^2}{3p^4}A_0\left(M_2\right) \\ &\quad + \frac{\lambda\left(-p^2,M_1^2,M_2^2\right)-3p^2M_1^2}{3p^4}B_0\left(p^2;M_1,M_2\right), \end{aligned}$$

with $$\Delta M_{12}^2 = M_1^2 - M_2^2. \tag{A.2.15}$$

They enter in the combination

$$\begin{aligned} B_f\left(p^2;M_1,M_2\right) &= 2\left[B_{21}\left(p^2;M_1,M_2\right)+B_1\left(p^2;M_1,M_2\right)\right] \\ &= -\frac{1}{3\bar{\varepsilon}} + 2\int_0^1 dx x(1-x)\ln\frac{p^2x(1-x)+M_1(1-x)+M_2x}{\mu^2}, \end{aligned} \tag{A.2.16}$$

which is often met in *fermionic* parts of self-energy functions (see Section A.3). For the case of equal masses ($M_1 = M_2$), the finite part of Eq. (2.2.44) may be cast in the following compact form:

$$p^2B_f^F\left(p^2;M,M\right) = \frac{p^2}{9} + \frac{2M^2}{3}\ln\frac{M^2}{M_W^2} + \frac{1}{3}\left(2M^2-p^2\right)B_0^F\left(p^2;M,M\right), \tag{A.2.17}$$

where

$$B_0^F\left(p^2;M,M\right) = -\ln\frac{M^2}{M_W^2} + 2 - \beta\ln\frac{\beta+1}{\beta-1}. \tag{A.2.18}$$

The counter-terms involve the derivative of B_0^F, which in the case of equal masses is very compact:

$$\begin{aligned} B_{0p}^F\left(p^2;M,M\right) &\equiv \frac{\partial B_0^F\left(p^2;M,M\right)}{\partial p^2} \\ &= -\frac{1}{p^2} + \frac{2M^2}{p^4}\frac{1}{\beta}\ln\frac{\beta+1}{\beta-1}. \end{aligned} \tag{A.2.19}$$

Finally, we use a subtracted B_0 function defined by

$$\Delta B\left(p^2;M_1,M_2\right) = B_0\left(p^2;M_1,M_1\right) - B_0\left(0;M_1,M_2\right). \tag{A.2.20}$$

Three- and four-point functions

The above presentation of scalar A_0 and B_0 functions is rather general. In what follows, only those C_0 and D_0 functions are described, which are used in ZFITTER. We will use a truncated argument list for these functions and omit masses of external particles, which are ignored in the calculations. There are only two generic scalar three-point integrals which one meets in our calculations. The first one arises in $Vf\bar{f}$ vertices if external

fermion masses are neglected and if the internal boson is not massless (i.e. not a photon). It is:

$$\begin{aligned} C_0(p^2;M_1,M_2,M_1) &= \int_0^1 ydy\int_0^1 dx\frac{1}{M_1^2(1-y)+M_2^2y+p^2y^2x(1-x)} \\ &= \frac{1}{p^2}\Bigg[\mathrm{Li}_2\left(\frac{x_0}{x_0-x_1}\right)-\mathrm{Li}_2\left(\frac{x_0-1}{x_0-x_1}\right)+\mathrm{Li}_2\left(\frac{x_0}{x_0-x_2}\right) \\ &\quad -\mathrm{Li}_2\left(\frac{x_0-1}{x_0-x_2}\right)-\mathrm{Li}_2\left(\frac{x_0}{x_0-x_3}\right)+\mathrm{Li}_2\left(\frac{x_0-1}{x_0-x_3}\right)\Bigg], \end{aligned} \tag{A.2.21}$$

with

$$x_0=\frac{M_1^2-M_2^2}{p^2}, \tag{A.2.22}$$

$$x_{1,2}=\frac{1}{2}\left(1\mp\sqrt{1+\frac{4M_2^2}{p^2}}\right), \tag{A.2.23}$$

$$x_3=\frac{M_1^2}{M_1^2-M_2^2}. \tag{A.2.24}$$

The generic four-point integral is:

$$\begin{aligned} D_0\left(p^2,I;M_1,0,M_1,M_2\right) &= \int_0^1 dz\int_0^1 ydy\int_0^1 dx \\ &\quad\times\frac{1}{\left[M_1^2(1-y)+M_2^2y+I(1-y)(1-z)+p^2z^2y^2x(1-x)\right]^2} \\ &= \frac{1}{p^2(I+M_1^2)\sqrt{d_4}} \\ &\quad\times\sum_{i=1,2}\Bigg[\mathrm{Li}_2\left(\frac{\bar{x}_i}{\bar{x}_i-x_1}\right)-\mathrm{Li}_2\left(\frac{\bar{x}_i-1}{\bar{x}_i-x_1}\right) \\ &\quad+\mathrm{Li}_2\left(\frac{\bar{x}_i}{\bar{x}_i-x_2}\right)-\mathrm{Li}_2\left(\frac{\bar{x}_i-1}{\bar{x}_i-x_2}\right)-\mathrm{Li}_2\left(\frac{\bar{x}_i}{\bar{x}_i-x_3}\right) \\ &\quad+\mathrm{Li}_2\left(\frac{\bar{x}_i-1}{\bar{x}_i-x_3}\right)+\mathrm{Li}_2\left(\frac{\bar{x}_i}{\bar{x}_i-x_4}\right)-\mathrm{Li}_2\left(\frac{\bar{x}_i-1}{\bar{x}_i-x_4}\right)\Bigg], \end{aligned} \tag{A.2.25}$$

where the new roots are:

$$\bar{x}_{1,2} = \frac{x_4}{2}\left(1\mp\sqrt{d_4}\right), \tag{A.2.26}$$

$$d_4 = 1+\frac{4M_2^2I(I+M_1^2-M_2^2)}{p^2(I+M_1^2)^2}, \tag{A.2.27}$$

$$x_4 = \frac{I+M_1^2}{I+M_1^2-M_2^2}, \tag{A.2.28}$$

and the $x_{1,2,3}$ are defined in Eq. (A.2.24).

The analytic continuation

$$p^2\to -s, \tag{A.2.29}$$

is well-defined if one understands all masses appearing in Eqs. (A.2.21)–(A.2.25) with infinitesimal imaginary parts

$$M_i^2 \to M_i^2 - i\epsilon. \tag{A.2.30}$$

The second generic scalar three-point integral is met in the infrared divergent $Vf\bar{f}$ vertex with a virtual photon and with external momenta on-shell. Here we must keep all arguments in the C_0 function:

$$\begin{aligned} C_0\left(-s; m_f, 0, m_f\right) &\equiv C_0\left(-m_f^2, -m_f^2, -s; m_f, 0, m_f\right) \\ &= \frac{\mu^{4-n}}{i\pi^2}\int d^n q \frac{1}{q^2\left[(q+p_1)^2+m_f^2\right]\left[(q-p_2)^2+m_f^2\right]}. \end{aligned} \tag{A.2.31}$$

We limit ourselves to the case $s \gg m_f^2$, where we have:

$$sC_0\left(-s; m_f, 0, m_f\right) \approx -\left(\frac{1}{\hat{\varepsilon}} + \ln\frac{m_f}{\mu^2}\right)\ln\frac{s}{m_f^2} - \frac{1}{2}\ln^2\frac{s}{m_f^2} + \frac{2}{3}\pi^2. \tag{A.2.32}$$

A.3. Building Blocks in the OMS Approach

In this Section we describe various *building blocks* used to construct the one-loop amplitudes of the processes $Z \to f\bar{f}$ and $e^+e^- \to f\bar{f}$ in terms of the A_0, B_0, C_0 and D_0 functions introduced in the previous Section. They are presented in the order of increasing complexity: self-energies, vertices, and boxes. The *on-mass-shell (OMS)* renormalization scheme is used in the unitary gauge [3,4].

A.3.1. Bosonic self-energies

Z, γ bosonic self-energies and Z–γ transition

In the unitary gauge there are only five diagrams which contribute to the *total* Z and γ bosonic self-energies and to the Z–γ transition. They are shown in Fig. A.1.

With S_{ZZ}, $S_{Z\gamma}$ and $S_{\gamma\gamma}$ standing for the sum of all diagrams, depicted by a grey circle in Fig. A.1, we define the three corresponding self-energy functions Σ:

$$S_{ZZ} = (2\pi)^4 i\frac{g^2}{16\pi^2 c_W^2}\Sigma_{ZZ}, \tag{A.3.1}$$

$$S_{Z\gamma} = (2\pi)^4 i\frac{g^2 s_W}{16\pi^2 c_W}\Sigma_{Z\gamma}, \tag{A.3.2}$$

$$S_{\gamma\gamma} = (2\pi)^4 i\frac{g^2 s_W^2}{16\pi^2}\Sigma_{\gamma\gamma}. \tag{A.3.3}$$

All **bosonic** self-energies and transitions may be naturally split into *bosonic* and *fermionic* components.

- Bosonic components of Z, γ self-energies and Z–γ transitions, diagrams Fig. A.1(2-5), are:

$$\begin{aligned}\Sigma^{\rm bos}_{ZZ}(s) &= M_W^2\Bigg\{c_W^4\left(-4-\frac{17}{3}\frac{1}{R_W}+\frac{4}{3}\frac{1}{R_W^2}+\frac{1}{12}\frac{1}{R_W^3}\right)B_0\left(-s;M_W,M_W\right)\\ &+\frac{1}{12}\left[\left(\frac{1}{c_W^4}-\frac{2}{c_W^2}r_W+{r_W}^2\right)R_W-\frac{10}{c_W^2}+2r_W-\frac{1}{R_W}\right]B_0\left(-s;M_H,M_Z\right)\\ &+c_W^2\left(-4+\frac{4}{3}\frac{1}{R_W}+\frac{1}{6}\frac{1}{R_W^2}\right)\frac{A_0\left(M_W\right)}{M_Z^2}\\ &+\frac{1}{12}\left(\frac{M_Z^2-M_H^2}{s}+1\right)\frac{\left[A_0\left(M_Z\right)-A_0\left(M_H\right)\right]}{M_Z^2}-\frac{1}{12}\frac{A_0\left(M_H\right)}{M_Z^2}\\ &-\left[\frac{1}{6c_W^2}+4c_W^4+\frac{1}{6}r_W-\left(\frac{1}{18}+\frac{4}{3}c_W^4\right)\frac{1}{R_W}+\frac{1}{9}c_W^4\left(5-\frac{1}{2}\frac{1}{R_W}\right)\frac{1}{R_W^2}\right]\Bigg\}, \qquad \text{(A.3.4)}\end{aligned}$$

$$\Sigma^{\rm bos}_{\gamma\gamma}(s) = -s\Pi^{\rm bos}_{\gamma\gamma}(s), \qquad \text{(A.3.5)}$$

$$\Sigma^{\rm bos}_{Z\gamma}(s) = -s\Pi^{\rm bos}_{Z\gamma}(s) = -c_W^2 s\Pi^{\rm bos}_{\gamma\gamma}(s). \qquad \text{(A.3.6)}$$

Here and below the following abbreviations are used:

$$c_W^2 = \frac{M_W^2}{M_Z^2}, \qquad \text{(A.3.7)}$$

$$s_W^2 = 1-c_W^2, \qquad \text{(A.3.8)}$$

$$r_W = \frac{M_H^2}{M_W^2}, \qquad \text{(A.3.9)}$$

$$r_Z = \frac{M_H^2}{M_Z^2}, \qquad \text{(A.3.10)}$$

$$R_W = \frac{M_W^2}{s}, \qquad \text{(A.3.11)}$$

$$R_Z = \frac{M_Z^2}{s}. \qquad \text{(A.3.12)}$$

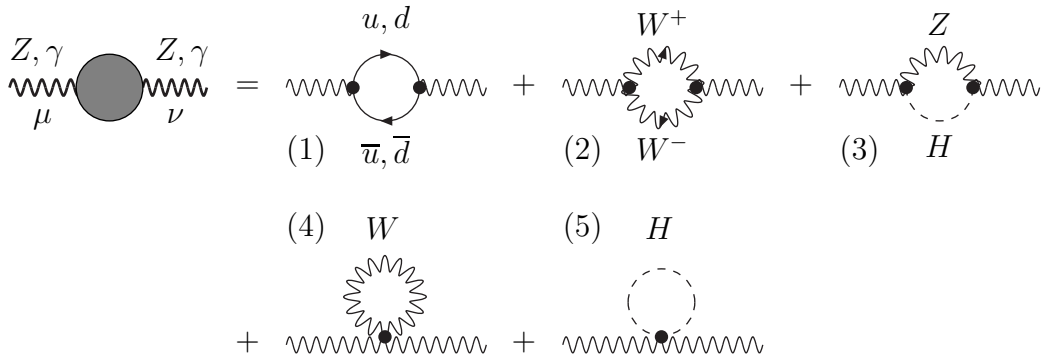

Figure A.1. *Photon and Z-boson self-energies and the Z–γ transition*

In the unitary gauge both $\Sigma^{\rm bos}_{\gamma\gamma}$ and $\Sigma^{\rm bos}_{Z\gamma}$ may be expressed in terms of one function,

$\Pi^{\rm bos}_{\gamma\gamma}$, the bosonic component of photonic vacuum polarization:

$$\begin{aligned}\Pi^{\rm bos}_{\gamma\gamma}(s) &= R_W\Bigg\{\left[4+\frac{17}{3}\frac{1}{R_W}-\frac{4}{3}\frac{1}{R_W^2}-\frac{1}{12}\frac{1}{R_W^3}\right]B_0\left(-s;M_W,M_W\right)\\ &\quad+\left(4-\frac{4}{3}\frac{1}{R_W}-\frac{1}{6}\frac{1}{R_W^2}\right)\left[\frac{A_0\left(M_W\right)}{M_W^2}+1\right]+\frac{1}{18}\frac{1}{R_W^2}\left(\frac{1}{R_W}-13\right)\Bigg\}. \qquad \text{(A.3.13)}\end{aligned}$$

Since only finite parts will contribute to resulting expressions for physical amplitudes which should be free from ultraviolet poles (after renormalization, or adding counter-terms, see below), it is convenient to split every divergent function into singular and finite parts:

$$\Pi^{\rm bos}_{\gamma\gamma}(s) = \left(-7+\frac{7}{6}\frac{1}{R_W}+\frac{1}{12}\frac{1}{R_W^2}\right)\left(\frac{1}{\bar{\varepsilon}}-\ln\frac{M_W^2}{\mu^2}\right)+\Pi^{{\rm bos},F}_{\gamma\gamma}(s), \qquad \text{(A.3.14)}$$

$$\Pi^{{\rm bos},F}_{\gamma\gamma}(s) = \left(4R_W+\frac{17}{3}-\frac{4}{3}\frac{1}{R_W}-\frac{1}{12}\frac{1}{R_W^2}\right)B_0^F\left(-s;M_W,M_W\right)+\frac{1}{18}\frac{1}{R_W}\left(\frac{1}{R_W}-13\right). \qquad \text{(A.3.15)}$$

With the Z boson self-energy, Σ_{ZZ}, one constructs a useful ratio:

$$\mathcal{D}_{Z}\left(s\right) = \frac{1}{c_W^2}\frac{\Sigma_{ZZ}\left(s\right)-\Sigma_{ZZ}\left(M_Z^2\right)}{M_Z^2-s}, \qquad \text{(A.3.16)}$$

which also has bosonic and fermionic parts, which in turn may be subdivided into pole and finite parts. The bosonic component is:

$$\begin{aligned}\mathcal{D}^{\rm bos}_{Z}\left(s\right) &= -\left[\frac{1}{6c_W^2}+\frac{7}{6}-7c_W^2+\left(\frac{1}{12c_W^2}+\frac{7}{6}\right)\frac{1}{R_Z}+\frac{1}{12c_W^2}\frac{1}{R_Z^2}\right]\left(\frac{1}{\bar{\varepsilon}}-\ln\frac{M_W^2}{\mu^2}\right)\\ &\quad+\mathcal{D}^{{\rm bos},F}_{Z}\left(s\right), \qquad \text{(A.3.17)}\\ \mathcal{D}^{{\rm bos},F}_{Z}\left(s\right) &= -\left[4c_W^4+\left(\frac{1}{12c_W^2}+\frac{4}{3}\right)\frac{1}{R_Z}+\frac{1}{12c_W^2}\frac{1}{R_Z^2}\right]B_0^F\left(-s;M_W,M_W\right)\\ &\quad+\left(\frac{1}{12c_W^2}+\frac{4}{3}-\frac{17}{3}c_W^2-4c_W^4\right)\\ &\quad\times\frac{sB_0^F\left(-s;M_W,M_W\right)-M_Z^2B_0^F\left(-M_Z^2;M_W,M_W\right)}{M_Z^2-s}\\ &\quad+\frac{1}{c_W^2}\left(1-\frac{1}{3}r_{Z}+\frac{1}{12}r_{Z}^2\right)\frac{M_Z^2\Big[B_0^F\left(-s;M_H,M_Z\right)-B_0^F\left(-M_Z^2;M_H,M_Z\right)\Big]}{M_Z^2-s}\\ &\quad-\frac{1}{12c_W^2}\left(1-r_{Z}\right)^2R_Z\Big[-B_0^F\left(-s;M_H,M_Z\right)+\ln c_W^2+1\Big]\\ &\quad-\frac{1}{12c_W^2}\left[B_0^F\left(-s;M_H,M_Z\right)-r_{Z}\left(1+r_{Z}\right)\frac{1}{R_Z}\ln r_{Z}\right]\\ &\quad-\frac{1}{18}\left[\frac{1}{c_W^2}+\left(\frac{1}{c_W^2}-13\right)\left(1+\frac{1}{R_Z}\right)+\frac{1}{c_W^2}\frac{1}{R_Z^2}\right]. \qquad \text{(A.3.18)}\end{aligned}$$

- Fermionic components of the Z and γ bosonic self-energies and of the Z–γ transition.

The fermionic components are represented as sums over all fermions of the theory, $\sum_f$. They, of course, depend on vector and axial couplings of fermions to the Z boson and photon, v_f, and a_f, and Q_f, correspondingly, and color factor c_f and fermion mass m_f. The couplings defined here deviate from Eq. (1.1.12) to Eq. (1.1.14):

$$v_f = I_f^{(3)} - 2Q_f s_W^2, \tag{A.3.19}$$

$$a_f = I_f^{(3)}, \tag{A.3.20}$$

with weak isospin $I_f^{(3)}$, and

$$Q_f = -1 \quad \text{for leptons,} \quad +\frac{2}{3} \quad \text{for up-,} \quad -\frac{1}{3} \quad \text{for down-quarks,} \tag{A.3.21}$$

$$c_f = 1 \quad \text{for leptons,} \quad 3 \quad \text{for quarks.} \tag{A.3.22}$$

The three main self-energy functions are

$$\Sigma_{ZZ}^{\text{fer}}(s) = \sum_f c_f \left[-\left(v_f^2 + a_f^2\right) s B_f\left(-s; m_f, m_f\right) - 2a_f^2 m_f^2 B_0\left(-s; m_f, m_f\right) \right], \tag{A.3.23}$$

$$\Sigma_{\gamma\gamma}^{\text{fer}}(s) = -s\Pi_{\gamma\gamma}^{\text{fer}}(s), \tag{A.3.24}$$

$$\Sigma_{Z\gamma}^{\text{fer}}(s) = -s\Pi_{Z\gamma}^{\text{fer}}(s). \tag{A.3.25}$$

However, $\Pi_{\gamma\gamma}^{\text{fer}}$ and $\Pi_{Z\gamma}^{\text{fer}}$ are now different owing to different couplings, but still proportional to one function B_f:

$$\Pi_{\gamma\gamma}^{\text{fer}}(s) = 4\sum_f c_f Q_f^2 B_f\left(-s; m_f, m_f\right), \tag{A.3.26}$$

$$\Pi_{Z\gamma}^{\text{fer}}(s) = \sum_f c_f \left(|Q_f| - 4s_W^2 Q_f^2\right) B_f\left(-s; m_f, m_f\right). \tag{A.3.27}$$

As usual, we split them into singular and finite parts:

$$\Pi_{Z\gamma}^{\text{fer}}(s) = -\frac{1}{3}\left(\frac{1}{2}N_f - 4s_W^2 \sum_f c_f Q_f^2\right)\left(\frac{1}{\bar{\varepsilon}} - \ln\frac{M_W^2}{\mu^2}\right) + \Pi_{Z\gamma}^{\text{fer},F}(s), \tag{A.3.28}$$

$$\Sigma_{ZZ}^{\text{fer}}(s) = \left[-\frac{1}{2}\sum_f c_f m_f^2 + \frac{s}{3}\left(\frac{1}{2}N_f - s_W^2 N_f + 4s_W^4 \sum_f c_f Q_f^2\right)\right]\left(\frac{1}{\bar{\varepsilon}} - \ln\frac{M_W^2}{\mu^2}\right) + \Sigma_{ZZ}^{\text{fer},F}(s).$$

In Eq. (A.3.28), $N_f = 24$ is the total number of fermions in the SM. We do not show explicit expressions for finite parts, marked with superscript F because these might be trivially derived from Eqs. (A.3.25)–(A.3.27) by replacing complete expressions for B_f and B_0 with their finite parts B_f^F and B_0^F, correspondingly.

W boson self-energy

Now we consider the W boson self-energy which in the unitary gauge is described by seven diagrams, shown if Fig. A.2.

Firstly, we present an explicit expression for its bosonic component:

$$\begin{aligned}
\Sigma^{\rm bos}_{WW}(s) &= M_W^2\Bigg\{\Bigg[\left(\frac{1}{12c_W^4}+\frac{2}{3}\frac{1}{c_W^2}-\frac{3}{2}+\frac{2}{3}c_W^2+\frac{1}{12}c_W^4\right)R_W \\
&+\frac{2}{3}\left(\frac{1}{c_W^2}-4-4c_W^2+c_W^4\right)-\left(\frac{3}{2}+\frac{8}{3}c_W^2+\frac{3}{2}c_W^4\right)\frac{1}{R_W} \\
&+\frac{2}{3}c_W^2\left(1+c_W^2\right)\frac{1}{R_W^2}+\frac{1}{12}c_W^4\frac{1}{R_W^3}\Bigg]B_0\left(-s;M_Z,M_W\right) \\
&-\frac{s_W^2}{6}\left(-5R_W+17+17\frac{1}{R_W}-5\frac{1}{R_W^2}\right)B_0\left(-s;0,M_W\right) \\
&-\frac{1}{12}\left[-\left(1-r_W\right)^2R_W-10+2r_W-\frac{1}{R_W}\right]B_0\left(-s;M_H,M_W\right) \\
&-\frac{1}{12}\Bigg\{\left(\frac{1}{c_W^2}-2+c_W^2-c_W^4-\frac{1}{R_W}\right)R_W-24+2c_W^2-c_W^4 \\
&+\left[10-\frac{c_W^2}{R_W}\left(1+c_W^2-\frac{c_W^2}{R_W}\right)\right]\frac{A_0\left(M_W\right)}{M_W^2} \\
&+\Bigg[\left(\frac{1}{c_W^2}+9-9c_W^2-c_W^4\right)R_W+1+14c_W^2+9c_W^4 \\
&+c_W^2R_W\left[\left(1-9c_W^2\right)-c_W^2R_W\right]\Bigg]\frac{A_0\left(M_Z\right)}{M_W^2}-\left(R_W+\frac{1}{r_W}+2\right)\frac{A_0\left(M_H\right)}{M_W^2}\Bigg\} \\
&-\frac{1}{6}\left(\frac{1}{c_W^2}+22+c_W^2+c_W^4+r_W\right)+\frac{1}{9}\Bigg[\left(6+3c_W^2+\frac{7}{2}c_W^4\right)R_W \\
&+\left(1+\frac{3}{2}c_W^2+\frac{5}{2}c_W^4\right)-\frac{c_W^4}{2}\frac{1}{R_W^3}\Bigg]\Bigg\}. \qquad \text{(A.3.29)}
\end{aligned}$$

Secondly, we give its fermionic component:

$$\Sigma^{\rm fer}_{WW}(s) = -s\sum_{f=d}c_fB_f\left(-s;m_{f'},m_f\right)+\sum_{f=d}c_fm_f^2B_1\left(-s;m_{f'},m_f\right), \qquad \text{(A.3.30)}$$

where summation extends on all *doublets* of the SM.

Bosonic self-energies and counter-terms

Bosonic self-energies and transitions enter one-loop amplitudes either directly via functions $\mathcal{D}_{_Z}(s)$, Eq. (A.3.16), or by means of bosonic counter-terms, which are made of self-energy functions at zero argument, owing to *electric charge renormalization* or at $p^2=-M^2$; that is, on-a-mass-shell, owing to *on-mass-shell renormalization*, (OMS scheme).

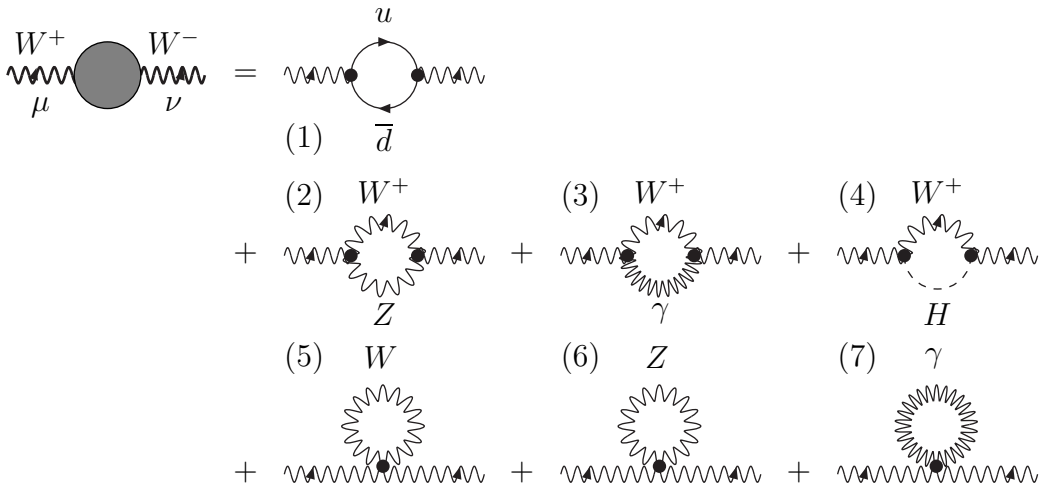

Figure A.2. *The W-boson self-energy*

- Electric charge renormalization.

The electric charge renormalization introduces the quantity $\Pi_{\gamma\gamma}(0)$ with bosonic and fermionic components:

$$\begin{aligned}
(z_\gamma - 1) &= \Pi_{\gamma\gamma}(0), \\
\Pi^{\rm bos}_{\gamma\gamma}(0) &= 7\left(\frac{1}{\bar{\varepsilon}} - \ln\frac{M_W^2}{\mu^2}\right) + \frac{2}{3}, \\
\Pi^{\rm fer}_{\gamma\gamma}(0) &= -\frac{4}{3}\sum_f c_f Q_f^2 \left(\frac{1}{\bar{\varepsilon}} - \ln\frac{M_W^2}{\mu^2}\right) + \Pi^{\rm fer,F}_{\gamma\gamma}(0). \qquad \text{(A.3.31)}
\end{aligned}$$

- Z boson wave-function renormalization.

In the treatment of Z decay one deals with the renormalization of an external Z boson line, which involves the on-shell derivative:

$$\begin{aligned}
(z_Z - 1) &= \frac{1}{c_W^2}\frac{\partial\,\Sigma_{ZZ}(p^2)}{\partial\,p^2}\bigg|_{p^2=-M_Z^2} \qquad \text{(A.3.32)} \\
&\equiv \frac{1}{c_W^2}\Sigma'_{ZZ}(M_Z^2), \qquad \text{(A.3.33)}
\end{aligned}$$

The bosonic components are:

$$\begin{aligned}
\frac{1}{c_W^2}\Big[\Sigma'_{ZZ}(M_Z^2)\Big]^{\rm bos} &= \left[-\frac{1}{3c_W^2} - \frac{7}{3} + 7c_W^2\right]\left(\frac{1}{\bar{\varepsilon}} - \ln\frac{M_W^2}{\mu^2}\right) + \frac{1}{c_W^2}\Big[\Sigma'_{ZZ}(M_Z^2)\Big]^{\rm bos,F}, \qquad \text{(A.3.34)} \\
\frac{1}{c_W^2}\Big[\Sigma'_{ZZ}(M_Z^2)\Big]^{\rm bos,F} &= -\left(\frac{1}{4c_W^2} + \frac{8}{3} - \frac{17}{3}c_W^2\right) B_0^F\left(-M_Z^2; M_W, M_W\right)
\end{aligned}$$

$$
\begin{aligned}
&-\left(\frac{1}{12c_W^2}+\frac{4}{3c_W^2}-\frac{17}{3}-4c_W^2\right)M_W^2 B_{0p}^F\left(-M_Z^2;M_W,M_W\right)\\
&-\frac{1}{6}r_W\left(1-\frac{1}{2}r_Z\right)B_0^F\left(-M_Z^2;M_H,M_H\right)\\
&-\left(1-\frac{1}{3}r_Z+\frac{1}{12}r_Z^2\right)\frac{M_Z^2}{c_W^2}B_{0p}^F\left(-M_Z^2;M_H,M_H\right)\\
&-\frac{1-r_Z}{12c_W^2}\left(\ln c_W^2+r_Z\ln r_W\right)\\
&-\frac{11}{36c_W^2}+\frac{13}{9}+\frac{1}{6}r_W\left(1-\frac{1}{2}r_Z\right). \qquad \text{(A.3.35)}
\end{aligned}
$$

The fermionic components are:

$$
\begin{aligned}
\frac{1}{c_W^2}\left[\Sigma'_{ZZ}(M_Z^2)\right]^{\rm fer} &= \left[\frac{1}{6}\left(\frac{1}{c_W^2}-2\right)N_f-\frac{4}{3}\frac{s_W^4}{c_W^2}\sum_f c_f Q_f^2\right]\left(\frac{1}{\bar\varepsilon}-\ln\frac{M_W^2}{\mu^2}\right)\\
&\quad+\frac{1}{c_W^2}\left[\Sigma'_{ZZ}(M_Z^2)\right]^{\rm fer,F}, \qquad \text{(A.3.36)}\\
\frac{1}{c_W^2}\left[\Sigma'_{ZZ}(M_Z^2)\right]^{\rm fer,F} &= \frac{1}{3c_W^2}\sum_f c_f\left(v_f^2+a_f^2\right)\left[\ln\frac{m_f^2}{M_W^2}+2\frac{m_f^2}{M_Z^2}-\frac{2}{3}\right.\\
&\quad\left.+\left(1-2\frac{m_f^2}{M_Z^2}+4\frac{m_f^4}{M_Z^4}\right)\frac{1}{\beta}\ln\frac{1+\beta}{1-\beta}\right]\\
&\quad-\frac{1}{2}\sum_f c_f\frac{m_f^2}{M_W^2}\left(1+2\frac{m_f^2}{M_Z^2}\frac{1}{\beta}\ln\frac{1+\beta}{1-\beta}\right). \qquad \text{(A.3.37)}
\end{aligned}
$$

- Renormalization constant due to Z–γ mixing:

$$
\frac{1}{M_Z^2}\Sigma_{Z\gamma}(M_Z^2)=\frac{1}{M_Z^2}\Sigma_{Z\gamma}^{\rm bos}(M_Z^2)+\frac{1}{M_Z^2}\Sigma_{Z\gamma}^{\rm fer}(M_Z^2). \qquad \text{(A.3.38)}
$$

Its bosonic and fermionic components are

$$
\begin{aligned}
\frac{1}{M_Z^2}\Sigma_{Z\gamma}^{\rm bos}(M_Z^2) &= \left(\frac{1}{12c_W^2}+\frac{7}{6}-7c_W^2\right)\left(\frac{1}{\bar\varepsilon}-\ln\frac{M_W^2}{\mu^2}\right)-\Pi_{Z\gamma}^{\rm bos,F}(M_Z^2), \qquad \text{(A.3.39)}\\
\frac{1}{M_Z^2}\Sigma_{Z\gamma}^{\rm fer}(M_Z^2) &= -\frac{1}{2}\left(\frac{8}{3}s_W^2\sum_f c_f Q_f^2-\frac{1}{3}N_f\right)\left(\frac{1}{\bar\varepsilon}-\ln\frac{M_W^2}{\mu^2}\right)-\Pi_{Z\gamma}^{\rm fer,F}(M_Z^2). \qquad \text{(A.3.40)}
\end{aligned}
$$

- ρ-parameter.

Finally, two self-energy functions enter Veltman's parameter $\Delta\rho$, a gauge-invariant combination of self-energies, which naturally appears in one-loop calculations:

$$
\Delta\rho = \frac{1}{M_W^2}\left[\Sigma_{WW}(M_W^2)-\Sigma_{ZZ}(M_Z^2)\right], \qquad \text{(A.3.41)}
$$

with individual components where we explicitly show the pole parts:

$$\Delta\rho^{\rm bos} = \left(-\frac{1}{6c_W^2}-\frac{41}{6}+7c_W^2\right)\left(\frac{1}{\bar{\varepsilon}}-\ln\frac{M_W^2}{\mu^2}\right)+\Delta\rho^{{\rm bos},F}, \quad \text{(A.3.42)}$$

$$\Delta\rho^{\rm fer} = \left[\frac{1}{6}N_f-\frac{1}{6}\left(2-\frac{1}{c_W^2}\right)N_f-\frac{4}{3}\frac{s_W^2}{c_W^2}\sum_f c_f Q_f^2\right]\left(\frac{1}{\bar{\varepsilon}}-\ln\frac{M_W^2}{\mu^2}\right)+\Delta\rho^{{\rm fer},F}. \quad \text{(A.3.43)}$$

The finite parts are not shown since they are trivially derived from the defining equation Eq. (2.3.7) replacing the total self-energies with their finite parts. Having all building blocks made of bosonic self-energies at our disposal, we continue with **fermionic** self-energy diagrams.

A.3.2. Fermionic self-energies

Fermionic self-energy diagrams

In the unitary gauge there are only four diagrams contributing to the total self-energy function of a fermion, see Fig. A.3.

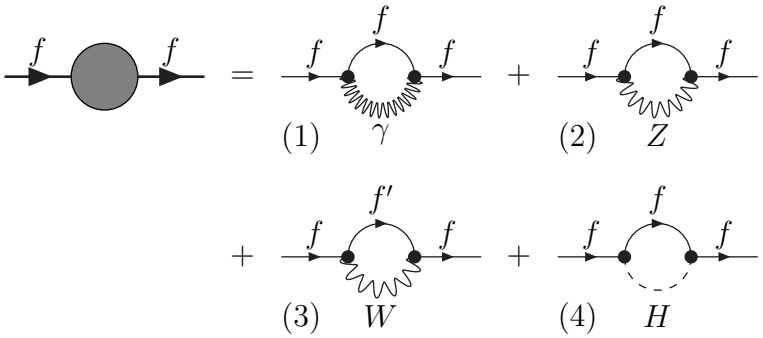

Figure A.3. *Fermion self-energies*

In Fig. A.3 and in what follows, f' denotes the weak isospin partner of fermion f.

Each self-energy diagram contains a B-boson line and will be denoted as $\Sigma_{B}(\not{p})$,

$$\Sigma_{B}(\not{p}) = (2\pi)^4\, i\frac{g^2}{16\,\pi^2}A_{B}, \quad \text{(A.3.44)}$$

with

$$\not{p} = p_\alpha\gamma_\alpha. \quad \text{(A.3.45)}$$

The first three A_{B}-functions in the unitary gauge read

$$A_\gamma(-s;m_f,0) = s_W^2\,Q_f^2\left\{i\not{p}\left[2B_1(-s;m_f,0)+1\right]-2m_f^2\left[2B_0(-s;m_f,0)-1\right]\right\}, \quad \text{(A.3.46)}$$

$$A_Z(-s;M_Z,m_f) = -\frac{1}{4c_W^2}\left\{i\not{p}\left(\sigma_f^{(2)}+2v_f a_f\gamma_5\right)\right.$$

$$\times\left[\frac{-s+m_f^2}{M_Z^2}B_1\left(-s;M_Z,m_f\right)+A\left(-s;M_Z,m_f\right)\right]$$
$$+m_f^2\delta_f^{(2)}\left[3B_0\left(-s;M_Z,m_f\right)+\frac{A_0\left(m_f\right)}{M_Z^2}-2\right]\Bigg\}, \qquad \text{(A.3.47)}$$

$$A_{_W}\left(-s;M_W,m_f\right) = -\frac{1}{4}i\not{p}\left(1+\gamma_5\right)\left\{\frac{-s+m_{f'}^2}{M_W^2}B_1\left(-s;M_W,m_f\right)+A\left(-s;M_W,m_f\right)\right\},$$

while the fourth function, $A_{_H}$, vanishes when masses of external fermions are ignored[1]

In Eq. (A.3.46) one uses an auxiliary function

$$A\left(-s;M,m\right)=2B_1\left(-s;M,m\right)+B_0\left(-s;M,m\right)+\frac{A_0\left(m\right)}{M^2}-1, \qquad \text{(A.3.48)}$$

and new short hand notations

$$\sigma_f^{(2)} = v_f^2+a_f^2, \qquad \text{(A.3.49)}$$
$$\delta_f^{(2)} = v_f^2-a_f^2. \qquad \text{(A.3.50)}$$

Fermionic renormalization constants

As can be seen from the previous subsection, in the Standard Model the contribution of any fermionic self-energy diagram with a virtual boson B, Fig. A.4(a), can be parameterized with three coefficients $a_1,\ a_3$ and a_4 (a_2 in the term $a_2\gamma_5$ is always equal to zero in the SM):

Figure A.4. *Generic self-energy (a) and counter-term (b) diagrams*

$$\Sigma_f\left(i\not{p}\right)=\left(2\pi\right)^4 i\Big[a_1+a_3i\not{p}+a_4i\not{p}\gamma_5\Big]. \qquad \text{(A.3.51)}$$

Kinetic and mass terms of a counter-term Lagrangian may be depicted as shown in Fig. A.4(b).

From the requirement that the sum of pairs of these diagrams vanishes on the fermion mass shell (a basic renormalization requirement of the OMS-scheme), one may fix all relevant counter-terms (mass and field renormalization constants) in the fermionic sector of the SM. In particular, we derive the following relations for the two renormalization constants that we need:

$$\left|\sqrt{z_{_L}}\right|^2-I = a_3-2m^2a_3^{'}+2ma_1^{'}+a_4, \qquad \text{(A.3.52)}$$
$$\left|\sqrt{z_{_R}}\right|^2-I = a_3-2m^2a_3^{'}-a_4, \qquad \text{(A.3.53)}$$

[1]Beware of two different definitions of v_f and a_f used in this description. We use here the definitions Eq. (2.4.14).

with derivatives

$$a_i^{'} = \partial a_i/\partial p^2|_{p^2=-m^2}. \tag{A.3.54}$$

Calculating derivatives straightforwardly and substituting the a_i's, one obtains explicit expressions for $\sqrt{z_{L,R}}$. It is convenient to distinguish the electromagnetic components,

$$\left(\sqrt{z_{\scriptscriptstyle L}} - I\right)_f^{em} = \left(\sqrt{z_{\scriptscriptstyle R}} - I\right)_f^{em} = s_{\scriptscriptstyle W}^2 Q_f^2 \left(-\frac{1}{2\bar{\varepsilon}} + \frac{1}{\hat{\varepsilon}} + \frac{3}{2}\ln\frac{m_f^2}{\mu^2} - 2\right), \tag{A.3.55}$$

and weak components,

$$\left|\sqrt{z_{\scriptscriptstyle R}}\right|^2 - I = \frac{3}{8}\frac{1}{c_{\scriptscriptstyle W}^2}\delta_f^2, \tag{A.3.56}$$

$$\left|\sqrt{z_{\scriptscriptstyle L}}\right|^2 - I = \frac{3}{4}r_t\left(\frac{1}{\bar{\varepsilon}} - \ln\frac{M_{\scriptscriptstyle W}^2}{\mu^2}\right) + \frac{3}{8c_{\scriptscriptstyle W}^2}\sigma_f^2 + \frac{1}{2}w_{\scriptscriptstyle W}^F, \tag{A.3.57}$$

where we introduced the short hand notation:

$$r_t = \frac{m_t^2}{M_{\scriptscriptstyle W}^2}, \tag{A.3.58}$$

and $w_{\scriptscriptstyle W}^F$ is a finite part:

$$w_{\scriptscriptstyle W}^F = \frac{5}{4}r_t + 3\left(1 - \frac{1}{2}r_t\right)\frac{1}{(1-1/r_t)^2}\ln r_t - \frac{3}{2}\frac{1}{r_t - 1}. \tag{A.3.59}$$

In Eq. (A.3.55) for the first time there appeared an infrared pole, $1/\hat{\varepsilon}$, which is explicitly distinguished from the ultraviolet pole, $1/\bar{\varepsilon}$; the infrared pole originates from a derivative. In the dimensional regularization scheme one may identify

$$\frac{1}{\hat{\varepsilon}} = -\frac{1}{\bar{\varepsilon}}. \tag{A.3.60}$$

However, it is reasonable to distinguish them since the poles cancel separately.

A.3.3. The $Zf\bar{f}$ and $\gamma f\bar{f}$ vertices

The *total* $\gamma(Z)f\bar{f}$ vertex depicted by a grey circle in Fig. A.5 consists of seven individual vertices, see Fig. A.5.

Diagrams Fig. A.5(5)-(7) do not contribute for massless external fermions. For the sum of all vertices in the unitary gauge and for $\gamma \to f\bar{f}$ and $Z \to f\bar{f}$ transitions, we use the standard normalization

$$i\pi^2 = (2\pi)^4 i\frac{1}{16\pi^2}, \tag{A.3.61}$$

and define

$$V_\mu^\gamma(s) = (2\pi)^4 i\frac{1}{16\pi^2}G_\mu(s), \tag{A.3.62}$$

$$V_\mu^Z(s) = (2\pi)^4 i\frac{1}{16\pi^2}Z_\mu(s), \tag{A.3.63}$$

while the individual vertices Fig. A.5(1-4) we denote as follows

$$G_\mu(s) = G_\mu^{\rm QED}(s) + G_\mu^Z(s) + G_\mu^{Wa}(s) + G_\mu^{Wn}(s), \quad (A.3.64)$$
$$Z_\mu(s) = Z_\mu^{\rm QED}(s) + Z_\mu^Z(s) + Z_\mu^{Wa}(s) + Z_\mu^{Wn}(s). \quad (A.3.65)$$

All vertices in the unitary gauge have the following structures:

$$G_\mu^{\rm QED}(s) = ig^3 Q_f^3 s_W^3 \gamma_\mu F_\gamma(s), \quad (A.3.66)$$
$$G_\mu^Z(s) = ig^3 Q_f \frac{s_W}{4c_W^2}\gamma_\mu\Big[\delta_f^2 + 2v_f a_f(1+\gamma_5)\Big]F_Z(s), \quad (A.3.67)$$
$$G_\mu^{Wa}(s) = ig^3 Q_{f'}\frac{s_W}{4}\gamma_\mu(1+\gamma_5)F_{Wa}(s), \quad (A.3.68)$$
$$G_\mu^{Wn}(s) = ig^3\frac{s_W}{2}\left(-I_f^{(3)}\right)\gamma_\mu(1+\gamma_5)F_{Wn}(s), \quad (A.3.69)$$
$$Z_\mu^{\rm QED}(s) = ig^3 Q_f^2\frac{s_W^2}{2c_W}\gamma_\mu\Big[\delta_f + a_f(1+\gamma_5)\Big]F_\gamma(s), \quad (A.3.70)$$
$$Z_\mu^Z(s) = ig^3\frac{1}{8c_W^3}\gamma_\mu\Big[\delta_f^3 + \left(3v_f^2 + a_f^2\right)a_f(1+\gamma_5)\Big]F_Z(s), \quad (A.3.71)$$
$$Z_\mu^{Wa}(s) = ig^3\frac{1}{4c_W}\gamma_\mu(1+\gamma_5)\left[\frac{\sigma_{f'}}{2}F_{Wa}(s) + a_{f'}\bar{F}_{Wa}(s)\right], \quad (A.3.72)$$
$$Z_\mu^{Wn}(s) = ig^3\frac{c_W}{2}\left(-I_f^{(3)}\right)\gamma_\mu(1+\gamma_5)F_{Wn}(s), \quad (A.3.73)$$

with the scalar form factors presented in the next subsection. We recall that f' stands for the isospin partner of a fermion f, moreover:

$$\delta_f = v_f - a_f = -2Q_f s_W^2, \quad (A.3.74)$$
$$\sigma_f = v_f + a_f. \quad (A.3.75)$$

Scalar form factors for the $\gamma f\bar{f}$ and $Zf\bar{f}$ vertices

In QED diagrams, Eqs. (A.3.66) and (A.3.70), a common QED scalar form factor enters

$$F_\gamma(s) = -2\left(-s+2m_f^2\right)C_0(-s;m_f,0,m_f) + B_0(-s;m_f,m_f) - 4B_{ff}(-s;m_f,m_f) - 2, \quad (A.3.76)$$

with a subtracted B-function,

$$B_{ff}(-s;m_f,m_f) = B_0(-s;m_f,m_f) - B_0\left(-m_f^2;m_f,0\right). \quad (A.3.77)$$

The $C_0(-s;m_f,0,m_f)$ function contains an infrared divergence (IRD), see Eqs. (A.2.31)–(A.2.32). Every scalar form factor is presented as a sum of its pole and finite parts:

$$F_\gamma(s) = \left(\frac{1}{\bar{\varepsilon}} - \ln\frac{M_W^2}{\mu^2}\right) + F_\gamma^F(s), \quad (A.3.78)$$
$$F_\gamma^F(s) = -4\ln\frac{m_f^2}{M_W^2} - 3\ln R_W + 2sC_0(-s;m_f,0,m_f). \quad (A.3.79)$$

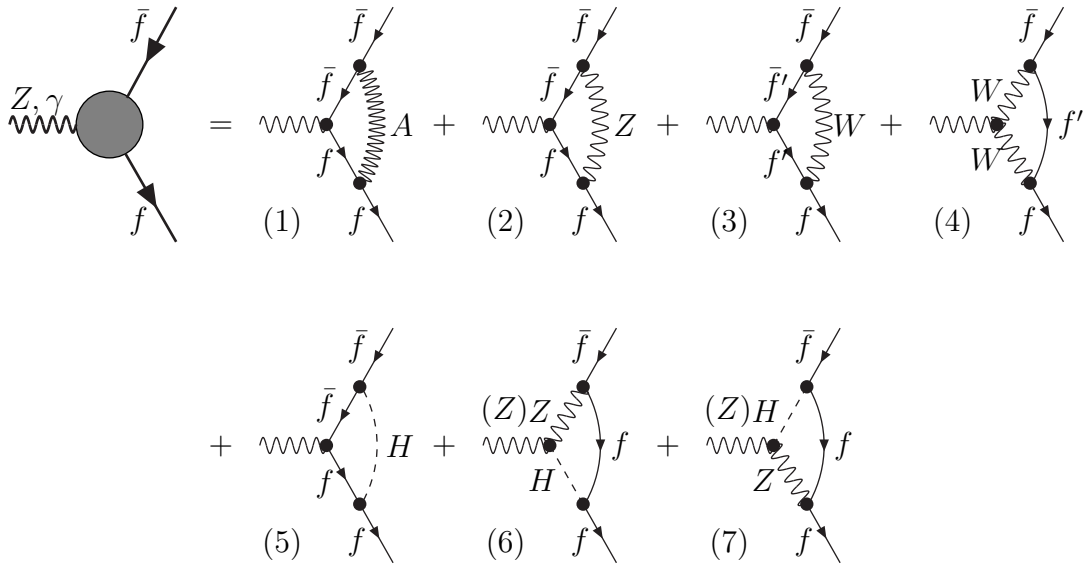

Figure A.5. *The $Zf\bar{f}$ and $\gamma f\bar{f}$ vertices. The symbol (Z) in some graphs indicates that they contribute only to the Z vertex*

The diagrams with the virtual Z boson, Eqs. (A.3.67) and (A.3.71), are described by another common scalar form factor:

$$F_{_Z}(s) \;=\; 2s(1+R_{_Z})^2 C_0(-s;0,M_{_Z},0) + (2R_{_Z}-3)\,\Delta B(-s;0,M_{_Z}) - 2, \tag{A.3.80}$$

with $\Delta B(-s;0,M_{_Z})$ defined in Eq. (A.2.20). Here we have no ultraviolet pole term since the poles from the two B-functions in ΔB cancel, and for the finite part we use a notation omitting the superscript F:

$$F_{_Z}(s) \;=\; -5 + (2R_{_Z}-3)\ln R_{_Z} + 2R_{_Z} + 2s\,(1+R_{_Z})^2\, C_0(-s;0,M_{_Z},0)\,. \tag{A.3.81}$$

Next, one has *abelian* diagrams with virtual W bosons, Eqs. (A.3.68) and (A.3.72). Again, there is a common scalar function:

$$\begin{aligned} F_{_{Wa}}(s) \;=\;& \left[(2+r_t)(1-r_t)^2 R_{_W} + (2-r_t)^2 + \frac{2}{R_{_W}}\right] M_{_W}^2 C_0(-s;m_t,M_{_W},m_t) \\ & - \frac{1}{2} r_t B_0(-s;m_t,m_t) - \Big[(2+r_t)(1-r_t)R_{_W} - 3 + r_t\Big]\Delta B(-s;m_t,M_{_W}) \\ & + \frac{A_0(m_t)}{M_{_W}^2} - \frac{1}{2} r_t - 2, \end{aligned} \tag{A.3.82}$$

which is subdivided into pole and finite parts:

$$F_{_{Wa}}(s) \;=\; -\frac{3}{2} r_t \left(\frac{1}{\bar{\varepsilon}} - \ln\frac{M_{_W}^2}{\mu^2}\right) + F^F_{_{Wa}}(s)\,, \tag{A.3.83}$$

$$F^F_{_{Wa}}(s) \;=\; \left[(2+r_t)(1-r_t)^2 R_{_W} + (2-r_t)^2 + \frac{2}{R_{_W}}\right] M_{_W}^2 C_0(-s;m_t,M_{_W},m_t)$$

$$+\left[3-\frac{1}{2}r_t+\left(2-r_t-r_t^2\right)R_W\right]B_0^F\left(-s;m_t,m_t\right) \tag{A.3.84}$$
$$+\left[\left(r_t+2\right)r_tR_W+\left(2+\frac{2}{r_t-1}\right)r_t-2\right]\ln r_t+1-\frac{5}{2}r_t-\left(r_t^2+r_t-2\right)R_W.$$

However, the abelian diagram, Fig. A.5(3), with incoming Z boson line, Eq. (A.3.72), has an additional contribution:

$$\begin{aligned}\bar{F}_{Wa}\left(s\right) &= r_t\Big\{\left[-(1-r_t)^2R_W-2\right]M_W^2C_0\left(-s;m_t,M_W,m_t\right)\\ &\quad-\frac{1}{2}B_0\left(-s;m_t,m_t\right)+(1-r_t)R_W\Delta B\left(-s;m_t,M_W\right)+\frac{1}{2}\Big\}.\end{aligned} \tag{A.3.85}$$

Its pole and finite parts of which vanish in the massless approximation, $r_t\to 0$:

$$\bar{F}_{Wa}\left(s\right) = -\frac{1}{2}r_t\left(\frac{1}{\bar{\varepsilon}}-\ln\frac{M_W^2}{\mu^2}\right)+\bar{F}_{Wa}^F\left(s\right), \tag{A.3.86}$$

$$\begin{aligned}\bar{F}_{Wa}^F\left(s\right) &= r_t\Big\{-\left[\left(1-r_t\right)^2R_W+2\right]M_W^2C_0\left(-s;m_t,M_W,m_t\right)\\ &\quad+\left[\left(r_t-1\right)R_W+\frac{1}{2}\right)B_0^F\left(-s;m_t,m_t\right)-\left[r_t\left(\ln r_t-1\right)+1\right]R_W+\frac{1}{2}\Big\}.\end{aligned} \tag{A.3.87}$$

Finally, there is a common scalar function entering Eqs. (A.3.68) and (A.3.73), which corresponds to a *non-abelian* diagram with two virtual W bosons, Fig. A.5(4):

$$\begin{aligned}F_{Wn}\left(s\right) &= \Big[(2+r_t)(1-r_t)^2R_W+4-\frac{5}{2}r_t+2r_t^2-\frac{1}{2}r_t^3\\ &\quad+r_t\left(2-\frac{1}{2}r_t\right)\frac{1}{R_W}\Big]M_W^2C_0\left(-s;M_W,m_t,M_W\right)\\ &\quad-\left[\frac{2}{3}-\frac{1}{2}r_t+\left(\frac{3}{2}-\frac{1}{4}r_t\right)\frac{1}{R_W}+\frac{1}{12R_W^2}\right]B_0\left(-s;M_W,M_W\right)\\ &\quad+\left[(2+r_t)(1-r_t)R_W+3-\frac{3}{2}r_t+\frac{1}{2}r_t^2\right]\Delta B\left(-s;M_W,m_t\right)\\ &\quad-\frac{1}{3}\left(2-\frac{1}{2R_W}\right)\frac{A_0\left(M_W\right)}{M_W^2}-\frac{A_0\left(m_t\right)}{M_W^2}\\ &\quad-\frac{2}{3}-\frac{1}{2}r_t+\left(\frac{4}{9}+\frac{1}{4}r_t\right)\frac{1}{R_W}-\frac{1}{18R_W^2}\\ &= \left[\frac{3}{2}r_t+\left(\frac{4}{3}-\frac{1}{4}r_t\right)\frac{1}{R_W}+\frac{1}{12}\frac{1}{R_W^2}\right]\left(\frac{1}{\bar{\varepsilon}}-\ln\frac{M_W^2}{\mu^2}\right)+F_{Wn}^F\left(s\right),\end{aligned} \tag{A.3.88}$$

with

$$\begin{aligned}F_{Wn}^F\left(s\right) &= \Big[(2+r_t)(1-r_t)^2R_W+4-\frac{5}{2}r_t+2r_t^2-\frac{1}{2}r_t^3+r_t\left(2-\frac{1}{2}r_t\right)\frac{1}{R_W}\Big]M_W^2\\ &\quad\times C_0\left(-s;M_W,m_t,M_W\right)\end{aligned}$$

$$
\begin{aligned}
&- \left[\left(2 - r_t - r_t^2\right) R_W + \frac{7}{3} - r_t\left(1 + \frac{r_t}{2}\right) - \left(\frac{3}{2} - \frac{r_t}{4}\right)\frac{1}{R_W} - \frac{1}{12}\frac{1}{R_W^2}\right] \\
&\times B_0^F\left(-s; M_W, M_W\right) \\
&- \left[\left(2 + r_t\right) R_W + 2 - \frac{2}{r_t - 1} + \frac{1}{2} r_t\right] r_t \ln r_t \\
&+ r_t R_W - 3 + 2 r_t - \frac{1}{2} r_t^2 + \left(\frac{11}{18} + \frac{r_t}{4}\right)\frac{1}{R_W} - \frac{1}{18}\frac{1}{R_W^2}\,. \qquad \text{(A.3.89)}
\end{aligned}
$$

Construction of $F^V_{\gamma(Z)Q}(s)$ and $F^V_{\gamma(Z)L}(s)$: vertices and counter-terms

Having in mind applications to Z resonance physics, in particular calculations of one-loop EWRC for the Z decay, it is useful to construct off-shell vertices: the sum of all vertex diagrams, Fig. A.5, and fermionic counter-terms, Eqs. (A.3.55) and (A.3.57). We will denote this sum by a black circle, see Fig. A.6.

The corresponding vertex functions may be parameterized by four scalar form factors $F_{\gamma(Z)L}(s)$ and $F_{\gamma(Z)Q}(s)$:

$$
\begin{aligned}
V_\mu^{\gamma f\bar f}(s) &= (2\pi)^4\, i\frac{ig^3 s_W}{16\pi^2}\gamma_\mu\left[\frac{1}{2} I_f^{(3)} F_{\gamma L}(s)\left(1+\gamma_5\right) + Q_f F_{\gamma Q}(s)\right], \qquad \text{(A.3.90)} \\
V_\mu^{Zf\bar f}(s) &= (2\pi)^4\, i\frac{ig^3}{16\pi^2 2c_W}\gamma_\mu\left[I_f^{(3)} F_{ZL}(s)\left(1+\gamma_5\right) - 2Q_f s_W^2 F_{ZQ}(s)\right]. \qquad \text{(A.3.91)}
\end{aligned}
$$

We note that the Born approximation would correspond to the replacements

$$
\begin{aligned}
\frac{g^2}{16\pi^2} F_{\gamma Q} &\to 1, \qquad \text{(A.3.92)} \\
\frac{g^2}{16\pi^2} F_{ZL} &\to 1, \qquad \text{(A.3.93)} \\
\frac{g^2}{16\pi^2} F_{ZQ} &\to 1. \qquad \text{(A.3.94)}
\end{aligned}
$$

This property justifies the normalization of these terms. Since the term with $F_{\gamma L}$ has no Born analog, its normalization is chosen in a convenient way.

We will understand that the second diagram of Fig. A.6 stands only for those counter-terms that originate from fermionic self-energy diagrams; i.e. those of Eqs. (A.3.55)–(A.3.57). They will be referred to as *fermionic* counter-terms. The rest will be called *bosonic* counter-terms. To distinguish the two types of counter-terms, we will use different drawings in Fig. A.6 and Fig. A.8 below.

The four contributions from the fermionic counter-terms to the four scalar form factors above are:

$$
\begin{aligned}
F_{\gamma Q}^{ct} &= 2\left(\sqrt{z_R} - I\right)^{em} = Q_f^2 s_W^2\left(-\frac{1}{\bar\varepsilon} + \frac{2}{\hat\varepsilon} + 3\ln\frac{M_W^2}{\mu^2}\right) + F_{\gamma Q}^{ct,F}, \qquad \text{(A.3.95)} \\
F_{\gamma Q}^{ct,F} &= Q_f^2 s_W^2\left(3\ln\frac{m_f^2}{M_W^2} - 4\right) + \frac{3}{8}\frac{1}{c_W^2}\delta_f^2, \qquad \text{(A.3.96)}
\end{aligned}
$$

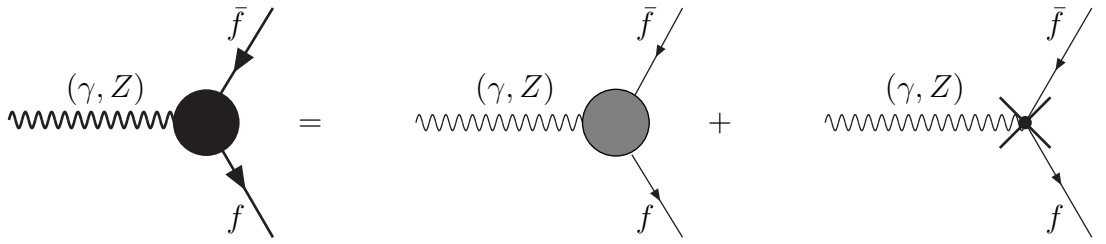

Figure A.6. *Off-shell $Zf\bar{f}$ and $\gamma f\bar{f}$ vertices*

$$F^{ct}_{\gamma L} = \left(\sqrt{z_{L}} - I\right) - \left(\sqrt{z_{R}} - I\right) = \frac{3}{8} r_t \left(\frac{1}{\bar{\varepsilon}} - \ln\frac{M_W^2}{\mu^2}\right) + F^{ct,F}_{\gamma L}, \tag{A.3.97}$$

$$F^{ct,F}_{\gamma L} = \frac{3}{4}\frac{a_f v_f}{c_W^2} + \frac{1}{4} w^F_W, \tag{A.3.98}$$

$$F^{ct}_{ZQ} = \delta_f \left(\sqrt{z_{R}} - I\right)^{em} = Q_f^3 s_W^4 \left(\frac{1}{\bar{\varepsilon}} - \frac{2}{\hat{\varepsilon}} - 3\ln\frac{M_W^2}{\mu^2}\right) + F^{ct,F}_{ZQ}, \tag{A.3.99}$$

$$F^{ct,F}_{ZQ} = -\frac{3}{8} Q_f \frac{s_W^2}{c_W^2}\delta_f^2 - Q_f^3 s_W^4 \left(3\ln\frac{m_f^2}{M_W^2} - 4\right), \tag{A.3.100}$$

$$\begin{aligned} F^{ct}_{ZL} &= \sigma_f^2 \left(\sqrt{z_{L}} - I\right) - \delta_f^2 \left(\sqrt{z_{R}} - I\right) \\ &= \frac{3}{2} Q_f^2 a_f s_W^2 \left(\frac{1}{\hat{\varepsilon}} + \ln\frac{M_W^2}{\mu^2}\right) + \frac{3}{16} r_t \sigma_f \left(\frac{1}{\bar{\varepsilon}} - \ln\frac{M_W^2}{\mu^2}\right) + F^{ct,F}_{ZL}, \end{aligned} \tag{A.3.101}$$

$$F^{ct,F}_{ZL} = \frac{3}{2} Q_f^2 a_f s_W^2 \left(\ln\frac{m_f^2}{M_W^2} - \frac{4}{3}\right) + \frac{3}{16}\frac{1}{c_W^2} a_f (3v_f^2 + a_f^2) + \frac{1}{8}\sigma_f w^F_W. \tag{A.3.102}$$

- Off-shell vertices.

Now we construct the four off-shell vertices, which are derived from the next four equations, two for $\gamma f\bar{f}$ vertices:

$$F^V_{\gamma Q}(s) = \frac{1}{Q_f s_W}\Big\{G_\mu(s)\left[\gamma_\mu i g^3\right] + Q_f s_W F^{ct}_{\gamma Q}\Big\}, \tag{A.3.103}$$

$$F^V_{\gamma L}(s) = \frac{2}{I_f^{(3)} s_W}\Big\{G_\mu(s)\left[\gamma_\mu(1+\gamma_5) i g^3\right] + Q_f s_W F^{ct}_{\gamma L}\Big\}; \tag{A.3.104}$$

and two for $Zf\bar{f}$ vertices:

$$F^V_{ZQ}(s) = \frac{2c_W}{(-2Q_f s_W^2)}\left\{Z_\mu(s)\left[\gamma_\mu i g^3\right] + \frac{1}{c_W} F^{ct}_{ZQ}\right\}, \tag{A.3.105}$$

$$F^V_{ZL}(s) = \frac{2c_W}{I_f^{(3)}}\left\{Z_\mu(s)\left[\gamma_\mu(1+\gamma_5) i g^3\right] + \frac{1}{c_W} F^{ct}_{ZL}\right\}. \tag{A.3.106}$$

The factors $1/(s_W Q_f)$ and $2/(s_W I_f^{(3)})$ for $\gamma f\bar{f}$ vertices, and the factors $2c_W/(-2Q_f s_W^2)$ and $2c_W/I_f^{(3)}$ for $Zf\bar{f}$ are due to the form factor definitions Eqs. (A.3.90)–(A.3.91).

The four off-shell vertices with separated ultraviolet poles read

$$F^V_{\gamma Q}(s) = F^V_{ZQ}(s) = 2Q_f^2 s_W^2 \left(\frac{1}{\hat{\varepsilon}} + \ln\frac{M_W^2}{\mu^2}\right) + F^{V,F}_{\gamma Q}(s), \tag{A.3.107}$$

$$F^{V,F}_{\gamma Q}(s) = Q_f^2 s_W^2 \left[3\ln\frac{m_f^2}{M_W^2} + F^F_\gamma(s) - 4\right] + \frac{\delta_f^2}{4c_W^2}\left[F^F_Z(s) + \frac{3}{2}\right], \tag{A.3.108}$$

$$F^V_{\gamma L}(s) = -\frac{1}{4}\frac{r_t}{R_W}\left(\frac{1}{\bar{\varepsilon}} - \ln\frac{M_W^2}{\mu^2}\right) + F^{V,F}_{\gamma L}(s), \tag{A.3.109}$$

$$F^{V,F}_{\gamma L}(s) = \frac{1}{R_W}\left(\frac{4}{3} + \frac{1}{12}\frac{1}{R_W}\right) + \frac{Q_f}{c_W^2}v_f\left[F^F_Z(s) + \frac{3}{2}\right] + \frac{1}{2}\frac{Q_f}{I_f^{(3)}}w_W^F - |Q_{f'}|\,F^F_{Wa}(s) - F^F_{Wn}(s), \tag{A.3.110}$$

$$F^V_{ZQ}(s) = 2Q_f^2 s_W^2 \left(\frac{1}{\hat{\varepsilon}} + \ln\frac{M_W^2}{\mu^2}\right) + F^{V,F}_{ZQ}(s), \tag{A.3.111}$$

$$F^{V,F}_{ZQ}(s) = Q_f^2 s_W^2 \left[3\ln\frac{m_f^2}{M_W^2} + F^F_\gamma(s) - 4\right] + \frac{\delta_f^2}{4c_W^2}\left[F^F_Z(s) + \frac{3}{2}\right], \tag{A.3.112}$$

$$F^V_{ZL}(s) = 2Q_f^2 s_W^2 \left(\frac{1}{\hat{\varepsilon}} + \ln\frac{M_W^2}{\mu^2}\right) + \left[\frac{c_W^2}{R_W}\left(\frac{1}{4}r_t + \frac{4}{3} + \frac{1}{12}\frac{1}{R_W}\right) + \frac{1}{4}r_t\right]\left(\frac{1}{\bar{\varepsilon}} - \ln\frac{M_W^2}{\mu^2}\right) + F^{V,F}_{ZL}(s), \tag{A.3.113}$$

$$F^{V,F}_{ZL}(s) = Q_f^2 s_W^2 \left[3\ln\frac{m_f^2}{M_W^2} + F^F_\gamma(s) - 4\right] + \frac{1}{4}\frac{1}{c_W^2}(3v_f^2 + a_f^2)\left[F^F_Z(s) + \frac{3}{2}\right] - c_W^2 F^F_{Wn}(s) + \frac{1}{4I_f^{(3)}}\left[2a_{f'}\bar{F}^F_{Wa}(s) + \sigma_f w_W^F + \sigma_{f'}F^F_{Wa}(s)\right]. \tag{A.3.114}$$

The expressions for these vertices are valid in case of a heavy virtual fermion (e.g. the top-quark). They may be used to construct the particular case when the virtual fermion is massless. It will be used to calculate one-loop EWRC for the initial electron vertex.

- Construction of the electron vertex.

The four individual off-shell electron vertices are derived from the general case Eq. (A.3.114) by setting:

$$m_{f'}^2 = m_{\nu_e}^2 = 0, \tag{A.3.115}$$

$$Q_f = Q_e, \tag{A.3.116}$$

$$Q_{f'} = Q_{\nu_e} = 0, \tag{A.3.117}$$

$$w_W^{F(0)} = \frac{3}{2}, \tag{A.3.118}$$

$$\bar{F}^F_{Wa}(s) = 0. \tag{A.3.119}$$

They are

$$F^{Ve}_{\gamma Q}(s) = F^{Ve}_{ZQ}(s) = 2Q_e^2 s_W^2 \left(\frac{1}{\hat{\varepsilon}} + \ln\frac{M_W^2}{\mu^2}\right) + F^{Ve,F}_{\gamma Q}(s), \tag{A.3.120}$$

$$F_{\gamma_Q}^{Ve,F}(s) = Q_e^2 s_W^2 \left[3\ln\frac{m_e^2}{M_W^2} + F_\gamma^F(s) - 4\right] + \frac{1}{4}\frac{\delta_e^2}{c_W^2}\left[F_Z(s) + \frac{3}{2}\right], \quad \text{(A.3.121)}$$

$$F_{\gamma_L}^{Ve}(s) = \frac{1}{3R_W}\left(4 + \frac{1}{4}\frac{1}{R_W}\right)\left(\frac{1}{\bar{\varepsilon}} - \ln\frac{M_W^2}{\mu^2}\right) + F_{\gamma_L}^{Ve,F}(s), \quad \text{(A.3.122)}$$

$$F_{\gamma_L}^{Ve,F}(s) = \frac{Q_e}{c_W^2} v_e \left[F_Z(s) - \frac{3}{2}\right] + \frac{3}{4}\frac{Q_e}{I_e^{(3)}} - |Q_{\nu_e}| F_{Wa}^{F(0)}(s) - F_{Wn}^{F(0)}(s), \quad \text{(A.3.123)}$$

$$F_{ZQ}^{Ve}(s) = 2Q_e^2 s_W^2 \left(\frac{1}{\hat{\varepsilon}} + \ln\frac{M_W^2}{\mu^2}\right) + F_{ZQ}^{Ve,F}(s), \quad \text{(A.3.124)}$$

$$F_{ZQ}^{Ve,F}(s) = Q_e^2 s_W^2 \left[3\ln\frac{m_e^2}{M_W^2} + F_\gamma^F(s) - 4\right] + \frac{\delta_e^2}{4c_W^2}\left[F_Z(s) + \frac{3}{2}\right], \quad \text{(A.3.125)}$$

$$F_{ZL}^{Ve}(s) = 2Q_e^2 s_W^2 \left(\frac{1}{\hat{\varepsilon}} + \ln\frac{M_W^2}{\mu^2}\right) + \frac{1}{3}\frac{c_W^2}{R_W}\left(4 + \frac{1}{4}\frac{c_W^2}{R_W}\right)\left(\frac{1}{\bar{\varepsilon}} - \ln\frac{M_W^2}{\mu^2}\right) + F_{ZL}^{Ve,F}(s), \quad \text{(A.3.126)}$$

$$F_{ZL}^{Ve,F}(s) = Q_e^2 s_W^2 \left[3\ln\frac{m_e^2}{M_W^2} + F_\gamma^F(s) - 4\right] + \frac{1}{4}\frac{(3v_e^2 + a_e^2)}{c_W^2}\left[F_Z(s) + \frac{3}{2}\right] - c_W^2 F_{Wn}^{F(0)}(s) + \frac{1}{4I_e^{(3)}}\left[\frac{3}{2}\sigma_e + \sigma_{\nu_e} F_{Wa}^{F(0)}(s)\right]. \quad \text{(A.3.127)}$$

Having constructed all these vertices, we may move to the last building blocks: electroweak boxes.

A.3.4. The WW box

Here we discuss only the WW box, see Fig. A.7. Only one diagram contributes for a given channel. The contribution of each diagram may be parameterized by only one scalar function:

$$WW_{box}^{d(c)} = (2\pi)^4 i \frac{g^4}{16\pi^2}\gamma_\mu(1+\gamma_5) \otimes \gamma_\mu(1+\gamma_5)\,\mathcal{B}_{WW}^{d(c)}(s,t), \quad \text{(A.3.128)}$$

where s, t, and u are the usual Mandelstamm variables and superscripts d and c denote the direct and crossed box diagrams. In this Appendix, the Mandelstam variables are defined such that they satisfy the identity:

$$s + t + u = 0. \quad \text{(A.3.129)}$$

- Direct box.

Only the direct box is the source of m_t-dependent terms. The general answer for the first diagram of Fig. A.7, valid for the case of a heavy virtual fermion, e.g. for *up=top*, reads:

$$\mathcal{B}_{WW}^{d}(s,t) = \left\{-t\left(1 + \frac{t^2}{u^2}\right) - 4\frac{M_W^2 t^2}{u^2} + 2\frac{M_W^4}{u}\left(1 + 2\frac{s}{u}\right) + m_t^2\left[2 + 3\frac{s}{u} + 2\frac{s^2}{u^2} - 2\frac{M_W^2}{u}\left(1 + 2\frac{s}{u}\right)\right] + \frac{m_t^4 s}{u^2}\right\} D_0(-s,-t;M_W,0,M_W,m_t)$$

$$
\begin{aligned}
&-\left\{2+2\frac{s}{u}+\frac{s^2}{u^2}-2\frac{M_W^2 s}{u^2}-\frac{1}{2}r_t\left[4-R_W\left(1+2\frac{s^2}{u^2}\right)\right]\right.\\
&\left.+\frac{1}{2}r_t^2\left(1-2R_W\right)-\frac{1}{2}r_t^3 R_W\right\}C_0\left(-s;M_W,m_t,M_W\right)\\
&-\left(2+2\frac{s}{u}+\frac{s^2}{u^2}-2\frac{M_W^2 s}{u^2}+\frac{m_t^2 s}{u^2}\right)C_0\left(-s;M_W,0,M_W\right)\\
&+\left(2+3\frac{s}{u}+\frac{s^2}{u^2}+2\frac{M_W^2 t}{u^2}-\frac{m_t^2 t}{u^2}\right)\left[C_0\left(-s;0,M_W,m_t\right)+C_0\left(-s;m_t,M_W,0\right)\right]\\
&-\frac{1}{s}\left[2\frac{s}{u}+\frac{5}{3}\frac{1}{R_W}+\frac{1}{12}\frac{1}{R_W^2}+\frac{1}{4}r_t\left(2-\frac{1}{R_W}\right)-\frac{1}{2}r_t^2\right]\\
&\times B_0\left(-s;M_W,M_W\right)+\frac{2}{u}B_0\left(-s;m_t,0\right)+\frac{1}{2}\frac{r_t}{s}\frac{A_0\left(m_t\right)}{M_W^2}\\
&-\frac{1}{3M_W^2}\left[\frac{1}{2}\left(1+3r_t R_W\right)\frac{A_0\left(M_W\right)}{M_W^2}-1-\frac{3}{4}r_t+\frac{1}{6}\frac{1}{R_W}\right]. \qquad \text{(A.3.130)}
\end{aligned}
$$

The expression for the WW box diagram with extracted pole is:

$$
\mathcal{B}^d_{WW}\left(s,t\right) = \frac{1}{M_W^2}\left(-\frac{3}{2}+\frac{1}{4}r_t-\frac{1}{12R_W}\right)\left(\frac{1}{\bar{\varepsilon}}-\ln\frac{M_W^2}{\mu^2}\right)+\mathcal{B}^{d,F}_{WW}\left(s,t\right), \qquad \text{(A.3.131)}
$$

$$
\begin{aligned}
\mathcal{B}^{d,F}_{WW}\left(s,t\right) = &\left\{-t\left(1+\frac{t^2}{u^2}\right)-4\frac{M_W^2 t^2}{u^2}+2\frac{M_W^4}{u}\left(1+2\frac{s}{u}\right)\right. \qquad \text{(A.3.132)}\\
&\left.+m_t^2\left[2+3\frac{s}{u}+2\frac{s^2}{u^2}-2\frac{M_W^2}{u}\left(1+2\frac{s}{u}\right)\right]+\frac{m_t^4 s}{u^2}\right\}D_0\left(-s,-t;M_W,0,M_W,m_t\right)\\
&-\left\{2+2\frac{s}{u}+\frac{s^2}{u^2}-2\frac{M_W^2 s}{u^2}-\frac{1}{2}r_t\left[4-R_W\left(1+2\frac{s^2}{u^2}\right)\right]\right.\\
&\left.+\frac{1}{2}r_t^2\left(1-2R_W\right)+\frac{1}{2}r_t^3 R_W\right\}C_0\left(-s;M_W,m_t,M_W\right)\\
&-\left(2+2\frac{s}{u}+\frac{s^2}{u^2}-2\frac{M_W^2 s}{u^2}+\frac{m_t^2 s}{u^2}\right)C_0\left(-s;M_W,0,M_W\right)\\
&+\left(2+3\frac{s}{u}+\frac{s^2}{u^2}+2\frac{M_W^2 t}{u^2}-\frac{m_t^2 t}{u^2}\right)\left[C_0\left(-t;0,M_W,m_t\right)+C_0\left(-t;m_t,M_W,0\right)\right]\\
&-\frac{1}{s}\left[\frac{2s}{u}+\frac{5}{3}\frac{1}{R_W}+\frac{1}{12R_W^2}+\frac{r_t}{4}\left(2-\frac{1}{R_W}\right)-\frac{r_t^2}{2}\right]B_0^F\left(-s;M_W,M_W\right)\\
&+\frac{2}{u}B_0^F\left(-t;m_t,0\right)-\frac{r_t^2}{2s}\left(1-\ln r_t\right)+\frac{1}{6M_W^2}\left(3r_t R_W+3+\frac{3}{2}r_t-\frac{1}{3R_W}\right).
\end{aligned}
$$

We note that C_0 and D_0 are both infrared finite.

- Crossed box.

The second diagram of Fig. A.7 may be computed below the $t\bar{t}$ production threshold ignoring fermion masses. Its answer is very compact:

$$
\mathcal{B}^c_{WW}\left(s,u\right) = -2u^2 D_0\left(-s,-u;M_W,0,M_W,0\right)+4C_0\left(-s;M_W,0,M_W\right) \qquad \text{(A.3.133)}
$$

$$+\frac{1}{3M_W^2}\left[\frac{1}{4}\left(20+\frac{1}{R_W}\right)B_0\left(-s;M_W,M_W\right)+\frac{1}{2}\frac{A_0\left(M_W\right)}{M_W^2}-1+\frac{1}{6R_W}\right].$$

And the same expression with extracted pole is

$$\mathcal{B}^c_{WW}\left(s,u\right) = \frac{1}{6M_W^2}\left(9+\frac{1}{2R_W}\right)\left(\frac{1}{\bar{\varepsilon}}-\ln\frac{M_W^2}{\mu^2}\right)+\mathcal{B}^{c,F}_{WW}\left(s,u\right), \tag{A.3.134}$$

$$\begin{aligned}\mathcal{B}^{c,F}_{WW}\left(s,u\right) &= -2u^2D_0\left(-s,-u;M_W,0,M_W,0\right)+4C_0\left(-s;M_W,0,M_W\right)\\ &\quad+\frac{1}{3M_W^2}\left[\frac{1}{4}\left(20+\frac{1}{R_W}\right)B_0^F\left(-s;M_W,M_W\right)-\frac{3}{2}+\frac{1}{6R_W}\right].\end{aligned} \tag{A.3.135}$$

It is instructive to compare the pole parts of Eq. (A.3.130) in the massless approximation with that of Eq. (A.3.135). They agree modulo an overall sign; that should be the case if one remembers that the Born amplitude has different sign for *down* and *up* final state fermions.

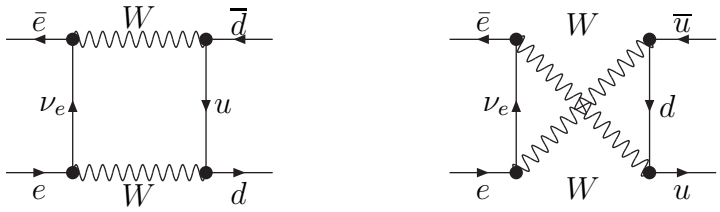

Figure A.7. *The WW boxes*

Finally, for the $d\bar{d}$ and $s\bar{s}$ channels one needs the direct WW box in top-less approximation: $m_t^2 \to 0$. It can trivially be derived from Eq. (A.3.130) and does not need to be additionally presented.

The contributions from the two ZZ boxes are presented in Subsection 3.3.2.

A.4. Amplitudes

A.4.1. Born amplitudes

We begin with the Born amplitude for the process $e\bar{e} \to f\bar{f}$ described by the two Feynman diagrams with γ and Z exchange, Fig. 1.1:

$$\begin{aligned}A^B_\gamma &= eQ_e\, eQ_f\gamma_\mu\otimes\gamma_\mu\frac{-i}{Q^2}\\ &= -i\,e^2\frac{Q_eQ_f}{Q^2}\gamma_\mu\otimes\gamma_\mu\\ &= -i\,4\pi\alpha(0)\frac{Q_eQ_f}{Q^2}\gamma_\mu\otimes\gamma_\mu\,,\end{aligned} \tag{A.4.1}$$

$$A^B_Z = \frac{e}{2s_Wc_W}\,\frac{e}{2s_Wc_W}\gamma_\mu\left[I_e^{(3)}\left(1+\gamma_5\right)-2Q_es_W^2\right]\otimes\gamma_\mu\left[I_f^{(3)}\left(1+\gamma_5\right)-2Q_fs_W^2\right]\frac{-i}{Q^2+M_Z^2}$$

$$
\begin{aligned}
&= -ie^2\frac{I_e^{(3)}I_f^{(3)}}{4s_W^2c_W^2(Q^2+M_Z^2)}\gamma_\mu\left[1+\gamma_5-4|Q_e|s_W^2\right]\otimes\gamma_\mu\left[1+\gamma_5-4|Q_f|s_W^2\right]\\
&= -ie^2\frac{I_e^{(3)}I_f^{(3)}}{4s_W^2c_W^2(Q^2+M_Z^2)}\Big[\gamma_\mu(1+\gamma_5)\otimes\gamma_\mu(1+\gamma_5)-4|Q_e|s_W^2\gamma_\mu\otimes\gamma_\mu(1+\gamma_5)\\
&\qquad -4|Q_f|s_W^2\gamma_\mu(1+\gamma_5)\otimes\gamma_\mu+16|Q_e||Q_f|s_W^4\gamma_\mu\otimes\gamma_\mu\Big]. \quad \text{(A.4.2)}
\end{aligned}
$$

The last representations for both amplitudes are identity transformations for the Born case. They are useful for the subsequent discussion of one-loop amplitudes showing explicitly five structures to which the complete amplitude may be reduced: one in the γ-exchange amplitude and four in the Z-exchange amplitude. The latter may be called LL, QL, LQ, and QQ structures, correspondingly; see last Eq. (A.4.2).

In the following we will use the propagator factor:

$$
\chi_Z(s) = \frac{1}{16s_W^2c_W^2}\frac{s}{s-M_Z^2+i\dfrac{\Gamma_Z}{M_Z}s}\,. \quad \text{(A.4.3)}
$$

In terms of these factors the Born amplitudes are

$$
A_\gamma^B = i\,4\pi\alpha(0)\frac{Q_eQ_f}{s}\gamma_\mu\otimes\gamma_\mu\,, \quad \text{(A.4.4)}
$$

$$
\begin{aligned}
A_Z^B &= i\,e^2\,4I_e^{(3)}I_f^{(3)}\frac{\chi_Z(s)}{s}\Big[\gamma_\mu(1+\gamma_5)\otimes\gamma_\mu(1+\gamma_5)-4|Q_e|s_W^2\gamma_\mu\otimes\gamma_\mu(1+\gamma_5)\\
&\qquad -4|Q_f|s_W^2\gamma_\mu(1+\gamma_5)\otimes\gamma_\mu+16|Q_e||Q_f|s_W^4\gamma_\mu\otimes\gamma_\mu\Big]. \quad \text{(A.4.5)}
\end{aligned}
$$

In this Section the presentation develops in two parallel streams: one for the $Z\to f\bar f$ decay, and another one for the process scattering $e\bar e\to(Z,\gamma)\to f\bar f$.

Here we discussed the Born amplitude only for the scattering process. For the decay it was already given in the second Eq. (A.3.91) followed by the formal replacement Eq. (A.3.94).

A.4.2. Towards one-loop amplitudes

The decay $Z\to f\bar f$

There are two basic ingredients contributing to the one-loop amplitude of the Z-decay.

1. Vertex correction for the Z-decay.

We recall diagram Fig. A.6, the second Eq. (2.4.26), which can be considered as the definition of the one-loop amplitude, and the two corresponding off-shell functions $F_{ZQ}^V(s)$ and $F_{ZL}^{V,F}(s)$ defined in Eq. (A.3.114). For the description of the Z-decay one should consider their on-mass-shell limit. For these two functions we introduce shortened notations omitting the subscript Z and the argument list (they are constants for the decay):

$$
F_Q^V \equiv F_{ZQ}^V(M_Z^2) = 2Q_f^2s_W^2\left(\frac{1}{\hat\varepsilon}+\ln\frac{M_W^2}{\mu^2}\right)+F_{ZQ}^{V,F}(M_Z^2), \quad \text{(A.4.6)}
$$

$$F_L^V \equiv F_{ZL}^V(M_Z^2) = 2Q_f^2 s_W^2 \left(\frac{1}{\hat{\varepsilon}} + \ln\frac{M_W^2}{\mu^2}\right) + \left(\frac{1}{2}r_t + \frac{4}{3} + \frac{1}{12}\frac{1}{R_W}\right)\left(\frac{1}{\bar{\varepsilon}} - \ln\frac{M_W^2}{\mu^2}\right) + F_{ZL}^{V,F}(M_Z^2). \quad (A.4.7)$$

2. Bosonic counter-terms.

Contributions to the decay amplitude from counter-terms originate from all relevant bosonic self-energy diagrams. They may be depicted the vertex in Fig. A.8.

The corresponding contributions are derived from the counter-term Lagrangian and may be expressed in terms of quantities introduced in Subsection A.3.1. We will call them *bosonic counter-terms*:

$$F_Q^{ct} = \frac{1}{2}\left[(z_Z - 1) - (z_\gamma - 1) - \frac{1}{s_W^2}\Delta\rho\right] + \frac{\Sigma_{Z\gamma}(M_Z^2)}{M_Z^2}, \quad (A.4.8)$$

$$F_L^{ct} = \frac{1}{2}\left[(z_Z - 1) - (z_\gamma - 1) + \frac{c_W^2 - s_W^2}{s_W^2}\Delta\rho\right]. \quad (A.4.9)$$

Now we jump to the scattering process.

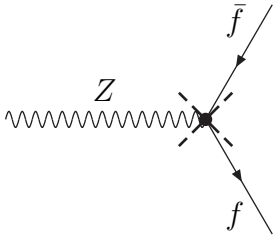

Figure A.8. *Bosonic counter-terms for* $Z \to f\bar{f}$

The process $e^+e^- \to (\gamma, Z) \to f\bar{f}$

For the scattering process there are many more ingredients than for the decay. Here we distinguish γ- and Z-exchanges; initial and final state vertex corrections; contributions from bosonic self-energies, counter-terms, and boxes.

- The process $e\bar{e} \to (\gamma) \to f\bar{f}$; final fermion vertex.

We begin with the final state vertex correction shown in Fig. A.9(b). Its amplitude is A_γ = Born electron vertex $\otimes$ dressed final state γ-vertex $\times$ γ-propagator:

$$A_\gamma = eQ_e\, e\gamma_\mu \otimes \gamma_\mu\left[\frac{1}{2}I_f^{(3)}\,(1+\gamma_5)\,F_{\gamma L}^V\,(s) + Q_f F_{\gamma Q}^V\,(s)\right]\frac{-i}{Q^2}\,. \quad (A.4.10)$$

- Process $e\bar{e} \to (\gamma) \to f\bar{f}$; initial electron vertex.

Similarly, there exists the initial state electron vertex correction shown in Fig. A.9(a).

We do not give its separate contribution but rather show both vertex corrections originating from the two γ-exchange diagrams:

$$\begin{aligned} A_\gamma &= (-ie^2)\Big\{\gamma_\mu\left[\frac{1}{2}I_e^{(3)}\left(1+\gamma_5\right)F_{\gamma L}^{V(0)}\left(s\right)+Q_eF_{\gamma Q}^{V(0)}\left(s\right)\right]\otimes\gamma_\mu Q_f \\ &\quad+\gamma_\mu Q_e\otimes\gamma_\mu\left[\frac{1}{2}I_f^{(3)}\left(1+\gamma_5\right)F_{\gamma L}^{V}\left(s\right)+Q_fF_{\gamma Q}^{V}\left(s\right)\right]\Big\}\frac{1}{Q^2}\,. \end{aligned} \tag{A.4.11}$$

- Process $e\bar{e}\to(Z)\to f\bar{f}$; final fermion vertex.

Analogously, one constructs the final state vertex for the Z-exchange diagram, Fig. A.10(b). Its amplitude is the product A_Z = Born electron vertex $\otimes$ dressed final state Z-vertex $\times$ Z-propagator:

$$\begin{aligned} A_Z &= \frac{e}{2s_Wc_W}\,\frac{e}{2s_Wc_W} \\ &\quad\times\gamma_\mu\left[I_e^{(3)}\left(1+\gamma_5\right)-2Q_es_W^2\right]\otimes\gamma_\mu\left[I_f^{(3)}\left(1+\gamma_5\right)F_{ZL}^{V}\left(s\right)-2Q_fs_W^2F_{ZQ}^{V}\left(s\right)\right]\frac{-i}{Q^2+M_Z^2}\,. \end{aligned} \tag{A.4.12}$$

- Process $e\bar{e}\to(Z)\to f\bar{f}$; initial electron vertex.

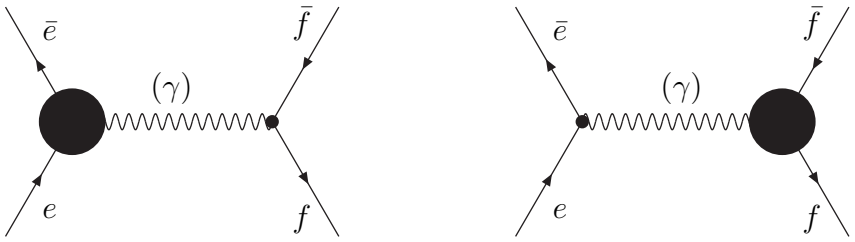

Figure A.9. *Electron (a) and final fermion (b) vertices in* $e\bar{e}\to(\gamma)\to f\bar{f}$

The initial state vertex for the Z-exchange diagram, Fig. A.10(a), is combined with the final state fermion vertex into:

$$\begin{aligned} A_Z &= \frac{-ie^2}{4s_W^2c_W^2}\Big\{\gamma_\mu\left[I_e^{(3)}\left(1+\gamma_5\right)F_{ZL}^{V(0)}\left(s\right)-2Q_es_W^2F_{ZQ}^{V(0)}\left(s\right)\right]\otimes\gamma_\mu\left[I_f^{(3)}\left(1+\gamma_5\right)-2Q_fs_W^2\right] \\ &\quad+\gamma_\mu\left[I_e^{(3)}\left(1+\gamma_5\right)-2Q_es_W^2\right]\otimes\gamma_\mu\left[I_f^{(3)}\left(1+\gamma_5\right)F_{ZL}^{V}\left(s\right)-2Q_fs_W^2F_{ZQ}^{V}\left(s\right)\right]\Big\}\frac{1}{Q^2+M_Z^2}\,. \end{aligned} \tag{A.4.13}$$

- All vertex corrections.

It is instructive to combine all four vertex corrections together, into a common expression where we restored omitted normalization factor $\dfrac{g^2}{16\pi^2}$:

$$\mathcal{A}_Z^{OLA} = -i\frac{g^2}{16\pi^2}\frac{e^2I_e^{(3)}I_f^{(3)}}{4s_W^2c_W^2(Q^2+M_Z^2)} \tag{A.4.14}$$

$$
\begin{aligned}
&\times\Big\{\gamma_\mu(1+\gamma_5)\otimes\gamma_\mu(1+\gamma_5)\left[F^{V(0)}_{ZL}(s)+F^{V}_{ZL}(s)\right]\\
&-4|Q_e|s^2_W\gamma_\mu\otimes\gamma_\mu(1+\gamma_5)\left[F^{V(0)}_{ZQ}(s)+F^{V}_{ZL}(s)+\frac{(Q^2+M_Z^2)4s^2_Wc^2_W|Q_e|}{Q^2(-4|Q_e|s^2_W)}F^{V}_{\gamma L}(s)\right]\\
&-4|Q_f|s^2_W\gamma_\mu(1+\gamma_5)\otimes\gamma_\mu\left[F^{V(0)}_{ZL}(s)+F^{V}_{ZQ}(s)+\frac{(Q^2+M_Z^2)4s^2_Wc^2_W|Q_f|}{Q^2(-4|Q_f|s^2_W)}F^{V(0)}_{\gamma L}(s)\right]\\
&+16|Q_e||Q_f|s^4_W\gamma_\mu\otimes\gamma_\mu\\
&\times\left[F^{V(0)}_{LQ}(s)+F^{V}_{ZQ}(s)+\frac{(Q^2+M_Z^2)4s^2_Wc^2_W|Q_e||Q_f|}{(16|Q_e||Q_f|s^4_W)Q^2}\left(F^{V(0)}_{\gamma Q}(s)+F^{V}_{\gamma Q}(s)\right)\right]\Big\}.
\end{aligned}
$$

It has the following Born-like structure:

$$
\begin{aligned}
\mathcal{A}^{OLA}_Z &= i\frac{g^2}{16\pi^2}e^2\,4I^{(3)}_eI^{(3)}_f\frac{\chi_Z(s)}{s}\\
&\times\Big\{\gamma_\mu(1+\gamma_5)\otimes\gamma_\mu(1+\gamma_5)F_{LL}(s,t)-4|Q_e|s^2_W\gamma_\mu\otimes\gamma_\mu(1+\gamma_5)F_{QL}(s,t)\\
&-4|Q_f|s^2_W\gamma_\mu(1+\gamma_5)\otimes\gamma_\mu F_{LQ}(s,t)+16|Q_eQ_f|s^4_W\gamma_\mu\otimes\gamma_\mu F_{QQ}(s,t)\Big\}. \qquad \text{(A.4.15)}
\end{aligned}
$$

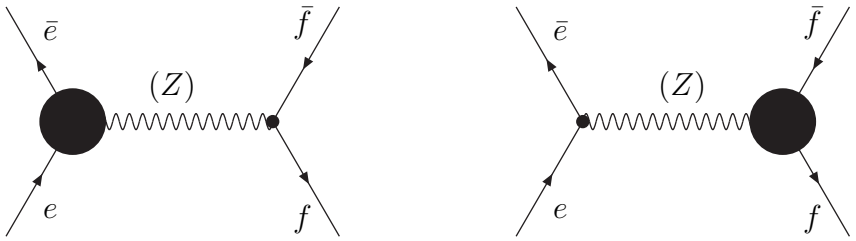

Figure A.10. *Electron (a) and final fermion (b) vertices in* $e\bar{e}\to(Z)\to f\bar{f}$

If one compares with the last Eq. (A.4.2), it is seen that the Born-factors '1' in front of the LL etc. structures are replaced by four scalar form factors $F_{LL}(s,t)$, $F_{QL}(s,t)$, $F_{LQ}(s,t)$ and $F_{QQ}(s,t)$. We allow for a t-dependence having in mind the contribution of EW boxes, see Subsection A.4.3.

- Bosonic self-energies and bosonic counter-terms.

The contributions to form factors from bosonic self-energy diagrams and counter-terms originating from bosonic self-energy diagrams come from four classes of diagrams; their sum is depicted by a black circle in Fig. A.11.

The contribution of these diagrams to the four scalar form factors is derived straightforwardly:

$$
\begin{aligned}
F^{ct}_{LL}(s) &= \mathcal{D}_Z(s)-s^2_W\left(z_\gamma-1\right)+\frac{c^2_W-s^2_W}{s^2_W}\Delta\rho, &\text{(A.4.16)}\\
F^{ct}_{QL(LQ)}(s) &= \mathcal{D}_Z(s)-\Pi_{Z\gamma}(s)-s^2_W\left(z_\gamma-1\right)-\Delta\rho, &\text{(A.4.17)}
\end{aligned}
$$

$$F_{QQ}^{ct,\mathrm{bos}}(s) = \mathcal{D}_z^{\mathrm{bos}}(s) - 2\Pi_{Z\gamma}^{\mathrm{bos}}(s) + c_W^2(1-R_Z)\left[\Pi_{\gamma\gamma}^{\mathrm{bos}}(s) - \left(z_\gamma^{\mathrm{bos}} - 1\right)\right] - s_W^2\left(z_\gamma^{\mathrm{bos}} - 1\right) - \frac{1}{s_W^2}\Delta\rho^{\mathrm{bos}}, \quad \text{(A.4.18)}$$

$$F_{QQ}^{ct,\mathrm{fer}}(s) = \mathcal{D}_z^{\mathrm{fer}}(s) - 2\Pi_{Z\gamma}^{\mathrm{fer}}(s) - s_W^2\left(z_\gamma^{\mathrm{fer}} - 1\right) - \frac{1}{s_W^2}\Delta\rho^{\mathrm{fer}}. \quad \text{(A.4.19)}$$

We note that the term $c_W^2(1-R_Z)\left[\Pi_{\gamma\gamma}^{\mathrm{fer}}(s) - (z_\gamma^{\mathrm{fer}} - 1)\right]$ is conventionally extracted from $F_{QQ}^{ct,\mathrm{fer}}(s)$. Recalling electron charge renormalization, Eq. (A.3.31), one may easily verify that this term gives rise to a 'dressed' γ-exchange amplitude:

$$A_\gamma^{OLA} = i\frac{4\pi Q_e Q_f}{s}\alpha(s)\gamma_\mu \otimes \gamma_\mu\,, \quad \text{(A.4.20)}$$

which is identical to the Born amplitude Eq. (A.4.2) modulo the replacement of $\alpha(0)$ by the running electromagnetic coupling $\alpha(s)$:

$$\alpha(s) = \frac{\alpha}{1 - \frac{\alpha}{4\pi}\left[\Pi_{\gamma\gamma}^{\mathrm{fer}}(s) - \Pi_{\gamma\gamma}^{\mathrm{fer}}(0)\right]}\,. \quad \text{(A.4.21)}$$

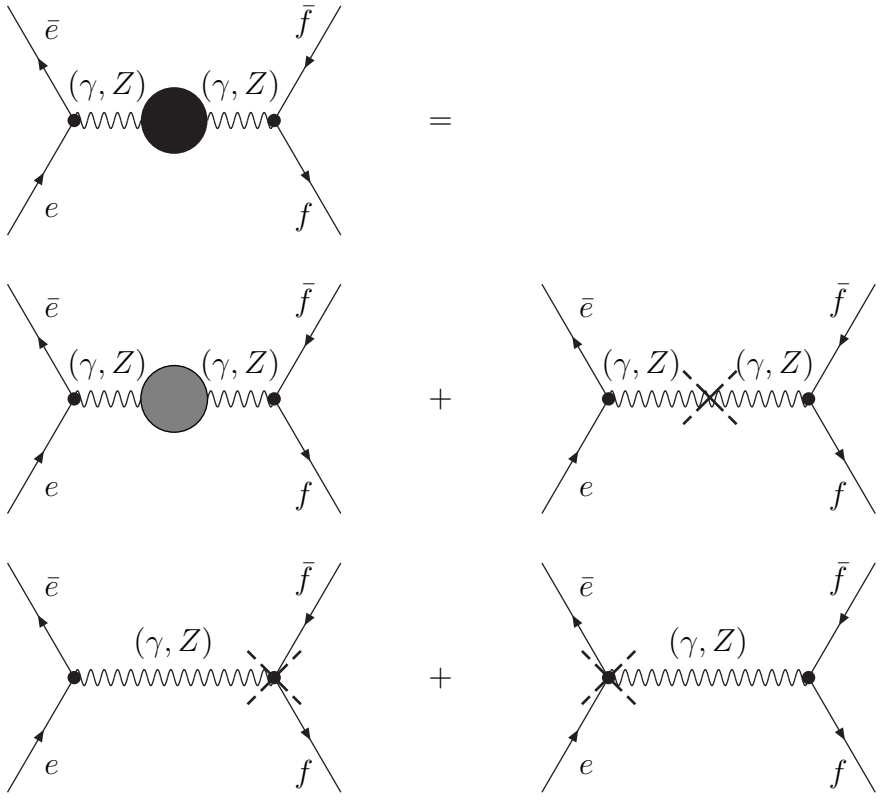

Figure A.11. *Bosonic self-energies and bosonic counter-terms for* $e\bar{e} \to (Z,\gamma) \to f\bar{f}$

A.4.3. The form factors Δr, F_L, F_Q, and $F_{LL}, F_{QL}, F_{LQ}, F_{QQ}$

Preliminaries

- Unified form factors.

If one looks at Eqs. (A.3.114) and (A.3.127) one may note that the finite parts of vertex functions, together with certain terms originating from fermionic counter-terms are forming several well-defined couples or larger families of terms. We will call them *unified form factors* and will denote them by a corresponding calligraphic symbol. In what follows we list all the unified form factors which are met.

The first family consists of various QED contributions:

$$\mathcal{F}^f_\gamma(s) = Q_f^2 s_W^2 \left[2\left(\frac{1}{\hat{\varepsilon}} + \ln\frac{M_W^2}{\mu^2} \right) + 3\ln\frac{m_f^2}{M_W^2} + F^{f,F}_\gamma(s) - 4 \right]. \tag{A.4.22}$$

The second is a simple couple associated with diagrams with a virtual Z boson:

$$\begin{aligned} \mathcal{F}_Z(s) &= F^F_Z(s) + \frac{3}{2} \\ &= 2(R_Z+1)^2 s C_0(-s;0,M_Z,0) - (2R_Z+3)\ln R_Z - 2R_Z - \frac{7}{2}. \end{aligned} \tag{A.4.23}$$

Now consider abelian and non-abelian diagrams with virtual W bosons:

$$\mathcal{F}_W(s) = -c_W^2 F^F_{Wn}(s) + \frac{1}{2}\left[\sigma^a_f w^F_W - \sigma^a_{f'} F^F_{Wa}(s) - \bar{F}^F_{Wa}(s) \right], \tag{A.4.24}$$

where

$$\sigma^a_f = |\sigma_f| = 1 - 2|Q_f| s_W^2, \tag{A.4.25}$$

and

$$\sigma^a_f + \sigma^a_{f'} = 2c_W^2. \tag{A.4.26}$$

It may be naturally rewritten in terms of three form factors:

$$\mathcal{F}_W(s) = c_W^2 \mathcal{F}_{Wn}(s) - \frac{1}{2}\sigma^a_{f'} \mathcal{F}_{Wa}(s) - \frac{1}{2}\overline{\mathcal{F}}_{Wa}(s), \tag{A.4.27}$$

where

$$\mathcal{F}_{Wa}(s) = F^F_{Wa}(s) + w^F_W, \tag{A.4.28}$$

$$\mathcal{F}_{Wn}(s) = -F^F_{Wn}(s) + w^F_W, \tag{A.4.29}$$

$$\overline{\mathcal{F}}_{Wa}(s) = -\bar{F}^F_{Wa}(s). \tag{A.4.30}$$

These three unified form factors, originating from diagrams with virtual W bosons as well as the contribution of the direct WW box diagram $\mathcal{B}^d_{WW}(s,t)$, contain the m_t^2-dependent terms. They may be naturally split into two terms: (i) their massless limit ($m_t^2 = 0$); (ii) top quark addition, vanishing when $m_t^2 \to 0$. We denote massless parts with superscript (0) and the additions with superscript (t):

$$\mathcal{F}(s) = \mathcal{F}^0(s) + \mathcal{F}^t(s), \tag{A.4.31}$$

$$\mathcal{B}^d_{WW}(s,t) = \mathcal{B}^{d,0}_{WW}(s,t) + \mathcal{B}^{d,t}_{WW}(s,t). \tag{A.4.32}$$

Below we present both parts of the three W unified form factors.

- Top-less limit.

The massless limit is compact:

$$\mathcal{F}^0_{Wa}(s) = 2(R_W+1)^2 sC_0(-s;0,M_W,0) - (2R_W+3)\ln(-R_W) - 2R_W - \frac{7}{2}, \quad \text{(A.4.33)}$$

$$\overline{\mathcal{F}}^0_{Wn}(s) = 0, \quad \text{(A.4.34)}$$

$$\begin{aligned}\mathcal{F}^0_{Wn}(s) &= -2(R_W+2)M_W^2 C_0(-s;M_W,0,M_W)\\ &\quad -\left(2R_W+\frac{7}{3}-\frac{3}{2R_W}-\frac{1}{12R_W^2}\right)B_0^F(-s;M_W,M_W)\\ &\quad +2R_W+\frac{9}{2}+\frac{11}{18R_W}-\frac{1}{18R_W^2}.\end{aligned} \quad \text{(A.4.35)}$$

- Top quark additions.

They are straightforwardly derived from the definitions:

$$\mathcal{F}^t_{Wa}(s) = \mathcal{F}_{Wa}(s) - \mathcal{F}^0_{Wa}(s) \quad \text{(A.4.36)}$$

$$\overline{\mathcal{F}}^t_{Wa}(s) = \overline{\mathcal{F}}_{Wa}(s) - \overline{\mathcal{F}}^0_{Wa}(s) \quad \text{(A.4.37)}$$

$$\mathcal{F}^t_{Wn}(s) = \mathcal{F}_{Wn}(s) - \mathcal{F}^0_{Wn}(s). \quad \text{(A.4.38)}$$

Now we give the list of the additions:

$$\begin{aligned}\mathcal{F}^t_{Wa}(s) &= 2(R_W+1)^2 s\Big[C_0(-s;m_t,M_W,m_t) - C_0(-s;0,M_W,0)\Big]\\ &\quad +(2R_W+3)\Big[-B_0^F(-s;m_t,m_t)+\ln R_W+2\Big]\\ &\quad -r_t\Bigg\{\Big(3R_W+2-r_t-r_t^2R_W\Big)M_W^2C_0(-s;m_t,M_W,m_t)\\ &\quad +\left(R_W+\frac{1}{2}+r_tR_W\right)\Big[1-B_0^F(-s;m_t,m_t)\Big]\\ &\quad -\left(2R_W+\frac{1}{2}-\frac{2}{r_t-1}+\frac{3}{2}\frac{1}{(r_t-1)^2}+r_tR_W\right)\ln r_t+\frac{3}{2}\frac{1}{r_t-1}+\frac{3}{4}\Bigg\},\end{aligned} \quad \text{(A.4.39)}$$

$$\begin{aligned}\overline{\mathcal{F}}^t_{Wa}(s) &= -r_t\Bigg\{\Big[R_W+2-r_t(2-r_t)R_W\Big]M_W^2C_0(-s;m_t,M_W,m_t)\\ &\quad -\left(\frac{1}{2}-R_W+r_tR_W\right)\Big[B_0^F(-s;m_t,m_t)+1\Big]+r_tR_W\ln r_t\Bigg\},\end{aligned} \quad \text{(A.4.40)}$$

$$\begin{aligned}\mathcal{F}^t_{Wn}(s) &= -2(R_W+2)M_W^2\Big[C_0(-s;M_W,m_t,M_W)-C_0(-s;M_W,0,M_W)\Big]\\ &\quad +r_t\Bigg\{\Bigg[3R_W+\frac{5}{2}-\frac{2}{R_W}-r_t\left(2-\frac{1}{2R_W}\right)\\ &\quad +{r_t}^2\left(\frac{1}{2}-R_W\right)\Bigg]M_W^2C_0(-s;M_W,m_t,M_W)\\ &\quad +\left[R_W+1-\frac{1}{4R_W}-r_t\left(\frac{1}{2}-R_W\right)\right]\Big[B_0^F(-s;M_W,M_W)-1\Big]\\ &\quad +\left[2R_W+\frac{1}{2}-\frac{2}{r_t-1}+\frac{3}{2}\frac{1}{(r_t-1)^2}-r_t\left(\frac{1}{2}-R_W\right)\right]\ln r_t+\frac{3}{2}\frac{1}{r_t-1}+\frac{1}{4}\Bigg].\end{aligned} \quad \text{(A.4.41)}$$

The decay $Z \to f\bar{f}$

The two decay form factors with restored normalization factors read:

$$F_{_Q} = \frac{g^2}{16\pi^2}\left(F_{_Q}^{V} + F_{_Q}^{ct}\right), \tag{A.4.42}$$

$$F_{_L} = \frac{g^2}{16\pi^2}\left(F_{_L}^{V} + F_{_L}^{ct}\right), \tag{A.4.43}$$

where $F_{_Q}^{V}$ and $F_{_L}^{V}$ are defined in Eq. (A.4.6) and Eq. (A.4.7) and $F_{_Q}^{ct}, F_{_L}^{ct}$ in Eq. (A.4.8) and Eq. (A.4.9). And the final expressions look quite compact:

$$\begin{aligned} F_{_Q} &= \frac{g^2}{16\pi^2}\Bigg[Q_f^2 s_{_W}^2 \mathcal{F}_{\gamma}\left(M_{_Z}^2\right) + \frac{\sigma_f^2}{4c_{_W}^2}\mathcal{F}_{_Z}\left(M_{_Z}^2\right) - \Pi_{_{Z\gamma}}(M_{_Z}^2) \\ &\quad -\frac{s_{_W}^2}{2}\Pi_{\gamma\gamma}^{F}(0) + \frac{1}{2}\Sigma_{_{ZZ}}^{'}(M_{_Z}^2) - \frac{1}{2s_{_W}^2}\Delta\rho^{F}\Bigg], \end{aligned} \tag{A.4.44}$$

$$\begin{aligned} F_{_L} &= \frac{g^2}{16\pi^2}\Bigg[Q_f^2 s_{_W}^2 \mathcal{F}_{\gamma}\left(M_{_Z}^2\right) + \frac{3v_f^2 + a_f^2}{4c_{_W}^2}\mathcal{F}_{_Z}(s) \\ &\quad +\mathcal{F}_{_W}\left(M_{_Z}^2\right) - \frac{s_{_W}^2}{2}\Pi_{\gamma\gamma}^{F}(0) + \frac{1}{2}\Sigma_{_{ZZ}}^{'}(M_{_Z}^2) - \frac{c_{_W}^2 - s_{_W}^2}{2s_{_W}^2}\Delta\rho^{F}\Bigg]. \end{aligned} \tag{A.4.45}$$

where

$$\Pi_{\gamma\gamma}^{F}(0) = \Pi_{\gamma\gamma}^{\mathrm{fer,F}}(0) + \Pi_{\gamma\gamma}^{\mathrm{bos}}(0), \tag{A.4.46}$$

$$\Pi_{\gamma\gamma}^{\mathrm{bos}}(0) = \frac{2}{3}\,. \tag{A.4.47}$$

The process $e\bar{e} \to (\gamma, Z) \to f\bar{f}$

For the scattering process we have to collect contributions from all off-shell vertices from self-energies and counter-terms, Eq. (A.4.19), and additionally from all boxes. However, conventionally the $Z\gamma$ and $\gamma\gamma$ boxes are shifted to the QED-corrections. So, in the electroweak form factors we are left with the purely $L \otimes L$ WW box and with the direct and crossed ZZ boxes. The latter two contribute to all four form factors and are free of ultraviolet and infrared divergences; they are *not* covered by the presentation below. From equations Eqs. (A.4.14) and (A.4.19) and adding only the WW box, one derives:

$$F_{_{LL}}(s,t) = F_{_{ZL}}^{V(0)}(s) + F_{_{ZL}}^{V}(s) + F_{_{LL}}^{ct}(s) - c_{_W}^2\left(R_{_Z} - 1\right) s\mathcal{B}_{_{WW}}^{d}(s,t), \tag{A.4.48}$$

$$F_{_{QL}}(s,t) = F_{_{ZQ}}^{V(0)}(s) + F_{_{ZL}}^{V}(s) + c_{_W}^2\left(R_{_Z} - 1\right) F_{\gamma L}^{V}(s) + F_{_{QL}}^{ct}(s)\,, \tag{A.4.49}$$

$$F_{_{LQ}}(s,t) = F_{_{ZL}}^{V(0)}(s) + F_{_{ZQ}}^{V}(s) + c_{_W}^2\left(R_{_Z} - 1\right) F_{\gamma L}^{V(0)}(s) + F_{_{LQ}}^{ct}(s)\,, \tag{A.4.50}$$

$$F_{_{QQ}}(s,t) = F_{_{ZQ}}^{V(0)}(s) + F_{_{ZQ}}^{V}(s) - \frac{c_{_W}^2}{s_{_W}^2}\left(R_{_Z} - 1\right)\left[F_{\gamma Q}^{V(0)}(s) + F_{\gamma Q}^{V}(s)\right] + F_{_{QQ}}^{ct}(s)\,, \tag{A.4.51}$$

where

$$F_{_{AB}}^{ct}(s) = F_{_{AB}}^{ct,\mathrm{bos}}(s) + F_{_{AB}}^{ct,\mathrm{fer}}(s)\,. \tag{A.4.52}$$

The final expressions for the basic quantities $F_{_{LL}}(s,t)$, $F_{_{QL}}(s,t)$, $F_{_{LQ}}(s,t)$ and $F_{_{QQ}}(s,t)$, are free of ultraviolet poles. But, as one may see from an inspection of the partial contributions, for instance from Eq. (A.4.35), there are terms rising with s,

$$\left[\frac{1}{R_{_W}}, \frac{1}{R_{_W}^2}\right] \otimes \left[1, B_0^{F}\left(-s; M_{_W}, M_{_W}\right)\right], \tag{A.4.53}$$

violating thereby unitarity. All these terms, which are called *non-unitary* terms, cancel identically in the sum. We introduce *hatted* quantities which are derived from the corresponding non-hatted objects by simply neglecting terms of the four kinds given in Eq. (A.4.53). The answers, now free of ultraviolet poles and of non-unitary terms are very compact:

$$\begin{aligned}
F_{LL}(s,t) &= \frac{g^2}{16\pi^2}\Bigg\{\mathcal{F}^e_\gamma(s)+\mathcal{F}^f_\gamma(s)-s^2_W\Pi^F_{\gamma\gamma}(0)+\frac{c^2_W-s^2_W}{s^2_W}\Delta\rho^F+\mathcal{D}^F_Z(s)\\
&+\frac{1}{4c^2_W}\left(3v^2_e+a^2_e+3v^2_f+a^2_f\right)\mathcal{F}_Z(s)+\hat{\mathcal{F}}^{(0)}_W(s)+\hat{\mathcal{F}}_W(s)\\
&-c^2_W(R_Z-1)\,s\hat{\mathcal{B}}^d_{WW}(s,t)+\frac{5}{3}B^F_0(-s;M_W,M_W)-\frac{1}{2}\\
&-\frac{r_t}{4}\Big[B^F_0(-s;M_W,M_W)+1\Big]\Bigg\}, \qquad \text{(A.4.54)}\\
F_{QL}(s,t) &= \frac{g^2}{16\pi^2}\Bigg\{\mathcal{F}^e_\gamma(s)+\mathcal{F}^f_\gamma(s)-s^2_W\Pi^F_{\gamma\gamma}(0)-\Delta\rho^F+\mathcal{D}^F_Z(s)+\Pi^F_{Z\gamma}(s)\\
&+\frac{1}{4c^2_W}\left(\delta^2_e+3v^2_f+a^2_f\right)\mathcal{F}_Z(s)+\hat{\mathcal{F}}_W(s)\\
&+c^2_W(R_Z-1)\left[\frac{|Q_f|}{2c^2_W}\left(1-4|Q_f|s^2_W\right)\mathcal{F}_Z(s)-|Q_{f'}|\mathcal{F}_{Wa}(s)+\hat{\mathcal{F}}_{Wn}(s)\right]\\
&+\frac{3}{2}B^F_0(-s;M_W,M_W)-\frac{11}{18}-\frac{r_t}{4}\Big[B^F_0(-s;M_W,M_W)+1\Big]\Bigg\}, \qquad \text{(A.4.55)}\\
F_{LQ}(s,t) &= \frac{g^2}{16\pi^2}\Bigg\{\mathcal{F}^e_\gamma(s)+\mathcal{F}^f_\gamma(s)-s^2_W\Pi^F_{\gamma\gamma}(0)-\Delta\rho^F+\mathcal{D}^F_Z(s)-\Pi^F_{Z\gamma}(s)\\
&+\frac{1}{4c^2_W}\left(3v^2_e+a^2_e+\delta^2_f\right)\mathcal{F}_Z(s)+\hat{\mathcal{F}}^{(0)}_W(s)\\
&+c^2_W(R_Z-1)\left[\frac{|Q_e|}{2c^2_W}\left(1-4|Q_e|s^2_W\right)\mathcal{F}_Z(s)+\hat{\mathcal{F}}^{(0)}_{Wn}(s)\right]\\
&+\frac{3}{2}B^F_0(-s;M_W,M_W)-\frac{11}{18}\Bigg\}, \qquad \text{(A.4.56)}\\
F_{QQ}(s,t) &= \frac{g^2}{16\pi^2}\Bigg\{\Big[\mathcal{F}^e_\gamma(s)+\mathcal{F}^f_\gamma(s)\Big]\left[1+\frac{c^2_W}{s^2_W}(1-R_Z)\right]-s^2_W\Pi^F_{\gamma\gamma}(0)\\
&-\frac{1}{s^2_W}\Delta\rho^F+\mathcal{D}^F_Z(s)-2\Pi^F_{Z\gamma}(s)-c^2_W(R_Z-1)\left[\hat{\Pi}^{\mathrm{bos},F}_{\gamma\gamma}(s)-\frac{2}{3}\right]\\
&-\frac{(R_W-1)}{4c^2_Ws^2_W}\left(\delta^2_e+\delta^2_f\right)\mathcal{F}_Z(s)+\frac{4}{3}B^F_0(-s;M_W,M_W)-\frac{13}{18}\Bigg\}, \qquad \text{(A.4.57)}
\end{aligned}$$

where we use the definitions

$$\mathcal{D}^F_Z(s) = \hat{\mathcal{D}}^{\mathrm{bos},F}_Z(s)+\mathcal{D}^{\mathrm{fer},F}_Z(s), \qquad \text{(A.4.58)}$$

$$\Pi^F_{Z\gamma}(s) = \hat{\Pi}^{\mathrm{bos},F}_{Z\gamma}(s)+\Pi^{\mathrm{fer,F}}_{Z\gamma}(s), \qquad \text{(A.4.59)}$$

and as usually decompose:

$$\Delta\rho^F=\Delta\rho^{\mathrm{bos},F}+\Delta\rho^{\mathrm{fer},F}. \qquad \text{(A.4.60)}$$

We complete this Subsection by presenting the massless limit of the WW box contribution:

$$\begin{aligned}
\hat{\mathcal{B}}^{d,0}_{WW}(s,t) &= \left[-t\left(1+\frac{t^2}{u^2}\right)-4\frac{M_W^2t^2}{u^2}+2\frac{M_W^4}{u}\left(1+2\frac{s}{u}\right)\right]D_0(-s,-t;M_W,0,M_W,0)\\
&-2\left(2+2\frac{s}{u}+\frac{s^2}{u^2}-2\frac{M_W^2s}{u^2}\right)C_0(-s;M_W,0,M_W)\\
&+2\left(2+3\frac{s}{u}+\frac{s^2}{u^2}+2\frac{M_W^2t}{u^2}\right)C_0(-t;0,M_W,0)\\
&-\frac{2}{u}\Big[B_0^F(-s;M_W,M_W)-B_0^F(-t;0,0)\Big], \qquad \text{(A.4.61)}
\end{aligned}$$

and of its addition with the m_t dependence:

$$\begin{aligned}
\hat{\mathcal{B}}^{d,t}_{WW}(s,t) &= \hat{\mathcal{B}}^{d}_{WW}(s,t)-\hat{\mathcal{B}}^{d,0}_{WW}(s,t)\\
&= \left[-t\left(1+\frac{t^2}{u^2}\right)-4\frac{M_W^2t^2}{u^2}+2\frac{M_W^4}{u}\left(1+2\frac{s}{u}\right)\right]\\
&\times\Big[D_0(-s,-t;M_W,0,M_W,m_t)-D_0(-s,-t;M_W,0,M_W,0)\Big]\\
&-\left(2+2\frac{s}{u}+\frac{s^2}{u^2}-2\frac{M_W^2s}{u^2}\right)\Big[C_0(-s;M_W,m_t,M_W)-C_0(-s;M_W,0,M_W)\Big]\\
&+\left(2+3\frac{s}{u}+\frac{s^2}{u^2}+2\frac{M_W^2t}{u^2}\right)\\
&\times\Big[C_0(-t;0,M_W,m_t)+C_0(-t;m_t,M_W,0)-2C_0(-t;0,M_W,0)\Big]\\
&+\frac{2}{u}\Big[B_0^F(-t;m_t,0)-B_0^F(-t;0,0)\Big]\\
&+r_t\Bigg\{\left[2+3\frac{s}{u}+2\frac{s^2}{u^2}-2\frac{M_W^2}{u}\left(1+2\frac{s}{u}\right)+\frac{m_t^2s}{u^2}\right]\\
&\times M_W^2D_0(-s,-t;M_W,0,M_W,m_t)\\
&-\frac{1}{2}\left[R_W\left(1+2\frac{s^2}{u^2}\right)-4+r_t(1-2R_W)+\frac{r_t^2}{R_W}\right]\\
&\times C_0(-s;M_W,m_t,M_W)-\frac{M_W^2s}{u^2}C_0(-s;M_W,0,M_W)\\
&-\frac{M_W^2t}{u^2}\Big[C_0(-t;0,M_W,m_t)+C_0(-t;m_t,M_W,0)\Big]\\
&+\frac{1}{2s}\Big[(1-r_t)\left[1-B_0^F(-s;M_W,M_W)\right]+r_t\ln r_t\Big]\Bigg\}. \qquad \text{(A.4.62)}
\end{aligned}$$

One-loop expression for Δr

In order to construct final expressions for ρ's and κ's we will need the well-known quantity Δr. It's derivation involves the full machinery of calculation of one-loop corrections for μ-decay that is similar to those presented for the decay and the scattering process here. However, the calculation is lengthy and we limit ourselves to the presentation of the resulting expression [3,4]. It is free of any singularities and reads as follows:

$$\Delta r = \frac{g^2}{16\pi^2}\left\{-\frac{2}{3}-\Pi^{\mathrm{fer,F}}_{\gamma\gamma}(0)+\frac{c_W^2}{s_W^2}\Delta\rho^F+\frac{1}{s_W^2}\left[\Delta\rho_W^F+\frac{11}{2}-\frac{5}{8}c_W^2(1+c_W^2)+\frac{9}{4}\frac{c_W^2}{s_W^2}\ln c_W^2\right]\right\},$$

(A.4.63)

where a new self-energy combination appears:

$$\Delta\rho_W^F = \frac{1}{M_W^2}\left[\Sigma_{WW}^F(0) - \Sigma_{WW}^F(M_W^2)\right]. \tag{A.4.64}$$

It is useful to present the *bosonic* components of the two ρ-factors entering Eq. (2.3.1):

$$\begin{aligned}\Delta\rho_W^{\mathrm{bos},F} &= \left(\frac{1}{12c_W^4}+\frac{4}{3c_W^2}-\frac{17}{3}-4c_W^2\right)B_0^F\left(-M_W^2;M_Z,M_W\right)\\ &+\left(1-\frac{1}{3}r_W+\frac{1}{12}r_W^2\right)B_0^F\left(-M_W^2;M_H,M_W\right)\\ &+\left(\frac{3}{4(1-r_W)}+\frac{1}{4}-\frac{1}{12}r_W\right)r_W\ln r_W+\left(\frac{1}{12c_W^4}+\frac{17}{12c_W^2}-\frac{3}{s_W^2}+\frac{1}{4}\right)\ln c_W^2\\ &+\frac{1}{12c_W^4}+\frac{11}{8c_W^2}+\frac{139}{36}-\frac{177}{24}c_W^2+\frac{5}{8}c_W^4-\frac{1}{12}r_W\left(\frac{7}{2}-r_W\right),\end{aligned} \tag{A.4.65}$$

and

$$\begin{aligned}\Delta\rho^{\mathrm{bos},F} &= \left(\frac{1}{12c_W^2}+\frac{4}{3}-\frac{17}{3}c_W^2-4c_W^4\right)\\ &\times\left[B_0^F\left(-M_Z^2;M_W,M_W\right)-\frac{1}{c_W^2}B_0^F\left(-M_W^2;M_Z,M_W\right)\right]\\ &-\left(1-\frac{1}{3}r_W+\frac{1}{12}r_W^2\right)B_0^F\left(-M_W^2;M_H,M_W\right)\\ &+\left(1-\frac{1}{3}r_Z+\frac{1}{12}r_Z^2\right)\frac{1}{c_W^2}B_0^F\left(-M_Z^2;M_H,M_W\right)\\ &+\frac{1}{12}s_W^2r_W^2\left(\ln r_W-1\right)-\left(\frac{1}{12c_W^4}+\frac{1}{2c_W^2}-2+\frac{1}{12}r_W\right)\ln c_W^2\\ &-\frac{1}{12c_W^4}-\frac{19}{36c_W^2}-\frac{133}{18}+8c_W^2.\end{aligned} \tag{A.4.66}$$

The expressions for their *fermionic* components are derived straightforwardly from the defining equations.

A.4.4. The form factors ρ_Z^f, κ_Z^f, and $\rho_{ef}, \kappa_{ef}, \kappa_e, \kappa_f$

In this Subsection we complete the construction of one-loop corrected amplitudes for the decay and the scattering process. First of all we observe that the final expressions for the one-loop form factors Eq. (A.4.45) (for the decay) and Eq. (A.4.57) (for the scattering process) contain common factors: $\mathcal{F}_\gamma^f\left(M_Z^2\right)$ and $\mathcal{F}_\gamma^e(s)+\mathcal{F}_\gamma^f(s)$. These factors have to be excluded from the electroweak form factors and shifted to the QED part of the corrections (together with $\gamma\gamma$ and γZ boxes) in order to be eventually combined with the bremsstrahlung contributions thus forming the infrared free complete QED correction.

Secondly, we change the normalization $\alpha(0)\to G_\mu$, thereby making profit of the precisely known quantity G_μ.

Expression for ρ_Z^f and κ_Z^f for the Z-decay

The sum of the one-loop Z-decay amplitude and the corresponding Born amplitude is being rewritten as:

$$V_\mu^{Zf\bar{f}}\left(M_Z^2\right) = (2\pi)^4\, i\, i\sqrt{\sqrt{2}G_\mu M_Z^2}\sqrt{\rho_Z^f} I_f^{(3)} \gamma_\mu \left[(1+\gamma_5) - 4|Q_f| s_W^2 \kappa_Z^f\right]. \tag{A.4.67}$$

The new electroweak effective couplings ρ_Z^f and κ_Z^f are related to the one-loop decay form factors of Eq. (A.4.45):

$$\rho_Z^f = 1 + 2F_{_L} - s_W^2 \Delta r, \tag{A.4.68}$$
$$\kappa_Z^f = 1 + F_{_Q} - F_{_L}. \tag{A.4.69}$$

One easily derives the final expressions for ρ_Z^f and κ_Z^f:

$$\rho_Z^f = 1 + \frac{g^2}{16\pi^2}\left[\Sigma'_{_{ZZ}}(M_Z^2) - \Delta\rho_Z^F - \frac{11}{2} + \frac{5}{8}c_W^2(1+c_W^2) - \frac{9}{4}\frac{c_W^2}{s_W^2}\ln c_W^2 + 2u_f\right], \tag{A.4.70}$$

$$\kappa_Z^f = 1 + \frac{g^2}{16\pi^2}\left[-\frac{c_W^2}{s_W^2}\Delta\rho^F + \Pi_{Z\gamma}^F(M_Z^2) + \frac{\delta_f^2}{4c_W^2}\mathcal{F}_{_Z}\left(M_Z^2\right) - u_f\right], \tag{A.4.71}$$

where two new quantities are used:

$$\Delta\rho_Z^F = \frac{1}{M_W^2}\left[\Sigma_{WW}^F(0) - \Sigma_{ZZ}^F(M_Z^2)\right], \tag{A.4.72}$$

$$u_f = \frac{3v_f^2 + a_f^2}{4c_W^2}\mathcal{F}_{_Z}\left(M_Z^2\right) + \mathcal{F}_{_W}\left(M_Z^2\right). \tag{A.4.73}$$

The first combination is a 'variation' of Veltman's ρ-parameter, which has the same asymptotic behaviour as $\Delta\rho^F$ and, as usually, may be presented as the sum of bosonic and fermionic components:

$$\Delta\rho_Z^F = \Delta\rho_Z^{\mathrm{bos},F} + \Delta\rho_Z^{\mathrm{fer,F}}. \tag{A.4.74}$$

Construction of ρ_{ef} and κ_{ij} for the scattering process

Similarly to Eq. (2.4.1), we define the net sum of Born and one-loop amplitudes for the scattering process in terms of four effective form factors $\rho_{ef}(s,t)$ and $\kappa_{ij}(s,t)$:

$$\begin{aligned}\mathcal{A}_Z^{_{OLA}}(s,t) = {} & i\sqrt{2}G_\mu I_e^{(3)} I_f^{(3)} M_Z^2 \chi_Z(s) \rho_{ef}(s,t)\Big\{\gamma_\mu(1+\gamma_5)\otimes\gamma_\mu(1+\gamma_5) \\ & -4|Q_e|s_W^2\kappa_e(s,t)\gamma_\mu\otimes\gamma_\mu(1+\gamma_5) - 4|Q_f|s_W^2\kappa_f(s,t)\gamma_\mu(1+\gamma_5)\otimes\gamma_\mu \\ & +16|Q_eQ_f|s_W^4\kappa_{e,f}(s,t)\gamma_\mu\otimes\gamma_\mu\Big\}.\end{aligned} \tag{A.4.75}$$

The form factors are simply related to the one-loop form factors Eq. (A.4.57):

$$\rho_{ef} = 1 + F_{_{LL}}(s,t) - s_W^2\Delta r, \tag{A.4.76}$$
$$\kappa_e = 1 + F_{_{QL}}(s,t) - F_{_{LL}}(s,t), \tag{A.4.77}$$
$$\kappa_f = 1 + F_{_{LQ}}(s,t) - F_{_{LL}}(s,t), \tag{A.4.78}$$
$$\kappa_{ef} = 1 + F_{_{QQ}}(s,t) - F_{_{LL}}(s,t). \tag{A.4.79}$$

After some trivial algebra one derives the final expressions:

$$\begin{aligned}
\rho_{ef} &= 1+\frac{g^2}{16\pi^2}\Bigg\{-\Delta\rho_{Z}^{F}+\mathcal{D}_{Z}^{F}\left(s\right)+\frac{5}{3}B_0^F\left(-s;M_W,M_W\right)-\frac{9}{4}\frac{c_W^2}{s_W^2}\ln c_W^2-6\\
&+\frac{5}{8}c_W^2\left(1+c_W^2\right)+\frac{1}{4c_W^2}\left(3v_e^2+a_e^2+3v_f^2+a_f^2\right)\mathcal{F}_{Z}\left(s\right)+\hat{\mathcal{F}}_{W}^{0}\left(s\right)+\hat{\mathcal{F}}_{W}\left(s\right)\\
&-\frac{r_t}{4}\Big[B_0^F\left(-s;M_W,M_W\right)+1\Big]-c_W^2\left(R_Z-1\right)s\hat{\mathcal{B}}_{WW}^{d}\left(s,t\right)\Bigg\}, \qquad \text{(A.4.80)}\\
\kappa_e &= 1+\frac{g^2}{16\pi^2}\Bigg\{-\frac{c_W^2}{s_W^2}\Delta\rho^F-\Pi_{Z\gamma}^{F}(s)-\frac{1}{6}B_0^F\left(-s;M_W,M_W\right)-\frac{1}{9}-\frac{v_e\sigma_e}{2c_W^2}\mathcal{F}_{Z}\left(s\right)\\
&-\hat{\mathcal{F}}_{W}^{0}\left(s\right)+\left(R_Z-1\right)\Bigg[\frac{|Q_f|}{2}\left(1-4|Q_f|s_W^2\right)\mathcal{F}_{Z}\left(s\right)+c_W^2\Big[\hat{\mathcal{F}}_{Wn}\left(s\right)\\
&-|Q_{f'}|\mathcal{F}_{Wa}\left(s\right)+s\hat{\mathcal{B}}_{WW}^{d}\left(s,t\right)\Big]\Bigg]\Bigg\}, \qquad \text{(A.4.81)}\\
\kappa_f &= 1+\frac{g^2}{16\pi^2}\Bigg\{-\frac{c_W^2}{s_W^2}\Delta\rho^F-\Pi_{Z\gamma}^{F}(s)-\frac{1}{6}B_0^F\left(-s;M_W,M_W\right)-\frac{1}{9}-\frac{v_f\sigma_f}{2c_W^2}\mathcal{F}_{Z}\left(s\right)\\
&-\hat{\mathcal{F}}_{W}\left(s\right)+\left(R_Z-1\right)\Bigg[\frac{|Q_e|}{2}\left(1-4|Q_e|s_W^2\right)\mathcal{F}_{Z}\left(s\right)+c_W^2\Big[\hat{\mathcal{F}}_{Wn}^{0}\left(s\right)\\
&-|Q_{e'}|\mathcal{F}_{Wa}\left(s\right)+s\hat{\mathcal{B}}_{WW}^{d}\left(s,t\right)\Big]\Bigg]-\frac{r_t}{4}\Big[B_0^F\left(-s;M_W,M_W\right)+1\Big]\Bigg\}, \qquad \text{(A.4.82)}\\
\kappa_{ef} &= 1+\frac{g^2}{16\pi^2}\Bigg\{-2\frac{c_W^2}{s_W^2}\Delta\rho^F-2\Pi_{Z\gamma}^{F}(s)-\frac{1}{3}B_0^F\left(-s;M_W,M_W\right)-\frac{2}{9}\\
&-\frac{1}{4c_W^2}\left[\frac{\delta_e^2+\delta_f^2}{s_W^2}\left(R_W-1\right)+3v_e^2+a_e^2+3v_f^2+a_f^2\right]\mathcal{F}_{Z}\left(s\right)\\
&-\hat{\mathcal{F}}_{W}^{0}\left(s\right)-\hat{\mathcal{F}}_{W}\left(s\right)-\frac{r_t}{4}\Big[B_0^F\left(-s;M_W,M_W\right)+1\Big]\\
&+c_W^2\left(R_Z-1\right)\left[\frac{2}{3}-\hat{\Pi}_{\gamma\gamma}^{\mathrm{bos},F}(s)+s\hat{\mathcal{B}}_{WW}^{d}\left(s,t\right)\right]\Bigg\}. \qquad \text{(A.4.83)}
\end{aligned}$$

In Eq. (A.4.83) we used the definitions:

$$\begin{aligned}
\hat{\mathcal{F}}_{W}\left(s\right) &= c_W^2\hat{\mathcal{F}}_{Wn}\left(s\right)-\frac{1}{2}\sigma_{f'}^{a}\mathcal{F}_{Wa}\left(s\right)-\frac{1}{2}\overline{\mathcal{F}}_{Wa}\left(s\right), \qquad \text{(A.4.84)}\\
\hat{\mathcal{F}}_{W}^{0}\left(s\right) &= c_W^2\hat{\mathcal{F}}_{Wn}^{0}\left(s\right)-\frac{1}{2}\mathcal{F}_{Wa}^{0}\left(s\right), \qquad \text{(A.4.85)}\\
\mathcal{D}_{Z}^{F}\left(s\right) &= \hat{\mathcal{D}}_{Z}^{\mathrm{bos},F}\left(s\right)+\mathcal{D}_{Z}^{\mathrm{fer},F}\left(s\right), \qquad \text{(A.4.86)}\\
\Pi_{Z\gamma}^{F}(s) &= \hat{\Pi}_{Z\gamma}^{\mathrm{bos},F}(s)+\Pi_{Z\gamma}^{\mathrm{fer},F}(s). \qquad \text{(A.4.87)}
\end{aligned}$$

These effective form factors are used in ZFITTER for the calculation of the one-loop EWRC.

A.5. Relations Between Earlier and Actual Notations

Here we provide some useful relations between notations used in this description and notations of Section 4.4 of [96].

A.5.1. N-point functions

Relations between definitions of two-point functions:

$$B_0^F(-s;M_W,M_W)-2 = \frac{1}{2s}L_{WW}(s)=\left(s^2-4M_W^2 s\right)\mathcal{F}(-s,M_W^2,M_W^2), \quad \text{(A.5.88)}$$

$$B_0^F(-s;M_H,M_Z) = \ln c_W^2-\frac{1}{2}\ln r_Z+2-\frac{1}{2}R_Z\left(r_Z-1\right)\ln r_Z+\frac{1}{2s}L_{ZH}(s). \quad \text{(A.5.89)}$$

The definitions of $\mathcal{F}(-s,M_W^2,M_W^2)$, $\mathcal{F}_3(s,M_W^2)$, and $\mathcal{F}_4(s,I_1,M_W^2)$ below were introduced in [8].

Relations between definitions of three- and four-point functions:

$$\begin{array}{lcll}
C_0(-s;m_t,M_W,m_t) & = & \texttt{XS3T}, & \\
C_0(-s;0,M_W,0) & = & \texttt{XS3T0}, & \\
C_0(-s;M_W,m_t,M_W) & = & \texttt{XS3W}, & \\
C_0(-s;M_W,0,M_W) & = & \texttt{XS3W0} & = -\dfrac{1}{s}\mathcal{F}_3(s,M_W^2), \\
C_0(-s;m_t,M_W,0) & = & \texttt{XJ3WT}, & \\
C_0(-s;0,M_W,0) & = & \texttt{XJ3W0}, & \\
D_0(-s,t;M_W,0,M_W,m_t) & = & \texttt{XS4WT}, & \\
D_0(-s,t;M_W,0,M_W,0) & = & \texttt{XS4W0} & = \dfrac{1}{s^2}\mathcal{F}_4(s,-u,M_W^2).
\end{array} \quad \text{(A.5.90)}$$

They are supplied by calls to different subroutines:

```
CALL S3WANA(AMT2,AMW2,-S,XJ0W,XS3W,XS3W0)
```

```
CALL S3WANA(AMW2,AMT2,-S,XJ0T,XS3T,XS3T0)
```

```
CALL J3WANA( 0D0,AMW2,AI12,XJ3W0)
```

```
CALL J3WANA(AMT2,AMW2,AI12,XJ3WT)
```

```
CALL S4WANA(AMT2,AMW2,-S,AI12,XS4WT)
```

```
CALL S4WANA( 0D0,AMW2,-S,AI12,XS4W0)
```

Here are the relations between the definitions of the self-energy contributions γ and Z (see Eqs. (A.3.14)–(A.3.18)):

$$A(s) = \hat{\Pi}_{\gamma\gamma}^{\mathrm{bos},F}(s), \quad \text{(A.5.91)}$$

$$D_{Z,f}(s) = \mathcal{D}_Z^{\mathrm{fer},F}(s), \quad \text{(A.5.92)}$$

$$D_{Z,b}(s) = \hat{\mathcal{D}}_Z^{\mathrm{bos},F}(s), \quad \text{(A.5.93)}$$

and the γZ-mixing functions (see Eqs. (A.3.27)–(A.3.28)):

$$M_f(s) = \texttt{XAMM1F} = -\Pi_{Z\gamma}^{\mathrm{fer},F}(s). \quad \text{(A.5.94)}$$

Relations between derivatives of the Z self-energy function (see Eqs. (A.3.35)–(A.3.37)) are:

$$\begin{aligned} Z_b^F(M_Z^2) &= \texttt{XZFM1} = \frac{1}{c_W^2}\left[\Sigma'_{ZZ}(M_Z^2)\right]^{\mathrm{bos},F}, \\ Z_f^F(M_Z^2) &= \texttt{XZFM1F} = \frac{1}{c_W^2}\left[\Sigma'_{ZZ}(M_Z^2)\right]^{\mathrm{fer},F}. \end{aligned} \tag{A.5.95}$$

Those for the bosonic parts of self-energy counter-terms (see Eq. (A.3.29)) are:

$$W_b(0) = \texttt{W0} = \frac{1}{M_W^2}\Sigma^{\mathrm{bos}}_{WW}(0), \tag{A.5.96}$$

$$W_b(M_W^2) = \texttt{XWM1} = \frac{1}{M_W^2}\Sigma^{\mathrm{bos}}_{WW}(M_W^2), \tag{A.5.97}$$

$$Z_b(M_Z^2) = \texttt{XZM1} = \frac{1}{c_W^2 M_Z^2}\Sigma^{\mathrm{bos}}_{WW}(M_Z^2), \tag{A.5.98}$$

and for the fermionic parts (see Eqs. (A.3.28) and (A.3.30)):

$$Z_f(M_Z^2) = \texttt{XZM1F} = \frac{1}{c_W^2 M_Z^2}\Sigma^{\mathrm{fer},F}_{ZZ}(M_Z^2), \tag{A.5.99}$$

$$W_f(M_W^2) = \texttt{XWM1F} = \frac{1}{M_W^2}\Sigma^{\mathrm{fer},F}_{WW}(M_W^2). \tag{A.5.100}$$

A.5.2. Vertex functions

For the vertex functions (see Eqs. (A.4.23) and (A.4.30)) the relations between different notations are:

$$V_{1_Z}(s) = \mathcal{F}_{_Z}(s), \tag{A.5.101}$$

$$V_{1_W}(s) = \mathcal{F}_{_{Wa}}(s), \tag{A.5.102}$$

$$V_{2_W}(s) = \hat{\mathcal{F}}^0_{_{Wn}}(s). \tag{A.5.103}$$

The vertex functions in the limit of vanishing fermion masses are calculated in subroutine VERTZW:

$$\texttt{V1ZZ} = \mathcal{F}_{_Z}\left(M_Z^2\right), \tag{A.5.104}$$

$$\texttt{V1ZW} = \mathcal{F}^0_{_{Wa}}\left(M_Z^2\right), \tag{A.5.105}$$

$$\texttt{V2ZWW} = \mathcal{F}^0_{_{Wn}}\left(M_Z^2\right). \tag{A.5.106}$$

Appendix B

Subroutine ZFTEST and Test Sample Output

B.1. Subroutine ZFTEST

The ZFITTER distribution package includes subroutine ZFTEST, which serves essentially for three purposes:

1. It is an example of how to use ZFITTER.
2. It is an internal consistency check of the different ZFITTER branches.
3. It allows one to check that ZFITTER has been properly installed on the machine.

The routine creates a Table of cross-sections and asymmetries as functions of $\sqrt{s}$ near the Z peak, below, and above.

An example of how to run ZFTEST is contained in the file zfmai6_21.f, which contains some useful information:

```
*
* MAIN to call ZFTEST
*
* to compile and link:
*
* f77 -K zfmai6_21.f zfitr6_21.f dizet6_21.f acol6_1.f m2tcor5_11.f pairho.f
* bcqcdl5_14.f bkqcdl5_14.f bhang4_67.f zf514_aux.f -o zfitr6_21.exe
*
* Warning! option -K is mandatory on some WS's while on the others
* leads to "illegal option -- K" while linking
*
* Starting 6.06, ZFITTER became Linux-compatible.
*
* In Dubna it is used under "Welcome to Linux 2.0.34"
* and compiled with the command suggested by G.Quast
*
```

```
* f77 *.f  -c -O3 -DCPU=596 -fno-automatic
*
      CALL ZFTEST(1)
      END
```

After compiling, linking, and running of the whole package of eleven files the results presented in Subsection B.1.2 should be reproduced.

B.1.1. Subroutine ZFTEST

```
      SUBROUTINE ZFTEST(IMISC)                                          *
*     ========== =============                                         *
************************************************************************
*                                                                       *
*     SUBR. ZFTEST                                                      *
*                                                                       *
*     Example program to demonstrate the use of the ZFITTER package.    *
*                                                                       *
************************************************************************
*
      IMPLICIT REAL*8(A-H,O-Z)
      COMPLEX*16 XALLCH,XFOTF
*
      DIMENSION XS(0:11,6),AFB(0:11,5),TAUPOL(2),TAUAFB(2),ALRI(0:11,2)
*
* constants
*
      PARAMETER(ALFAI=137.0359895D0,ALFA=1.D0/ALFAI,CONS=1.D0)
      PARAMETER(ZMASS=91.1867D0,TMASS=173.8D0,HMASS=100.D0)
      PARAMETER(ALFAS=.119D0)
      PARAMETER(RSMN=87.D0,DRS=1.D0,NRS=9)
      PARAMETER(ANG0=35D0,ANG1=145D0)
      PARAMETER(QE=-1.D0,AE=-.5D0,QU= 2.D0/3.D0,AU= .5D0,
     +                            QD=-1.D0/3.D0,AD=-.5D0)
*
* ZFITTER common blocks
*
      COMMON /ZUPARS/QDF,QCDCOR(0:14),ALPHST,SIN2TW,S2TEFF(0:11),
     & WIDTHS(0:11)
*
      COMMON /CDZRKZ/ARROFZ(0:10),ARKAFZ(0:10),ARVEFZ(0:10),ARSEFZ(0:10)
     &              ,AROTFZ(0:10),AIROFZ(0:10),AIKAFZ(0:10),AIVEFZ(0:10)
      COMMON /CDZAUX/PARTZA(0:10),PARTZI(0:10),RENFAC(0:10),SRENFC(0:10)
*
      COMMON /EWFORM/ XALLCH(5,4),XFOTF
*
*---------------------------------------------------------------------
*
* initialize
```

```
*
      CALL ZUINIT
*
* set ZFITTER flags and print flag values
*
      CALL ZUFLAG('PRNT',1)
      CALL ZUFLAG('MISC',IMISC)
      CALL ZUFLAG('ISPP',1)
      ICUTC=-1
*
* do weak sector calculations
*
      DAL5H=2.8039808929734D-02
*
      CALL ZUWEAK(ZMASS,TMASS,HMASS,DAL5H,ALFAS)
*
* define cuts for fermion channels and print cut values
*
      CALL ZUCUTS(11,0,15.D0,10.D0,0.D0,ANG0,ANG1,0.D0)
      CALL ZUINFO(0)
*
* make table of cross-sections and asymmetries
*
      PI   = DACOS(-1.D0)
*
* DO loop over S
*
      DO I = 1,8
*
* array of RS=SQRT(S)
*
        IF(I.EQ.1) RS=35D0
        IF(I.EQ.2) RS=65D0
        IF(I.EQ.3) RS=ZMASS-2D0
        IF(I.EQ.4) RS=ZMASS
        IF(I.EQ.5) RS=ZMASS+2D0
        IF(I.EQ.6) RS=100D0
        IF(I.EQ.7) RS=140D0
        IF(I.EQ.8) RS=175D0
*
* Changing of default, for instance:
* 1) NO PAIRS at PETRA and TRISTAN
*
        IF(I.LT.3.) CALL ZUFLAG('ISPP',0)
        IF(I.GE.3.) CALL ZUFLAG('ISPP',1)
*
* The OUTPUT is adjusted for hp WS at Zeuthen
*
```

```
      IF(I.EQ.5.OR.I.EQ.8) THEN
        PRINT *
        PRINT *
        PRINT *
          ELSE
        PRINT *
      ENDIF
* table header
        PRINT *,' SQRT(S) = ',REAL(RS)
        PRINT *
        PRINT 1000
 1000   FORMAT(1X,'     '
     +  ,'<-------------- Cross-section -------------->'
     +  ,'  <------- Asymmetry ------->','  <--Tau_Pol-->',
     +   '  <----A_LR--->')
        PRINT 1001
 1001   FORMAT(1X,'INDF   ZUTHSM   ZUXSEC    ZUXSA   ZUXSA2   ZUXAFB'
     +,'   ZUTHSM  ZUXSA ZUXSA2 ZUXAFB ZUTPSM  ZUTAU  ZULRSM  ZUALR')
*
* loop over fermion indicies
*
        DO INDF = 0,11
         S=RS**2
         IF(INDF.NE.11)
     +   CALL ZUCUTS(INDF,ICUTC,0D0,0D0,1D-2*S,0D0,180D0,.25D0*S)
* standard model interf. (INTRF=1)
         CALL ZUTHSM(INDF,RS,ZMASS,TMASS,HMASS,DAL5H,ALFAS,
     +     XS(INDF,1),AFB(INDF,1))
         IF(INDF.EQ.3) CALL ZUTPSM(RS,ZMASS,TMASS,HMASS,DAL5H,ALFAS,
     +     TAUPOL(1),TAUAFB(1))
* cross-section interf. (INTRF=2)
           GAME = WIDTHS(   1)/1000.
           GAMF = GAME
           GAMZ = WIDTHS(11)/1000.
           IF(INDF.NE.11) GAMF = WIDTHS(INDF)/1000.
           CALL ZUXSEC(INDF,RS,ZMASS,GAMZ,GAME,GAMF,XS(INDF,2))
* cross-section & forward-backward asymmetry interf. (INTRF=3)
         IF(INDF.NE.0 .AND. INDF.NE.10) THEN
           IF(IMISC.EQ.0) THEN
             ROEE= AROTFZ(1)
           ELSE
             ROEE= ARROFZ(1)
           ENDIF
          IF(IMISC.EQ.0) THEN
            GAE= SQRT(AROTFZ(1))/2
          ELSE
            GAE= SQRT(ARROFZ(1))/2
          ENDIF
```

```
          GVE  = ARVEFZ(1)*GAE
*
           IF(INDF.LT.11) THEN
             IF(IMISC.EQ.0) THEN
               ROFI= AROTFZ(INDF)
               GAF = SQRT(AROTFZ(INDF))/2
             ELSE
               ROFI= ARROFZ(INDF)
               GAF = SQRT(ARROFZ(INDF))/2
             ENDIF
             GVF = ARVEFZ(INDF)*GAF
           ELSEIF(INDF.EQ.11) THEN
             GAF = GAE
             GVF = ARVEFZ(1)*GAF
           ENDIF
           CALL ZUXSA(INDF,RS,ZMASS,GAMZ,0,GVE,GAE,GVF,GAF,
CB: MODE=1 CALL ZUXSA(INDF,RS,ZMASS,GAMZ,1,GVE/GAE,ROEE,GVF/GAF,ROFI,
     +     XS(INDF,3),AFB(INDF,3))
         ENDIF
* tau polarization interf. (INTRF=3)
         IF(INDF.EQ.3) CALL ZUTAU(RS,ZMASS,GAMZ,0,GVE,GAE,GVF,GAF,
     +     TAUPOL(2),TAUAFB(2))
* left-right polarization Asymmetry (IBRA=4)
         IF((INDF.GE.4.AND.INDF.LE.7).OR.INDF.EQ.9) THEN
          POL=.63D0
          CALL
     &    ZULRSM(INDF,RS,ZMASS,TMASS,HMASS,DAL5H,ALFAS,POL,XSPL,XSMI)
          ALRI(INDF,1)=(XSMI-XSPL)/(XSMI+XSPL)/POL
         ENDIF
         IF(INDF.EQ.10) THEN
          POL=.65D0
          XSMINS=0D0
          XSPLUS=0D0
          DO 2004 IALR=4,9
           IF(IALR.EQ.8) GO TO 2004
           CALL
     &     ZULRSM(IALR,RS,ZMASS,TMASS,HMASS,DAL5H,ALFAS,POL,XSPL,XSMI)
           XSMINS=XSMINS+XSMI
           XSPLUS=XSPLUS+XSPL
2004       CONTINUE
          ALRI(INDF,1)=(XSMINS-XSPLUS)/(XSMINS+XSPLUS)/POL
         ENDIF
*
* cross-section & forward-backward asymmetry interf. for gv**2 and ga**2(IBRA=4)
*
         IF(INDF.GE.1 .AND. INDF.LE.3 .OR. INDF.EQ.11) THEN
           IF(INDF.LT.11) THEN
             IF(IMISC.EQ.0) THEN
```

```
              ROFI= AROTFZ(INDF)
              GAF = SQRT(AROTFZ(INDF))/2
            ELSE
              ROFI= ARROFZ(INDF)
              GAF = SQRT(ARROFZ(INDF))/2
            ENDIF
            GVF = ARVEFZ(INDF)*GAF
          ELSEIF(INDF.EQ.11) THEN
            IF(IMISC.EQ.0) THEN
              ROFI= AROTFZ(1)
              GAF = SQRT(AROTFZ(1))/2
            ELSE
              ROFI= ARROFZ(1)
              GAF = SQRT(ARROFZ(1))/2
            ENDIF
            GVF = ARVEFZ(1)*GAF
          ENDIF
          GVF2= GVF**2
          GAF2= GAF**2
          CALL ZUXSA2(INDF,RS,ZMASS,GAMZ,0,GVF2,GAF2,
CB: MODE=1 CALL ZUXSA2(INDF,RS,ZMASS,GAMZ,1,GVF2/GAF2,ROEE**2,
     +     XS(INDF,4),AFB(INDF,4))
*
* cross-section & forward-backward asymmetry interf. for gve*gae*gvf*gaf,
* gve**2+gae**2 and gvf**2+gaf**2 (IBRA=6)
*
          PFOUR=GVE*GVF*GAE*GAF
          PVAE2=GVE**2+GAE**2
          PVAF2=GVF**2+GAF**2
          IF(INDF.NE.11) THEN
           CALL ZUXAFB(INDF,RS,ZMASS,GAMZ,PFOUR,PVAE2,PVAF2,
     +      XS(INDF,5),AFB(INDF,5))
          ENDIF
        ENDIF
* S-matrix interf. (ISMA=1, via SMATASY)
* results
        IF(INDF.EQ.0) THEN
          PRINT 9000,INDF,(XS(INDF,J),J=1,2)
        ELSEIF(INDF.EQ.1) THEN
          PRINT 9010,INDF,(XS(INDF,J),J=1,5),AFB(INDF,1),
     +     (AFB(INDF,J),J=3,5)
        ELSEIF(INDF.EQ.2) THEN
          PRINT 9010,INDF,(XS(INDF,J),J=1,5),AFB(INDF,1),
     +     (AFB(INDF,J),J=3,5)
        ELSEIF(INDF.EQ.3) THEN
          PRINT 9015,INDF,(XS(INDF,J),J=1,5),AFB(INDF,1),
     +     (AFB(INDF,J),J=3,5),(TAUPOL(J),J=1,2)
        ELSEIF(INDF.EQ.10) THEN
```

```
          PRINT 9025,INDF,(XS(INDF,J),J=1,2),(ALRI(INDF,J),J=1,2)
        ELSEIF(INDF.EQ.11) THEN
          PRINT 9011,INDF,(XS(INDF,J),J=1,4),AFB(INDF,1),
     +      (AFB(INDF,J),J=3,4)
        ELSE
          PRINT 9020,INDF,(XS(INDF,J),J=1,3),AFB(INDF,1),AFB(INDF,3)
     +                 ,(ALRI(INDF,J),J=1,2)
         ENDIF
       ENDDO
       PRINT *
      ENDDO
      RETURN
 9000 FORMAT(1X,I4, 2F9.5)
 9010 FORMAT(1X,I4, 5F9.5, 2X,4F7.4)
 9011 FORMAT(1X,I4, 4F9.5,11X,4F7.4)
 9015 FORMAT(1X,I4, 5F9.5, 2X,6F7.4)
 9020 FORMAT(1X,I4, 3F9.5,20X,2F7.4,28X,2F7.4)
 9025 FORMAT(1X,I4, 2F9.5,71X,2F7.4)
*                                                          END ZFTEST
      END
```

B.1.2. ZFTEST Results

Here we include the standard test-outputs, produced by a call to `ZFTEST(0/1)` for two values of flag `MISD`.

The first one corresponds to `MISD=0`. The numbers from different interfaces agree only at $s = M_Z^2$.

The second output, produced with `MISD=1`, exhibits a beautiful agreement of numbers from different interfaces in a wide energy range, $\sqrt{s}$ from 35 to 175 GeV (with the only exclusion for `INDF=10` for $\sqrt{s} > 100$ GeV). It is remarkable that due to a non-straightforward coding the CPU time increase with s-dependent remnants is only about 20% compared to the use of `MISD=0`.

```
**************************************************
**************************************************
**           This is ZFITTER version 6.21       **
**                    99/07/26                  **
**************************************************
** http://www.ifh.de/theory/publist.html        **
**************************************************

ZUINIT> ZFITTER defaults:

ZFITTER flag values:
AFBC:  1 SCAL:  0 SCRE:  0 AMT4:  4 BORN:  0
BOXD:  1 CONV:  1 FINR:  1 FOT2:  3 GAMS:  1
DIAG:  1 INTF:  1 BARB:  2 PART:  0 POWR:  1
PRNT:  0 ALEM:  3 QCDC:  3 VPOL:  1 WEAK:  1
FTJR:  1 EXPR:  0 EXPF:  0 HIGS:  0 AFMT:  1
CZAK:  1 PREC:10 HIG2:  0 ALE2:  3 GFER:  2
ISPP:  2 FSRS:  1 MISC:  0 MISD:  1 IPFC:  5
IPSC:  0 IPTO:  3


ZFITTER cut values:
  INDF   ICUT     ACOL     EMIN     S_PR     ANGO     ANG1      SPP
     0     -1     0.00     0.00     0.00     0.00   180.00     0.00
     1     -1     0.00     0.00     0.00     0.00   180.00     0.00
     2     -1     0.00     0.00     0.00     0.00   180.00     0.00
     3     -1     0.00     0.00     0.00     0.00   180.00     0.00
     4     -1     0.00     0.00     0.00     0.00   180.00     0.00
     5     -1     0.00     0.00     0.00     0.00   180.00     0.00
     6     -1     0.00     0.00     0.00     0.00   180.00     0.00
     7     -1     0.00     0.00     0.00     0.00   180.00     0.00
     8     -1     0.00     0.00     0.00     0.00   180.00     0.00
     9     -1     0.00     0.00     0.00     0.00   180.00     0.00
    10     -1     0.00     0.00     0.00     0.00   180.00     0.00
    11     -1     0.00     0.00     0.00     0.00   180.00     0.00


ZFITTER input parameters:
 ZMASS =   91.18670;   TMASS =  173.80000
 HMASS =  100.00000
 DAL5H =    0.02804;  ALQED5 =  128.88524
 ALFAS =    0.11900;   ALFAT =    0.10837

ZFITTER intermediate results:
 WMASS =   80.37380;  SIN2TW =    0.22310

ALPHST =    0.11900;
QCDCOR =  1.00000 1.04005 1.04725 1.03944 1.03225 1.04008 1.04700 1.03944 1.03225 1.04005 1.04725 1.04003 1.02575-0.00002 0.20202

CHANNEL          WIDTH          RHO_F_R         RHO_F_T         SIN2_EFF
-------          -------        --------        --------        --------
nu,nubar        167.234        1.008182        1.008182        0.231221
e+,e-            83.995        1.005428        1.005281        0.231601
mu+,mu-          83.995        1.005428        1.005281        0.231601
tau+,tau-        83.805        1.005428        1.005281        0.231601
u,ubar          300.154        1.006027        1.005976        0.231495
d,dbar          382.996        1.006951        1.006943        0.231368
c,cbar          300.092        1.006027        1.005976        0.231495
s,sbar          382.996        1.006951        1.006943        0.231368
t,tbar            0.000        0.000000        0.000000        0.000000
b,bbar          375.993        0.994243        0.994243        0.232950
hadron         1742.231
total          2495.727
```

```
USE OF AN OBSOLETED OPTION, ICUT=0;
Might be useful for backcompatibility with 5.xx;
Presently, ICUT=2,3 recommended for realistic cuts.
ZFITTER flag values:
AFBC: 1 SCAL: 0 SCRE: 0 AMT4: 4 BORN: 0
BOXD: 1 CONV: 1 FINR: 1 FOT2: 3 GAMS: 1
DIAG: 1 INTF: 1 BARB: 2 PART: 0 POWR: 1
PRNT: 1 ALEM: 3 QCDC: 3 VPOL: 1 WEAK: 1
FTJR: 1 EXPR: 0 EXPF: 0 HIGS: 0 AFMT: 1
CZAK: 1 PREC:10 HIG2: 0 ALE2: 3 GFER: 2
ISPP: 1 FSRS: 1 MISC: 0 MISD: 1 IPFC: 5
IPSC: 0 IPTO: 3


 SQRT(S) =   35.

     <-------------- Cross Section -------------->  <------- Asymmetry ------->  <--Tau_Pol-->  <----A_LR--->
INDF   ZUTHSM   ZUXSEC    ZUXSA   ZUXSA2   ZUXAFB   ZUTHSM  ZUXSA ZUXSA2 ZUXAFB ZUTPSM  ZUTAU  ZULRSM  ZUALR
   0  0.00057  0.00057
   1  0.09502  0.09502  0.09502  0.09502  0.09502  -0.0647-0.0647-0.0647-0.0647
   2  0.09527  0.09527  0.09527  0.09527  0.09527  -0.0646-0.0646-0.0646-0.0646
   3  0.09410  0.09410  0.09410  0.09410  0.09410  -0.0644-0.0644-0.0644-0.0644 0.0067 0.0067
   4  0.13281  0.13281  0.13281                    -0.1108-0.1108                          -0.0561 0.0000
   5  0.03389  0.03389  0.03389                    -0.1993-0.1993                          -0.1950 0.0000
   6  0.13290  0.13290  0.13290                    -0.1112-0.1112                          -0.0561 0.0000
   7  0.03389  0.03389  0.03389                    -0.1993-0.1993                          -0.1950 0.0000
   8  0.00000  0.00000  0.00000                     0.0000 0.0000                           0.0000 0.0000
   9  0.03244  0.03244  0.03244                    -0.2108-0.2108                          -0.2027 0.0000
  10  0.36594  0.36594                                                                     -0.0948 0.0000
  11  1.47311  1.46902  1.46902  1.46902             0.8513 0.8491 0.8491


 SQRT(S) =   65.

     <-------------- Cross Section -------------->  <------- Asymmetry ------->  <--Tau_Pol-->  <----A_LR--->
INDF   ZUTHSM   ZUXSEC    ZUXSA   ZUXSA2   ZUXAFB   ZUTHSM  ZUXSA ZUXSA2 ZUXAFB ZUTPSM  ZUTAU  ZULRSM  ZUALR
   0  0.00558  0.00558
   1  0.03188  0.03188  0.03188  0.03188  0.03188  -0.3670-0.3670-0.3670-0.3670
   2  0.03196  0.03196  0.03196  0.03196  0.03196  -0.3662-0.3662-0.3662-0.3662
   3  0.03196  0.03196  0.03196  0.03196  0.03196  -0.3650-0.3650-0.3650-0.3650 0.0247 0.0247
   4  0.04977  0.04977  0.04977                    -0.4735-0.4735                          -0.2290 0.0000
   5  0.02196  0.02196  0.02196                    -0.4879-0.4879                          -0.4450 0.0000
   6  0.04979  0.04979  0.04979                    -0.4742-0.4742                          -0.2290 0.0000
   7  0.02196  0.02196  0.02196                    -0.4878-0.4878                          -0.4450 0.0000
   8  0.00000  0.00000  0.00000                     0.0000 0.0000                           0.0000 0.0000
   9  0.02169  0.02169  0.02169                    -0.4983-0.4983                          -0.4511 0.0000
  10  0.16516  0.16516                                                                     -0.3156 0.0000
  11  0.45481  0.45471  0.45471  0.45471             0.8370 0.8366 0.8366


 SQRT(S) =   89.1866989

     <-------------- Cross Section -------------->  <------- Asymmetry ------->  <--Tau_Pol-->  <----A_LR--->
INDF   ZUTHSM   ZUXSEC    ZUXSA   ZUXSA2   ZUXAFB   ZUTHSM  ZUXSA ZUXSA2 ZUXAFB ZUTPSM  ZUTAU  ZULRSM  ZUALR
   0  0.79394  0.79394
   1  0.41251  0.41251  0.41251  0.41251  0.41251  -0.1892-0.1892-0.1892-0.1892
   2  0.41268  0.41268  0.41268  0.41268  0.41268  -0.1892-0.1892-0.1892-0.1892
   3  0.41182  0.41182  0.41182  0.41182  0.41182  -0.1895-0.1895-0.1895-0.1895-0.1194-0.1194
   4  1.44081  1.44081  1.44081                    -0.0483-0.0483                           0.0827 0.0000
   5  1.81553  1.81553  1.81553                     0.0533 0.0533                           0.1016 0.0000
   6  1.44059  1.44059  1.44059                    -0.0483-0.0483                           0.0827 0.0000
   7  1.81554  1.81554  1.81554                     0.0533 0.0533                           0.1016 0.0000
   8  0.00000  0.00000  0.00000                     0.0000 0.0000                           0.0000 0.0000
   9  1.78197  1.78197  1.78197                     0.0526 0.0526                           0.1002 0.0000
  10  8.29444  8.29444                                                                      0.0947 0.0000
  11  0.70042  0.70060  0.70049  0.70049             0.4313 0.4312 0.4312
```

SQRT(S) = 91.1866989

INDF	ZUTHSM	ZUXSEC	ZUXSA	ZUXSA2	ZUXAFB	ZUTHSM	ZUXSA	ZUXSA2	ZUXAFB	ZUTPSM	ZUTAU	ZULRSM	ZUALR
	<-------------- Cross Section -------------->					<------- Asymmetry ------->				<--Tau_Pol-->		<----A_LR--->	
0	2.91053	2.91053											
1	1.47542	1.47542	1.47542	1.47542	1.47542	-0.0003	-0.0003	-0.0003	-0.0003				
2	1.47594	1.47594	1.47594	1.47594	1.47594	-0.0003	-0.0003	-0.0003	-0.0003				
3	1.47288	1.47288	1.47288	1.47288	1.47288	-0.0005	-0.0005	-0.0005	-0.0005	-0.1418	-0.1418		
4	5.23978	5.23978	5.23979			0.0605	0.0605					0.1404	0.0000
5	6.66702	6.66702	6.66703			0.0960	0.0960					0.1427	0.0000
6	5.23898	5.23898	5.23899			0.0606	0.0606					0.1404	0.0000
7	6.66706	6.66706	6.66706			0.0960	0.0960					0.1427	0.0000
8	0.00000	0.00000	0.00000			0.0000	0.0000					0.0000	0.0000
9	6.54739	6.54739	6.54738			0.0965	0.0965					0.1422	0.0000
10	30.36023	30.36022										0.1418	0.0000
11	1.37052	1.37061	1.37052	1.37052		0.1868	0.1868	0.1868					

SQRT(S) = 93.1866989

INDF	ZUTHSM	ZUXSEC	ZUXSA	ZUXSA2	ZUXAFB	ZUTHSM	ZUXSA	ZUXSA2	ZUXAFB	ZUTPSM	ZUTAU	ZULRSM	ZUALR
	<-------------- Cross Section -------------->					<------- Asymmetry ------->				<--Tau_Pol-->		<----A_LR--->	
0	1.21994	1.21994											
1	0.62814	0.62814	0.62814	0.62814	0.62814	0.1204	0.1204	0.1204	0.1204				
2	0.62838	0.62838	0.62839	0.62839	0.62838	0.1204	0.1204	0.1204	0.1204				
3	0.62715	0.62715	0.62715	0.62715	0.62715	0.1203	0.1203	0.1203	0.1203	-0.1516	-0.1516		
4	2.21170	2.21170	2.21170			0.1284	0.1284					0.1748	0.0000
5	2.80422	2.80422	2.80422			0.1224	0.1224					0.1681	0.0000
6	2.21140	2.21140	2.21140			0.1286	0.1286					0.1748	0.0000
7	2.80423	2.80423	2.80424			0.1224	0.1224					0.1681	0.0000
8	0.00000	0.00000	0.00000			0.0000	0.0000					0.0000	0.0000
9	2.75524	2.75524	2.75524			0.1237	0.1237					0.1682	0.0000
10	12.78678	12.78676										0.1704	0.0000
11	0.52304	0.52301	0.52296	0.52296		0.2174	0.2174	0.2174					

SQRT(S) = 100.

INDF	ZUTHSM	ZUXSEC	ZUXSA	ZUXSA2	ZUXAFB	ZUTHSM	ZUXSA	ZUXSA2	ZUXAFB	ZUTPSM	ZUTAU	ZULRSM	ZUALR
	<-------------- Cross Section -------------->					<------- Asymmetry ------->				<--Tau_Pol-->		<----A_LR--->	
0	0.20697	0.20697											
1	0.11687	0.11687	0.11687	0.11687	0.11687	0.2402	0.2402	0.2402	0.2402				
2	0.11694	0.11694	0.11694	0.11694	0.11694	0.2401	0.2401	0.2401	0.2401				
3	0.11675	0.11675	0.11676	0.11676	0.11675	0.2402	0.2402	0.2402	0.2402	-0.1507	-0.1507		
4	0.38972	0.38972	0.38972			0.1995	0.1995					0.2065	0.0000
5	0.48043	0.48043	0.48044			0.1508	0.1508					0.1949	0.0000
6	0.38969	0.38969	0.38969			0.1997	0.1997					0.2065	0.0000
7	0.48044	0.48044	0.48044			0.1508	0.1508					0.1949	0.0000
8	0.00000	0.00000	0.00000			0.0000	0.0000					0.0000	0.0000
9	0.47255	0.47255	0.47255			0.1530	0.1530					0.1959	0.0000
10	2.21283	2.21282										0.1992	0.0000
11	0.19397	0.19395	0.19394	0.19394		0.6381	0.6383	0.6383					

SQRT(S) = 140.

	<-------- Cross Section -------->				<------- Asymmetry ------->				<--Tau_Pol-->		<----A_LR--->	
INDF	ZUTHSM	ZUXSEC	ZUXSA	ZUXSA2	ZUXAFB	ZUTHSM	ZUXSA	ZUXSA2	ZUXAFB	ZUTPSM	ZUTAU	ZULRSM	ZUALR
0	0.02249	0.02249											
1	0.01749	0.01749	0.01749	0.01749	0.01749	0.2926	0.2927	0.2927	0.2926				
2	0.01751	0.01751	0.01751	0.01751	0.01751	0.2923	0.2923	0.2923	0.2923				
3	0.01750	0.01750	0.01750	0.01750	0.01750	0.2923	0.2923	0.2923	0.2923	-0.1163	-0.1163		
4	0.04834	0.04834	0.04834			0.2476	0.2477					0.2114	0.0000
5	0.05363	0.05363	0.05363			0.1686	0.1687					0.2039	0.0000
6	0.04834	0.04834	0.04834			0.2478	0.2478					0.2114	0.0000
7	0.05363	0.05363	0.05363			0.1686	0.1686					0.2039	0.0000
8	0.00000	0.00000	0.00000			0.0000	0.0000					0.0000	0.0000
9	0.05297	0.05297	0.05297			0.1734	0.1734					0.2092	0.0000
10	0.25691	0.25642										0.2077	0.0000
11	0.08494	0.08497	0.08497	0.08497		0.8995	0.8997	0.8997					

SQRT(S) = 175.

	<-------- Cross Section -------->				<------- Asymmetry ------->				<--Tau_Pol-->		<----A_LR--->	
INDF	ZUTHSM	ZUXSEC	ZUXSA	ZUXSA2	ZUXAFB	ZUTHSM	ZUXSA	ZUXSA2	ZUXAFB	ZUTPSM	ZUTAU	ZULRSM	ZUALR
0	0.01070	0.01070											
1	0.00934	0.00934	0.00934	0.00934	0.00934	0.2824	0.2824	0.2824	0.2824				
2	0.00936	0.00936	0.00936	0.00936	0.00936	0.2819	0.2819	0.2819	0.2819				
3	0.00935	0.00935	0.00935	0.00935	0.00935	0.2819	0.2819	0.2819	0.2819	-0.1000	-0.1000		
4	0.02405	0.02405	0.02405			0.2459	0.2459					0.2031	0.0000
5	0.02563	0.02563	0.02563			0.1624	0.1624					0.1981	0.0000
6	0.02405	0.02405	0.02405			0.2460	0.2460					0.2031	0.0000
7	0.02563	0.02563	0.02563			0.1624	0.1624					0.1981	0.0000
8	0.00000	0.00000	0.00000			0.0000	0.0000					0.0000	0.0000
9	0.02536	0.02536	0.02536			0.1696	0.1696					0.2081	0.0000
10	0.12472	0.12428										0.2019	0.0000
11	0.05490	0.05490	0.05490	0.05490		0.9019	0.9021	0.9021					

117.190u 0.090s 1:59.22 98.3%

REFERENCES

1. D. Bardin, M. Bilenky, A. Chizhov, P. Christova, O. Fedorenko, M. Jack, L. Kalinovskaya, A. Olshevsky, S. Riemann, T. Riemann, M. Sachwitz, A. Sazonov, Y. Sedykh, I. Sheer, and L. Vertogradov, Fortran program `ZFITTER`;
   obtainable from `afs/cern.ch/user/b/bardindy/public`
   and from `http://www.ifh.de/~riemann/Zfitter/`.
2. A. Akhundov, D. Bardin, M. Bilenky, P. Christova, L. Kalinovskaya, S. Riemann, T. Riemann, M. Sachwitz, and H. Vogt, Fortran program `DIZET`.
3. D. Bardin, P. Christova, and O. Fedorenko, "On the lowest order electroweak corrections to spin-$\frac{1}{2}$ fermion scattering (I). The one loop diagrammar", *Nucl. Phys.* **B175** (1980) 435.
4. D. Bardin, P. Christova, and O. Fedorenko, "On the lowest order electroweak corrections to spin-$\frac{1}{2}$ fermion scattering (II). The one-loop amplitudes", *Nucl. Phys.* **B197** (1982) 1.
5. D. Bardin, M. Bilenky, P. Christova, T. Riemann, M. Sachwitz, and H. Vogt, "`DIZET`: A program package for the calculation of electroweak one loop corrections for the process $e^+e^- \to f^+f^-$ around the Z^0 peak", *Comput. Phys. Commun.* **59** (1989) 303.
6. D. Bardin, M. Bilenky, A. Chizhov, O. Fedorenko, S. Ganguli, A. Gurtu, M. Lokajicek, G. Mitselmakher, A. Olshevsky, J. Ridky, S. Riemann, T. Riemann, M. Sachwitz, A. Sazonov, D. Schaile, Y. Sedykh, and L. Vertogradov, "`ZFITTER` v.4.5: An analytical program for fermion pair production in e^+e^- annihilation", preprint CERN-TH. 6443/92 (1992), `hep-ph/9412201`.
7. D. Bardin, P. Christova, M. Jack, L. Kalinovskaya, A. Olshevski, S. Riemann, and T. Riemann, Fortran program `ZFITTER` v.6.21 (26 July 1999).
8. D. Bardin, M. S. Bilenky, G. Mitselmakher, T. Riemann, and M. Sachwitz, "A realistic approach to the standard Z peak", *Z. Phys.* **C44** (1989) 493.
9. D. Bardin, M. Bilenky, A. Chizhov, A. Sazonov, O. Fedorenko, T. Riemann, and M. Sachwitz, "Analytic approach to the complete set of QED corrections to fermion pair production in e^+e^- annihilation", *Nucl. Phys.* **B351** (1991) 1–48.
10. D. Bardin, M. Bilenky, A. Sazonov, Y. Sedykh, T. Riemann, and M. Sachwitz, "QED corrections with partial angular integration to fermion pair production in e^+e^- annihilation", *Phys. Lett.* **B255** (1991) 290–296.
11. P. C. Christova, M. Jack, and T. Riemann, "Hard photon emission in $e^+e^- \to \bar{f}f$ with realistic cuts", *Phys. Lett.* **B456** (1999) 264.
12. A. Akhundov, D. Bardin, and T. Riemann, "Electroweak one loop corrections to the decay of the neutral vector boson", *Nucl. Phys.* **B276** (1986) 1.
13. D. Bardin and A. Chizhov, "On the $O(\alpha_{em}\alpha_s)$ corrections to electroweak observables", in *Proc. Int. Topical Seminar on Physics of e^+e^- Interactions at LEP energies, 15-16 Nov 1988, JINR Dubna, USSR,* JINR preprint E2-89-525 (1989) (D. Bardin *et al.*, eds.), pp. 42–48.
14. D. Bardin, G. Passarino, and W. Hollik (eds.), "Reports of the working group on precision calculations for the Z resonance", report CERN 95–03 (1995).
15. D. Bardin, M. Bilenky, A. Chizhov, A. Sazonov, Y. Sedykh, T. Riemann, and M. Sachwitz, "The convolution integral for the forward - backward asymmetry in e^+e^- annihilation", *Phys. Lett.* **B229** (1989) 405.
16. D. Bardin, W. Hollik, and T. Riemann, "Bhabha scattering with higher order weak loop corrections", *Z. Phys.* **C49** (1991) 485–490.
17. M. Grünewald, S. Kirsch, and T. Riemann, Fortran program `SMATASY` v.6.10 (27 May 1999), obtainable from `/afs/cern.ch/user/g/gruenew/public/smatasy/smata6_10.fortran`

or from `http://l3www.cern.ch/homepages/gruenew/welcome.html`.
18. S. Kirsch and T. Riemann, *Comp. Phys. Commun.* **88** (1995) 89–108.
19. A. Leike, T. Riemann, and J. Rose, *Phys. Lett.* **B273** (1991) 513–518.
20. T. Riemann, *Phys. Lett.* **B293** (1992) 451–456.
21. S. Riemann, Fortran program `ZEFIT`, obtainable from `http://www.ifh.de/~riemanns/`.
22. A. Leike, S. Riemann, and T. Riemann, *Phys. Lett.* **B291** (1992) 187–194.
23. I. N. Silin, Fortran subroutine `SIMPS`.
24. Y. Sedykh, Fortran subroutine `FDSIMP`.
25. T. Matsuura, Fortran subroutines `TRILOG` and `S12`.
26. F. Jegerlehner, Fortran function `hadr5` (Feb 1995).
27. S. Eidelman and F. Jegerlehner, *Z. Phys.* **C67** (1995) 585–602.
28. H. Burkhardt, Fortran function `HADRQQ` (1989).
29. H. Burkhardt, F. Jegerlehner, G. Penso, and C. Verzegnassi, *Z. Phys.* **C43** (1989) 497.
30. G. Degrassi, Fortran program `m2tcor` (Oct 1996).
31. G. Degrassi, S. Fanchiotti, F. Feruglio, B. Gambino, and A. Vicini, "Two-loop electroweak top corrections: are they under control?", in *Reports of the Working Group on Precision Calculations for the Z Resonance,* report CERN 95–03 (1995) (D. Bardin, W. Hollik, and G. Passarino, eds.), pp. 163–174.
32. G. Degrassi, S. Fanchiotti, F. Feruglio, P. Gambino, and A. Vicini, "Two loop corrections to the heavy top limit in the ρ parameter", New York Univ. preprint NYU-TH-01-04-95 (1995).
33. G. Degrassi, F. Feruglio, A. Vicini, S. Fanchiotti, and P. Gambino, "Two loop corrections for electroweak processes", in *Proc. of the 30^{th} Rencontre de Moriond, Les Arcs, France, March 1995* (J. Tran Than Van, ed.), vol. 1, pp. 77–86, Editions Frontieres, 1995.
34. G. Degrassi, P. Gambino, and A. Vicini, *Phys. Lett.* **B383** (1996) 219–226.
35. G. Degrassi, P. Gambino, and A. Sirlin, *Phys. Lett.* **B394** (1997) 188–194.
36. G. Degrassi and P. Gambino, "Two loop heavy top corrections to the Z^0 boson partial widths", Padua Univ. preprint DFPD-99-TH-19 (1999), `hep-ph/9905472`.
37. A. Arbuzov, "Light pair corrections to e^+e^- annihilation at LEP/SLC", `hep-ph/9907500`.
38. B. A. Kniehl, *Nucl. Phys.* **B347** (1990) 86–104.
39. D. Bardin and G. Passarino, "The Standard Model in the Making" (Clarendon Press, Oxford, 1999).
40. M. Jack, "QED radiative corrections to $e^+e^- \to \bar{f}f$ with realistic cuts at LEP energies and beyond", DESY 99-166 (1999), talk given at *14th International Workshop on High Energy Physics and Quantum Field Theory*, Moscow, Russia, 27 May - 2 Jun 1999, `hep-ph/9911296`.
41. P. Christova, M. Jack, S. Riemann and T. Riemann, "Radiative corrections to $e^+e^- \to \bar{f}f$", LC-TH-2000-008 (2000), `hep-ph/0002054`; to appear in: R. Heuer, F. Richard and P. Zerwas (eds.), "Physics Studies for a Future Linear Colider", Proc. of *2nd Joint ECFA/DESY Study on Physics and Detectors for a Linear Electron-Positron Collider*, held at Orsay, Lund, Frascati, Oxford, and Obernai from April 1998 until Oct 1999, DESY report 123F (in preparation).
42. D. Bardin, A. Leike, T. Riemann, and M. Sachwitz, *Phys. Lett.* **B206** (1988) 539–542.
43. P. Christova, M. Jack, S. Riemann, and T. Riemann, "Predictions of `ZFITTER` v.6 for fermion-pair production with acollinearity cut", DESY preprint 99-037 (1999), `hep-ph/9908289`.
44. T. Riemann and Z. Was, *Mod. Phys. Lett.* **A4** (1989) 2487.
45. M. Bilenky and A. Sazonov, "QED corrections at Z^0 pole with realistic kinematical cuts", Dubna preprint JINR-E2-89-792 (1989).
46. T. Riemann, M. Sachwitz, and D. Bardin, "The Z boson line shape at LEP", in *Proc. of the*

11th Warsaw Symp. on Elementary Particle Physics: New Theories in Physics, Kazimierz, Poland, May 23-27, 1988 (Z. Ajduk, S. Pokorski, and A. Trautman, eds.), pp. 238–246, World Scientific, Singapore, 1989, Zeuthen preprint PHE 88-11 (1988), scanned image in KEK library, entry 8901077.

47. D. Bardin, O. Fedorenko, and T. Riemann, "The electromagnetic $O(\alpha^3)$ contributions to e^+e^- annihilation into fermions in the electroweak theory. Total cross-section σ_T and integrated asymmetry A_{FB}", Dubna preprint JINR E2-87-663 (1987).
48. D. Bardin, M. Bilenky, O. Fedorenko, and T. Riemann, "The electromagnetic $O(\alpha^3)$ contributions to e^+e^- annihilation into fermions in the electroweak theory. Total cross-section σ_T and integrated asymmetry A_{FB}", Dubna preprint JINR E2-88-324 (1988), scanned image in KEK library, entry 8808103.
49. P. Christova, M. Jack, and T. Riemann, in preparation.
50. G. Passarino, *Nucl. Phys.* **B204** (1982) 237–266.
51. E. Byckling and K. Kajantie, "Particle Kinematics" (Wiley, London, 1973).
52. G. Bonneau and F. Martin, *Nucl. Phys.* **B27** (1971) 381.
53. E. A. Kuraev and V. S. Fadin, *Yad. Phiz. (in Russian)* **41** (1985) 733–742.
54. D. Bardin *et al.*, "Z line shape", in *Proc. of Workshop on Z Physics at LEP, Geneva, Switzerland, Feb 20-21 and May 8-9, 1989,* report CERN 89–08 (1989) (G. Altarelli, R. Kleiss, and C. Verzegnassi, eds.), vol. 1, pp. 89–128.
55. M. Skrzypek, *Acta Phys. Polon.* **B23** (1992) 135.
56. B. A. Kniehl, M. Krawczyk, J. H. Kühn, and R. G. Stuart, *Phys. Lett.* **209B** (1988) 337.
57. D. Bardin, M. Grünewald, and G. Passarino, "Precision calculation project report", `hep-ph/9902452`.
58. S. Jadach, M. Skrzypek, and M. Martinez, *Phys. Lett.* **B280** (1992) 129–136.
59. F. A. Berends, G. Burgers, and W. L. van Neerven, *Nucl. Phys.* **B297** (1988) 429; E: ibid., **B304** (1988) 921.
60. G. Montagna, O. Nicrosini, and F. Piccinini, *Phys. Lett.* **B406** (1997) 243–248.
61. W. Beenakker, F. Berends, and W. van Neerven, "Applications of renormalization group methods to radiative corrections", in *Proc. of the Int. Workshop on Radiative Corrections for e^+e^- Collisions, Schloß Ringberg, Tegernsee, Germany, April 1989* (J. H. Kühn, ed.), p. 3, Springer, Berlin, 1989.
62. M. W. Grünewald, "Combined Analysis of Precision Electroweak Results", talk at ICHEP 98, July 1998, Vancouver, Canada, Berlin Humboldt-Univ. preprint HUB-EP-98/67 (1998).
63. LEPEWWG – LEP electroweak working group, `http://www.cern.ch/LEPEWWG/`.
64. C. Caso *et al.*, *Eur. Phys. J.* **C3** (1998) 1.
65. G. Källén and A.Sabry, *K. Dan. Vidensk. Selsk. Mat.-Fys. Medd.* **17** (1955) 29.
66. M. Steinhauser, *Phys. Lett.* **B429** (1998) 158–161.
67. A. Sirlin, *Phys. Rev.* **D22** (1980) 971–981.
68. D. A. Ross and M. Veltman, *Nucl. Phys.* **B95** (1975) 135.
69. M. Veltman, *Nucl. Phys.* **B123** (1977) 89.
70. A. Djouadi, *Nuovo Cim.* **100A** (1988) 357.
71. F. Halzen and B. A. Kniehl, *Nucl. Phys.* **B353** (1991) 567–590.
72. L. Avdeev, J. Fleischer, S. Mikhailov, and O. Tarasov, *Phys. Lett.* **B336** (1994) 560–566, E: ibid., **B349** (1995) 597.
73. K. G. Chetyrkin, J. H. Kühn, and M. Steinhauser, *Phys. Lett.* **B351** (1995) 331–338.
74. S. Fanchiotti and A. Sirlin, "Higher order contributions to Δr", New York Univ. preprint NYU-TH-91-02-04 (1991).
75. M. Consoli, W. Hollik, and F. Jegerlehner, "Electroweak radiative corrections for Z physics",

in *Proc. of Workshop on Z Physics at LEP, Geneva, Switzerland, Feb 20-21 and May 8-9, 1989,* report CERN 89–08 (1989) (G. Altarelli, R. Kleiss, and C. Verzegnassi, eds.), vol. 1, p. 7.
76. R. Barbieri, M. Beccaria, P. Ciafaloni, G. Curci, and A. Vicere, *Phys. Lett.* **B288** (1992) 95–98.
77. J. Fleischer, O. V. Tarasov, and F. Jegerlehner, *Phys. Lett.* **B319** (1993) 249–256.
78. G. Degrassi and P. Gambino, private communication.
79. J. van der Bij and M. Veltman, *Nucl. Phys.* **B231** (1984) 205.
80. J. J. van der Bij, *Nucl. Phys.* **B248** (1984) 141.
81. B. A. Kniehl, "Estimation of higher-order QCD effects on electroweak parameters", in *Reports of the Working Group on Precision Calculations for the Z Resonance,* report CERN 95–03 (1995) (D. Bardin, W. Hollik, and G. Passarino, eds.), pp. 299–312.
82. A. Sirlin, "On the QCD corrections to $\delta\rho$", in *Reports of the Working Group on Precision Calculations for the Z Resonance,* report CERN 95–03 (1995) (D. Bardin, W. Hollik, and G. Passarino, eds.), pp. 285–298.
83. K. Chetyrkin, J. Kühn, and A. Kwiatkowski, "QCD corrections to the e^+e^- cross-section and the Z boson decay rate", in *Reports of the Working Group on Precision Calculations for the Z Resonance,* report CERN 95–03 (1995) (D. Bardin, W. Hollik, and G. Passarino, eds.), pp. 175–263.
84. A. Czarnecki and J. H. Kühn, *Phys. Rev. Lett.* **77** (1996) 3955–3958.
85. R. Harlander, T. Seidensticker, and M. Steinhauser, *Phys. Lett.* **B426** (1998) 125–132.
86. D. Bardin, S. Riemann, and T. Riemann, *Z. Phys.* **C32** (1986) 121.
87. G. Mann and T. Riemann, *Annalen Phys.* **40** (1984) 334.
88. W. Beenakker and W. Hollik, *Z. Phys.* **C40** (1988) 141.
89. J. Bernabéu, A. Pich, and A. Santamaria, *Phys. Lett.* **200B** (1988) 569.
90. J. Bernabéu, A. Pich, and A. Santamaria, *Nucl. Phys.* **B363** (1991) 326–344.
91. G. Buchalla and A. J. Buras, *Nucl. Phys.* **B398** (1993) 285–300.
92. J. Fleischer, O. V. Tarasov, F. Jegerlehner, and P. Raczka, *Phys. Lett.* **B293** (1992) 437–444.
93. G. Degrassi, *Nucl. Phys.* **B407** (1993) 271–289.
94. K. G. Chetyrkin, A. Kwiatkowski, and M. Steinhauser, *Mod. Phys. Lett.* **A8** (1993) 2785–2792.
95. T. Riemann, "The Z boson resonance parameters", in *Irreversibility and Causality, Lecture Notes in Physics, vol. 504* (A. Bohm *et al.*, eds.), pp. 157–177, Springer, Berlin, 1998, `hep-ph/9709208`.
96. D. Bardin *et al.*, "Electroweak working group report", in *Reports of the Working Group on Precision Calculations for the Z Resonance,* report CERN 95–03 (1995) (D. Bardin, W. Hollik, and G. Passarino, eds.), pp. 7–162, `hep-ph/9709229`.
97. L. Kalinovskaya, "Finite top mass effects in $e^+e^- \to \bar{f}f$ at LEP energies", talk at LEP-EWWG meeting, 30 Oct 1998, obtainable from `http://www.ifh.de/~riemann/Zfitter/LK_LEPEWWG_30_10_98/`.
98. E. Accomando *et al.*, "Standard model processes", in *Physics at LEP2,* report CERN 96–01 (1996) (G. Altarelli, T. Sjöstrand, and F. Zwirner, eds.), pp. 207–248, 1996, `hep-ph/9601224`.
99. A. Djouadi and C. Verzegnassi, *Phys. Lett.* **195B** (1987) 265.
100. A. B. Arbuzov, D. Bardin, and A. Leike, *Mod. Phys. Lett.* **A7** (1992) 2029–2038, E: ibid. **A9** (1994) 1515.
101. A. L. Kataev, *Phys. Lett.* **B287** (1992) 209–212.
102. K. G. Chetyrkin, A. L. Kataev, and F. V. Tkachev, *Phys. Lett.* **85B** (1979) 277.

103.M. Dine and J. Sapirstein, *Phys. Rev. Lett.* **43** (1979) 668.
104.W. Celmaster and R. J. Gonsalves, *Phys. Rev. Lett.* **44** (1980) 560.
105.S. G. Gorishny, A. L. Kataev, and S. A. Larin, *Phys. Lett.* **B273** (1991) 141–144.
106.S. Riemann, "A comparison of programs used in L3 for the analysis of Bhabha scattering", Zeuthen preprint PHE 91–04 (1991), scanned image in KEK library, entry 9105486.
107.W. Beenakker, "Theoretical developments in large angle Bhabha scattering", in *Proc. of the Joint Int. Symposium on Lepton and Photon Interactions and Europhysics Conference on High Energy Physics, Geneva, Switzerland, 25 July - 1 August 1991* (S. Hegarty *et al.*, eds.), vol. 1, p. 28, World Scientific, Singapore, 1992.
108.D. Bardin and T. Riemann, Fortran package `BHASHA` (1990), unpublished.
109.G. Passarino and M. Veltman, *Nucl. Phys.* **B160** (1979) 151.
110.D. Bardin and V. Dokuchaeva, *Nucl. Phys.* **B246** (1984) 221.
111.D. Bardin and V. Dokuchaeva, "On the radiative corrections to the neutrino deep inelastic scattering", Dubna preprint JINR-E2-86-260 (1986).
112.A. Akhundov, D. Bardin, L. Kalinovskaya, and T. Riemann, *Fortsch. Phys.* **44** (1996) 373–482.
113.A. Arbuzov, D. Bardin, J. Blümlein, L. Kalinovskaya, and T. Riemann, *Comput. Phys. Commun.* **94** (1996) 128.
114.S. Jadach, B. F. L. Ward, and Z. Was, *Comput. Phys. Commun.* **79** (1994) 503–522.
115.J. H. Field and T. Riemann, *Comput. Phys. Commun.* **94** (1996) 53–87.
116.F. Jegerlehner, "Renormalizing the standard model", in *Testing the Standard Model: Proceedings of the Theoretical Advanced Study Institute in Elementary Particle Physics (TASI), Boulder, CO, Jun 3-29, 1990* (M. Cvetic and P. Langacker, eds.), pp. 476–590, World Scientific, Teaneck, N.J., 1991.
117.F. Jegerlehner, *Prog. Part. Nucl. Phys.* **27** (1991) 1–76.
118.J. J. van der Bij and F. Hoogeveen, *Nucl. Phys.* **B283** (1987) 477.
119.R. Barbieri, P. Ciafaloni, and A. Strumia, *Phys. Lett.* **B317** (1993) 381.
120.R. Barbieri, private communication.
121.S. M. Berman, *Phys. Rev.* **112** (1958) 267.
122.T. Kinoshita and A. Sirlin, *Phys. Rev.* **113** (1959) 1652.
123.G. Källen, *Springer Tracts in Modern Physics* **46** (1968) 67–132.
124.T. van Ritbergen and R. G. Stuart, *Phys. Rev. Lett.* **82** (1999) 488.
125.T. van Ritbergen and R. G. Stuart, *Phys. Lett.* **B437** (1998) 201.
126.P. Christova, M. Jack, S. Riemann, and T. Riemann, "Predictions for fermion-pair production at LEP", preprint DESY 98-184 (1998), to appear in the proceedings of RADCOR98, Sep 8-12, 1998, Barcelona, Spain, `hep-ph/9812412`.